BAW-2127
December 1990

THE B&W OWNERS GROUP

MATERIALS COMMITTEE

FINAL SUBMITTAL

FOR

NUCLEAR REGULATORY COMMISSION
BULLETIN 88-11

"PRESSURIZER SURGE LINE
THERMAL STRATIFICATION"

B&W NUCLEAR SERVICE COMPANY

BAW-2127
December 1990

FINAL SUBMITTAL

IN RESPONSE TO

NUCLEAR REGULATORY COMMISSION

BULLETIN 88-11

"PRESSURIZER SURGE LINE THERMAL STRATIFICATION"

Prepared for

Arkansas Power and Light Company
Duke Power Company
Florida Power Corporation
General Public Utilities Nuclear
Toledo Edison Company

Prepared by
(see Section 10 for document signatures)

M.T. Matthews
R.J. Gurdal
D.E. Costa
G.L. Weatherly

B&W Nuclear Service Company
P.O. Box 10935
Lynchburg, Virginia 24506-0935

EXECUTIVE SUMMARY

On December 20, 1988 the Nuclear Regulatory Commission issued NRC Bulletin 88-11. The bulletin addressed technical concerns associated with thermal stratification in the pressurizer surge line and required utilities to establish and implement a program to ensure the structural integrity of the surge line. Subsequent to issuance of the bulletin, the B&W Owners Group has developed a comprehensive program to address the requirements of the bulletin. A committee which includes representatives from each member utility has closely participated in all phases of the program. This report summarizes the B&WOG program and its results.

The surge line for each B&W-designed lowered loop plant has been evaluated for the effects of thermal stratification. Davis-Besse Unit 1 (DB-1), the only B&WOG raised loop plant, is undergoing a plant specific evaluation which will be reported in a supplement to this report. The evaluation of the lowered loop plants involved comprehensive instrumentation of Oconee Unit 1 as the representative plant. The evaluation also involved assessment of operating practices and procedures, collection and review of historical plant data from all six lowered loop B&W plants, and development of new design basis transient conditions for the surge line to conservatively account for thermal cycling, thermal stratification, and thermal striping. The evaluation of thermal striping incorporated the best available data to characterize this phenomenon as it may occur in the surge line.

The structural analysis for the new design conditions has shown that the lowered loop surge line can meet its 40 year design life. Detailed finite element analyses have been performed on the pressurizer surge nozzle, on the surge line to hot leg nozzle, and on the limiting portions (the elbows) of the pressurizer surge line piping. At all points in the surge line and the associated nozzles the cumulative fatigue usage factor remains less than one for the design life.

CONTENTS

List of Tables

List of Figures

1. INTRODUCTION

This report summarizes the B&W Owners Group program addressing the technical issues described in NRC Bulletin 88-11 (reference 1). The analyses described in this report confirm that all surge line pressure boundary components (including all nozzles) satisfy applicable code stress allowables for the operating B&W lowered loop plants: Arkansas Nuclear One Unit 1, Crystal River Unit 3, Oconee Unit 1, Oconee Unit 2, Oconee Unit 3, and Three Mile Island Unit 1, considering the effects of thermal stratification and thermal striping. The Davis Besse Unit 1 (raised loop plant) surge line is currently being evaluated and will be addressed in a future supplement to this report.

In light of the extensive technical program developed to respond generically to NRC Bulletin 88-11, the Babcock and Wilcox Owners Group formed a Thermal Stratification Working group. The Working Group included representatives from each member utility. The represenatives were chosen for their expertise in thermal-hydraulics or structural mechanics. The Working Group has been extensively involved in this program and has functioned as technical overseers, technical coordinators between the utilities and BWNS, and program managers.

The introduction provides the background for the thermal stratification, striping and cycling issues and a summary of the surge line fatigue analysis results and conclusions. The remaining sections of the report are as follows:

- Section 2 describes the technical approach which has been developed by the B&W Owners Group,
- Section 3 discusses the justification for the generic approach taken by the lowered loop plant owners,
- Section 4 describes the development of the new design basis thermal-hydraulic conditions for the surge line,
- Sections 5 and 6 describe the stress and fatigue analyses performed for

the surge line piping and its nozzles,

- Section 7 provides conclusions resulting from the B&W Owners Group program with regard to new design basis transients which represent surge line thermal conditions and the structural integrity of the surge line,
- Section 8 states the conditions which form the basis for the analysis,
- Section 9 lists all references, and
- The appendices provide a detailed discussion of the striping and stratification tests which were used as aids in developing the design basis transients.

1.1. Background

The surge line in B&W 177FA plants contains approximately 50 feet of piping which connects the pressurizer lower head and the reactor coolant hot leg piping. During plant operation, the reactor coolant system (RCS) is pressurized with a steam bubble in the pressurizer. Thus, the pressurizer contains saturated fluid while the remainder of the RCS is subcooled with temperatures generally at least 50F cooler than the pressurizer fluid. The surge line provides the means by which the pressurizer accommodates changes in RCS inventory. Thus, RCS fluid flows through the surge line during surges into and out of the pressurizer. During RC pump operations, there is an outflow from the pressurizer due to pressurizer bypass spray flow.

Due to differences in density, the reactor coolant can stratify in the horizontal piping section whereby the fluid temperature varies from top to bottom with the warmer fluid located above the denser (cooler) fluid. This phenomenon, known as thermal stratification, is most pronounced during outsurges from the pressurizer. During an insurge or outsurge under stratified conditions, a phenomenon known as thermal striping may occur at the fluid layer interface. Thermal striping is a rapid oscillation of the thermal boundary interface caused by interfacial waves and turbulent effects. The original surge line fatigue analyses performed for the B&W 177FA plants assumed that uniform temperatures existed at each surge line location and did not account for thermal stratification which causes additional bending moments in the piping. The original surge line fatigue analyses also did not account for thermal striping which affects the fatigue usage at the inner

considered in the original stress analysis. The effects of this bowing have been observed in the surge line of the Portland General Electric Company Trojan plant during each refueling outage since 1982. The piping deflections have been observed to have resulted in reduced clearances at the pipe restraints and, in some instances, contact of the piping and the pipe restraints has been observed. Similar occurrences have also been noted at Beaver Valley Unit 2.

In order to confirm pressurizer surge line integrity, the Nuclear Regulatory Commission issued NRC Bulletin Number 88-11, Pressurizer Surge Line Thermal Stratification (December 20, 1988). This bulletin requires certain actions of licensees of all operating pressurized water reactors (PWRs). The actions applicable to the case at hand are paraphrased below.

1a. At the first available cold shutdown after receipt of the bulletin, and which exceeds seven days, conduct a visual inspection of the pressurizer surge line.

1b. Within four months of receipt of the bulletin, licensees of plants in operation over ten years are requested to demonstrate that the pressurizer surge line meets the applicable design codes and other FSAR and regulatory commitments for the licensed life of the plant, considering thermal stratification and thermal striping in the fatigue and stress evaluations. (For licensees of plants which have been in operation less than ten years, this action must be completed within one year of receipt of the bulletin.) Or provide the staff with a justification for continued operation while a detailed analysis of the surge line is performed by implementing Items 1c and 1d below.

1c. If necessary, obtain plant specific surge line thermal and displacement data. Data can be obtained through collective efforts if sufficient similarities in geometry and operation can be demonstrated.

1d. Update the fatigue and stress analyses to ensure compliance with the applicable Code requirements.

A portion of the B&W Owners Group program was presented to the Nuclear Regulatory Commission Staff on September 29, 1988 and April 7, 1989. An interim evaluation, BAW-2085 dated May 1989, provided the staff with a justification for near term operation for all of the operating B&W 177FA plants (reference 2). The NRC concluded that sufficient information had been provided to justify near term operation for B&W plants until the final report could be completed (reference 3).

This report summarizes the entire B&W Owners Group program and documents compliance with action items 1b, 1c, and 1d of NRC Bulletin 88-11 to demonstrate code compliance for the 40 year life of the surge line.

1.2. Conclusion

The surge lines for the six B&W lowered loop plants are shown to fulfill the 40 year design life. The structural analysis of the surge line and associated nozzles has accounted for thermal conditions (thermal stratification, thermal striping, and thermal cycling) existing during the life of the plants. The highest cumulative usage factor for 40 years of operation occurs in the vertical elbow located at the bottom of the riser (elbow B on Figure 3-1). This elbow has been calculated to have the largest cumulative usage factor for the Oconee Unit 2 surge line, with a value of 0.82 for the 40 year design life and based on 360 heatup/cooldown cycles. For the non-Oconee lowered-loop plants, the highest cumulative usage factor occurs in the same elbow for Arkansas Nuclear One Unit 1 (ANO-1) and is equal to 0.66 for the 40 year design life and based on 240 heatup/cooldown cycles.

2. OVERVIEW OF B&W OWNER'S GROUP PROGRAM

Revised surge line design basis transients have been developed based on an assessment of information from all the B&W plants including detailed thermal stratification data taken at Oconee Unit 1, thermal striping data collected by Battelle-Karlsruhe, other plant heatup, cooldown, and operational data, and plant operating and surveillance procedures. The number of occurrences for each design basis transient has been determined for each plant from operating histories and a fatigue stress evaluation has been performed for the surge line of each plant.

The B&W Owners Group Materials Committee has developed a comprehensive program to address all technical concerns identified in NRC Bulletin 88-11. The program is divided into two basic sections. The first addresses the need to understand relevant thermal-hydraulic phenomena occurring in the surge lines, to develop operational recommendations, as appropriate, to reduce the severity and impact of thermal stratification in the surge line, and lastly to develop a new thermal-hydraulic design basis for the structural analysis and fatigue evaluation of the surge line and the associated nozzles. The design basis thermal transients represent the final product of the first part of the program. The second part of the program addresses all structural analyses required to assess the integrity of the surge line and associated nozzles for the balance of the design life of each of the plants.

This report is a summary of the entire program. Figure 2-1 shows the relationship of the key elements of the program, which is further described in the following two subsections.

2.1. Development of New Design Basis Conditions

The thermal-hydraulic phenomena which had to be accounted for in the surge line were thermal stratification, thermal striping, and thermal cycling. These phenomena occur to some degree in almost all modes of plant operation. As a

result, the surge line conditions had to be carefully considered from cold shutdown through heatup, power escalation and cooldown.

Operational events at power also cause surge line thermal cycling although these cycles have been shown to be relatively inconsequential as a result of evaluations performed in this program. This is primarily due to the small difference in temperature between the pressurizer fluid and the RCS hot leg fluid.

Thermal cycling is a transient phenomenon and is thus associated with mass or temperature changes in the RCS. Thermal stratification can occur in the surge line only during moderate to low flow rates through the surge line and may exist in a steady state as well as in a transient condition. Thermal striping requires the existence of thermal stratification. Quantitative treatment of these phenomena requires knowledge of the following:

1. Previous operating experience (surge line operating experience),
2. Operating practices that influence surge line conditions,
3. Thermal stratification, and
4. Relationship between thermal striping and thermal stratification.

Previous operating experience includes the total of all thermal cycles and stratification conditions that have existed since plant startup. Data does not exist in order to describe the complete history of the surge line transients in the plants. Therefore, two things have been done to estimate the operational history. First, each utility reviewed plant operating logs to identify each heatup and cooldown performed since plant startup. The utilities then retrieved data sets for the overall RCS parameters for the heatup and cooldown events to typify these evolutions. These data sets have provided the bases for key operational characteristics such as the average times for the various phases of a plant heatup, the frequency and magnitudes of surge line flow transients, and the relationship between the pressurizer and reactor coolant loop temperatures.

To understand surge line thermal-hydraulic service conditions, the Oconee Unit 1 surge line was thoroughly instrumented to record the thermal transients in the surge line for plant heatup, power escalation, full power operation, and plant cooldown. Surge line displacement instrumentation was also added to all major

sections of the Oconee Unit 1 surge line. The Oconee data collection effort, described in more detail in Appendix A, has provided circumferential temperature measurements at several different axial locations along the surge line in addition to displacement measurements for each major displacement axis. These data have been used to develop a correlation of surge line temperature responses to the surge line flow rate for given end point pressurizer and RC loop temperatures.

In parallel with the Oconee Unit 1 measurement program and the collection of historical plant data, a review of the operating procedures for all plants has been performed to better understand those plant evolutions likely to cause surge line upsets. This review has been supplemented with interviews of plant operators at each site. Evolutions causing significant surge flows have been identified and quantified, within the limits of the plant data. Plant data indicated many more surge line upsets than could be described and quantified as determined from the procedures. Hence, the mechanistic surge line events have been augmented with random, or unexplained, surge line flow events. The random events have been based on typical plant data for changes in pressurizer level during heatup and cooldown operations. The total number of surge line flow occurrences have been based on plant data. The results of the overall effort have provided the bases for assumed surge line upsets that take place during heatup, cooldown, and power operation.

An important part of the operating procedure review has dealt with the potential upper bound for the pressurizer to hot leg temperature differences. The B&W Owners chose to relate the potential upper limit on the surge line end point differential temperatures to pressure limits imposed according to 10CFR50, Appendix G (see Figure 2-2.). The Appendix G limits have been reviewed for each plant and a bounding composite pressure/temperature (P/T) limit has been developed to cover all plants for the 0 to 2 Effective Full Power Years (EFPY) period, the 2 EFPY to 1990 time period, and the period from 1991 to the end of life. Since no B&W-designed lowered loop plant transient has been identified to have approached or exceeded the pressure/temperature limits at or near cold RCS conditions (50F-120F), these limits represent an upper bound on the pressurizer temperature to hot leg temperature difference. The survey of plant heatup and cooldown data has shown that none of the recorded transients approached the

pressure-temperature relationship adopted for this program. The maximum theoretical surge line top-to-bottom temperature difference is 397F, as discussed in Section 4.5.1.2. The maximum surge line top-to-bottom temperature difference measured at Oconee Unit 1 was 280F.

The third item on the list of key elements addresses thermal striping. A review of the literature on thermal striping has been made to identify potentially useful experimental data for application to the surge line analyses. As noted in the interim submittal (reference 2), most experimental work reported in the literature applies to fluid conditions very different from those that exist in a PWR surge line. The majority of work has been done at low pressures and relatively low temperatures. Some of the experiments used different concentrations of solutions to simulate the density gradients that can exist at higher fluid temperatures. One set of experiments, those performed by Battelle-Karlsruhe Laboratories, stood out as clearly superior in simulating the PWR surge line conditions. BWNS performed a detailed review of published reports on the experimental apparatus and partial test results and has followed this review up with direct contact with the principal investigator, Dr. Lothar Wolf. The B&W Owners Group decided to purchase the raw data from Battelle for the series of nine test runs made at typical PWR surge line conditions. Details of the experimental setup and tested conditions are addressed in Section 4.3. The important results that have been derived from the Battelle data are the relationship of thermal striping amplitude and frequency to the pipe fluid conditions. The thermal striping data correlation allows the determination of striping characteristics for any given surge line flow rate and imposed top-to-bottom temperature difference.

The product of the thermal-hydraulic program is a revised set of surge line design basis transient descriptions that account for thermal cycling, thermal stratification, and thermal striping. All design transients considered in the previous design basis for the surge line have been modified to account for all three thermal phenomena. All design basis transients involving surges have been considered in the evaluation.

Results of the thermal-hydraulics part of the program consist of the input for the stress analysis of the surge line itself, the associated nozzles at each end, and the one-inch diameter drain nozzle connection at the bottom of the lower

horizontal run. The stress analysis portion of the program is described in the next subsection.

2.2. Stress Analysis

The first phase of the stress analysis involved building a structural mathematical model containing the pressurizer, the surge line, the hot leg, the reactor vessel and the steam generator. This structural mathematical model has been verified by using the measured surge line temperature data from the Oconee Unit 1 heat-up of February 1989 to predict surge line displacements. These predicted surge line displacements agree well with the measured surge line displacements (see subsection 5.1.4 and Figures 5-2 through 5-4).

The structural loading analysis has been performed using the new thermal-hydraulic design basis. This generates the internal forces and moments which have been used for the stress analysis of the surge line and the nozzles associated with its endpoints.

The applicable piping code is the 1986 Edition of ASME Code NB-3600, in accordance with NRC Bulletin 88-11 which states: "Fatigue analysis should be performed in accordance with the latest ASME Section III requirements incorporating high cycle fatigue". A Code reconciliation has been performed for each plant to remove all concerns associated with using the later Code (1986 Edition) for the fatigue stress analysis of the surge line. For the Code reconciliation, each plant's surge line stress report has been reviewed (the code of record for piping analysis is not the same for all the surge lines).

Using finite element analysis for the elbows and simplified equations elsewhere in the surge line, all stress intensity values (Equations 12 and 13, and Thermal Stress Ratchet) have been found to be within their allowables (taken from ASME Section III, Appendix I). Therefore, the elastc-plastic fatigue analysis has been performed in accordance with NB-3653.6(c). To account for the thermal-hydraulic conditions defined in the new design basis, the surge line fatigue analysis includes thermal stratification, pressure ranges between the thermal stratification conditions, thermal striping, fluid flow and temperature changes leading to through-wall temperature gradients, and the additional localized stress due to the non-linearity of the top-to-bottom temperature profile.

In the NB-3600 elasto-plastic fatigue analysis, all applicable surge line locations have been analyzed, including the drain line nozzle considered as a branch connection. The design basis transients are generally the same for each one of the six B&W lowered-loop plants. The number of occurrences of those transients, however, is unique to the plant to be analyzed due to differences in operating history. The elasto-plastic fatigue analysis has been performed and applied to each of the six plants being analyzed. For each one of the six B&W lowered-loop plants, the total cumulative usage factor is less than 1.0 at all surge line locations.

In addition to the structural analysis of the surge line described above, detailed stress analyses of the pressurizer and hot leg nozzles have been performed to demonstrate compliance with the ASME Code, Section III.

Finite element models have been made of both nozzles and the thermal and pressure stresses have been calculated using the revised design basis transient descriptions as input. Piping loads acting on the nozzles have been taken from the structural analysis of the surge line and have been combined with the pressure and thermal stresses. Stress and fatigue analyses were performed in accordance with the requirements of the 1986 Edition of the ASME Code, Section III, NB-3200 and NB-3600. The analyses demonstrate that the cumulative usage factor for each nozzle is less than 1.0.

Figure 2-1. B&W Owners Group Surge Line Stratification Program Key Elements

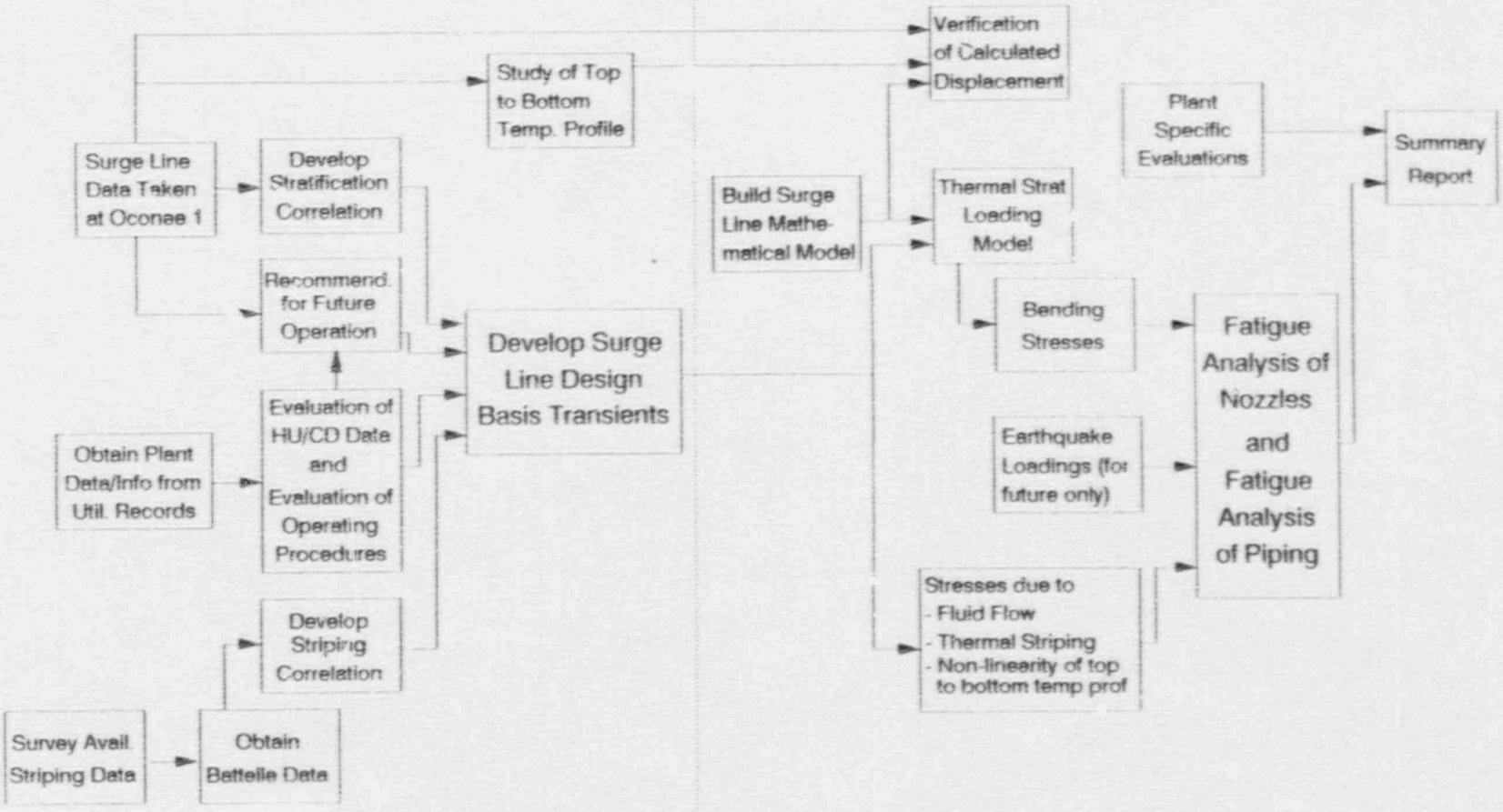

Figure 2-2. Maximum Pressurizer to RC Temperature Differences Imposed by Appendix G Limits

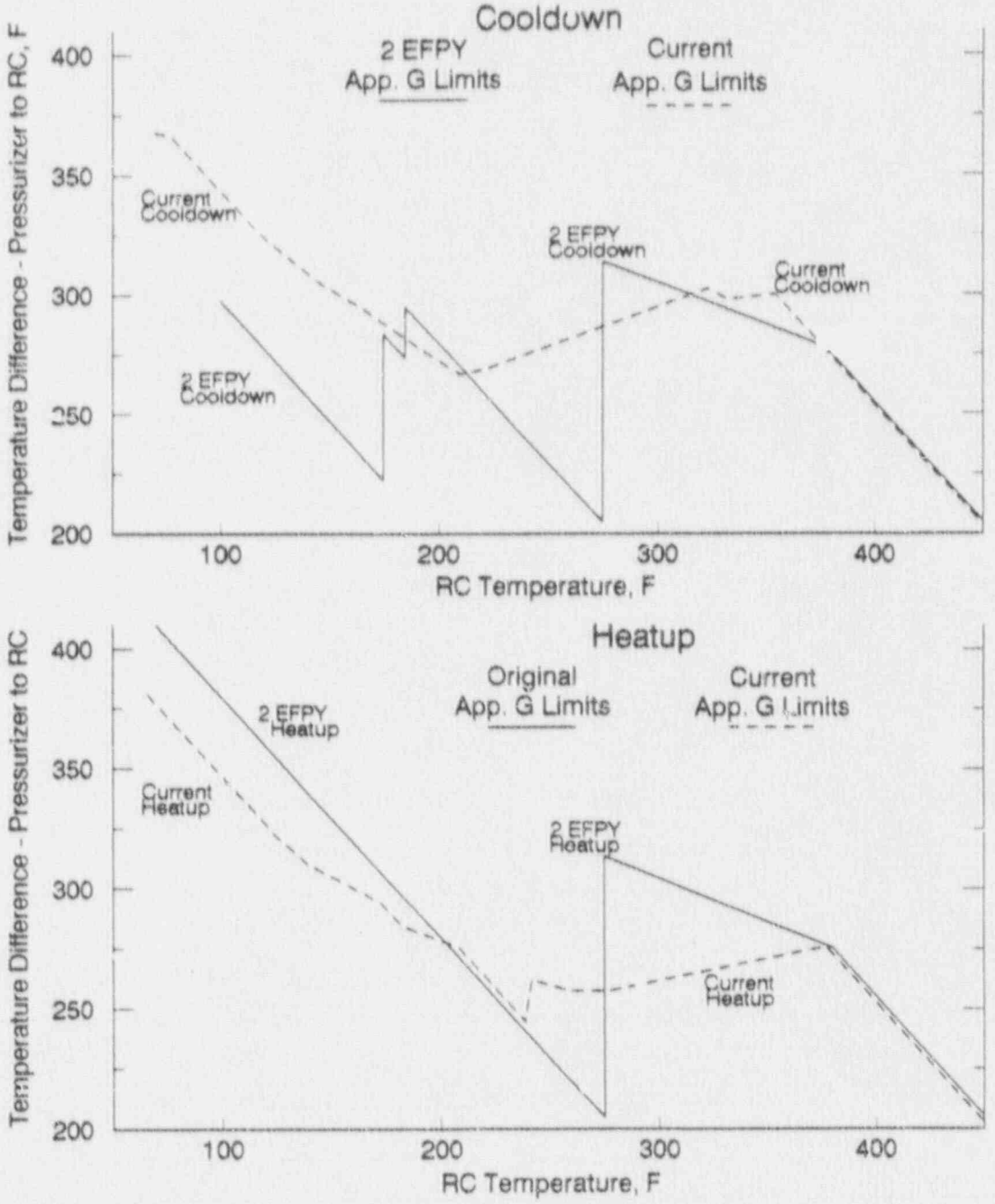

NOTES: 1) These curves were determined by taking a composite from the least restrictive (i.e.highest allowable) App.G pressures for the lowered loop plants.
2) Portions of the Appendix G limits are less restrictive than the original 2EFPY limits due to improvements in the analytical methods used to develop the limits. In spite of this, the Appendix G limits are expected to become more restrictive in the future. Consequently, the maximum pressurizer to RC temperature differences are expected to decrease.

3. GENERIC APPLICATION

Factors affecting surge line thermal stratification have been assessed to determine if the B&WOG plants can be evaluated generically. The assessment addressed two different types of factors: (1) those that are inherent in the equipment design and (2) the plant specific operating and surveillance procedures that may influence the surge line conditions. The following two subsections summarize these evaluations.

3.1. Comparison of Configurations

A review of the surge line piping for all B&W 177 fuel assembly plants shows that, with the exception of Davis-Besse Unit 1 (DB-1), all plants have the same nominal dimensions and configuration. The lowered loop and raised loop (DB-1) surge lines are shown in Figures 3-1 and 3-2, respectively.

The surge line for each configuration is constructed of 10" diameter schedule 140 austenitic stainless steel pipe (inside diameter 8.75") with a wall thickness of 1". The surge lines are insulated with a reflective/mirror insulation having similar characteristics for all B&W plants as tabulated in Table 3-1. The end nozzles connect the surge line to the hot leg and to the pressurizer. In the lower horizontal piping run, a one inch diameter nozzle made of austenitic material connects a drain line to the surge line. The drain nozzle itself (dimensions and material) is the same for all six lowered loop surge lines. The plant specific location of this drain nozzle is indicated in Figure 5-1 of this report.

With the exception of TMI-1, snubber restraints are positioned to restrain the surge line in case of a seismic event, and allow for pipe movement during design thermal cycles. The snubbers are placed at different locations along the surge line at each plant. As long as the snubber displacement is within the range of free travel, the effect on surge line stresses is negligible. The TMI-1 surge line does not contain any seismic snubbers, restraints, or supports.

At Davis-Besse Unit 1, a fixed pipe whip restraint construction is used at eight locations along the surge line. At each whip restraint location, an impact collar acting as a spacer is affixed to the pressurizer surge line. Free movement of the surge line is determined by preset gaps between shims, applied to the inside of the whip restraint, and the pressurizer surge line collar. Eight pipe whip restraints, one spring hanger, and three snubbers provide support for the surge line under the various design loading conditions.

Surge line pipe hangers are used only at the Davis Besse and Crystal River plants (these hangers are variable spring hangers). The surge line piping for the other B&W-177 plants is free hanging. Crystal River has three dead weight hangers located on the surge line. The available travel in the hangers is sufficient to prevent each one of these hangers from bottoming out. Therefore, the hangers have a negligible impact on the surge line stresses.

Other than nozzles at the pressurizer and the hot leg connections, the only other piping connection on the surge line is a one-inch drain nozzle located in the lower horizontal section. During the heatup, cooldown, and power operation of a lowered loop plant, this drain pipe is valved off and has no effect on the surge line response to surges.

Based upon an evaluation of the surge line configurations and plant operations, the lowered loop plants are sufficiently similar to be evaluated generically. However the differences between Davis-Besse Unit 1 and the lowered loop plants led to the decision to install special instrumentation at Davis-Besse to gather data during the heatup from the 6th refueling outage in the summer of 1990. Considerations leading to this decision are the following:

- The Davis-Besse surge line configuration differs significantly from the lowered loop plants. The lower horizontal run is somewhat shorter, and there is an upper horizontal run in excess of 20 feet compared to the 2.5 foot length in the lowered loop plants.
- The surge line at Davis Besse incorporates eight fixed pipe whip restraint structures, with impact collars clamped to the surge line. These impact collars interrupt the insulation, permitting gaps on either side. The increased heat loss potentially affects the degree of stratification.

- At Davis-Besse the power operated relief valve (PORV) inlet condensate drain is connected to the surge line drain upstream of the drain isolation valve. Condensate reflux into the surge line depends upon heat losses from the line, and could have some influence on the surge line stratification response.

The data from the special instrumentation at Davis-Besse are being used as the basis for a plant-specific stress and fatigue analysis which will be submitted as a supplement to this report.

3.2. Plant Operations

The plant operational aspects which affect the magnitude and number of thermal cycles applied to the pressurizer surge line have been evaluated in order to formulate the design basis cycles.

During the evaluation, the applicable plant operating procedures and plant data have been reviewed. In addition, plant operators have been interviewed at each plant. The results indicate that all of the B&W plants basically operate in a similar fashion with some minor differences. The focus of the operational review has been the heatup/cooldown and initial RCS pressurization phases, since the potential for significant thermal stratification conditions exists only during these phases.

During power operating conditions and during operating conditions wherein RCS temperature is near "Hot Standby" (approximately 530F) all of the plants operate in a similar fashion and the thermal stratification potential (pressurizer saturation temperature minus RCS hot leg temperature) is relatively small.

During design basis event transients, the transients imposed on the surge line are virtually identical for all of the lowered loop plants.

Since the reactor vessel operational P/T limits, in accordance with 10CFR50 Appendix G, provide the upper limit of the pressurizer surge line thermal stratification potential during the heatup/cooldown and initial pressurization phases, and these limits are a function of the effective full power years (EFPY) of operation, the magnitude of the thermal stratification gradients as well as the actual number of heatup/cooldown cycles have been grouped on the basis of the

periods of the applicable Appendix G limits. Actual plant data have shown that operation of the B&W plants has been below the reactor vessel P/T limits.

Plant data from the instrumented Oconee Unit 1 surge line as well as the installed pressurizer surge line thermocouple and pressurizer level data from each of the other B&W plants have been utilized to define the number and magnitude of thermal stratification cycles for the generic design basis.

Based on the P/T path taken by each of the plants during past heatups and cooldowns, the magnitude of future thermal stratification cycles was developed and has formed the basis for evaluating future surge line fatigue.

The design basis thermal stratification cycles developed for this evaluation are generically conservative in both number and magnitude. Recognition of the operational actions which produce such cycles will reduce the actual future cycles, in number and magnitude, to less than those which have been evaluated.

3.3. Conclusion

The lowered loop plant configuration and plant operations are quite similar and a generic development of design basis transients is justified. The number of occurrences of each type of generic transient will vary based on each plant's operating history.

Davis-Besse Unit 1, which is a raised loop B&W plant, requires a plant specific analysis due to the differences discussed in Section 3.1. The analysis for Davis-Besse Unit 1 will be addressed in a supplement to this report. The methodology described in this report is generally applicable to the Davis-Besse Unit 1 analysis. This includes the correlation of stratification and striping, the synthesis of design transients, the structural modeling techniques, the structural loading analysis, and the fatigue analyses of the surge line and its associated nozzles. Differences from the material contained in this report, due to plant specific structural and operating conditions will be identified and justified in the supplement containing the analysis for Davis-Besse Unit 1.

Table 3-1. Surge Line Insulation Comparison

PLANT	INSULATION MFG.	TYPE	THICKNESS	HEAT LOSS BTU/(HR-FT^2)
ANO-1	Transco	Reflective	3"	59-54
CR-3	Transco	Reflective	3.5"	57-61
DB-1	Diamond	Mirror	4"	74-86
OC-1	Diamond	Mirror	3"	74-86
OC-2	Diamond	Mirror	3"	74-86
OC-3	Diamond	Mirror	3"	74-86
TMI-1	Transco	Reflective	4"	55-79

Figure 3-1. Lowered Loop Surge Line Configuration

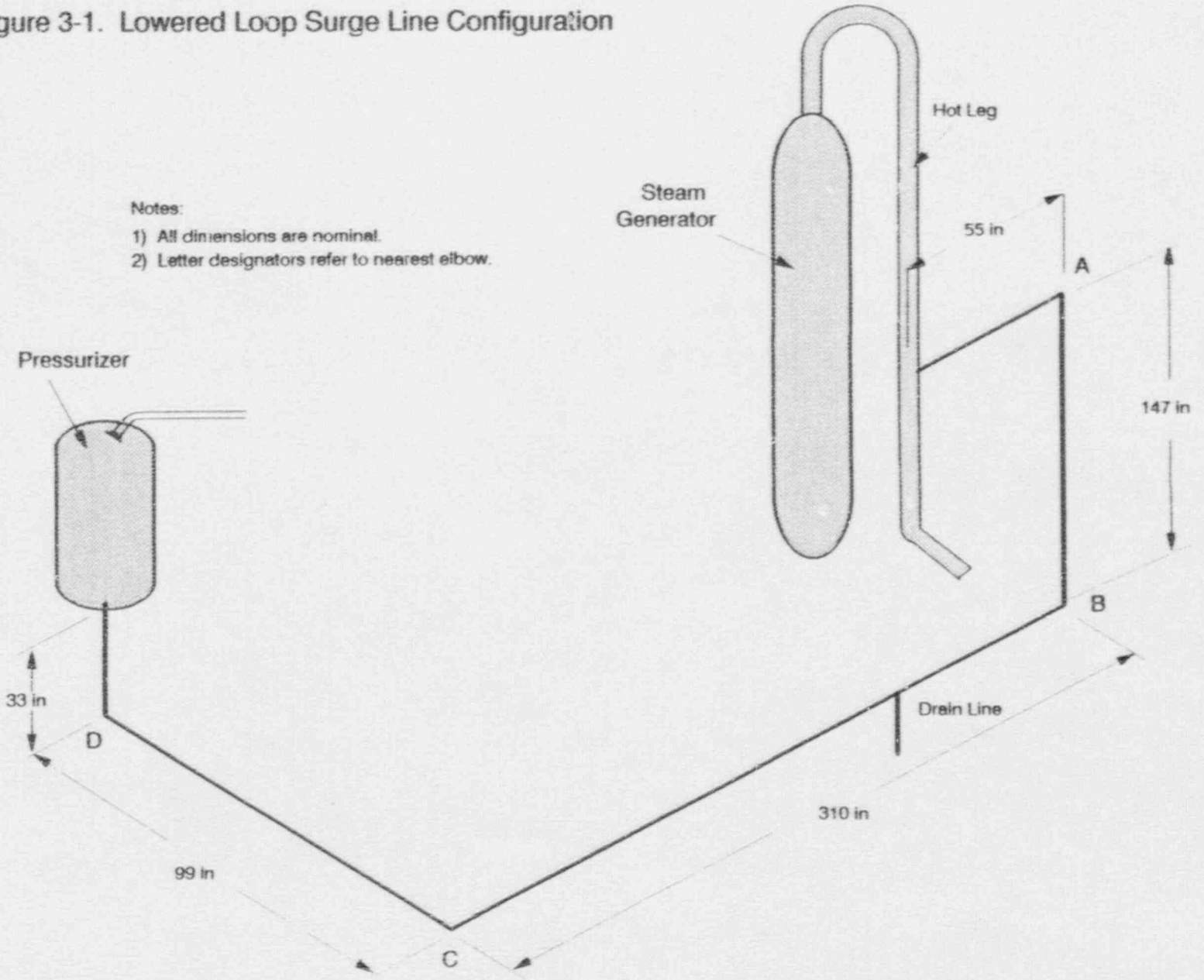

Figure 3-2. DB-1 Surge Line Configuration

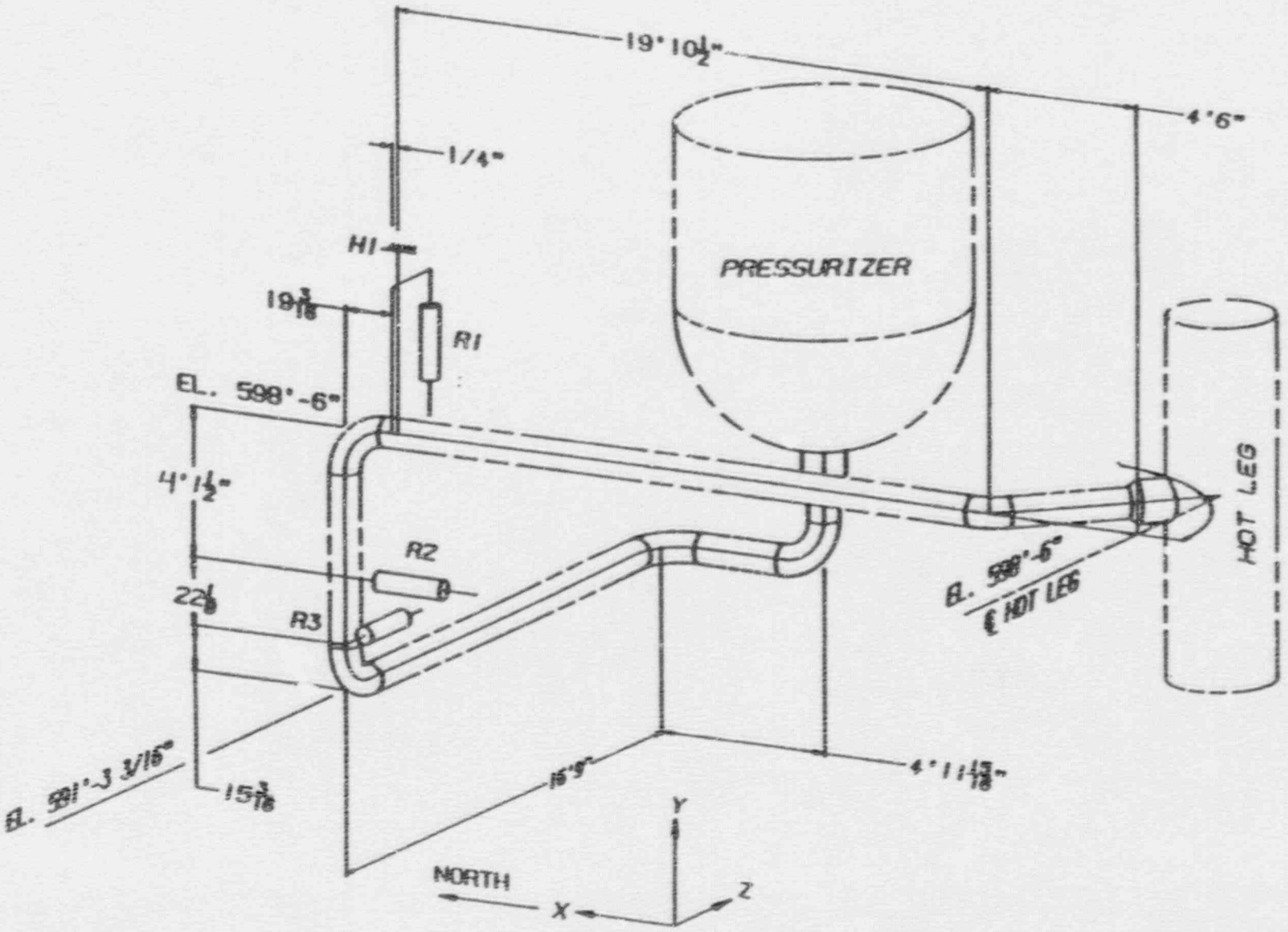

4. REVISED DESIGN TRANSIENTS FOR THE SURGE LINE

The purpose of NSSS design basis transients is to provide conservative thermal-hydraulic conditions for representative plant transients that are used in the structural analysis and fatigue evaluation of the reactor coolant system components. Transients described in the design basis include normal plant evolutions (such as heatup and cooldown), upset conditions (such as reactor trips), emergency events (such as rapid RCS depressurization following a steam generator tube rupture), and faulted events (such as a steam line break). Depending on the classification of the transient, various stress criteria must be met and demonstrated in the stress report for the NSSS components. For normal and upset transients, i.e. those that will occur during the normal course of plant operation, the fatigue of each NSSS component must be evaluated. The design basis transients provide the thermal-hydraulic input for the fatigue evaluations.

Typical parameters that are specified for each design basis transient include the applicable temperatures and pressures during the transient condition. Other parameters, such as the flow rate, are also specified to enable the determination of heat transfer coefficients from the fluid to the metal wall. In the case of thermal stratification, several additional parameters are of interest to the stress analyst. These include:

- Temperature difference from top to bottom of the surge line,
- Changes in the magnitude of stratification,
- Top-to-bottom cross-sectional temperature profile, and
- Location of the temperature interface between stratified fluid layers.

The development of the new design basis transients involved the following:

1. Measurement of surge line data at Oconee Unit 1,
2. Development of surge line stratification correlations,
3. Development of thermal striping correlations,
4. Review of operational histories, and
5. Formulation of new design basis transients.

Each of these areas is addressed in subsequent subsections.

4.1. Instrumentation of Oconee Unit 1

The original Reactor Coolant System instrumentation package in each B&W-designed plant included temperature detectors in the hot and cold legs of the reactor coolant loops, in the lower half of the pressurizer (i.e. the liquid space), and on the outside of the surge line. The single detector on the surge line is a thermocouple mounted on the lower horizontal run. The surge line thermocouple, generally mounted on the side of the pipe, is for use in monitoring for gross changes in surge line temperature such as those that might exist if the pressurizer spray bypass flow is stopped. However, this thermocouple measurement is not adequate for use in determining the existence of stratified conditions in the surge line.

Following comparisons of the as-built dimensions of the surge lines it was concluded that a single plant could be instrumented to provide typical data for thermal response under conditions of thermal stratification. Oconee Unit 1 was selected as the plant to be instrumented.

The objectives of the instrumentation program have been to determine:

- The magnitude of the thermal stratification including the maximum top-to-bottom piping temperature differential,
- Variations in the thermal stratification with axial position along the surge line,
- The changes in surge line displacement that result from thermal stratification,
- The plant operations that cause thermal stratification cycles, and

- The temperature response of the surge line to pressurizer level changes.

To meet the above objectives, a comprehensive instrumentation package was prepared including 54 thermocouples mounted on the outside circumference of the surge line and 14 displacement instruments affixed to various parts of the line. The thermocouples and displacement instruments were connected to a data acquisition system allowing continuous monitoring of all instruments. The system also recorded numerous permanent plant computer signals which have provided data for the determination of changes in RCS conditions that affect the surge line flow rates. Details of the instrumentation and the data acquisition system are included in Appendix A.

The instrumentation package and data acquisition system were installed during the refueling outage of January 1989. Data were recorded as the plant prepared for and went into its normal heatup in early February. There was no interference with normal plant operations and no changes to procedures were made to accommodate the data acquisition or to reduce the effects of potential thermal stratification. Data were recorded throughout the heatup, power escalation, and for several days at full power.

The Oconee data clearly show that thermal stratification develops after the pressurizer is heated in preparation for starting the first reactor coolant pump. Thermal stratification cycles of varying magnitude occurred throughout the heatup and power escalation. Figure 4-1 is a sample of the data from the February 1989 heatup. The correlation between pressurizer level changes and the surge line temperature response is easily seen. The quantification of this and other relationships is the next step in the preparation of revised design basis transients. This quantification has been viewed as an essential element of the overall program since no two plant evolutions will occur in exactly the same way. A means to predict the surge line conditions for any given event, based on the RCS parameters and plant conditions, is needed. The next subsection addresses the development of the surge line correlations based on Oconee Unit 1 data.

4.2. Thermal Stratification Correlation

Stratification correlations have been developed from plant surge line temperature measurements recorded at Oconee Unit 1. The plant measurements cover a wide

range of system conditions and evolutions, including power operation, heatup, cooldown, pump starts and stops, and spray. Stratification correlations have been developed for each of the key surge line locations. These correlations have been based on observed temperature responses to changes in surge line conditions; they have been adjusted as necessary to ensure that the predictions are conservative as well as realistic. The temperature differences predicted by these correlations have been compared to the observed temperature differences. The same coding used to generate these predictions has also been used to analyze the synthesized plant transients, to produce revised design basis thermal transients for the surge line analysis. The following sections provide additional information regarding the plant measurements, the development and refinement of the prediction correlations, and their performance.

A number of assumptions are implicit in the development of the stratification correlations. Principal among them is the application of outside-wall temperature measurements to predict inside-wall temperatures. The time constant of the surge line pipe wall is on the order of four minutes (and varies with the convective heat transfer coefficient). Therefore, rapid temperature fluctuations occurring at the inside surface are attenuated at the outside measuring surface. (Indeed, the high-frequency fluctuations associated with thermal striping are not observable at the outside wall.) The extreme temperature changes of greatest interest in stress analyses generally develop over relatively long periods, equivalent to many pipe wall time constants. Therefore, the application of outside measurements to predict inside-wall stratification is acceptable.

4.2.1. Plant Temperature Measurements

Plant surge line temperatures have been recorded at nine cross sections spaced throughout the line, as shown in Figure 4-2. At each of the six instrumented cross sections in the horizontal piping runs, from 5 to 10 thermocouples were distributed circumferentially to provide complete coverage of temperature profile across the height of the pipe. Temperature measurements were recorded at either 20-second or 1-minute intervals.

The following three sets of data have been selected for this analysis:

1) Power operation of 19 Sept 89,

2) Cooldown beginning 22 Sept 89, and

3) Heatup beginning 02 Oct 89.

These data sets span a wide variety of plant conditions and evolutions. The power-operation data include a reactor coolant pump trip. The cooldown data span a period of three days of operations. It includes pump trips and the actuation of both regular and auxiliary pressurizer spray. The third data set, the October heatup, spans approximately one week. The plant was initially cold, with no pumps running. Data recording continued through the intermittent operation of the reactor coolant pumps, heatup using pumps, and power escalation. A period of pressurizer recirculation is also included with pressurizer heaters manually energized and pressurizer spray control in automatic.

The acquired plant data has been extensively cross-plotted and compared. The temperature distributions at each cross section, the sequential response of temperature versus location in the surge line, and temperature responses to insurges and outsurges, confirm the sensitivity and self-consistency of the surge line temperature measurements.

4.2.2. Processing the Measurements

The measured t eratures at instrumented cross sections have been used to estimate the elevation of the current, local, average temperature, as well as the elevations at which the local temperature reaches one-fourth and three-fourths of the differential from the lowest local temperature to the highest. These elevations provide indications of the location and vertical extent of the thermal interface. The top-to-bottom temperature difference has also been obtained as a function of time.

The top-to-bottom temperature differences at each measurement section in the horizontal piping runs and time have been compared to determine the overall maximum temperature difference versus tim (the vertical piping runs were observed to be approximately isothermal). With the exception of the short horizontal run at the hot leg, the local temperature differences among the several measurement locations have been within 20% of each other. The

temperature difference at location 11, approximately midway in the horizontal run nearest to the pressurizer, has generally been observed to be slightly larger than the temperature difference at other locations. Therefore, the top and bottom temperatures at location 11 have been used for subsequent comparisons of predictions to observations.

The overall maximum observed top-to-bottom temperature difference has been processed further to identify the most limiting stratification cycles. First, the times and temperatures at which the time-rate-of-change of the maximum temperature difference changed sign have been identified. These arrays of extreme temperature differences and times have been analyzed using the Ordered Overall Range method of cycle counting developed by Fuchs et al (reference 4). For a specified threshold temperature difference, the Ordered Overall Range method has identified those large and small temperature differences (commonly referred to as "peaks" and "valleys", or "PVs") which are significant in terms of stress. These results have been compared to the significant PVs which have been predicted rather than measured, as discussed in the following subsection.

4.2.3. Development of the Prediction Correlations

Correlations have been developed to predict plant surge line temperatures versus time using the following global plant conditions:

- System pressure (or saturation temperature)
- Hot leg temperature
- Pressurizer level (or surge line flow rate)
- Reactor coolant pump operating status
- Spray valve status

A prediction correlation has been developed for each temperature of interest. As mentioned previously, the top-of-pipe and bottom-of-pipe temperatures at location 11 (see Figure 4-6) have been of primary interest for stratification in the horizontal piping. Predictions have also been developed for the measurement locations nearest the hot leg-to-surge line nozzle and the pressurizer nozzle, to provide estimates of the fluid temperatures at these nozzles.

The measured surge line temperatures often respond to an insurge or outsurge in a decaying exponential fashion. They have also exhibited threshold surge line flow rates below which they are unresponsive, and time delays before they begin to respond. Therefore, the prediction correlations have consisted of the corresponding four temperature characteristics, as follows:

- Threshold,
- Time delay,
- Final temperature, and
- Time constant.

The threshold flow rate and time delay are self-explanatory. The final temperature and time constant are combined to describe the decaying exponential temperature change from the initial temperature to the final temperature; the time constant is the elapsed time required for the fractional temperature change to approach the total temperature change by a factor of $(1-e^{-1})$.

The prediction correlations also identified the "mode" of current surge line conditions -- insurge, outsurge, or bypass. Spray and pressurizer-recirculation modes are also assigned. The bypass mode is the default mode, and is used when no other mode of surge line conditions is currently active.

The prediction correlations have been developed by examining brief periods of data when the observed surge line temperatures appear to be responding to a single or predominant event, such as the outsurge associated with a reduction of pressurizer level. The apparent time constant and final temperature have been estimated. These parameters have been estimated for several intervals, at a variety of plant and surge line conditions, and have been combined to form the basic prediction correlations. These correlations are based on calculated surge line flow rates obtained from changes in pressurizer level and do not require knowledge of specific operations occurring in the plant.

Preliminary correlations based on identifiable discrete events have been refined and adjusted in two steps. First, the predicted temperatures have been compared to their observations. The temperatures predicted were adjusted as required to ensure the predictions are realistic but conservative. The prediction of the top-of-pipe temperatures have been skewed to render them slightly more responsive

than observed, and the bottom-of-pipe predictions have been adjusted to make them slightly cooler, and less responsive, than observed.

The final adjustments have been based on the predicted versus observed significant temperature differences.[1] As was done for the observed (maximum) temperature differences, the top-to-bottom differences of the predicted temperatures have been processed to yield the extreme differences (PVs), and the differences which are significant in terms of stress (the significant PVs). The predicted and observed significant PVs have been compared over each of the data sets and evolutions. The prediction correlations have been adjusted, if necessary, to yield conservative but realistic predictions of the significant PVs. The hot/cold fluid interface elevations have been predicted and compared to the observations in a similar fashion; the predicted interface elevations have been skewed towards the centerline of the pipe for conservatism.

Figures 4-3 and 4-4 demonstrate the predicted and observed temperatures and temperature differences at location 11, during the period containing the overall extreme PV.

4.2.4. Application of the Correlations and Conclusions

The stratification correlations have been used to process the synthesized plant transients, described later in Section 4.5. The coding used to compare the predictions to observations has also been used for processing the synthesized plant transients to generate revised design transients for surge line analysis.

The stratification correlations provide predictions which are appropriate for surge line stress analyses. The stratification correlations have been developed from plant data spanning a wide variety of conditions and evolutions. The correlations are responsive to basic surge line conditions, rather than to the

---

[1]The "significant" temperature differences in the comparisons of predictions to observations were the results of the Ordered Overall Range method of cycle counting. This method identified those PV-pairs which were of the proper time sequence and which defined a temperature change greater than the specified threshold. For the comparisons of predictions to measurements, this threshold was set to obtain a number of PVs suitable for comparison. When the predictions were applied to synthesized plant transients, as described later herein, the counting threshold was set to identify those PVs which were of significance to stress or fatigue. The fatigue analysis has shown that thermal cycles occurring with a temperature difference greater than 50F must be accounted for.

specific type of plant evolution. Finally, the stratification correlations provide realistic but conservative estimates of the extreme surge line stratification conditions.

4.3. Thermal Striping

Surge line striping has been estimated using a correlation of experimentally-observed striping and is based on the "TEMR-PWR" experiments performed at Battelle Institute, Karlsruhe, FRG. These experiments have been performed at plant-typical fluid conditions and used large-diameter, horizontal, insulated, metal pipe which is characteristic of the horizontal piping runs of PWR surge lines. The acquired experimental data has been self-consistent; moreover, it provided adequate temperature versus time definition of the high-frequency, localized thermal-hydraulic interactions which characterize striping. The temperature data have been processed to determine interface characteristics as well as striping frequencies and amplitudes. The interface information has facilitated the interpretation of the observed striping variations among tests. The maximum striping amplitude has been correlated with the governing fluid conditions, as has been the distribution of striping frequency versus amplitude. These striping efforts are described below; Appendix C provides a summary of the striping literature and a description of the Battelle experiments.

4.3.1. Selection of the Battelle Striping Data

There are four major sources of striping information:

- Boiling Water Reactor (BWR) feedwater nozzle tests,
- Liquid Metal Fast Breeder Reactor (LMFBR) tests,
- Argonne National Laboratory (ANL) tests, and
- Battelle-Karlsruhe tests (HDR).

The BWR feedwater nozzle striping tests results (reference 5) were quite extensive. The associated studies demonstrate the ability to combine low-temperature test data with high temperature test data and with plant striping data. The application of these results illustrate the use of probability distribution functions. But the geometry and hence the striping interaction of the feedwater nozzle are not like those of the surge line, therefore these results are not applicable to the surge line.

Woodward (reference 6) has investigated striping and stratification in a 1/5-scale model of an LMFBR. The temperature fluctuations in transparent, horizontal pipes have been examined using dye and thermocouples. Results were based on inside diameters of 4 and 6.5 inches, and hot and cold fluid temperatures of approximately 130F and 70F. Woodward references the experimental work of Fujimoto et al (reference 7) for a fluid-to-wall heat transfer coefficient. The Fujimoto tests also pertain to low temperature conditions, but employ the addition of calcium chloride to the warmer fluid stream to obtain plant-typical differences of fluid densities. (The fluid temperatures were used simply as tracers of the streams of differing densities.)

Kasza et al, at ANL (references 8 through 10), have conducted extensive tests of stratification and striping. Combinations of horizontal and vertical piping runs have been tested, including bends in both the vertical and horizontal planes. These tests also employed the relatively low bounding fluid temperatures of the tests previously mentioned. Kasza et al have published a limited amount of power-spectral-density information for striping; the reported signal energy peaks between 0.1 and 0.6 Hz, and decays exponentially with increasing frequency.

Wolf et al (references 11 through 15) have also conducted extensive experimental studies of stratification and striping in the HDR facility at Battelle Institute, Karlsruhe, FRG. Unlike the other experimental efforts, the HDR tests were performed in a large-diameter, insulated, metal pipe using plant-typical fluid conditions. The pipe was extensively instrumented with fast-response thermocouples.

The thermal-hydraulic conditions governing striping (buoyancy, inertia, and viscosity) are the appropriate bases on which to compare the several striping tests discussed above. High-frequency fluctuations of wall temperature, namely, striping, are due to rapid undulations of the fluid thermal interface -- the relatively narrow zone between fluids of dissimilar temperatures and densities. These undulations are commonly caused by the interactions among the fluid buoyant, viscous, and inertial forces. Buoyancy tends to stratify the fluid, whereas the fluid inertia and viscosity tend to mix the fluid and to disrupt stratification. These competing effects give rise to interface instabilities.

The interacting fluid forces are conveniently quantified in terms of two dimensionless ratios of fluid forces. These are the Reynolds number, which is the ratio of inertial to viscous forces, and the Grashof number, which is the ratio of buoyant to viscous forces. A third dimensionless ratio is commonly used to gauge the presence and significance of stratification, and has also been extensively referenced in studies of interface instabilities. This is the Richardson number, which is the ratio of buoyant to inertial forces.

The LMFBR, ANL, and HDR tests previously mentioned have been compared on the bases of these governing force ratios, in Figure 4-5. The Reynolds number is readily varied experimentally, but the Grashof number is more intractable. It includes the difference between the bounding (hot and cold) fluid temperatures, and the fluid thermal expansion coefficient. In a low-pressure facility, the maximum temperature difference is limited. Similarly, the thermal expansion coefficient of water is a strong function of temperature; it increases almost threefold going from 200F to 500F. The low-pressure facilities are again limited in this regard. Thus the Grashof numbers of the low-pressure tests are far below those obtained at plant-typical conditions. Only the HDR tests by Wolf et al lie in the appropriate range. For this reason, the HDR data has been selected for use in this investigation of surge line striping.

4.3.2. Data Checks

Thermal stratification and striping in a horizontal line were examined by Wolf et al in the "TEMR" series of tests. Multiple temperature measurements have been made in a 20-foot long horizontal section of 15.6-in inside diameter pipe (Figures 4-6 and 4-7). Three subseries of TEMR tests were distinguished by differing obstructions placed at the junction of the pipe with the reservoir of hot fluid. The junction was left unobstructed in the "PWR" subseries of tests; these tests are considered to be the most relevant to the surge line geometry, therefore the "PWR" tests have been examined.

The complete test measurements have been obtained. These consisted of hundreds of measurements processed at 10 Hz, for tests ranging up to 1000 seconds in duration. The acquired data has been subjected to rudimentary tests as it has been transferred to the analysis computer. Each temperature reading has been scanned for out-of-range measurements, and each signal has been checked to verify

that it did not remain constant throughout a test. Offending temperature measurements have been set to negative infinity, to prevent their processing and plotting.

The vast majority of the instruments and readings have passed these checks. The few temperature readings and instruments which failed these tests have generally corresponded to those which had been identified as suspect by the experimenters, in their test report (reference 16). Two sets of temperature measurements contained out-of-range readings, both in Test 33.14. The earlier failure occurred just after 640 seconds of an 872.7-second test, therefore data processing has been interrupted at 640 seconds with little net impact on the ability to draw conclusions from this test.

Each of the tests was initialized with the pipe hot and isothermal, providing a convenient cross-check of all the temperature measurements. The tests were initiated by introducing cold water at the bottom of one end of the horizontal pipe -- the responses to this cold stream provided another straightforward check of thermocouple response. Finally, the thermocouples were spaced sufficiently closely in the circumferential direction that multiple adjacent thermocouples often responded to the passage of an individual interface undulation, as demonstrated in Figure 4-8.

The temperature measurements consisted primarily of thermocouple triplets -- these measured the temperatures of the fluid near the wall, of the inside wall, and of the outside wall. Several cross-sections of the pipe were instrumented. At the most-heavily instrumented cross section, the thermocouple triplets were placed every 2-1/2 angular degrees near the mid-height of the pipe, from 90 to 105 degrees, increasing to 30-degree spacing at the top and bottom of the pipe.

4.3.3. Interface Calculations

This investigation of striping depended on the response of individual thermocouples, and hence on there being a temperature measurement within the thermal interface, which is the region of steep temperature gradients and maximum striping potential. The striping calculations have been preceded by an examination of the characteristics of the thermal interface, in particular the proximity of this interface to the installed thermocouples.

The thermal interface has been characterized using three fractional temperatures, "T1", "T2", and "T3". Fractional temperature T1 has been defined as the coldest local fluid temperature plus one-fourth of the difference between the hottest and coldest local temperatures; similarly, T2 has been defined to be one-half of the way from the coldest to the hottest temperature, and T3 has been defined to be three-quarters of the way. The definition of these fractional temperatures is somewhat arbitrary -- they could have been assigned other fractional values, for example. They have simply been defined as convenient intermediate temperatures. The elevation of the average temperature (T2) is approximately located at the center of the interface, and the difference between the elevations of T3 and T1 indicated the vertical extent of the (half-) interface. The elevations of the fractional temperatures have been extracted from time-smoothed data.

At two measurement cross-sections and each time of measurement, each group of measurements from three adjacent thermocouples which bracketed a fractional temperature has been curve fit using a second-order relation of temperature to (thermocouple) elevation. This relation has been solved for the elevation of the corresponding fractional temperature. The elevations "Z1", "Z2", and "Z3" of the corresponding fractional temperatures demonstrated interface development and stabilization in each test. Comparisons of the interface location and thickness among the tests have permitted their correlation in terms of the governing fluid forces. More importantly, the elevation of the stabilized interface has been compared to the thermocouple elevations, to identify those tests in which the observed striping most closely corresponded to the actual maximum striping.

4.3.4. Correlation of Striping Calculations

The recorded temperatures provided good definition of the temperature trends, but slightly underestimated the extreme temperatures. The actual extreme temperatures are estimated by solving for the zero-slope point of the second-order fit to the three temperature measurements bracketing the apparent extreme. The results of these estimates are illustrated in Figure 4-9.

The Ordered Overall Range method of Fuchs et al (reference 4) has been used to count striping cycles. Counting has been performed separately for each inside-wall thermocouple at the three instrumented cross sections. Counting focused on the relatively stable period which followed the initial realignment of

temperatures and interface development. The stable period has been counted both overall and by halves, to provide a gauge of self-consistency. For each instrument and counting period, the counting threshold has been decremented from the highest threshold, which just passed the difference between the most extreme temperatures throughout the period, down to a minimum threshold. The cycles counted at each threshold, divided by the counting interval, formed the so-called "cumulative frequency of occurrence". This is the rapidity at which temperature changes larger than the threshold have been observed. The distribution of these cumulative frequencies of occurrence versus striping amplitude formed readily-correlated relations.

The maximum striping amplitude for each test has been compared and correlated with the governing fluid conditions. The maximum striping amplitude of each test has been indexed according to the proximity of the thermal interface to the measurement thermocouples. Generally, the largest striping amplitudes over a range of governing conditions have been observed when the interface bracketed a thermocouple, and vice versa. The correlation of maximum striping amplitude versus governing conditions has been constructed to reproduce these largest-amplitude points. The maximum striping amplitudes of the final correlation have been increased by 10% (of the imposed temperature difference) to allow for residual uncertainties. Finally, the frequency-versus-amplitude distributions obtained by Kasza et al (reference 10) have been consulted to check the correlated trends at the highest frequencies; the decreasing amplitudes at higher frequencies-of-occurrence have been confirmed by the distributions obtained by Kasza et al.

4.3.5. Conclusion

Stratification and striping information have been extracted from the HDR data, and correlated with the governing fluid forces. The HDR data is singular in that it alone was taken at conditions typical of the plant surge line. The experimental data has been found to be self consistent. The HDR data was taken over a fairly broad range of fluid conditions. Moreover, the striping correlations have been based on the ratios of governing fluid forces, rather than fluid properties. Therefore, these correlations provide useful estimates of striping over the expected range of plant evolutions and surge line conditions.

The striping correlations can be used with confidence to predict striping effects in the plant surge lines.

4.4. Review of Operational Histories

The revised design basis transients are intended to represent the operational history of the plants and to bound future transients. Hence, past operational information is required to generate revised transients. An information base which includes plant operating data, operating procedures, surveillance procedures and operational limits has been collected from utility and BWNS records. In addition, discussions with plant operators have provided records of first hand experience.

Representative operational data for sixteen heatups and fifteen cooldowns have been supplied by the plant utilities. The parameters provided include:

RC Temperature (Hot leg and Cold leg)
RC Pressure
Pressurizer Temperature
Pressurizer Level
Makeup flow rate
Letdown flow rate
Surge Line Temperatures (original thermocouple)
RC flow
RC spray valve status (open/close)
Steam Generator Pressures
Steam Generator Levels

The data for these parameters provide the general bases for describing heatup and cooldown design basis transients.

In conjunction with the plant data review, operation and surveillance procedures have been reviewed to identify events that might cause stratification cycles. In deciding whether or not generic design basis transients are appropriate, operational procedures have been reviewed for differences. It has been determined from the surveillance procedure review that valve testing involving RCS inventory changes has been the most significant type of surveillance procedure in terms of thermal cycling of the surge line. As a result of this review, Transient 22 of the design basis transients has been revised to account for HPI check valve testing. The operating procedures have been used to determine the major flow events to be accounted for in the heatup and cooldown

transients. Random flow events have also been added to ensure that all pressurizer level changes observed in the plant data are taken into account.

All applicable pressure-temperature (P/T) limits and requirements have been collected to determine the bound of operation for heatups and cooldowns. These pressure-temperature limits and requirements are comprised of 10CFR50 Appendix G limits, decay heat removal system (DHRS) limits, Net Positive Suction Head (NPSH) requirements for RC pumps, minimum sub-cooling pressure requirements, and fuel compression limits. The actual pressure-temperature history indicated by the historical heatup/cooldown data and the Appendix G limits has been used to create both representative and bounding pressure-temperature relationships for the heatup and cooldown transients.

4.5. Development of Revised Design Basis Transients

The revised surge line design basis include the transients listed in Table 4-1. It is the redefinition of the surge line conditions for these transients that forms the bases for reanalysis of the structural integrity of the surge line piping and its associated nozzles.

The greatest impact of stratification and striping occurs during conditions when the temperature difference between the pressurizer and the RCS hot leg is large. The largest temperature differences occur during plant heatup and cooldown. These transients contribute most of the cumulative fatigue usage for the surge line piping. Therefore an extensive effort has been made to develop detailed descriptions for these plant evolutions. The design basis plant heatup and cooldown transients have been completely redefined in this program. Other transients included in the design basis have generally been retained in terms of the existing surge line boundary conditions (pressurizer temperature, RCS temperature and flow rates), but thermal stratification and striping have been included in the surge line transient descriptions.

Typical variation of RC hot leg temperature as a function of time has been determined for heatup and cooldown transients based on plant data. The pressurizer pressure variation is based on pressure-temperature (P/T) relationships, both the 2 EFPY P/T limit and available plant data. Pressurizer temperature has been developed as a function of RC temperatures from the P/T relationships.

The Oconee design basis differ from the current design basis for other plants in that the Oconee design basis include different heatup rates. For the purposes of this evaluation, these heatup rate differences have been disregarded and the time for heatup has been set at one conservatively long period for the heatup events. The various heatup rates given in the design basis are important for the major components, i.e., reactor vessel and steam generator, but are not necessarily conservative for description of the surge line conditions.

Operational events that affect surge line flow during heatup and cooldown have been identified by a review of plant data, operating procedures, and surveillance test procedures for the lowered loop plants. Surge line flow rates resulting from these operational events have been characterized using available plant data, analysis, and engineering judgement. All operational events which affect RCS inventory, volume and spray flow are included. The number of surge events per plant transient and time between occurrences have been estimated for each significant type of event affecting the surge line flows. Random surge line flow events have been included to ensure that the total number of surge events corresponds to the number based on plant data.

Composite heatup and cooldown transients with an appropriate sequence of events, timing, and surge line flows have been generated. The total number of surge line flow events for each type of transient has been described and categorized according to severity in terms of pressurizer to RC temperature differences. Probable past operations and the projected improvements in operations affecting surge line conditions have been taken into account in defining the heatup and cooldown transients. The correlations discussed in Section 4.2.2 and 4.2.3 have been used to generate the surge line thermal response to the flow events.

The number of occurrences for each type of heatup and cooldown transient are based on operational records and on the total number of heatups and cooldowns stated in the original design basis. The original design basis assumptions for the number of occurrences for the other transients has generally been retained.

The following sub-sections describe the detailed development of the heatup, cooldown, and other events.

4.5.1. Heatup Transients

4.5.1.1. Heatup Transient Descriptions and Number of Occurrences

Heatups are categorized into five transients (Transients 1A1 - 1A5) in order to conservatively represent plant heatup transients occurring during the 40 year life of the plant. The RC and pressurizer temperatures for these transients are shown in Figure 4-10. A heatup transient is defined as the operations from a RC temperature of 70F to 8% power. The first three transients (1A1, 1A2, and 1A3) represent past operations and the last two transients (1A4 and 1A5) represent future operations. The surge line flow events occurring during the heatup have been defined to be identical for all five types of transients; however, the RCS and pressurizer temperatures vary. The development of these transients is represented by the schematic in Figure 4-11 and is discussed below.

Transient 1A1 — This transient has been conservatively defined to bound past plant operations in terms of the maximum possible pressure in the RCS. The resulting surge line temperatures are shown in Figure 4-12. For these heatups, core decay heat has been assumed to heat the RCS to 120F prior to the operator achieving the pressure necessary for starting an RC pump. Pressurizer temperature is based on the pressure-temperature relationship defined by the 2 EFPY Appendix G limit.

Transient 1A2 — The RC temperature for this transient represents heatups in which decay heat has not been available for initial heatup and the RC pumps were started with an RC temperature of 70F. The pressure-temperature relationship for this transient represents the fraction of plant heatups which have occurred with a higher than average RC pressure for given RC temperatures based on plant historical data.

Transient 1A3 — This transient represents typical plant heatups for the past operating history of B&W lowered loop plants. Decay heat has been assumed available for these heatups and the RC temperature has been assumed to be 120F at the time the pressure required to start the first RC pump has been reached.

The pressure-temperature relationship for this transient is representative of historical plant data.

Transient 1A4 — The RCS temperature as a function of time represents the heatups for which decay heat will not be available for the initial portion of the heatup. The pressure-temperature relationship has been based upon plant data in which the pressure required for the first RC pump start was reached at an approximate RC temperature of 70F. The pressure-temperature limits discussed in Section 8 will help ensure that this basis remains valid for future heatups.

Transient 1A5 — The RCS temperature as a function of time represents the heatups for which decay heat will be available for the initial portion of the heatup. The pressure-temperature relationship *has been based upon plant data in which the pressure required* for the first RC pump start was reached at an approximate RC temperature of 120F. The pressure-temperature limits specified in Section 8 will help ensure that this basis remains valid for future heatups.

Some plants do not start RC pumps until a higher RC temperature than those represented in the transients (>120F) is obtained. The pressurizer to RC temperature difference for these heatups is usually lower due to a lower system pressure for RC temperatures. To conservatively represent all lowered loop B&W plants, the transients are described with RC pump starts at RC temperatures at 70F and 120F.

The number of occurrences for each type of heatup transient, tabulated for each lowered loop plant in Table 4-2, has been determined using utility records and plant data as the schematic shows in Figure 4-13. The number of Transient 1A1 events has been obtained by taking a conservative estimated fraction of the total number of heatup events occurring over the first two years of operation and an equivalent number of heatups that occur during hot functional tests. The remaining fraction of events occurring over the first two years are grouped with the events that have been distributed between Transients 1A2 and 1A3 based on plant experience to date. Based on plant data, approximately 15% of these past

heatup events are categorized as type 1A2. The remainder of events are included in type 1A3. For future events, approximately 15% are categorized as type 1A4 and the remainder of design events are included in type 1A5.

4.5.1.2. Maximum Pressurizer-to-RCS Temperature Difference

A maximum stratification temperature differential has been specified for a small fraction of the total number of design transients to account for operating conditions in which the system pressure corresponds to the maximum allowed by the 2 EFPY P/T curve (Transient 1A1). It has been assumed that the RCS temperature reached approximately 80F at the time the pressurizer temperature reaches 480F (saturation temperature for the pressure limit of 565 psia at RC temperatures below 275F). The resulting temperature differential between the pressurizer and the RC loop of 400F is considered to be a realistic, conservative upper bound for this temperature difference. Although lower RC loop temperatures are possible during typical heatup operations, it is considered very unlikely that the simultaneous occurrence of lower RC loop temperatures with RCS pressures approaching the RCS P/T limits has occurred at any plant. The maximum value of stratification (surge line top to bottom temperature difference) that resulted for the revised surge line design transients is 397F.

4.5.1.3. Boundary Temperatures as a Function of Time

The RC temperature versus time for the revised heatup transients is similar to the existing transients contained in the original design basis except that the duration of the heatup has been extended to be more representative of actual plant operations. Temperature holds have been added and heatup rates adjusted to give reasonable agreement between the heatup for analysis and the available plant data. The pressurizer temperature versus time plots for Transients 1A1 through 1A3 have been developed based on the relationship of pressurizer temperature to RCS temperature corresponding to available plant data. Transients 1A4 and 1A5 represent future operations based upon B&W Owners Group recommendations for plant operation discussed in Section 8.

The time for heatup is based on actual plant experience, which shows average heatup times of approximately 60 hours. The surge line analysis conservatively

assumes each heatup requires 75 hours. The time durations for each portion of the heatup have been developed from available plant data for the following:

RC loops cold (<100F), pressurizer hot (>200F)
Heatup operations (RCS temperature increase)
RCS held at constant temperature throughout all modes
Hot, zero power
Power Escalation 0 to 8%

4.5.1.4. Surge Line Flow Rates for Heatup

Changes of flow of pressurizer or hot leg fluid through the surge line leads to thermal stratification transients. Unlike the RCS and pressurizer temperature relationship, direct operator guidance does not exist for pressurizer level control. Procedures and operations have changed over the years with some changes decreasing the number and magnitude of surges while others have increased this number. It is not possible to describe every plant event that influenced the surge line flow rate and consequently the effects on the thermal transients for the surge line piping and nozzles. However, by supplementing the major flow events with random flow events, a typical heatup transient has been generated which realistically represents the number and magnitude of surge flow events.

Each heatup transient case (Transient 1A1 - 1A5), has been assumed to have the same flow events. On the average, these transients represent the typical operations occurring during the life of a lowered loop plant. The five heatup transients differ in the relationship between RCS and pressurizer temperature as discussed in Section 4.5.1.1.

Typical plant heatup operations that may affect the makeup flow to the RCS are listed in Table 4-3. The operations that have been judged as significant and quantifiable are considered the major events which have been accounted for in the transients. RCS temperature changes affecting RCS inventory are accounted for in addition to events such as RC pump starts, certain surveillance tests, and venting operations. The response of makeup flow rate to each of these events is accounted for in the development of the transients.

Transient surge line flow events found in Oconee and other plant data from unidentifiable causes have been incorporated in the design transients as random events. The available plant data has been statistically analyzed to characterize

the random flow events in terms of flow rates and changes in pressurizer level. To accomplish this, the following steps have been taken:

1) Plant heatup data have been evaluated to determine the average and standard deviations for pressurizer level changes (inches) and flow rates during operation over various ranges of RCS operating temperatures. Also, the average number of flow events has been determined for the heatup operations.

2) The average number of flow events has been adjusted so that the number of events per unit time is consistent between the prescribed heatup length and the data.

3) The number of random flow events has been determined by taking the total number of flow upsets derived from the plant data less the number of defined flow events.

4) Flow change data have been treated as a normally distributed, random variable and divided into three ranges based on the normal distribution curve. Flow rates representing the three regions have been sequentially repeated for the level events in the synthesized transients.

5) Random flow events have been uniformly spaced over the appropriate time corresponding to RCS operating temperature ranges.

Pressurizer spray operation for the B&W plants is classified in one of three modes: pressurizer-RCS boron equilibration, automatic actuation of spray and bypass spray. The bypass spray operation is identical for all B&W plants with a four pump operation bypass flow rate between 1.5 and 5 gpm. Surge line flow rates are accounted for based on the number of pumps operating.

The operation of full spray differs between the Oconee Units and the other three B&W lowered-loop plants. The original modulating spray valves have been replaced with on-off acting Target Rock spray valves for the Oconee Units. All other plants have operated their entire life with the original modulating spray valves. When the spray is actuated for heater/spray operation to bring the pressurizer boron into equilibrium with the RCS boron concentration, the Target Rock solenoid-operated valve cycling results in periodic spray flow, whereas the modulating valve allows the spray flow to be held constant. The Oconee Target

Rock valves supply approximately 315 gpm maximum flow rate and the typical modulating valve supplies 190 gpm maximum flow rate.

Spray operation occurs for the following two operations as part of the design basis heatup transients: (1) pressurizer-RCS boron equilibration occurs at hot shutdown conditions (Tavg = 532F) and (2) spray cycling occurs during the increase from 0 to 8% power due to the increase in Tavg causing the spray setpoint to be reached.

Although the Oconee spray valve and the modulating spray valve types do differ, their differences do not have an impact on thermal stratification. When the spray is actuated automatically, the difference in flow rate between the Oconee Target Rock spray valve and the standard modulating type of valve is not significant in terms of stratification since both flows are large enough to flush the surge line of any stratified fluid. The action of the spray flow in flushing the line of stratified fluid also effectively eliminates the conditions that can lead to the occurrence of striping. Automatic actuation of the spray valve in either case, Target Rock or modulating valve, rid the line of the conditions required for striping to exist.

4.5.2. Cooldown Transients

4.5.2.1. Cooldown Transient Descriptions and Number of Occurrences

Cooldowns are categorized into two transients in order to conservatively represent RC cooldowns from 8% FP to refueling temperatures for the 40 year life of the plant. The RC and pressurizer temperatures for these two transients are shown in Figure 4-14. The time duration and the surge flow events are the same for both transients, but different pressure-temperature relationships are used. All lowered loop plant cooldown transients are represented by the two transients discussed in the following paragraphs.

Transient 1B1 — The pressure-temperature relationship for this cooldown transient has been based on the least restrictive Appendix G limits and available plant data. The least restrictive Appendix G limits (highest allowed RC pressure for a given RC temperature) are used to determine the pressurizer temperature for RC temperatures below 200F and above 400F. It has been determined by a review of plant data that the plants operated well below the cooldown Appendix G limits for RC temperatures between 200F and 400F. The pressurizer temperature has been assumed to be 250F above the RC temperature for this RC temperature region as this bounds the available plant data.

Transient 1B2 — The pressure-temperature relationship for this transient is identical to Transient 1B1 except for the intermediate (200F<Trcs<400) pressure-temperature relationship for which representative data is used instead of the bounding plant data.

Based on plant data, approximately 15% of the past cooldown events have been categorized as type 1B1. The remainder of events have been included in type 1B2. Future cooldowns have also been categorized with 15% as type 1B1 and the remaining 85% as type 1B2.

4.5.2.2. Boundary Temperatures as a Function of Time

The average time required for cooldowns, from plant data experience, indicates an average time for a complete cooldown of 46 hours. The surge line analysis assumes that each cooldown transient requires 75 hours. This long duration conservatively allows surge line thermal events to stabilize. The time durations for each portion of the cooldown transient have been estimated using available plant data for the following phases of the cooldown operations:

Power Decrease from 15 to 0% Power
Cooldown operations (RC temperature decrease)
Cooldown hold throughout all modes
RCS below 200F, Pressurizer hot
Pressurizer cooldown

The RC temperatures versus time for the cooldown transients have been based on the existing transients contained in the original design basis with the exception

that the times have been extended to be more representative of actual plant operations. Temperature holds have been added and cooldown rates adjusted to give reasonable agreement between the cooldown for analysis and the available plant data. The pressurizer temperature versus time plots for the cooldown transients have been developed based on the relationship of pressurizer temperature to RCS temperature based on the available plant data.

4.5.2.3. Surge Line Flow Rates for Cooldown

Cooldown flow events have been developed in a manner similar to that method used for determining heatup flow events as discussed in Section 4.5.1.4.

The operations that have been judged as significant and quantifiable are considered the major events to be accounted for in the cooldown transients. Actual makeup system response to each flow event is accounted for in the development of the transients. The spray flow required throughout a cooldown for depressurization is included in the surges specified for the cooldown transients.

Random flow events have been added to ensure that the total number of flow events for the transients adequately represent actual operating experience. Available plant data has been statistically analyzed to describe the flow events required. The same method which determined the random heatup flow events, outlined in Section 4.5.1.4, has been used to determine the number of random cooldown events.

4.5.3. Other Transients

Existing spray flow rates, temperatures, and pressures from the original RCS design basis transients have remained unchanged for most transients other than plant heatups and cooldowns. The design basis transients in which thermal stratification and striping require evaluation are listed in Table 4-1.

Spray flow rates, temperatures, and pressures from the original design basis transients have generally been used to define the boundary conditions used to evaluate thermal stratification and striping. The numbers assigned to this transient are similar to the original design basis. Surge line flow events caused by changes in the volume average temperature in the RCS have been generated by calculating the surge rate from the existing plots of RC temperature versus time contained in the original design basis transients. A few

modifications and additions to the list of transients have been made as discussed in the next few sections.

4.5.3.1. Steady State Temperature Variations - Transient 13

Transient 13 has been redefined to be more realistic in terms of the flow conditions experienced in the plants for normal steady state operations at power. The previous description conservatively and unrealistically described the steady state transient as an oscillation in reactor power of 1 percent and a temperature oscillation of 2F on an approximate period of 6 minutes. Based on the results of an evaluation of actual plant characteristics from observations of experienced control room operators, the variation is more appropriately described as a variation of temperature with an amplitude of 0.5F on a 15 minute period. This transient has been arbitrarily defined to occur over a two hour period and the number of transients have been determined accordingly for the forty year life of the plant.

4.5.3.2. Pressurizer-RCS Boron Equilibration - Transient 20D

Transient 20D has been added to describe the effects of spray and heater operations to equalize the pressurizer and RCS boron concentrations. This transient has been described both for operation with the on/off type of spray valve (Oconee Target Rock valves) and the modulating valves. The operation involves use of spray flow through the pressurizer to cause the boron concentration to approach that in the RCS. A modulated spray flow of about 50 gpm has been used in the transient description. The maximum flow rate used for the Target Rock valve is 315 gpm.

The operation of pressurizer spray and heaters to circulate reactor coolant for purposes of bringing the pressurizer boron concentration to within range of the concentration in the RCS is performed roughly twice a week. The operation will normally last approximately eight hours. The number of these transients occurring during the 40 year life of the plant has been determined accordingly.

4.5.3.3. HPI Safety Injection and Check Valve Test - Transient 22

Core Flood Tank (CFT) check valve test operations have been combined with the heatup and the cooldown transient descriptions. However, the HPI safety injection and the check valve tests are described separately. The present

description of the HPI transient given in the original design basis transients corresponds to the safety injection test only, and is intended to conservatively describe the conditions at the injection nozzles. An additional transient has been added to describe the HPI check valve tests and the resulting effects on the surge line thermal conditions.

The HPI safety injection test and the HPI check valve test have been described for four different operating conditions which represent appropriate points during past and future heatups and cooldowns. The test conditions for the pressurizer and RC temperatures are summarized as follows:

Safety Injection Test	Check Valve Test	RCS Temperature	Pressurizer Temperature
22A-1	22A-2	90F	480F
22B-1	22B-2	70F	400F
22C-1	22C-2	280F	530F
22D-1	22D-2	280F	500F

Transient 22D is based on future HPI safety injection and check valve tests not being performed with a pressurizer to RC temperature difference greater than 220F.

For the safety injection tests, a flow rate of 100 gpm per nozzle (total of 400 gpm) is assumed to be established for a period of about 30 seconds. The HPI check valve test flow rates have been set to approximate the change in pressurizer level and surge line temperature response based on the measured response at Oconee as part of the data acquisition discussed in Appendix A. The length of time between flow increases has been set to give a decrease in temperature of about 180F at the top of the surge line after every flow event, which is in agreement with the measured plant data. An offsetting outsurge flow of 15 gpm for a two hour period counters the 100 gpm insurge flows and maintains the final level approximately equal to the level at the start of the simulated test. The plant data collected at Oconee Unit 1 indicated at least three flow pulses based on measured level in the pressurizer. The number of flow pulses for analysis purposes is four for each test series.

In estimating the number of HPI safety injection tests and check valve tests for the 40 year plant life, plant operators have been consulted and the surveillance requirements have been reviewed. Requirements for some plants stipulate only that tests be conducted every 18 months as a maximum, whereas other plants are required to test during shutdown conditions if the test has not been performed in the last 90 days (or if maintenance or modifications have been performed that would affect the HPI system flow characteristics). In estimating the number of Transient 22 events, the 90 day requirement has been used to conservatively estimate the number of events. Frequent check valve tests were not required prior to about 1980. Therefore there have not been many of these tests during the period when the 2 EFPY P/T limit curves were in effect.

Table 4-1. Surge Line Design Basis Transient List

Transient ID	Transient Description	Modification from Original Transients (ODB - Original Design Basis)
1A1	Past Heatups - Trc of 70F to 8%FP, 2 EFPY Appendix G limits specifies P/T relationship, decay heat available.	Completely redefined to realistically represent the most severe heatup occurring during the life cycle of the plant.
1A2	Past Heatups - Trc of 70F to 8%FP, higher than usual RC pressures specify P/T relationship, no decay heat.	Completely redefined to realistically represent heatups occurring with higher than usual pressures for all RC temperatures.
1A3	Past Heatups - Trc of 70F to 8%FP, P/T relationship based on average P/T relationships, decay heat available.	Completely redefined to realistically represent an average heatup.
1A4	Future heatups - Trc of 70F to 8%FP, P/T relationship based on plant data in which decay heat is not available.	Completely redefined to represent future heatups for which decay heat is not used to heat RCS before starting pumps. (see path ABE in Figure 8-1)
1A5	Future heatups - Trc of 70F to 8%FP, P/T relationship based on plant data for which decay heat is available.	Completely redefined to represent future heatups for which decay heat is used to heat the RCS to 120F before starting RC pumps. (see path CDE in Figure 8-1)
1B1	Cooldown - 15%FP to refueling temperature, P/T relationship based on maximum RC pressures.	Completely redefined to represent a bounding cooldown based on least limiting Appendix G limits (highest pressures) and plant data.
1B2	Cooldown - 15%FP to refueling temperature, P/T relationship based on average pressures.	Completely redefined to represent an average cooldown based on least limiting Appendix G limits and average plant data.
2A	Power Change from 0% to 15% FP	Surge line temperatures based on ODB boundary conditions.

Transient ID	Transient Description	Modification from Original Transients (ODB - Original Design Basis)
2B	Power Change from 15% to 0% FP	Surge Line temperatures based on ODB boundary conditions.
3	Power loading 8% to 100% FP	Surge Line temperatures based on ODB boundary conditions.
4	Power unloading 100 to 8 percent	Surge Line temperatures based on ODB boundary conditions.
5	Ten percent step load power increase	Surge Line temperatures based on ODB boundary conditions.
6	Ten percent step load power decrease	Surge Line temperatures based on ODB boundary conditions.
7	Step Load decrease 100 to 8% FP	Surge Line temperatures based on ODB boundary conditions.
8	Reactor Trip	All trips now included in Transient 8. Previously, certain trips were included in other transients.
9	Rapid Depressurization	SL temps based on ODB boundary conditions.
10	Change of RC Flow Rate	SL temps based on ODB boundary conditions.
13	Steady State Temperature Variations	SL temps based on ODB boundary conditions.
14	Control Rod Drop	SL temps based on ODB boundary conditions.
19	Feed and Bleed Operations	SL temps based on ODB boundary conditions.
20	Miscellaneous Transients	A complete transient was added to describe pressurizer spray and heater operations used to equilibrate pressurizer & RCS boron concentrations.
22	Test Transients	Complete transients were added for the HPI check valve test. The HPI Safety Injection Test was completely modified.

Table 4-2. Design Basis Heatup Transient Definitions

Transient ID	Past/ Future Events	P/T Relationship	Number of Events					
			ANO-1	CR-3	OC-1	OC-2	OC-3	TMI-1
1A1	Past	Original P-T Limits	10	10	11	13	10	10
1A2	Past	Orig. Design Basis	13	8	12	14	6	6
1A3	Past	Orig. Design Basis	68	45	64	70	33	30
1A4	Future	Plant Data	24	29	45	43	51	32
1A5	Future	Plant Data	125	148	228	220	260	162
EVENT TOTAL			240	240	360	360	360	240

Note: 1) Pressurizer level versus time is identical for all five transients.

2) An appropriate number of heatups is included in Transient 1A1 to account for hot functional tests.

3) This table is based on data as of November, 1990 and does not include the ANO-1 heatup in late December, 1990.

Table 4-3. Events Affecting Surge Line Flow for Plant Heatup and Cooldown

Pressurizer pressurization (affects letdown rate and RCS volume and mass)
Purging of Pressurizer nitrogen along with RCS fill/vent operations
Degassing Pressurizer using heaters/spray
Adjusting Pressurizer level setpoint
Controlling Pressurizer level in auto (w/ valve and controller deadbands)
Drawing of Pressurizer chemistry sample
Forcing fill of RC loops by pressurizing Pressurizer
PORV testing
Control Rod Drive and RCS venting
Decay Heat Removal System testing (i.e., throttling DHR flow)
Starting makeup pump
Adjusting of RCP seal injection/return flows (adjusting seal backpressure)
Adjusting flow in RC pump seal bypass line
HPI check valve testing
RCS heatup without RCP operating (throttle back on LPI cooler flow)
Closing letdown orifice manual bypass
Drawing of vacuum in steam generator (OTSG)
Starting first RC pump with thermally stratified RCS
Starting first RC pumps
Cycle auxiliary spray valve (for flushing of pressurizer)
Venting of Pressurizer to Letdown Storage Tank (LDST)
Changing RC pump combinations (affects minimum bypass spray flow)
Adjusting letdown flow rate with increasing RCS pressure
Actuating spray (spray controls in hand)
Opening turbine bypass valves
Testing Core Flood system
Adjusting heatup rate with turbine bypass valves (TBVs) (heatup hold/proceed)
Pressurizer spray controlling in auto, heaters on for boron equilibration
Opening spray line block valve
Adjusting makeup nozzle warming flow(s) (nozzle-warming throttle valves)
Placing TBV's in auto, steam pressure maintained within control band
Adjusting boron concentration in RCS (changing MU/LD)
Increasing power to 8 percent
Surveillance testing
Degassifying Pressurizer and RCS (vent pressurizer to waste gas header)
Placing TBV's in hand and shutting down turbine
Tripping turbine

Reducing core power and reducing Tavg to 532F
Sampling boron concentration in RCS
Adjusting TBV positions for desired cooling rate (TBV's in manual)
Performing Safety Injection functional test
Controlling Pressurizer level in auto (w/ valve and controller deadbands)
Discharging CFT's to RCS (test at <700 psig)
Closing HPI injection and bypass injection valves (at <350F)
Securing steam generator hot blowdown
Initiating hot soak of SG's (optional)
Decreasing pressurizer level control setpoint to 100 inches
Valving in the LPI system and starting 1 LPI pump
Throttling LPI cooler flow to establish proper RCS cooldown rate
Securing OTSG's by closing TBV's
Filling OTSG's for Fill, Drain, Layup (optional)
Lining up and using auxiliary spray
Adjusting LPI cooler outlet temperature to cold leg temperature
Securing last RCP (RC loop temperature differential increases)
Adjusting LPI cooler outlet temperature to resume RCS cooling
Securing RCP seal injection/return flows
Opening letdown orifice manual bypass
Adjusting letdown flow to lower pressurizer level to about 115 inches
Regulating LPI flow as RCS is depressurized
Going to 1 LPI pump
Raising and lowering pressurizer level when on DHR
Cooling loops by fill, soak, drain of SG (optional)

Figure 4-1. Plant Data taken at Oconee Unit 1
during HPI Check Valve Test (2/10/89)
(see Appendix B for details on the events occuring during this period)

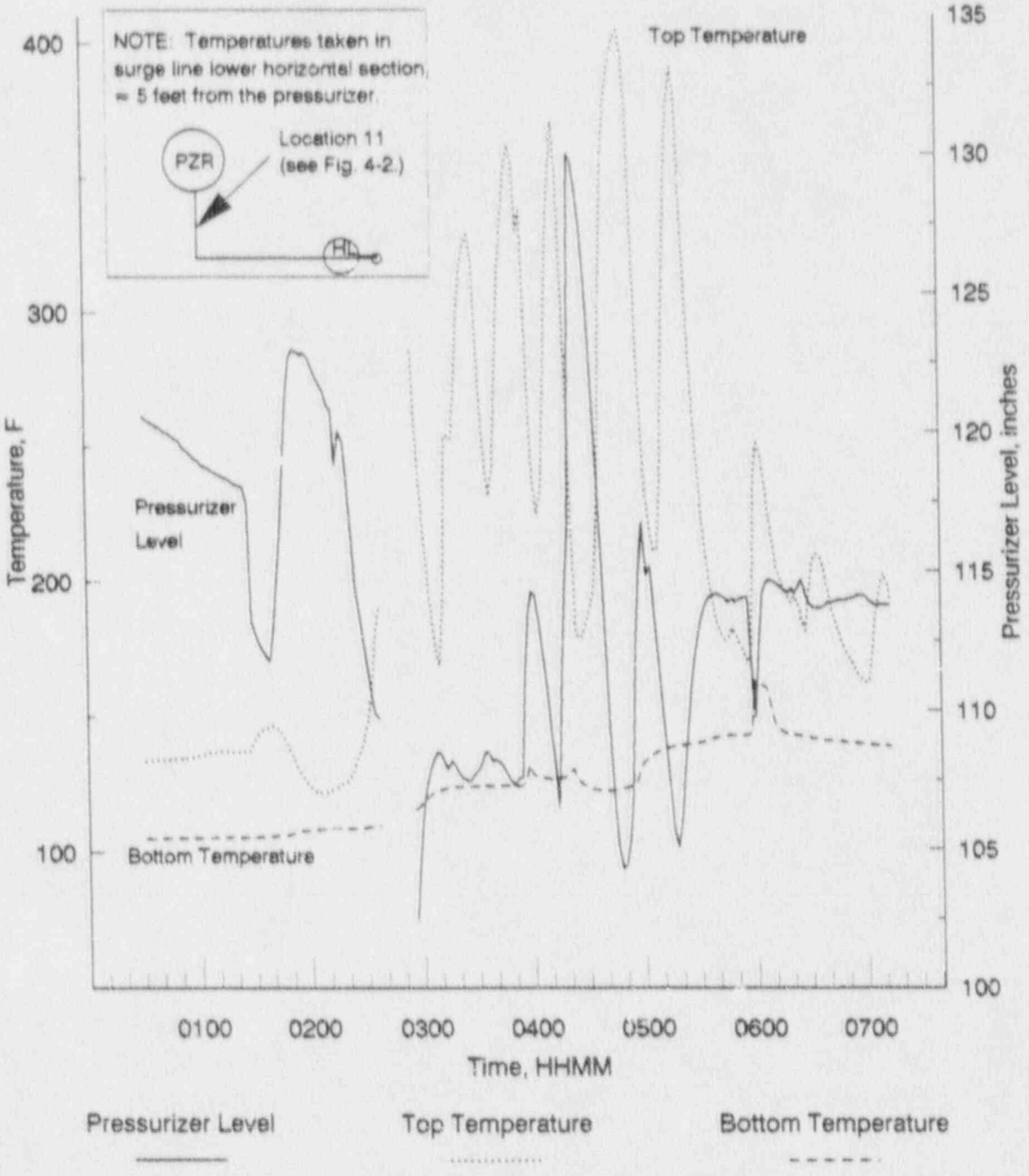

Figure 4-2. Thermocouple Locations at Oconee Unit 1

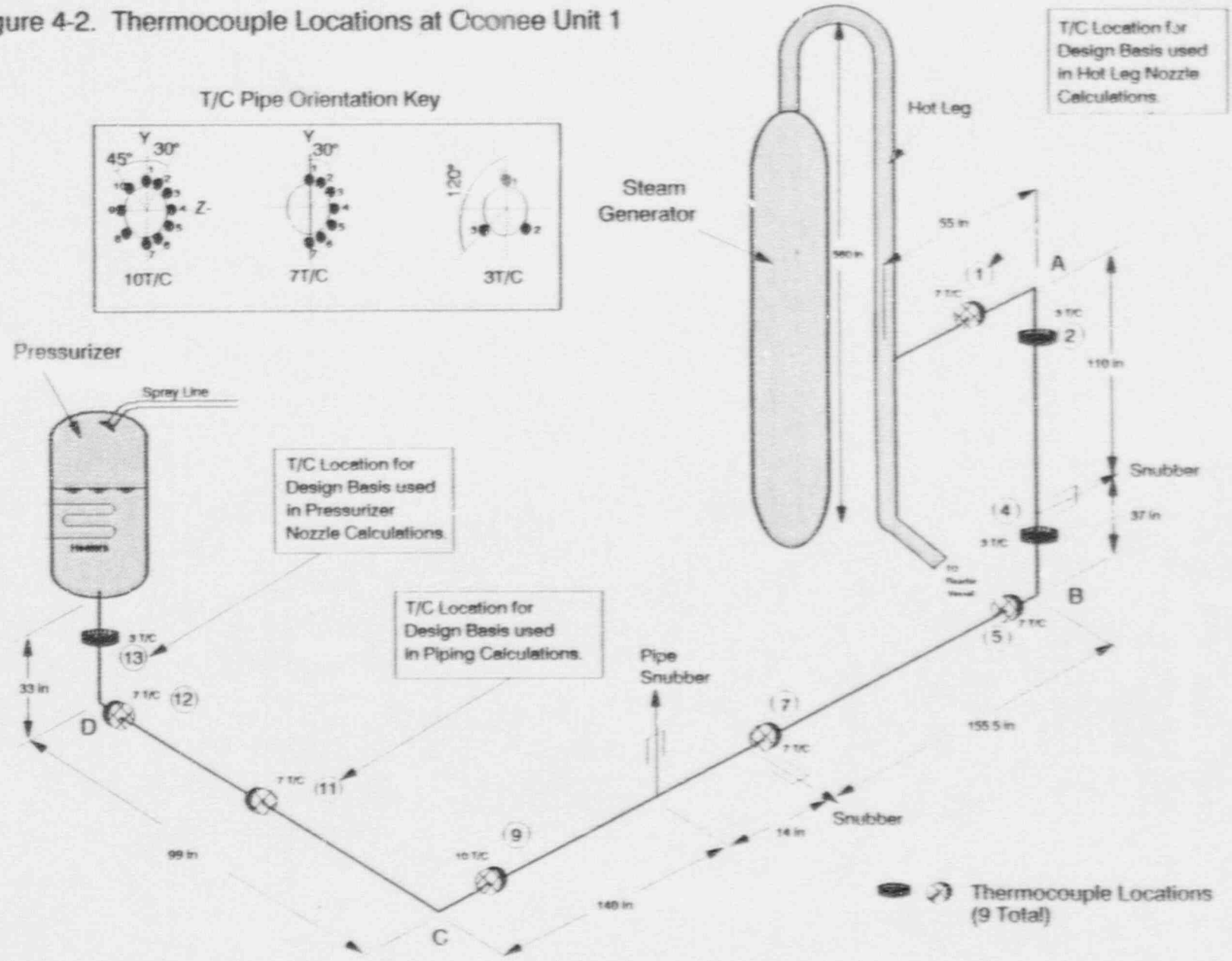

Figure 4-3. October 89 Oconee Heatup

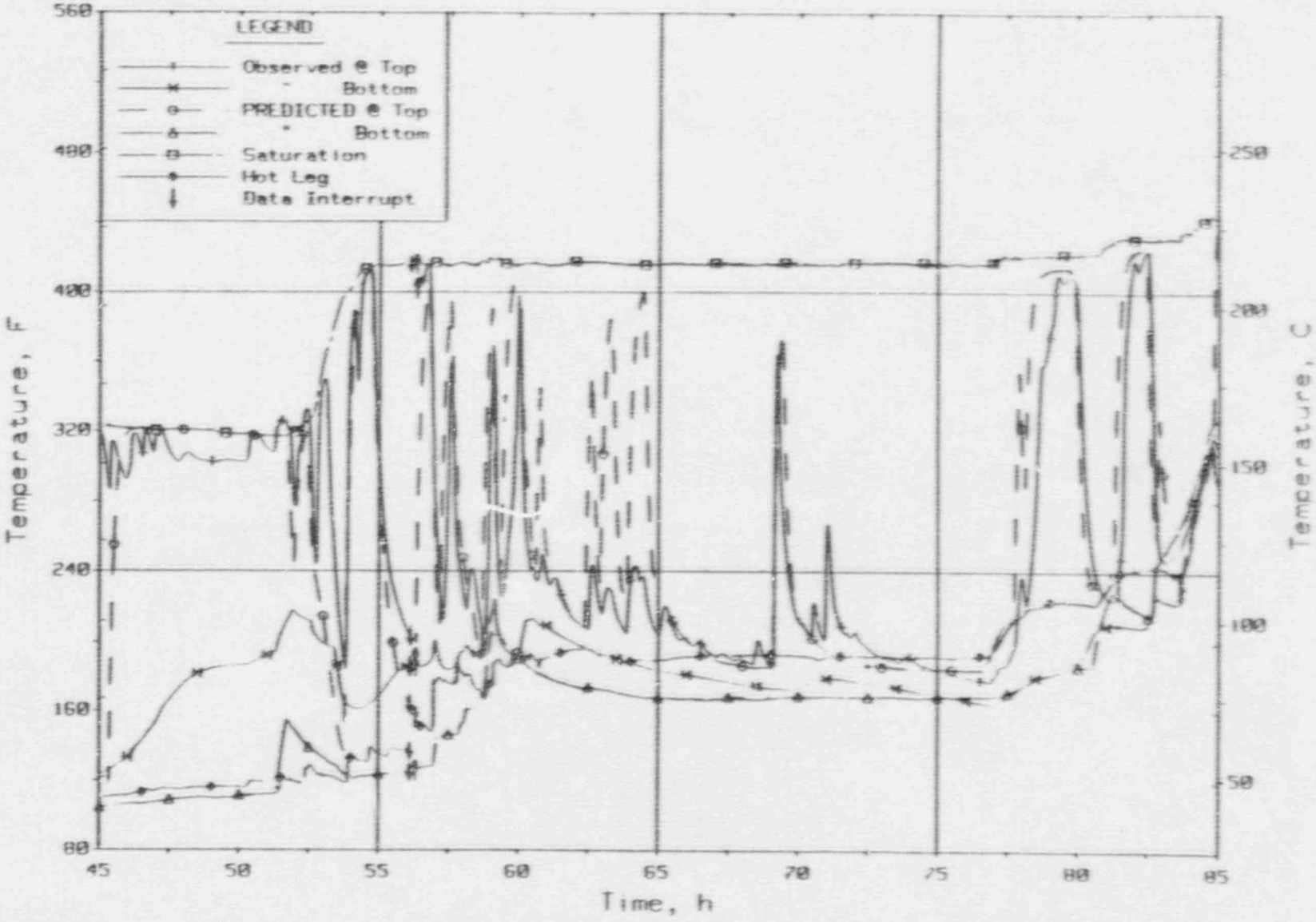

Wall Temperatures @ Location 11

Wed Jun 27 10:43:33 1990

TL11

Figure 4-4. October 89 Oconee Heatup

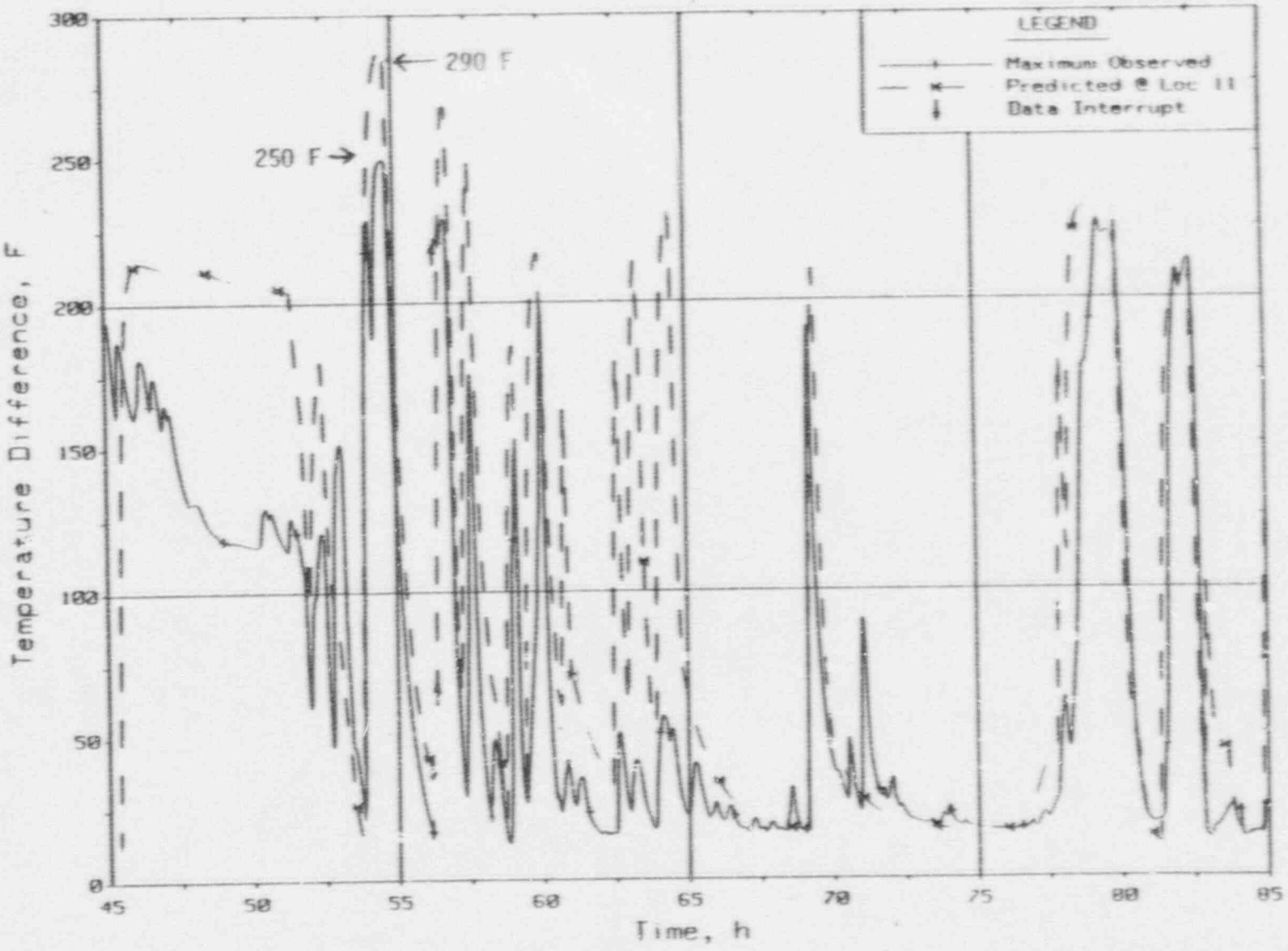

Top-To-Bottom Temperature Differences

Wed Jun 27 10:51:51 1990

DTMPIX

Figure 4-5. Striping Conditions

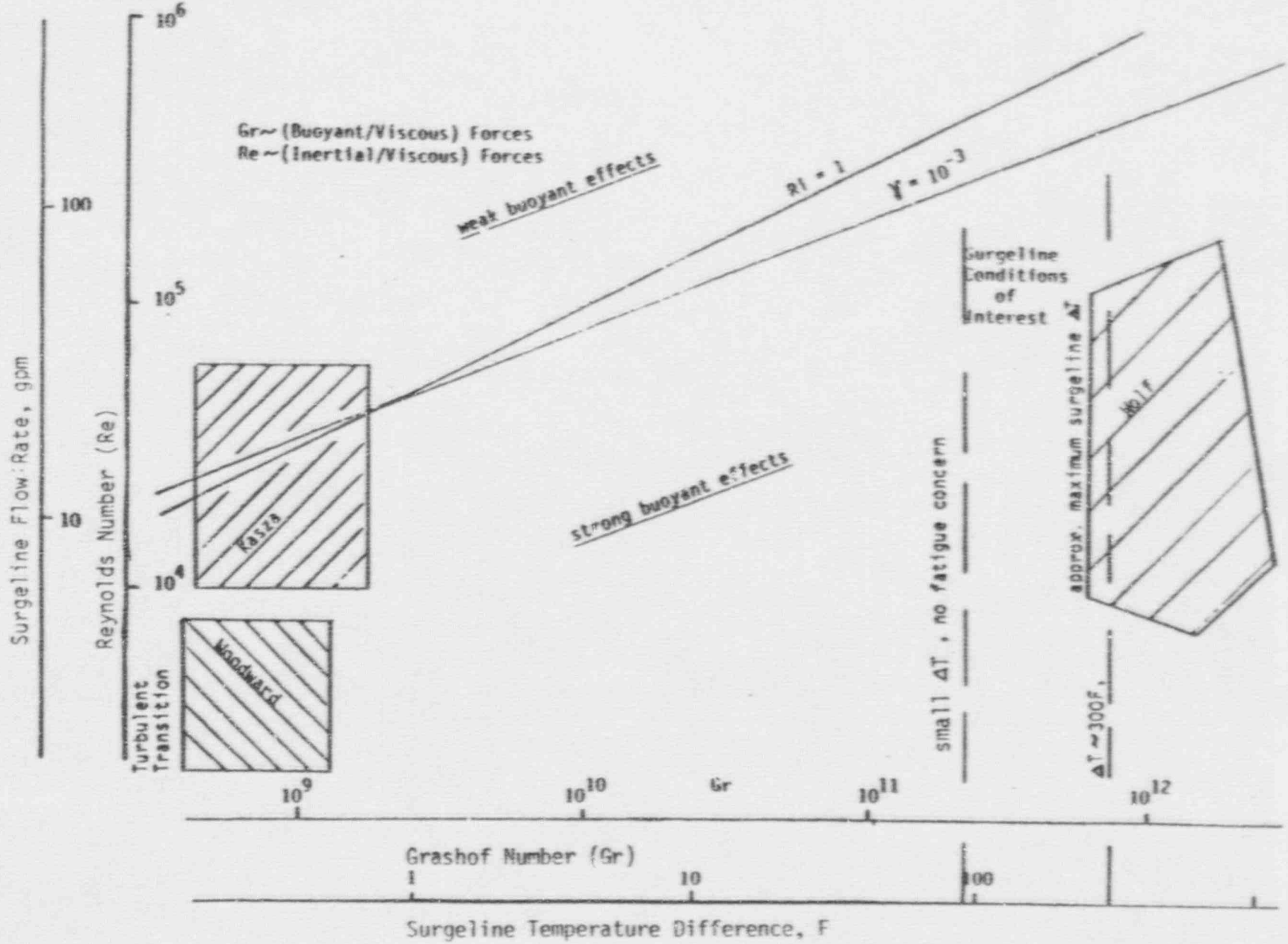

Figure 4-6. Test Loop

Extracted from Figure 4.2-1 of reference 1.
Dimensions in mm.

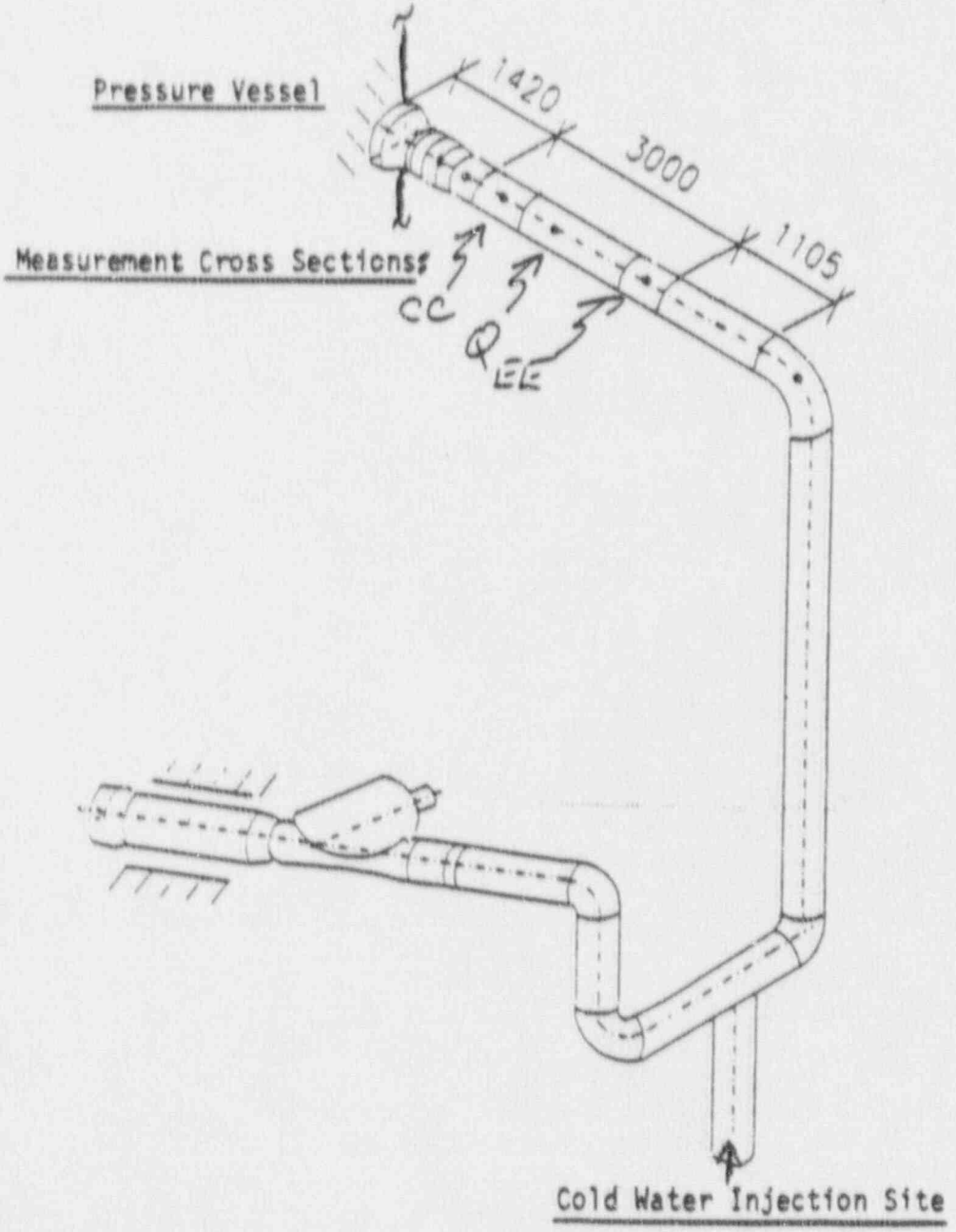

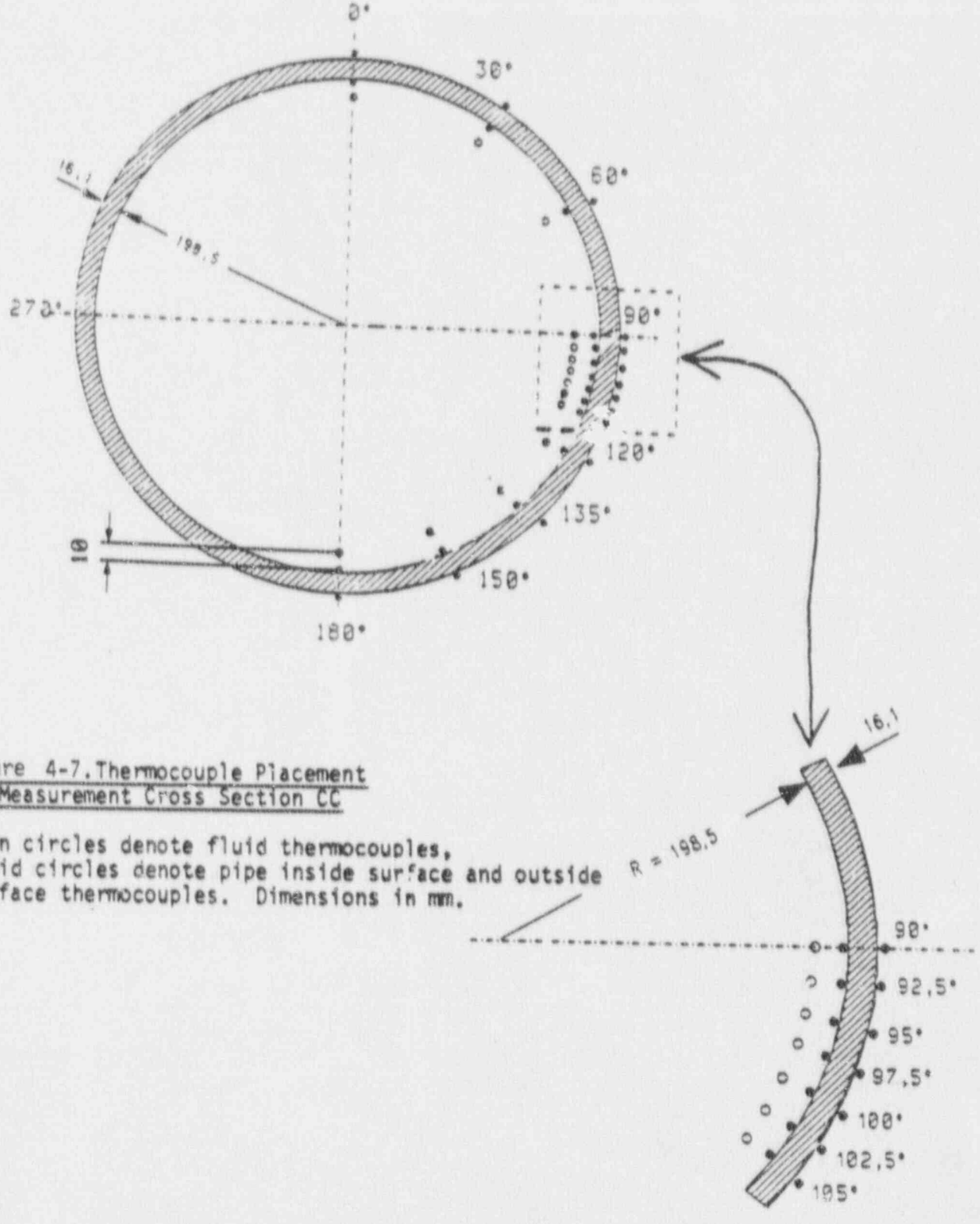

Figure 4-7. Thermocouple Placement
At Measurement Cross Section CC

Open circles denote fluid thermocouples,
Solid circles denote pipe inside surface and outside surface thermocouples. Dimensions in mm.

Figure 4-8. Inside Wall Temperature Between 90 and 95 Degrees, Cross Section CC

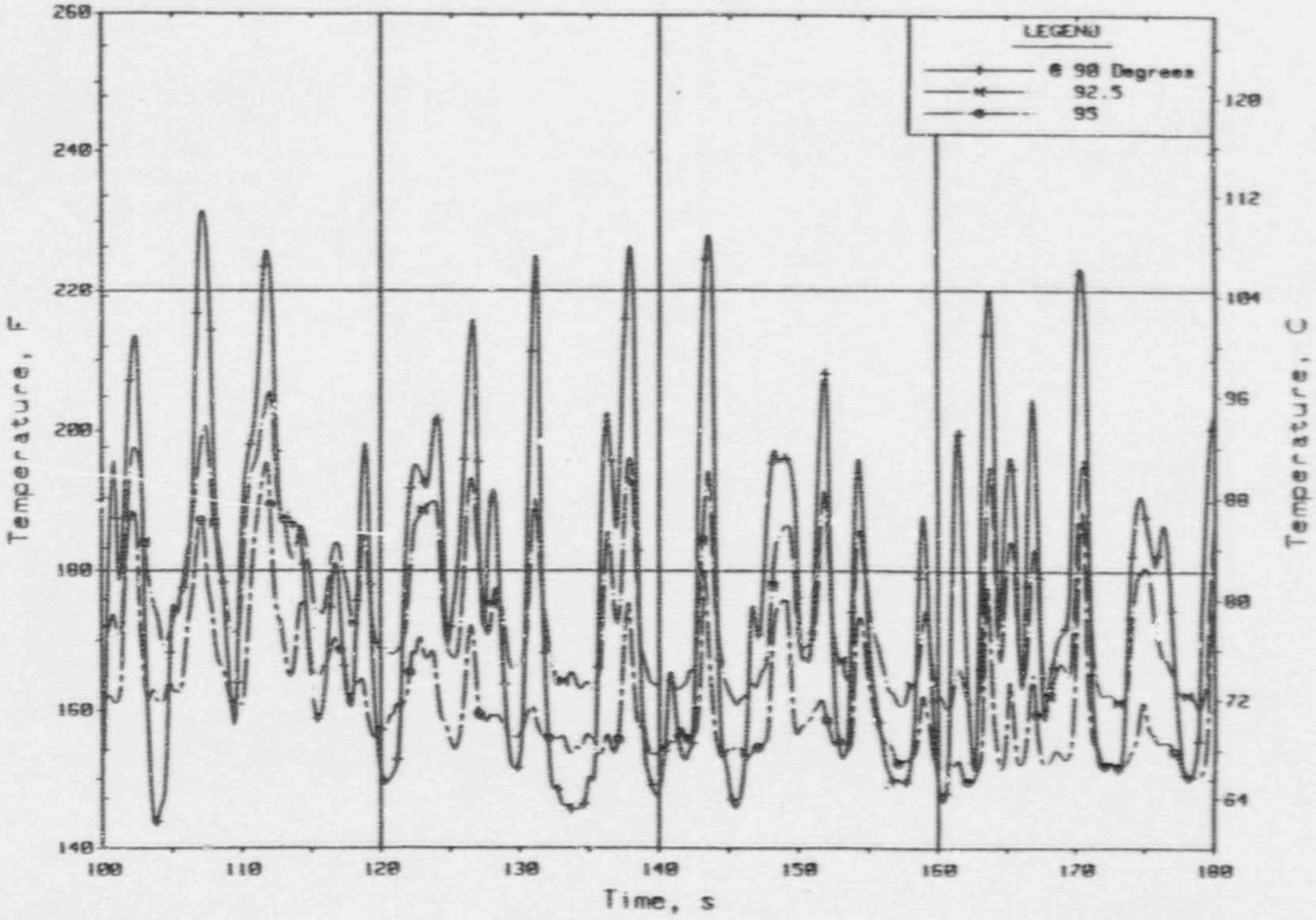

Battelle-Karlsruhe Test 33.16, DT = 190 F

TICC96

Figure 4-9. Inside Wall Temperature Fluctuations @ 100 Degrees, Cross Section CC

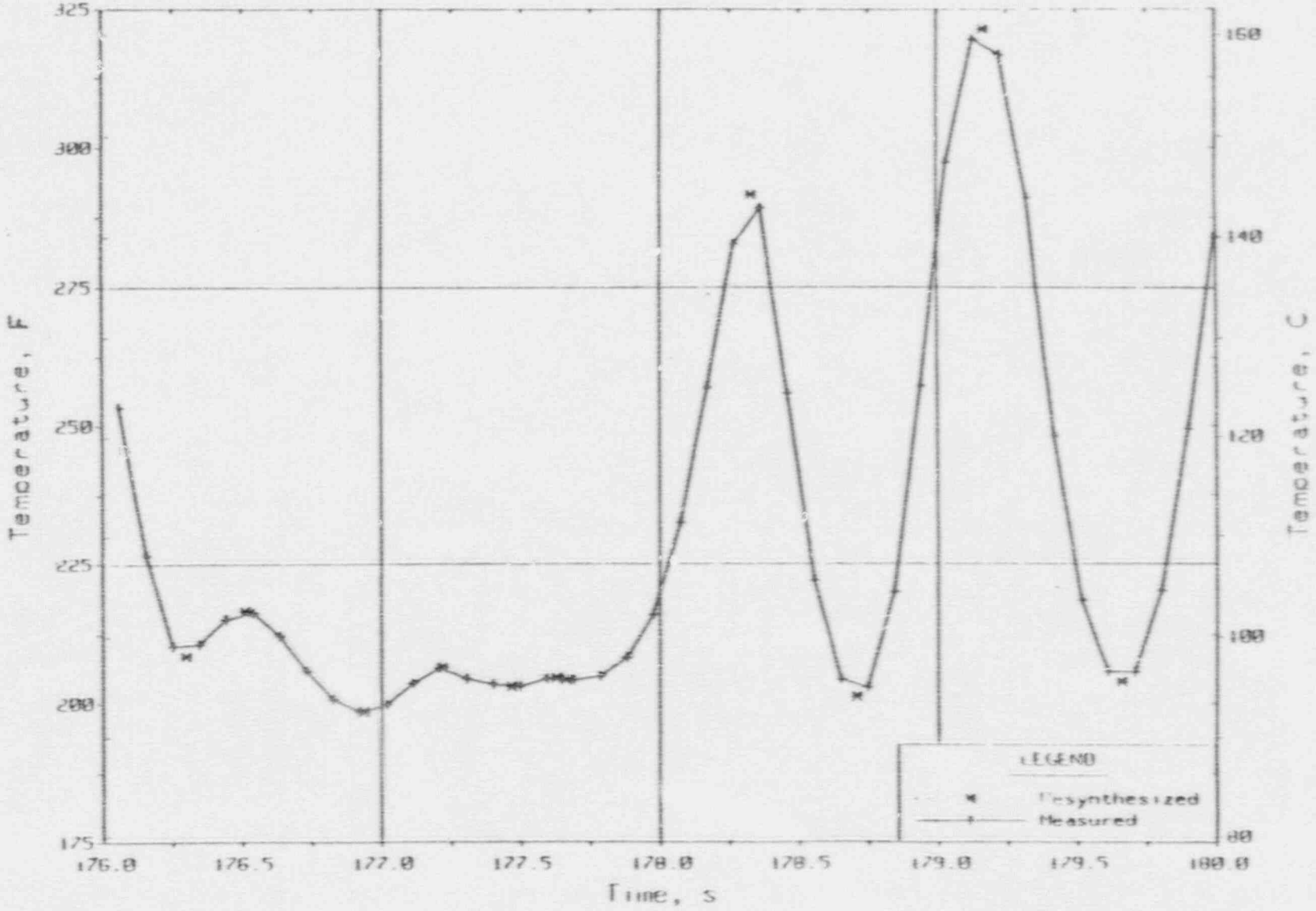

Test 53, Phase 3 of Battelle-Karlsruhe Test 33.25, DT = 322 F

Figure 4-10. Heatup Design Bases Transient Temperatures

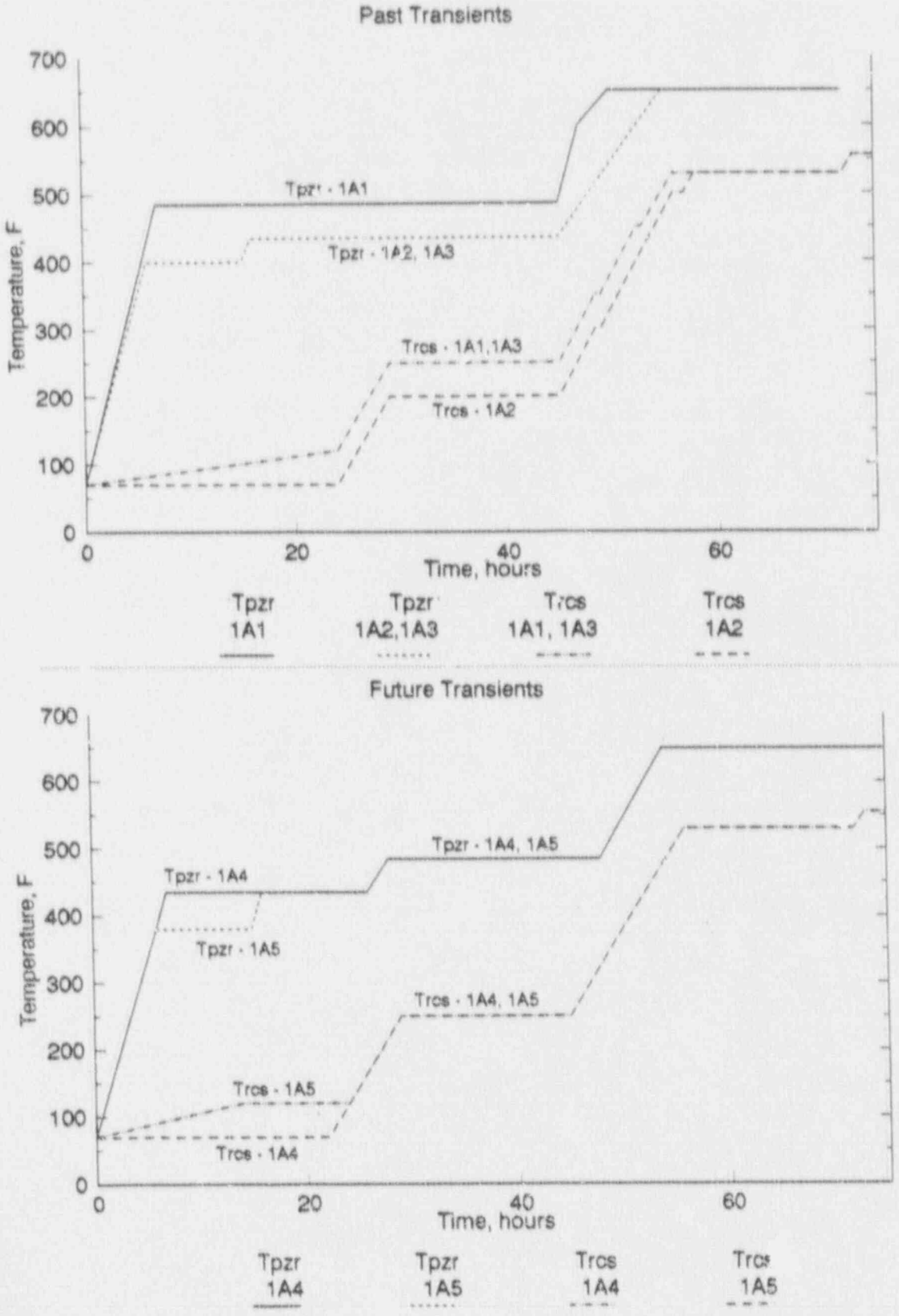

Figure 4-11. Development of Heatup Design Bases Transients

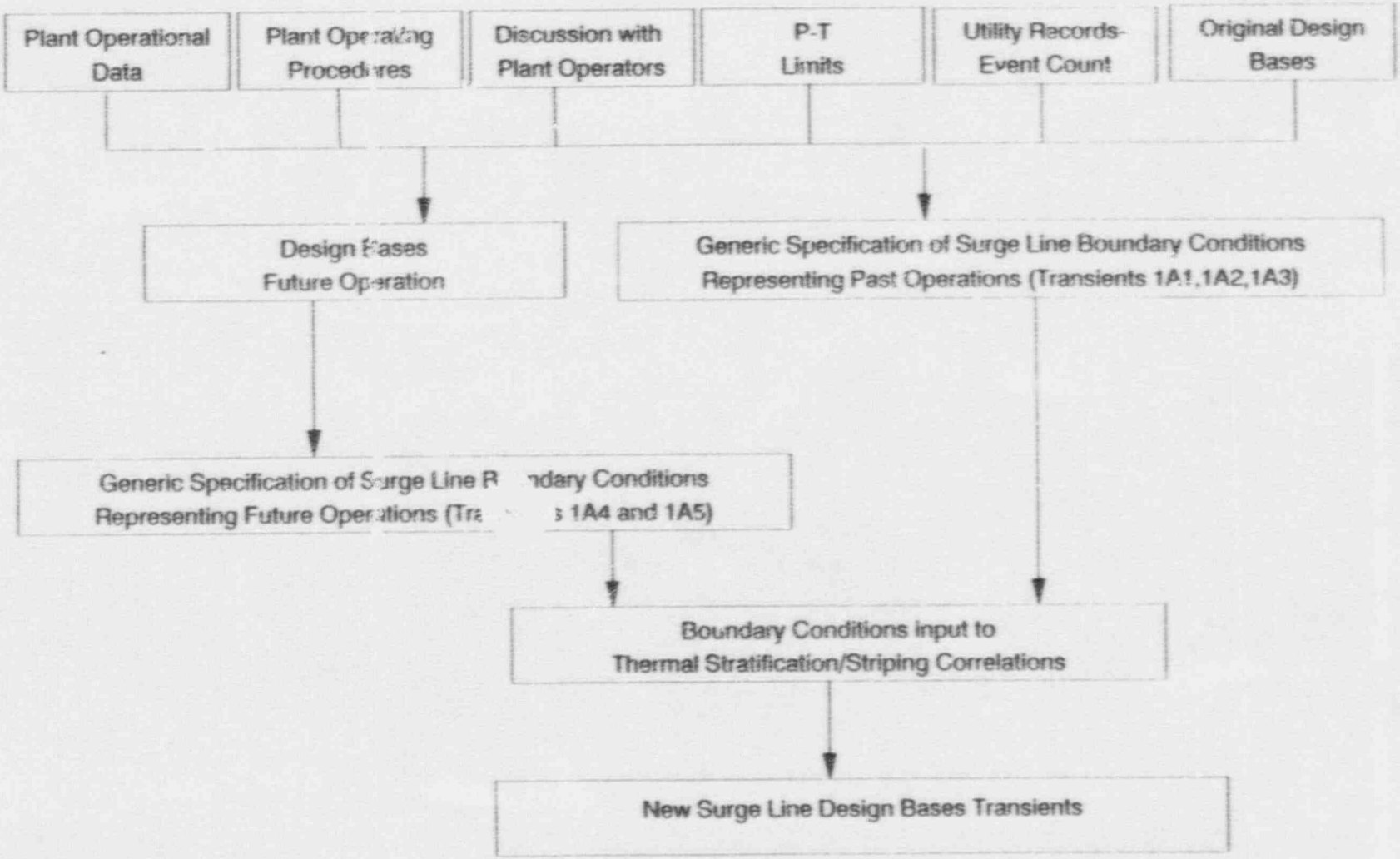

Figure 4-12. Plant Heatup Transient 1A1
Temperatures - Pzr, Surge Line (top/bottom), RC

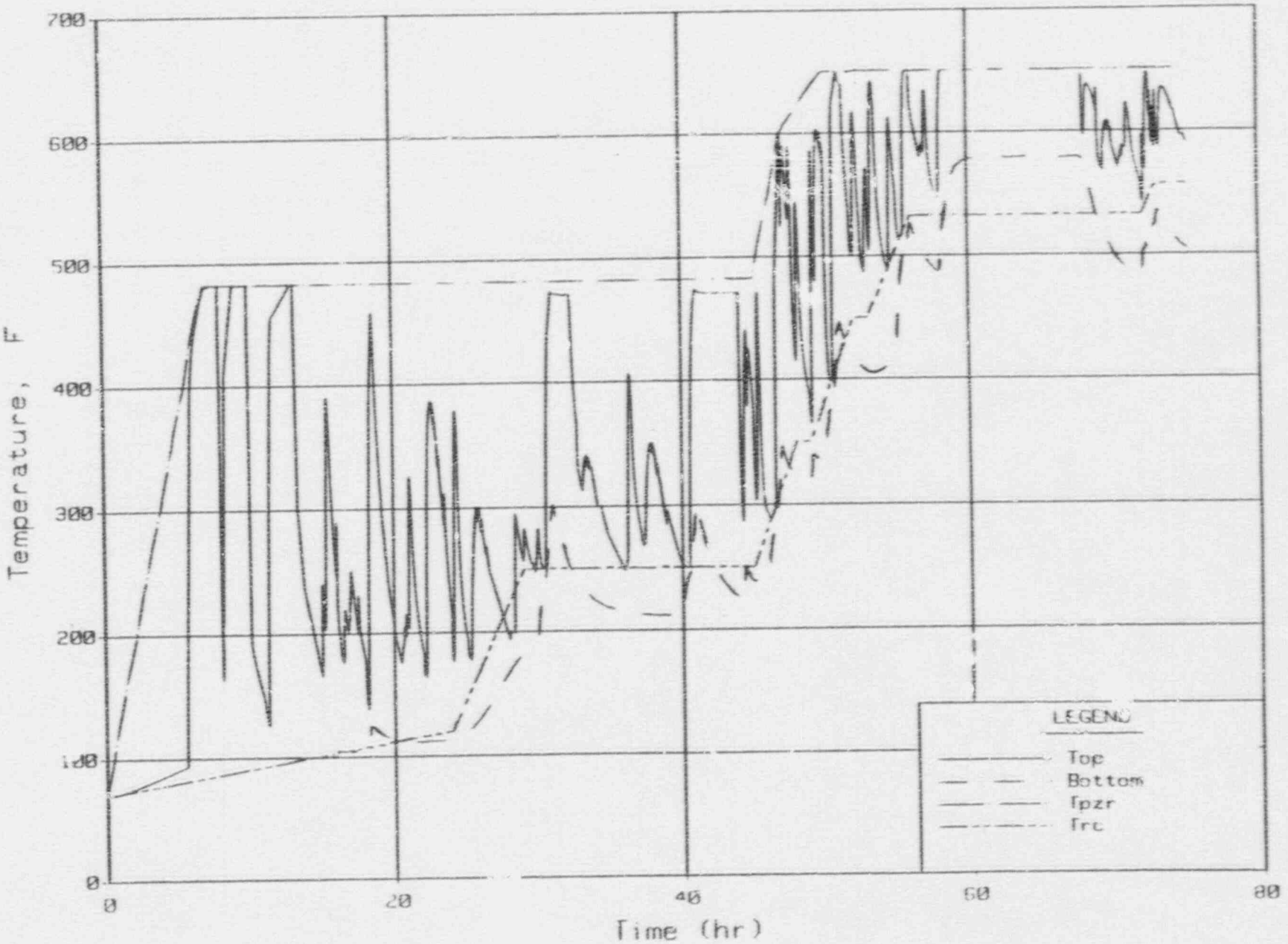

Figure 4-13. Determining the Number of Events for Each Heatup Transient

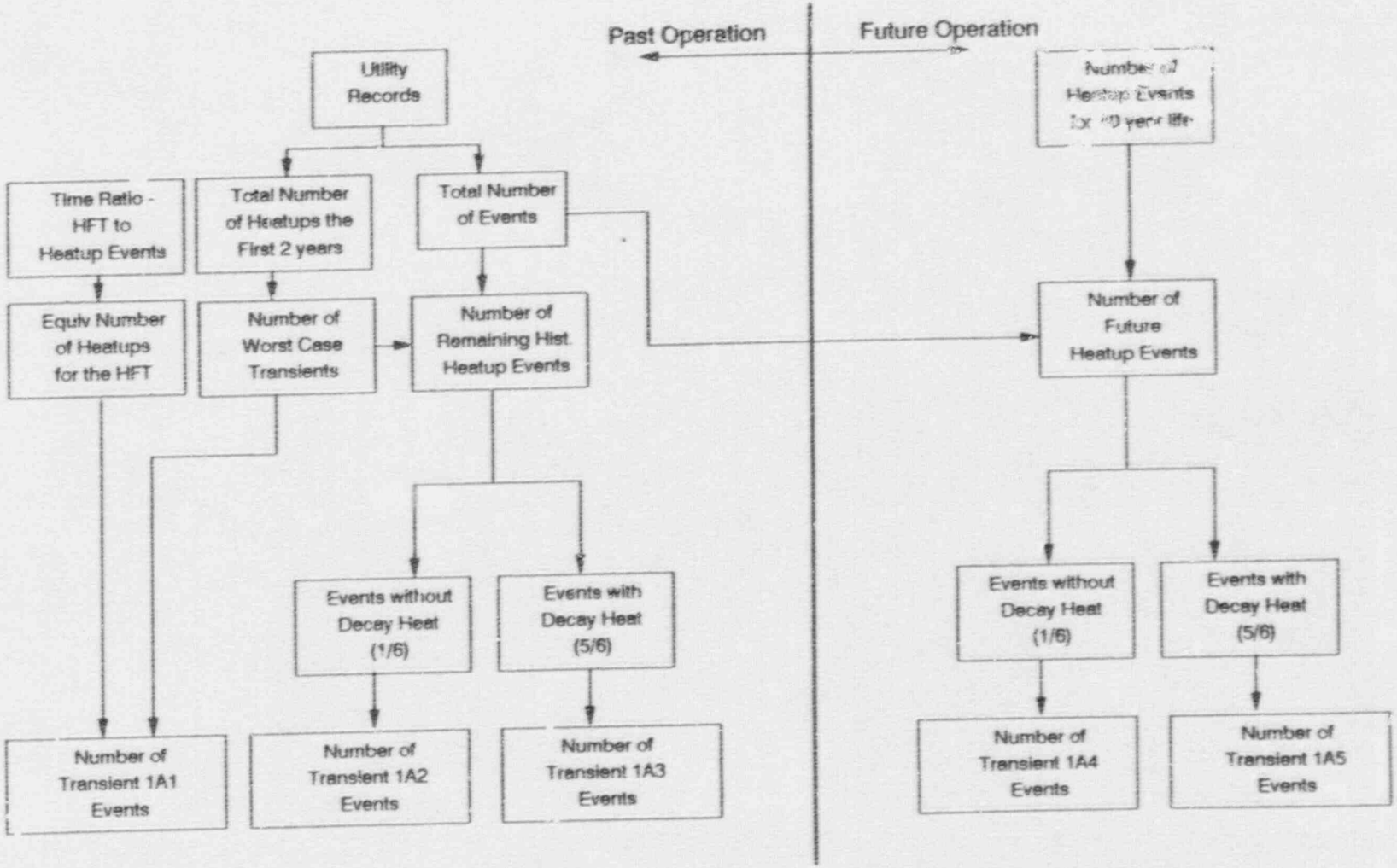

Figure 4-14. Cooldown Design Bases Transient Temperatures

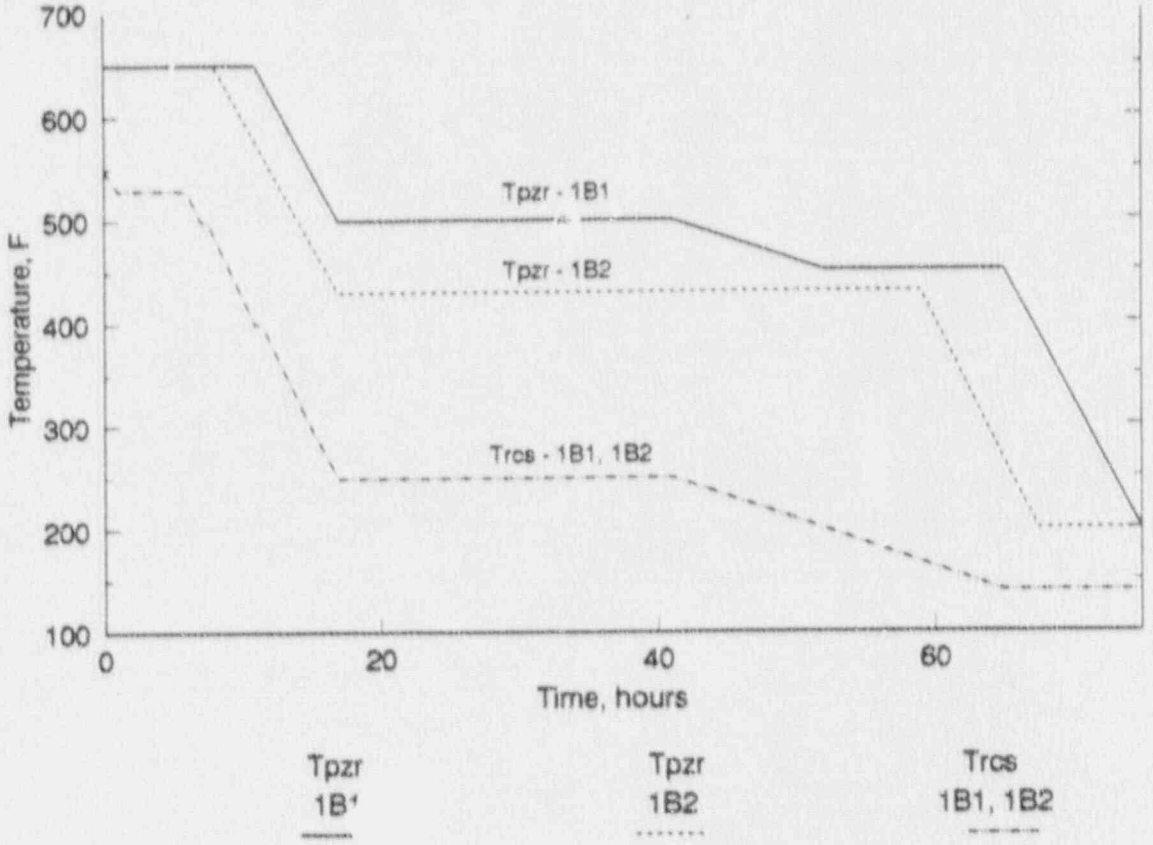

Tpzr 1B1	Tpzr 1B2	Trcs 1B1, 1B2

5. PIPING ANALYSIS

5.1. Structural Loading Analysis

The purpose of the structural loading analysis is to generate the internal forces and moments in the surge line for the thermal stratification conditions defined in the design basis transients.

5.1.1. Choice of Computer Program

The Structural Loading Analysis of the surge line has been performed using the computer program ANSYS (reference 17). The decision to use ANSYS is based on the fact that both the straight pipe element STIF20 and the pipe elbow element STIF60 have been used extensively in the past. In addition, these two ANSYS elements allow the user to define a variation of temperature on the pipe cross-section. This capability is necessary for thermal stratification, as a top-to-bottom temperature difference exists in the horizontal portion of the surge line.

5.1.2. Building of Mathematical Model

To accurately simulate the deformation of the surge line as a result of thermal stratification, an "extended" mathematical model has been built. It consists of the pressurizer, surge line, hot leg, reactor vessel, and steam generator. The boundaries of this "extended" mathematical model are the pressurizer support at approximately mid-elevation of the pressurizer (where a stiffness matrix is applied to simulate the flexibility of the support frame), the base of the reactor vessel skirt, and the base of the steam generator pedestal. The mathematical model of the surge line is given in Figure 5-1. The purpose of adding the pressurizer at one end of the surge line and the hot leg, reactor vessel, and steam generator at the other end is twofold: it allows the surge line nozzles to experience the correct displacements and rotations due to the global thermal expansion of the primary system, and it correctly simulates the

flexibility of the components adjacent to the surge line (the pressurizer and the hot leg).

5.1.3. Non-Linear Temperature Profile

As mentioned in Section 5.1.1, both the straight pipe element and the pipe elbow element allow the user to define a variation of temperature on the pipe cross-section, the maximum temperature being at the top of the pipe, and the minimum temperature being at the bottom of the pipe. This variation of temperature, however, can only be applied as a linear function on the pipe cross-section. This is a limitation, as the temperature measurements taken during heatups at Oconee Unit 1, in February 1989 and again in October 1989, have shown that the temperature profile on the pipe cross-section is non-linear.

To study the influence of a non-linear temperature profile on the pipe cross-section, the concept of "equivalent linear temperature profile" is introduced: the equivalent linear temperature profile is the linear temperature profile which generates exactly the same rotation of the pipe cross-section as the one generated by the non-linear temperature profile. The main steps of that non-linear temperature profile study are as follows:

- Evaluation of the non-linear temperature profiles measured at Oconee Unit 1 (outside surface temperature profiles).
- Selection of the most critical of those non-linear temperature profiles (temperature profiles which experience a constant maximum temperature for a considerable height at the top of the pipe cross-section, and a constant minimum temperature for a considerable height at the bottom of the pipe).
- Selection of a simple temperature profile at the inside surface of the pipe cross-section.

  Finite element conduction run to arrive at the temperature profile at the outside surface of the pipe cross-section.
- Repetition of the previous two steps, in an iterative manner, in an effort to determine the temperature profile at the inside surface which matches almost exactly the "most critical" non-linear temperature profile at the outside surface.

These iterative analyses have been performed for two non-linear measured temperature profiles at the outside surface: one for the Oconee Unit 1 February 1989 heatup and the other for the Oconee Unit 1 October 1989 heatup. These measured temperature profiles have been chosen for their particularly non-linear profile.

From the results of finite element conduction runs for which the calculated outside temperature profile corresponds almost exactly to the measured outside temperature profile, the average temperature profile can be calculated easily.

This average temperature profile is then applied as input in the mathematical formulation of the "equivalent linear" temperature profile. In addition to being a function of the average temperature profile, this mathematical formulation is also a function of the modulus of elasticity and the coefficient of thermal expansion, which are both dependent on the temperature.

The non-linearity coefficient is defined as the ratio between the top-to-bottom temperature difference of the equivalent linear temperature profile and the top-to-bottom temperature difference of the measured non-linear temperature profile. As the analysis described above has been performed for two non-linear measured temperature profiles, two different non-linearity coefficients are calculated: 1.32 and 1.35. It is not surprising that these two coefficients are not equal, as they are, in general, a function of the following three parameters: the temperature at the top of the pipe, the temperature at the bottom of the pipe, and the elevation of the fluid interface centerline, the fluid interface being the height on which there is a non-negligible variation of the temperature at the inside surface of the pipe cross-section.

Finally, the mathematical formula of the non-linearity coefficient has been developed, as a function of the temperature at the top of the pipe, the temperature at the bottom of the pipe and the elevation of the fluid interface centerline. The variations with temperature of the modulus of elasticity and of the coefficient of thermal expansion have been embedded in that mathematical formula.

5.1.4. Verification Run for Displacements

During the Oconee Unit 1 February 1989 heat-up, the temperature and the displacements of the surge line have been recorded.

During that heat-up, the maximum recorded top-to-bottom temperature difference is 280F (T_{top} = 403F; T_{bottom} = 123F). For that exact time point, the temperature at other locations of the surge line and the surge line displacements are known. At that particular time point, the top-to-bottom temperature difference varies along the horizontal portion of the surge line from 280F maximum to 200F minimum.

Also, the top-to-bottom temperature profile is not exactly the same at each location where temperature data have been measured. Therefore, the non-linearity coefficient is calculated at each one of these locations, using the mathematical formula developed as explained in Section 5.1.3.

The resulting equivalent linear temperature profiles have been given as input for the horizontal portion of the surge line, together with the other temperature data measured at the same exact time point in the surge line riser, in the hot leg, and in the pressurizer.

Using the "extended" mathematical model of the surge line, (documented in Section 5.1.2), an ANSYS computer run has been performed. The resulting displacements have been compared with the measured displacements, as shown in Figures 5-2 through 5-4. These comparisons have shown a very good agreement between the calculated and the measured displacements. (See Figures 5-2 through 5-4.)

This has verified that the "extended" mathematical model of the surge line is accurate for the generation of the internal forces and moments in the structural loading analysis. It has also verified the method used to correct for the influence of the non-linearity of the temperature profile on the pipe cross-section. (An ANSYS computer-run without the non-linearity coefficient gave displacements that do not compare well with the measured displacements.)

5.1.5. Structural Loading Analysis for the Thermal Stratification Conditions

The thermal stratification conditions have been defined in the design basis transients documented in Section 4.5. In these design basis transients, the thermal stratification conditions are evenly divided in peaks and valleys, where the peaks are characterized by maximum top-to-bottom temperature differences and

the valleys by minimum top-to-bottom temperature differences. Among the peak conditions, the three most critical thermal stratification conditions occur during the heatup transient 1A1. These three thermal stratification conditions are characterized by top-to-bottom temperature differences of 397F, 393F and 386F.

For each one of these three stratification conditions, a structural loading analysis has been performed, using the ANSYS mathematical model documented in Section 5.1.2. For each of these stratification conditions, the top-to-bottom temperature difference has been multiplied by the non-linearity coefficient, to arrive at the "equivalent linear" top-to-bottom temperature difference which has been given as an input for the ANSYS computer run. Also, the pressurizer and hot leg temperatures have been defined in the design basis transients and are given as input. The temperature in the riser of the surge line is given as T_{top} in the lower half of the riser (the temperature at the top of the pipe in the horizontal run), and as the average between T_{top} and $T_{hot\ leg}$ in the upper half of the riser. This temperature distribution in the riser is known from the measurements performed at Oconee Unit 1, and is the same as already used in the Verification Run of Section 5.1.4.

In addition to the three ANSYS computer-runs performed for the three most critical thermal stratification conditions, the structural loading analysis has also been performed for a spectrum of seven other thermal stratification conditions defined in the design basis transients. These conditions have been chosen to cover a wide range of different top-to-bottom temperature differences. Also, the structural loading analysis has been performed for the 100% power thermal conditions characterized by a complete lack of top-to-bottom temperature difference.

As a result of each thermal stratification condition above, the internal forces and moments in the surge line have been calculated (in separate ANSYS computer-runs). Furthermore, having these 11 sets of internal forces and moments allows the generation of an interpolation scheme to determine the internal forces and moments everywhere in the surge line. The variables included in this interpolation scheme are the location on the surge line (coordinates), the "equivalent linear" top-to-bottom temperature difference, the average between T_{top} and T_{bottom}, and the temperatures of the pressurizer and the hot leg.

5.2. Generic Stress Indices for the Surge Line Elbows

The thermal expansion secondary stress has to be verified in NB-3600 through the Equation 12 stress which is required to be within the 3*Sm allowable. This Equation 12 stress contains the stress index C_2. For the elbows, NB-3600 gives the same values for the secondary stress index C_2 and for $K_2 * C_2$, which is the multiplication of stress indices to be used for the elbow peak stress (K_2 is defined as 1.0 for the elbows). Using the definitions of secondary and peak stresses given in NB-3213.11 and NB-3213.13, the C_2 and K_2 stress indices have been recalculated for the surge line elbows. The following finite element analyses are for all four surge line elbows, as they are identical to each other (90 degree elbows, 10 inch schedule 140, stainless steel A 403, grade WP316).

The computer program ABAQUS (reference 19) is used for the purely elastic and elasto-plastic finite element analyses described in the next subsections. ABAQUS is a general-purpose finite element program for linear and non-linear structural applications. ABAQUS has been chosen for these finite element analyses, because, while it is well suited for purely linear analyses, the overall program design is dominated by features especially suited for non-linear and elasto-plastic problems.

5.2.1. Purely Elastic Finite Element Analysis

A finite element model of the surge line elbow has been built as shown in Figure 5-5. A purely elastic finite element analysis has been performed, using the computer program ABAQUS, for the following two loading conditions: in-plane bending of the elbow, and out-of-plane bending of the elbow.

The most critical stresses from these two loading cases are compared with the stresses which can be calculated by using the formulas given in Table NB-3685.1-2. From both loading conditions, the highest stress index for these maximum stresses occurs when applying in-plane bending: 2.32, using Table NB-3685.1-2, and 2.33 from the ABAQUS finite element Analysis. This verifies the ABAQUS finite element model and reinforces the fact that the formulas given in Table NB-3685.1-2 are calculating peak stresses.

5.2.2. Elasto-Plastic Finite Element Analysis

To study the influence of the peak stress on the distortion of the surge line elbow, an ABAQUS elasto-plastic finite element analysis has been performed for the same two loading conditions as in subsection 5.2.1: in-plane bending and out-of-plane bending.

In the case of in-plane bending, the highest stress in the elbow reaches the 3*Sm allowable at the loading level for which K2 * C2 is equal to 2.33. After passing this loading level, the inside and outside fibers on the elbow thickness enter the elasto-plastic domain in very localized regions of the cross-section and do not contribute further to the strength of the elbow. As a result, the surge line elbow no longer behaves in a purely elastic manner. However, when plotting these displacements as a function of the increasing loading level, it can be seen that the general distortion of the surge line elbow remains an essentially linear function of the loading level. This means that, for a reasonable range of loading above the loading level which causes initial yielding, the highest stresses at the inside and outside fibers on the elbow thickness do not contribute significantly to the distortion of the elbow. (This is because initial yielding is localized.)

In other words, these stresses are peak stresses which should be considered in the fatigue analysis, but not secondary stresses, as they do not cause any appreciable distortion. In the case of out-of-plane bending, the surge line elbow behaves in a very similar fashion as in the case of in-plane bending.

5.2.3. Calculation of a Generic Stress Index C2 for Secondary Stress in the Surge Line Elbow

The determination of the generic stress index C_2 for calculating the maximum secondary stress in the surge line elbow has been based on the fact that the secondary stress is the stress which contributes to the general distortion of the elbow. Therefore, the maximum state of stress has been linearized on the pipe cross-section, and the resulting stress at the outside fiber of the pipe cross-section is the maximum secondary stress, after an additional factor of safety is applied (using the fact that this is a displacement controlled phenomenon).

The resulting stress indices C_2 from the finite element analysis are as follows:

- For in-plane bending, $C_2 = 1.30$
- For out-of-plane bending, $C_2 = 1.58$

Therefore, the generic stress indices for the surge line elbows are: $C_2 = 1.58$ and $K_2 = 1.48$, leading to a total peak stress index $K_2 * C_2$ equal to 2.34. These stress indices have been used in the Fatigue Analysis of the surge line.

5.3 Verification of NB-3600 Equations (Equations 12 and 13, and Thermal Stress Ratcheting)

When accounting for the most critical thermal stratification cycles, the Primary Plus Secondary Stress Intensity Range, Equation 10 of NB-3653 (reference 18), exceeds the 3*Sm limit. This occurs typically for the thermal stratification cycles associated with the very high top-to-bottom temperature differences in the surge line (such as the past heatup transients). For all other thermal stratification cycles, the Equation 10 Stress Intensity Range is verified to be less than the 3*Sm limit. To be able to perform the simplified elasto-plastic fatigue analysis in accordance with NB-3600, it is necessary to verify Equations 12 and 13 of NB-3653.6, and the Thermal Stress Ratcheting Equation of NB-3653.7. These verifications (described below) are performed using the 3*Sm limit based on the ASME Code allowable yield stress for the material.

Equation 13 consists of calculating the primary plus secondary membrane plus bending stress intensity, excluding thermal expansion, and comparing the total resulting stress with the 3*Sm limit. Equation 13 stress is due to dead weight, operating pressure and Operating Basis Earthquake (OBE). The surge line does not contain any material or thickness discontinuity. Therefore, the third term of Equation 13 stress is equal to zero (no variation of modulus of elasticity and no abrupt variation of average temperature in the axial direction of the piping). Equation 13 stress has been shown to be acceptable at every surge line location for all six B&W lowered-loop plants. The maximum Equation 13 stress occurs in the elbow just below the pressurizer (elbow D) for the TMI Unit 1 surge line. It is equal to 26.8 Ksi, which is 56% of the 3*Sm limit of 48 Ksi.

The verification of Thermal Stress Ratcheting consists of comparing the highest occurring Delta T_1 range with an allowable value to be calculated in accordance with NB-3653.7 of reference 18 (Delta T_1 range is the range of the linear

through-wall temperature gradients). This verification is performed in the fatigue analysis of the surge line described in subsection 5.5. This is because the right hand side of the equation (the allowable Delta T_1 range) includes the yield strength value which has to be taken at the average fluid temperature of the transient under consideration. However, for a yield strength value taken at the maximum possible temperature in the surge line (650F), the allowable Delta T_1 range is still more than 15% higher than the maximum Delta T_1 range occurring during the thermal stratification cycles. Therefore, Thermal Stress Ratcheting is verified to be acceptable (by more than 15%).

Equation 12 consists of calculating the secondary stress range due to thermal expansion and comparing it with the 3 * Sm allowable. To do so, the internal forces and moments due to each one of the three most severe thermal stratification conditions have been compared.

Applying the thermally adjusted internal forces and moments from the most severe thermal stratification conditions, Equation 12 secondary stress has been verified at every surge line location, using the simplified ASME-Code equations and the conservative generic elbow stress indices (derived earlier), except for three elbows. These three elbows are elbows B, C and D (see Figure 3-1).

The three elbows which failed the simplified Equation 12 have been addressed via the elasto-plastic finite element analysis. For each one of these elbows, the thermally adjusted internal forces and moments from the most severe thermal stratification conditions have been applied on the elbow finite element model documented in Section 5.2. The method used to calculate the resulting maximum secondary stress was exactly the same as the one used for the generation of the generic stress index C_2 in Section 5.2.4. For these elasto-plastic finite element analyses, the 3 * Sm allowable is taken (conservatively) at the maximum possible temperature in each elbow. This maximum possible temperature is, for all three elbows B, C and D, the temperature at the top of the horizontal portion of the surge line. The maximum resulting secondary stress is calculated to be smaller than the 3 * Sm allowable.

5.4. Development of Peak Stresses

5.4.1. Peak Stresses due to Fluid Flow

The design basis transients specify the temperature data necessary for the Structural Loading Analysis documented above (subsection 5.1.5). In addition, they specify the maximum flow rate in the surge line for each time span between two consecutive PV's (either between a valley and a peak, or between a peak and a valley). Also, the maximum variation of the fluid temperature with time can be found in the design basis transients for the nozzles.

During an outsurge, the hot temperature fluid from the pressurizer flows on top of the relatively stagnant lower temperature fluid. This leads to a hot temperature flow, into a relatively cold inside wall. The maximum flow rate for the transient has been assumed to be constant for conservatism; and the variation of the fluid temperature has been taken at the highest temperature gradient given in the design basis transients for all the outsurges. The flow cross-section has been reduced to the upper portion of the inside pipe cross-section, thus maximizing the flow velocity and the through-wall temperature gradients Delta T_1 and Delta T_2. These temperature gradients occur at the top of the pipe.

During an insurge, the cold temperature fluid from the hot leg flows through the surge line. As a result, the temperature at the bottom of the pipe does not change significantly, but the top of the pipe experiences a temperature decrease from T_p (top, peak) to T_v (top, valley). Therefore, the insurge is analyzed similarly to the way the outsurge is analyzed: cold temperature flow, into a relatively hot inside wall. The maximum flow rate for the transient has been assumed to be constant for conservatism; and the variation of the fluid temperature has been taken at the highest temperature gradient given in the design basis transients for all the insurges. The flow cross-section is the whole inside cross-section of the pipe. (Buoyancy is minimal since hot leg water has approximately the same temperature as the water at the bottom of the pipe.) The maximum through-wall temperature gradients Delta T_1 and Delta T_2 occur at the top of the pipe.

The Peak Stress Intensity Range is a direct function of the through-wall temperature gradients Delta T_1 and Delta T_2. (NB-3600 Equation 11). Both the

insurges and the outsurges have been utilized to obtain the total Peak Stress Intensity Range.

The through-wall temperature gradients Delta T_1 and Delta T_2 calculated as described above are very conservative. This is due to the fact that, for both the outsurges and the insurges, all temperature data, flow rates and fluid temperature variations are taken at their conservative extreme values (either maximum or minimum). Also, no consideration has been given to the loss of temperature as a result of thermal conduction around the pipe cross-section (which would mitigate the effect of the extreme fluid temperature ramp assumed).

5.4.2. Peak Stresses due to Thermal Striping

The thermal striping temperature data are given in the design basis transients. These temperature data are maximum inside wall temperature ranges occurring in the region of the fluid interface centerline.

To calculate the temperature distribution through the thickness of the surge line at different points in time, a mathematical model has been built, using the Finite Element program ANSYS. The time-dependent wall temperature has been simulated as a "cut-sawtooth" wave which is very close to a sine wave. From the experimental thermal striping work described in Section 4.3, it is known that the thermal striping fluctuations have a period of approximately 1.0 second. Therefore, a sensitivity analysis is performed to determine for which thermal striping period the peak stress intensity range is the highest. The thermal striping periods considered in this sensitivity analysis are 0.5, 1.0, 2.0 and 4.0 seconds, to cover the entire range of periods which could be expected.

For each thermal striping period studied, the ANSYS computer-run produces time-dependent temperature profiles through the pipe thickness. There are two extreme temperature profiles: one above the average temperature and with the inside wall temperature reaching a maximum, and the other below the average temperature and with the inside wall temperature reaching a minimum. For these two temperature profiles, the linear and non-linear through-wall temperature gradients have been calculated, leading to the maximum peak stress intensity range.

This evaluation has been repeated for each one of the four thermal striping periods. It is found that there is not one most critical thermal striping period. This is because the maximum peak stress intensity range is a function of the

stress index K_3 which acts on the peak stress contribution from the linear through-wall temperature gradient Delta T_1, but not on the one from the non-linear through-wall temperature gradient Delta T_2 (which does not have any stress index). For a stress index K_3 equal to 1.7 (girth butt welds, as-welded), the most critical period is 4.0 seconds, because the higher the period, the greater the linear temperature gradient Delta T_1 is. On the other hand, for K_3 equal to 1.0 (locations remote from welds), the most critical period is 0.5 seconds. In that case, the maximum peak stress is the so-called "skin stress", due to Delta T_2 (in the surge line, 1.7 and 1.0 are the only two possible values for K_3).

For the Fatigue Analysis of the surge line, the peak stress intensity range due to thermal striping has been taken at its maximum possible value: at the as-welded locations, it is the peak stress intensity range corresponding to a striping period of 4.0 seconds; and at the locations remote from welds, it is the peak stress intensity range corresponding to a striping period of 0.5 second.

5.4.3. Peak Stresses Due to the Non-Linearity of the Temperature Profile

As already mentioned in subsection 5.1.3, the top-to-bottom temperature profile on the pipe cross-section is not linear. In the Structural Loading Analysis of the surge line, the "equivalent linear" temperature profile has been applied for the generation of the internal forces and moments. The difference between the actual non-linear and the "equivalent linear" temperature profiles is a relatively small temperature difference which is referred to as the Delta T_4 temperature difference. It causes a peak stress very similar to the one produced by the non-linear through-wall temperature gradient Delta T_2.

The two most severe measured top-to-bottom temperature profiles have been analyzed (see subsection 5.1.3). These two measured top-to-bottom temperature profiles have been selected for their particularly non-linear shapes. Therefore, these non-linear shapes will lead to the highest possible temperature differences Delta T_4. To better study the influence of Delta T_4 on the localized state of stress in the pipe, an ABAQUS Finite Element model has been built (reference 19); and the temperature differences have been applied as input. The ABAQUS Finite Element analysis is performed for each one of the two measured top-to-bottom temperature profiles.

From the two ABAQUS Finite Element analyses, it has been found that the maximum peak stress intensity occurs at the inside radius of the pipe cross-section. This maximum peak stress intensity takes into account all localized effects in the pipe cross-section, including the localized bending on the pipe thickness.

A correlation has been developed to calculate the maximum temperature difference Delta T_4, as a function of the top-to-bottom temperature difference and the elevation of the fluid interface centerline, and give the maximum peak stress intensity in the pipe cross-section, as a function of the maximum temperature difference Delta T_4, the top-to-bottom temperature difference and the elevation of the fluid interface centerline.

5.5. Fatigue Analysis of the Surge Line.

As described in Section 5.3, Equations 12 and 13 of NB-3653.6 and the Thermal Stress Ratcheting Equation of NB-3653.7 have been verified to be acceptable. Therefore, the fatigue analysis of the surge line can be performed in accordance with NB-3653.6(c). The verification of Equations 12 and 13, the Thermal Stress Ratcheting verification, and the fatigue analysis of the surge line have been performed in accordance with the 1986 Edition of NB-3600. This is a requirement of NRC Bulletin 88-11: "Fatigue Analysis should be performed in accordance with the latest ASME Section III requirements incorporating high cycle fatigue" (reference 1). A Code reconciliation has been performed to remove all concerns associated with using the later Code (1986 Edition) for this fatigue stress analysis. For this Code reconciliation, each plant's surge line stress report has been reviewed (the code of record for piping analysis is not the same for all the surge lines). The Code reconciliation has shown that:

1) research performed since the publication of the B-31.7 USA Standards (1968 and 1969) has led, in general, to more sophisticated mathematical formulas for the stress indices,

2) the allowables used in this final analysis are either equal to or smaller than the ones used in the original stress reports (therefore, the allowables used in this final analysis are conservative),

3) the fatigue analysis of the surge line incorporates the fatigue curves up to 10^{11} cycles, in comparison with the fatigue curves of the B-31.7 USA Standards (which are restricted to 10^6 cycles, and therefore do not

contribute any additional fatigue usage for relatively low alternating stresses).

For each of the thermal stratification peaks and valleys from the design basis transients, the total Equation 11 peak stress intensity has been calculated. The complete "loading map" for the peak stress intensity values is as follows:

- Moment loadings due to thermal stratification ("Equivalent linear" top-to-bottom temperature difference),
- Internal pressure in the surge line,
- The additional localized peak stress due to the non-linearity of the top-to-bottom temperature profile, and
- The maximum stress (for a given thermal stratification condition) between the peak stress due to thermal striping and the one due to Fluid Flow. The maximum is used, because these two peak stress intensities occur at two different locations in the pipe cross-section during the same thermal stratification condition (in the region around the fluid interface centerline for thermal striping and at the top of the pipe for the Fluid Flow conditions). This maximum peak stress intensity is added for the thermal stratification peaks and subtracted for the thermal stratification valleys.

A sort of all the total peak stress intensity values has been performed, and a selection table has been built for the combination of the thermal stratification peaks and valleys into pairs. This selection table is built in such a way that the peak stress intensity ranges are maximized.

For each pair of thermal stratification conditions (one peak and one valley), the alternating stress intensity (Sa) has been calculated, as a function of the peak stress intensity range and of Equation 10 primary plus secondary stress intensity range. The usage factor associated with the Sa value has been calculated, using the "extended" fatigue curves of the ASME-Code, Section III, Appendix I (up to 10^{11} cycles). A summation of all usage factors on all pairs of thermal stratification conditions has resulted in the main fatigue usage. This main fatigue usage includes all the thermal stratification conditions characterized

by a top-to-bottom temperature difference. Also, the surge line internal moments due to an Operating Basis Earthquake have been added conservatively to the most critical thermal stratification internal moments, for consideration of future OBE occurrences.

As required by ASME-Code NF -3600, all stress intensity ranges from the different contributions given in the "loading map" above have been combined to generate the maximum total stress intensity range to be used for fatigue.

Also, as part of this fatigue analysis, the Thermal Stress Ratchet has been verified to be acceptable, in accordance with NB-3653.7. This verification is performed for every range of linear through-wall temperature gradients (Delta T_1 range).

The following fatigue contributions have been added to the main fatigue usage:

- Fatigue due to highly cyclic thermal striping ranges. The design basis transients define, for each event, the number of occurrences of each thermal striping range.
- Fatigue due to the future Operating Basis Earthquake ranges (cycles which are not associated with the thermal stratification events).
- Fatigue due to additional Fluid Flow conditions which are not associated with significant thermal stratification conditions.

The fatigue usage factor due to the highly cyclic thermal striping ranges has been found to be in the following ranges: between 0.10 and 0.15 at the locations with a stress index K_3 equal to 1.7 (girth butt welds, as welded), and between 0.06 and 0.09 at the locations with a stress index K_3 equal to 1.0 (locations remote from welds). The reason for the 50% difference between the extreme values in each range is the fact the number of design transients is not the same for each B&W lowered-loop plant.

The fatigue usage factors associated with the future OBE cycles and with the additional fluid flow conditions are very small. However, in order to complete the total fatigue picture, they have been added to the sum of the usage factors from the main fatigue and from the highly cyclic thermal striping ranges.

5.6. Fatigue Analysis Results for the Surge Line

Table 5-1 is a plant-specific table of the total fatigue usage factors for a 40 year plant life (including past and future fatigue). This table is plant-specific because the number of occurrences of the events defined in the design basis transients is unique to each B&W lowered-loop plant.

Table 5-1. Specific Total Fatigue Usage Factors for the Surge Line

Surge Line Locations	Oconee Unit 1	Oconee Unit 2	Oconee Unit 3	CR-3	ANO-1	TMI-1
Most Critical Straight	0.48	0.48	0.47	0.37	0.38	0.38
Most Critical Elbow	0.79	0.82	0.76	0.64	0.66	0.65
Second Most Critical Elbow	0.76	0.79	0.75	0.60	0.60	0.61
Drain Nozzle Branch	0.35	0.37	0.33	0.25	0.26	0.25

(See Section 6 for the pressurizer surge nozzle and the surge line / hot leg nozzle).

All total fatigue usage factors are smaller than their allowable of 1.0. The highest cumulative damage is 0.82 (this value is for Oconee Unit 2).
The most critical locations are the same for all six surge lines: the highest cumulative damage occurs in the vertical elbow at the bottom of the surge line riser (elbow B); and the second highest cumulative damage occurs in the vertical elbow just below the pressurizer (elbow D). Elbows B and D are indicated in Figures 3-1 and 5-1.

Figure 5-1. Surge Line Mathematical Model

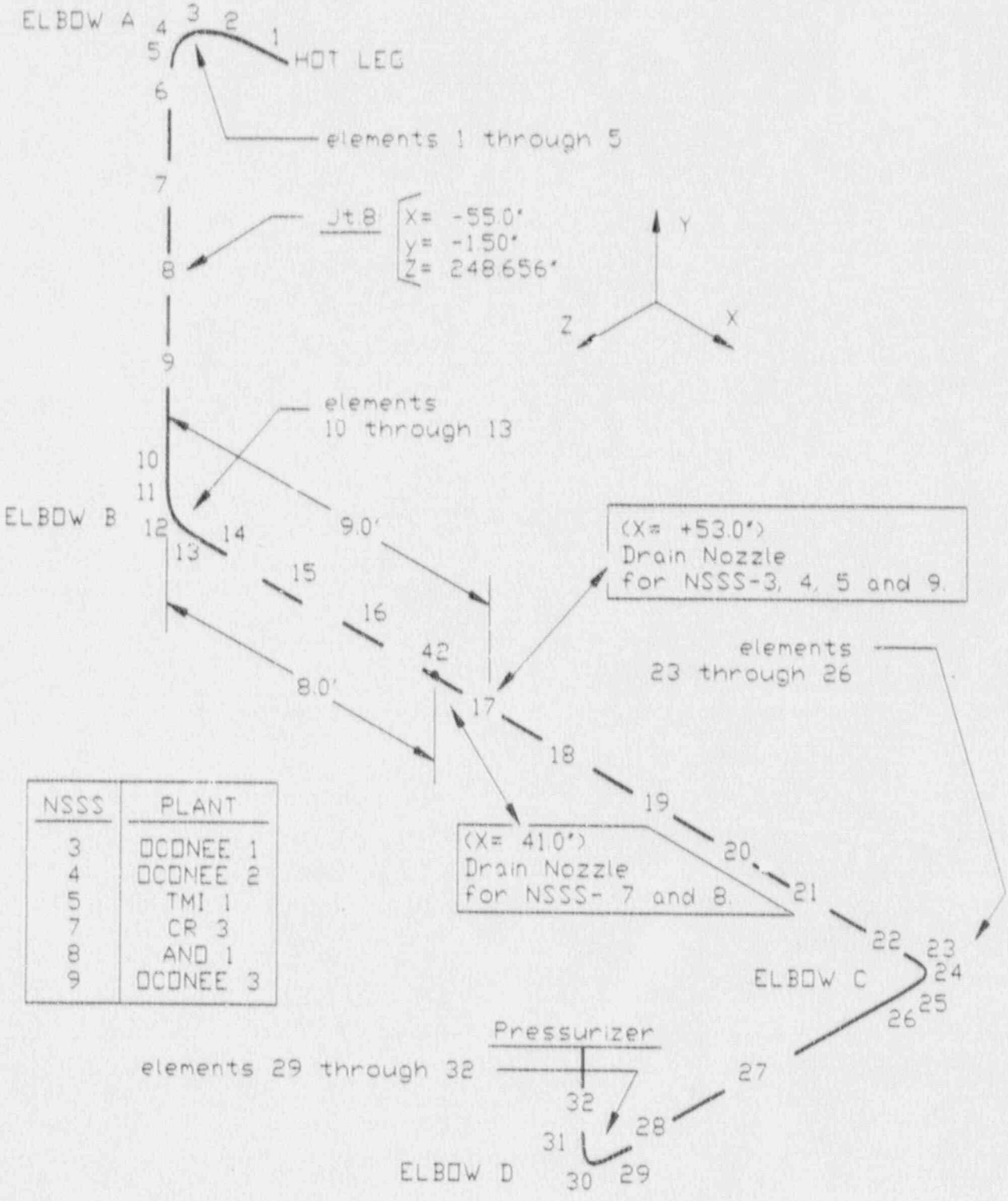

NSSS	PLANT
3	OCONEE 1
4	OCONEE 2
5	TMI 1
7	CR 3
8	ANO 1
9	OCONEE 3

Figure 5-2. Comparison of Surge Line Displacements, X - direction
(Calculated vs. Measured with DT=280F)

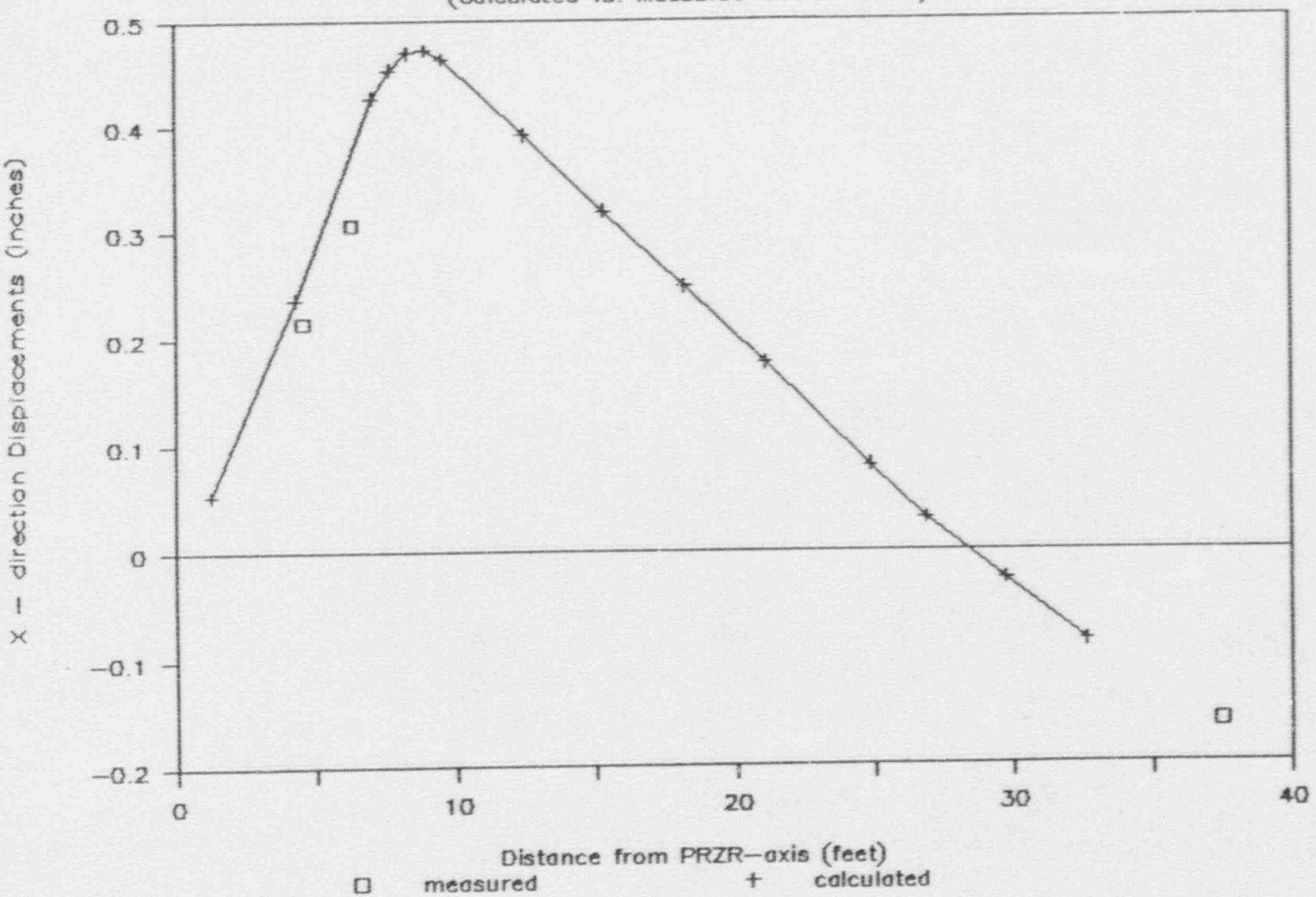

Figure 5-3. Comparison of Surge Line Displacements, Y - direction
(Calculated vs. Measured with DT=280F)

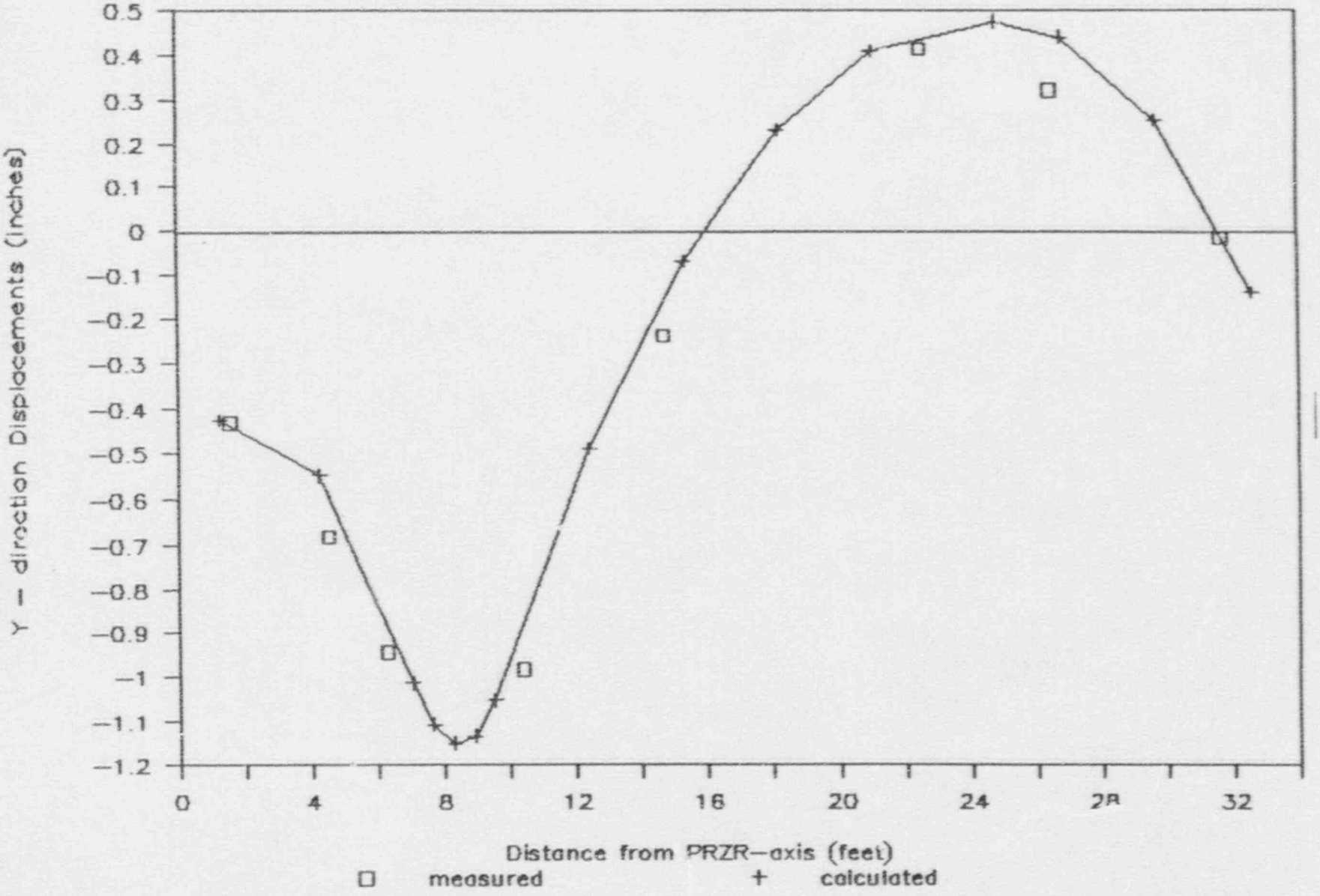

Figure 5-4. Comparison of Surge Line Displacements, Z - direction
(Calculated vs. Measured with DT=280F)

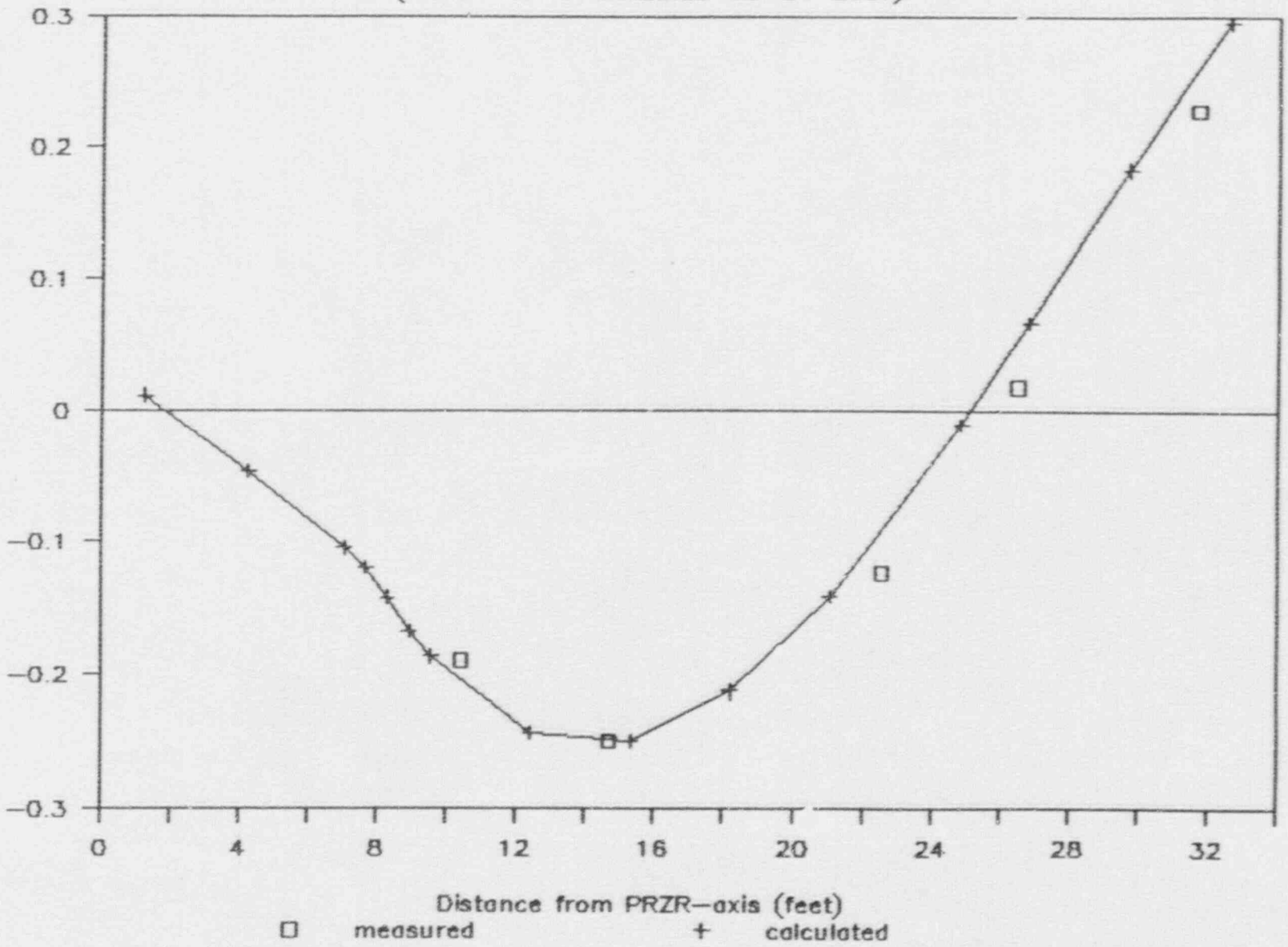

Figure 5-5. Finite Element Model of Surge Line Elbow

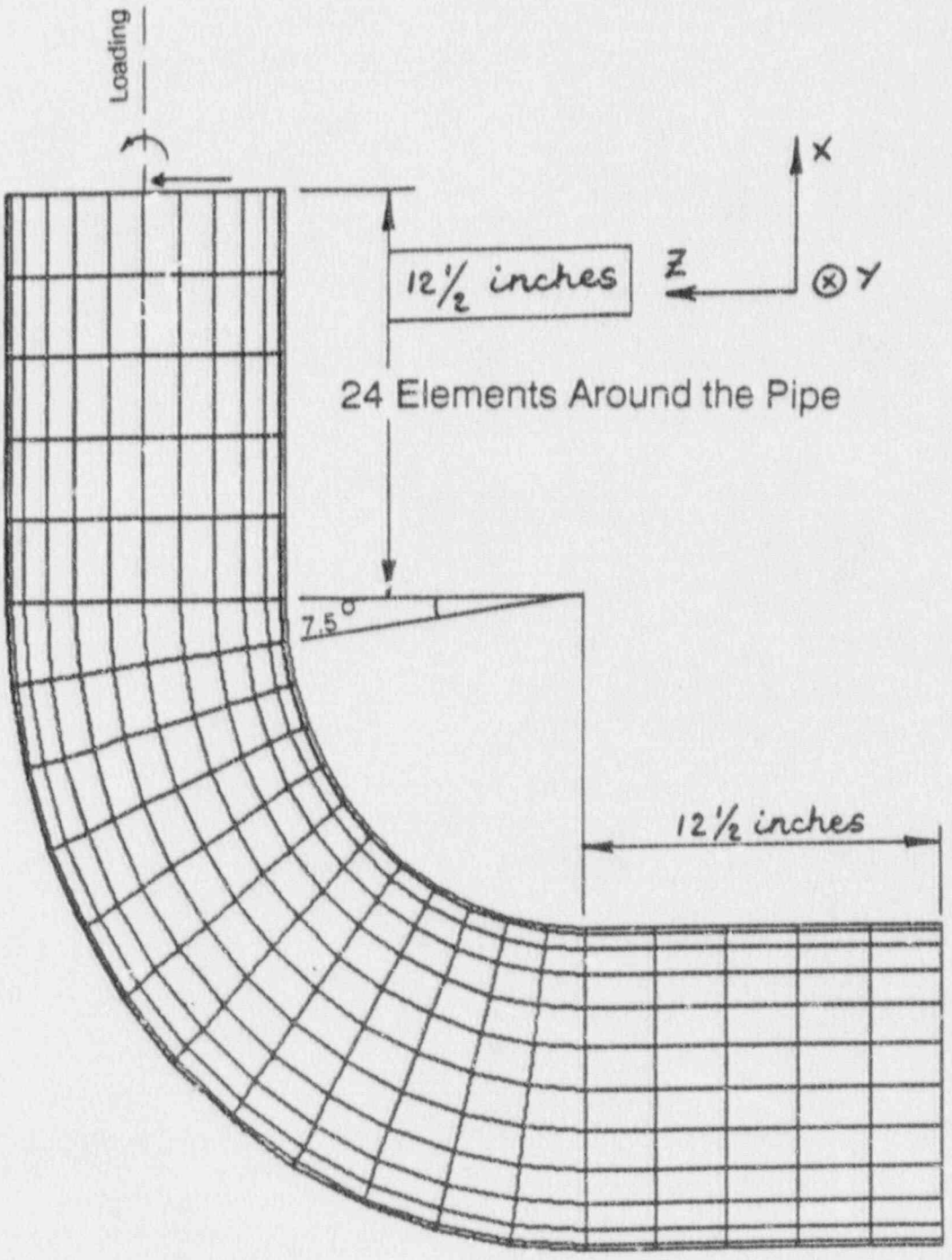

6. NOZZLE ANALYSES

In addition to the structural analysis of the surge line described in Section 5, detailed stress analyses of the pressurizer and hot leg nozzles have been performed to demonstrate compliance with the requirements of the ASME Code, Section III. The thermal and pressure parameters for each nozzle are described in the design basis transients of Section 4.5. In addition, each nozzle is subjected to piping loads from the surge line itself. These loads have been taken from the piping analysis described in Section 5 and the resulting stresses have been combined with those from pressure and thermal loadings.

Detailed descriptions of the analyses of the pressurizer surge nozzle and of the surge line to hot leg nozzle are contained in the following sections. The analysis of the surge drain nozzle is part of the surge line structural analysis described in Section 5 (Table 5-1 gives the total fatigue usage for the surge drain nozzle of each plant).

6.1. Pressurizer Surge Nozzle

The purpose of this section is to describe the evaluation of the pressurizer surge nozzle. The analysis of the nozzle, safe end, and safe end-to-pipe weld has been performed using the finite element method as implemented by the "ANSYS" computer code, Reference 17. The loads used for evaluation were the thermal and pressure loads identified in the design basis transients for the surge line [illegible]cation (see Section 4.5). The acceptance criteria for the evaluation [illegible]e requirements for Class 1 components of the ASME B&PV code, Section III, [illegible] edition with no Addenda, reference 18. The safe end, nozzle, and [illegible]urizer head were evaluated using the requirements of NB-3200. The safe end-to-elbow weld was evaluated to the requirements of NB-3600.

6.1.1. Geometry

The pressurizer surge nozzle is shown in Figure 6-1 and consists of a carbon steel nozzle welded to the carbon steel lower head. Both the nozzle and pressurizer head are clad with stainless steel to prevent reactor coolant fluid from contacting the carbon steel base metal. The nozzle and head are also protected from thermal shock by a stainless steel thermal sleeve.

A stainless steel safe end is welded to the end of the surge nozzle and then welded to the stainless steel surge line piping in the field. The weld between the safe end and pipe is critical since it is in the "as-welded" condition and requires special consideration (stress indices) in the stress evaluation.

6.1.2. Description of Loadings

The loadings on the pressurizer surge nozzle consist of thermal gradients, internal pressure, and external piping loads. Since the pressurizer surge nozzle is vertically oriented, there are no significant thermal stratification loads (ie. temperature gradients from one side of the nozzle to the other).

The thermal gradients are caused by the various temperature swings (peaks and valleys) associated with the in- and out- surges of fluid between the pressurizer and the RC pipe. The temperature swings are defined in the design basis for the surge line. The thermal gradients and stresses due to these temperature swings are determined using the ANSYS finite element code.

The RC system pressure is applied to the internal surfaces of the nozzle, safe end, and head. The pressures are defined in the design basis and the resulting stresses are determined using ANSYS.

There are significant external loads developed due to the heating and cooling of the surge line as well as the stratification in the surge line. The external loads, forces and moments, for each peak and valley are given in the documentation of the surge line analysis. The stresses due to these moments are calculated using classical solutions (e.g. Mc/I).

6.1.3. Discussion of Analysis

An axisymmetric thermal and thermal stress analysis has been performed using the ANSYS finite element computer code. The transient thermal analysis consists of imposing time dependent boundary conditions (bulk fluid temperatures and heat

transfer coefficients) on the finite element model. Nodal temperatures from the thermal analysis have been stored on magnetic tape for each iteration (time step) of the transient. The ANSYS postprocessor "POST 26" has used the nodal temperatures to calculate Delta-T's between various locations in the structure. Tables of the Delta-T's versus time for each transient have been used to determine when the maximum and minimum stresses are likely to occur. The nodal temperatures for each critical time step are input to the ANSYS stress routine for the determination of stresses. The ANSYS postprocessor, "POST 11", has been used to linearize the stresses at critical sections of the structure. Pressure stresses at the critical sections have also been determined using ANSYS and POST11. Stresses due to external loads are hand calculated and combined with the thermal and pressure stresses for comparison to ASME code allowables.

Due to the large number of temperature swings (peaks and valleys) associated with the thermal stratification transients it was not practical to evaluate each peak and valley as an individual case. Instead, a few "base cases" were created to envelop the large number of identified peaks and valleys. The base cases were chosen to cover both up and down ramps, various starting temperatures, various ramp rates, and various changes in temperature (Delta-T). The temperature distribution and resulting thermal stresses for each of the base cases have been determined using the procedure described above. A summary of the parameters used in the base cases and the resulting stresses is given in Table 6-1. The actual transients identified in the design basis were reviewed and each peak and valley have been assigned a representative "base case". The selection of "base case" was such that the starting temperature, ramp rate, and Delta-T of the actual transient were bounded by those of the "base case". The linear and maximum thermal stresses from the chosen "base case" have been used directly for combining with stresses due to pressure and external loads.

Pressure stresses for a base case with an internal pressure of 2200 psi have been determined using ANSYS. The pressure stresses for each peak and valley have been determined by multiplying the stresses from the base case by the ratio of the actual pressure for the peak or valley from the design basis to the pressure used in the pressure base case (2200 psi).

The external load stresses for each peak and valley have been determined by taking the moments from the surge line evaluation at the time nearest the peak

or valley and calculating the resulting stress using classical solutions (e.g. Mc/I).

The thermal, pressure, and external load stresses have been multiplied by the appropriate stress indices (Table NB-3681(a)-1) or stress concentration factors and then combined for determination of maximum stress and fatigue usage. The results are given in Section 6.1.7.

6.1.4. List of Assumptions/Inputs Used in Analysis

1) Since the surge line elbow is a 3D structure it cannot be included in an axisymmetric model, therefore it has been modeled as a straight pipe. This change should have a negligible effect on the resulting stresses in the safe end-to-elbow weld. The actual stresses in the elbow have been considered in the evaluation of the surge line, Section 5.0.

2) Because the exact fluid boundary conditions on the inside surface of the lower head are difficult to determine, it has been assumed that the fluid boundary conditions (fluid temperature) are similar to those in the surge nozzle. In other words, the cold fluid entering the pressurizer has been assumed to fall to the bottom where it contacts the lower head.

3) The outside of the lower head, nozzle, and piping have been assumed to be fully insulated (no heat loss).

4) It has been assumed that the water between the thermal sleeve OD and nozzle ID is stagnant (no flow of water behind thermal sleeve).

5) The nozzle and pressurizer head are assumed to be at a uniform temperature at the beginning of each up ramp (peak) or down ramp (valley). This is conservative since it maximizes the radial and axial gradients in the structure. Example: For an up ramp from 250F to 550F, the ramp begins with the nozzle and head at 250F.

6) The fluid temperature ramp rate (F/Hr) used in the analysis has been the maximum ramp rate at any time throughout the temperature change as defined in the design basis.

7) The stress indices from Table NB-3681(a)-1 for an "as-welded transition" have been used in the evaluation of the safe end-to-elbow weld.

8) The OBE seismic events have been assumed to occur at steady state conditions and not at the point of maximum or minimum transient stress. Even if an event were to occur during a time of maximum transient stress, the effect on fatigue usage for only one occurrence of OBE would be minimal.

6.1.5. Thermal Analysis

An axisymmetric heat transfer analysis using the finite element code ANSYS has been performed to obtain the temperature distributions in the nozzle, safe end, welds, and pressurizer head. The thermal transients evaluated are those specified in the design basis and discussed in Section 6.1.5.1. The resulting nodal temperatures from the thermal analysis have been used as input to the stress analysis.

The finite element model of the pressurizer surge nozzle is shown in Figure 6-2. The nozzle, safe end, welds, and pressurizer head are represented by isoparametric quadrilateral thermal elements, STIF 55. The required inputs for this element are four nodal points and material properties: thermal conductivity, density, and specific heat.

6.1.5.1. Selection of Transients

The operating transients for the surge line (and nozzles) have been identified in the design basis for the surge line and discussed in Section 4.5. A review of the transients revealed a significant number of temperature fluctuations during each transient. The temperature fluctuations involved approximately 70 different peaks or valleys per heatup and cooldown transient. The fluctuations include temperature changes from approximately 50 to 450 degrees F. An example of one of these transients, HU1A1, is shown in Figure 6-3. As previously stated, an evaluation of each peak and valley is not practical, therefore only a few cases are considered. These cases are referred to as "base cases" and have been selected to insure all peaks and valleys have been enveloped. A summary of the base case parameters and resulting stresses is given in Table 6-1.

6.1.5.2. Thermal Boundary Conditions

The thermal boundary conditions consist of convective heat transfer at the inside surfaces of the pipe elbow, safe end, thermal sleeve, and pressurizer head.

Because of the low velocities (generally less than 0.5 ft/sec) associated with the in- and out- surges, the heat transfer is by natural convection and is caused by the difference in temperature between the metal surface and the reactor coolant fluid. The film coefficient versus Delta-T is input in tabular form to the ANSYS thermal runs. ANSYS uses the actual surface-to-fluid Delta-T at each time step (iteration) to determine the appropriate film coefficient. A sample of the film coefficients for the various regions of the model is given below.

REGION	LOCATION	FILM COEF. (BTU/Hr-Ft^2-F)
1	LOWER HEAD	288
2*	BEHIND THERMAL SLEEVE COLLAR	145
3*	BEHIND THERMAL SLEEVE, WATER REGION	19
4*	BEHIND THERMAL SLEEVE, CONTACT ROLL	225
5	SAFE END AND PIPE, BEYOND SLEEVE	465

* Effective film coefficient, takes into account thermal resistance of thermal sleeve, contact pressure, and water behind sleeve.

The outside surfaces of the pipe elbow, safe end, nozzle, and pressurizer head have been assumed to be fully insulated. In addition, for symmetry, the ends of the pipe elbow and head have been assumed to be insulated.

A summary of the thermal boundary conditions is shown in Figure 6-4.

6.1.5.3. Results of Thermal Analysis

The results of the thermal analysis are in the form of nodal temperatures. These nodal temperatures are read into the thermal stress analysis and provide the model with the axial and radial thermal gradients that produce the thermal stress. The times at which the maximum gradients occur are used for the thermal stress analysis since they will produce the maximum stresses. To determine when the maximum gradients occur the ANSYS postprocessor, POST 26, has been used. POST 26 provides a time history of the gradients at defined locations for the duration of the transient. For the surge nozzle evaluation fifteen pairs of nodes have been used to examine the thermal response (Delta-T) of the structure. The locations of these 15 node pairs are shown in Figure 6-5. Since all the

transient peaks and valleys are defined by a fluid temperature ramp, the maximum thermal gradients (and maximum stress) occur at the end of the applied ramp.

6.1.6. Stress Analysis

An axisymmetric stress analysis using the finite element code ANSYS has been performed to obtain the stress distribution in the pipe, safe end, nozzle, and pressurizer head. The loadings for the analysis are the nodal temperatures from the thermal analysis (Section 5.1.5) and pressures from the design basis.

6.1.6.1. Description of Finite Element Model

The finite element model used for the thermal analysis has also been used for the stress analysis. The only difference between the two models is the element type designation. The nozzle, safe end, welds, and pressurizer head are represented by isoparametric quadrilateral stress elements, STIF 42. The model representing these components is the same as that shown in Figure 6-2. The required inputs for this element are four nodal points and material properties: density, coefficient of thermal expansion, Young's Modulus, and Poisson's ratio.

6.1.6.2. Structural Boundary Conditions

The structural boundary conditions applied were required to simulate those portions of the structure that had not been modeled. The end of the model representing the pressurizer head has been restrained from motion in the meridional direction (UY displacement = 0.0). This restraint simulates the restraint of the adjacent head material. The nodes at the end of the pipe (elbow) have been coupled together in the axial direction for symmetry. A summary of these boundary conditions is shown in Figure 6-6.

6.1.6.3. Selection of Transient Times

As stated in Section 6.1.5.3, the selection of transient times for use in the stress analysis is dependent upon the thermal gradients through the structure. The thermal gradients cause differential growth between adjacent material which results in thermal stresses. The times at which the maximum radial and axial gradients (Delta-T) occur have been evaluated for stress. The results of the analysis shows that the radial gradient was the major contributor for maximum stress and almost always occurs at the end of the defined thermal ramp.

6.1.6.4. Finite Element Stress Results

The results from the ANSYS stress runs were not in a format which can be directly compared to ASME code allowables. In order to get stresses compatible with the ASME code requirements it was necessary to use the ANSYS postprocessor POST 11. POST 11 performs stress linearization by converting the non-linear through-wall stress distributions into the stress components required for an ASME code evaluation: membrane stress, bending stress, and peak stress. The pertinent information about the linearization methods and detailed input is given in Section 6.31 of the ANSYS users manual. Eleven stress classification lines (SCL) have been selected to evaluate stresses in the various regions of the model. The line locations are shown in Figure 6-7. After being combined, the linearized stresses have been used to compare to the ASME code limit for the range of primary-plus-secondary stress intensities (3*Sm limit). An example of the linearized thermal and pressure stresses for the various "base cases" evaluated is shown in Table 6-1. The tabulated stresses are those for the safe end-to-elbow weld, SCL 10.

Also contained in Table 6-1 are the maximum stresses for the different "base cases". The maximum stresses represent the stresses at the surface of the component and are given in the ANSYS element stress printout as the element surface stress. When combined, the maximum stresses are used in the evaluation for fatigue usage.

6.1.6.5. ASME Code Calculations

The linearized thermal, pressure, and external load stresses for each peak and valley were multiplied by the appropriate stress indices and combined to obtain the total linearized stress. The linearized stresses for all peaks and valleys have been tabulated and the difference between the maximum and minimum linearized stresses have been used for comparison to the ASME code limit of 3Sm. A sample of the linearized stresses for HU1A1 at the safe end-to-elbow weld is given in Table 6-2. When the 3Sm limit has been exceeded, NB-3228.5 "Simplified Elastic-Plastic Analysis" has been used to justify the stress conditions.

The maximum thermal, pressure, and external load stresses for each peak and valley have been multiplied by the appropriate stress indices or stress concentration factor and combined to obtain the total maximum stress. The

maximum stresses for all peaks and valleys have been tabulated for evaluation of fatigue. A sample of the maximum stresses for HU1A1 at the safe end-to-elbow weld is given in Table 6-3.

The fatigue evaluation took into account the number of cycles for each peak and valley, the maximum stress ranges, the linearized stress range associated with the maximum stress range, and the resulting Ke factor for the maximum stress range when the linearized stress range exceed the 3Sm allowable.

The maximum linearized stress and fatigue usage factor for both the stainless steel and carbon steel portions of the surge nozzle are given in Section 6.1.7. All stresses and fatigue usage factors meet the ASME code limits.

6.1.7. Summary of Results and Conclusion

A summary of results for the pressurizer surge nozzle evaluation is given in the following table. Although the 3Sm limit is exceeded for both the carbon steel and stainless steel, the requirements of the ASME code have been satisfied by performing a "Simplified Elastic-Plastic Analysis" as defined in NB-3228.5 of the code.

PRESSURIZER SURGE NOZZLE CALCULATED FATIGUE USAGE FACTORS						
LOCATION	Oconee Unit 1	Oconee Unit 2	Oconee Unit 3	TMI-1	CR-3	ANO-1
SAFE END-TO-ELBOW WELD (STAINLESS STEEL)	.40	.41	.41	.33	.32	.32
NOZZLE-TO-HEAD CORNER (CARBON STEEL)	.35	.35	.35	.32	.32	.32

In conclusion, the pressurizer surge nozzle, safe end, and safe end-to-elbow weld meet the requirements for Class 1 components of the ASME code, Section III, 1986 Edition with no Addenda for the revised design basis transients discussed in Section 4.5.

6.2. Hot Leg Surge Nozzle

The purpose of this section is to describe the evaluation of the hot leg surge nozzle. The stress analysis of the nozzle and nozzle-to-surge line weld has been performed using the finite element method as implemented by the "ANSYS" computer code, reference 17. The loads used for evaluation were the thermal and pressure loads identified in the design basis transients for the surge line stratification (see Section 4.5). The acceptance criteria for the evaluation were the requirements for Class 1 components of the ASME B&PV code, Section III, 1986 edition with no Addenda, reference 18. The nozzle and nozzle-to-surge line weld were evaluated using the detailed requirements of NB-3200 as permitted by NB-3600.

6.2.1. Geometry

An axisymmetrical representation of a small segment of the surge line, hot leg surge nozzle, and hot leg is shown in Figure 6-8 with an effective radius for the sphere (hot leg) equal to 3.2 times the hot leg pipe radius. The 3.2 to 1 equivalent spherical vessel is a modeling technique recommended by reference 20. Using the 3.2 factor instead of the more common 2.0, assures that the maximum pressure stress at the critical location in the nozzle is adequately predicted by the axisymmetric model. This modeling technique is conservative for predicting the membrane stress but is accurate for predicting the maximum stress in the critical locations for use in a fatigue analysis. This piping junction consists of a carbon steel nozzle welded to the carbon steel hot leg. Both the nozzle and hot leg are clad with stainless steel to prevent reactor coolant fluid from contacting the carbon steel base metal.

6.2.2. Description of Loadings

The loadings on the hot leg surge nozzle consist of thermal gradients, internal pressure, and external piping loads.

The thermal gradients are caused by the various fluid temperature swings (peaks and valleys) associated with the in- and out- surges of fluid between the pressurizer (hot) and the hot leg pipe (cold). The surge line fluid becomes stratified near the hot leg nozzle producing circumferential temperature gradients and thermal striping which are in addition to the axisymmetric (radial and longitudinal) temperature gradients produced by the transient. Also, the

temperature differential between the surge line fluid and the hot leg fluid contribute to these temperature gradients. The temperature swings for the surge nozzle and hot leg fluids are defined in the design basis for the surge line. The thermal gradients and stresses due to these temperature swings are determined using the ANSYS finite element code.

The RC system pressure is applied to the internal surfaces of the nozzle and hot leg pipe. The pressures are defined in the design basis and the resulting stresses are determined using the ANSYS finite element code.

There are significant external loads developed due to the heating and cooling of the surge line as well as the stratification in the surge line. The external loads, forces and moments, for each peak and valley are given in the documentation of the surge line analysis. The stresses due to these moments and forces are calculated using the ANSYS finite element code.

6.2.3. Discussion of Analysis

In a typical fluid temperature spike, the top fluid in the nozzle will have a larger temperature change than the bottom fluid. Thus, for the determination of the radial and longitudinal temperature gradients and the associated thermal stress, it is conservative to use an axisymmetric analysis with the top fluid as the fluid boundary. An axisymmetric thermal and thermal stress analysis has been performed using the ANSYS finite element computer code. The transient thermal analysis consists of imposing time dependent boundary conditions (bulk fluid temperatures and heat transfer coefficients) on the finite element model. Nodal temperatures from the thermal analysis are stored on magnetic tape for each iteration (time step) of the transient. The ANSYS postprocessor "POST 26" uses the nodal temperatures to calculate Delta-T's between various locations in the structure. Tables of the Delta-T's versus time for each transient are used to determine when the maximum and minimum stresses are likely to occur. The nodal temperatures for each critical time step are input to the ANSYS stress routine for the determination of stresses. The ANSYS postprocessor, "POST 11", is used to linearize the stresses at critical sections of the structure. Stresses due to pressure and resultant external force (along the nozzle axis) are also determined at the critical sections using ANSYS and POST11.

Due to the large number of temperature swings (peaks and valleys) associated with the thermal stratification transients it was not practical to evaluate each peak and valley as an individual case. Instead, a few "base cases" were created to envelop the large number of identified peaks and valleys. The base cases were chosen using the following parameters; the maximum instantaneous ramp rate for the top fluid temperature excursion in the stratified nozzle, the hot leg temperature, the convective heat transfer coefficients for the nozzle and hot leg, and the top fluid temperature change (Delta-T) between a peak and valley in the nozzle. The temperature distribution and resulting thermal stresses for each of the base cases were determined using the procedure described above. A summary of the parameters used in the base cases is given in Table 6-4. Parameters describing the actual transients identified in the design basis were used to determine a representative base case for each peak and valley which will now approximate the actual transient. The linearized and maximum thermal stresses from the chosen "base case" were used directly for combining with stresses due to pressure, resultant external force, and non-axisymmetic load stresses.

Pressure stresses for a base case with an internal pressure of 1000 psi were determined using ANSYS. The pressure stresses for each peak and valley were determined by multiplying the stresses from the base case by the ratio of the actual pressure for the peak or valley from the design basis to the pressure used in the pressure base case.

The stresses due to a axial load of 10^5 lbs were determined using ANSYS. The axial load stresses for each peak and valley were determined by multiplying the stresses from the base case by the ratio of the axial force from the surge line evaluation at the time nearest the peak or valley to the force used in the base case.

As described above, the thermal analysis performed is axisymmetric in that it assumes that the top fluid completely fills the nozzle and creates the two-dimensional axisymmetrical temperature fields in the nozzle for the various thermal transients. The task now is to determine the additional stresses due to circumferential temperature gradients produced by the fluid stratification in the nozzle. The stresses due to this fluid stratification will conservatively be assumed to occur at the time of maximum thermal stresses due to the radial and longitudinal temperature gradients.

The stresses due to thermal stratification are determined for two base cases by use of the ANSYS harmonic element STIF 25. This element is used for two-dimensional modeling of an axisymmetric structure with nonaxisymmetric loading. In the case being considered, the nonaxisymmetric loading is the temperature field in the nozzle which varies in the circumferential direction as well as in the radial and axial directions. The stresses due to a circumferential temperature gradient are independent of the radial and axial gradients. These stresses are primarily a function of the temperature difference between the top and bottom fluid and the transition zone between the two fluid temperatures.

The circumferential temperature gradient is approximated by assuming the top and bottom of the nozzle are at a steady state condition for a thermal peak and valley, respectively. The transition between these two temperature fields is assumed to be linear over the same 1" height of nozzle that contains the fluid interface zone between the hot and cold fluid. From the design basis, the centerline elevation of this interface zone in the hot leg nozzle, relative to the centerline of the nozzle, varies from 0.0" to -3.88" during the various PV temperature excursions. The elevation (Z) of the interface zone is assumed to be at 0.0" for actual elevations of $-2.0" < Z \leq 0.0"$ and -3.88" for actual elevations of $-3.88" \leq Z \leq -2.0"$. Thus, only two thermal stratification load base cases are required.

The two stratification base cases used a 229F temperature differential between the hot and cold fluid. Therefore, the stress due to the base case circumferential temperature gradient can be determined by subtracting the steady state stress due to the radial and axial temperature gradients from the combined stress due to radial, axial, and circumferential temperature gradients (from harmonic element results which included the same steady state temperatures as were used in the axisymmetric load).

The thermal stratification stresses due to the circumferential temperature gradient for each peak and valley were determined by multiplying the stresses from the appropriate circumferential temperature gradient base case by the ratio of the actual stratification Delta T for the peak or valley from the design basis to the Delta T used in the stratification base case (229F).

Stresses for a base case nozzle bending moment of 10^6 in-lbs (in the plane of the surge line) were also determined by using the ANSYS harmonic element, STIF 25. The bending moment stresses for each peak and valley were determined by multiplying the stresses from the base case by the ratio of the moment from the surge line evaluation at the time nearest the peak or valley to the moment used in the base case.

The thermal, stratification, pressure, and external load stresses were multiplied by the appropriate stress indices (Table NB-3681(a)-1) or stress concentration factors and then combined for determination of maximum stress and fatigue usage. The results are given in Section 6.2.9.

6.2.4. List of Assumptions/Inputs Used in Analysis

1) The surge line nozzle to hot leg junction is a 3D structure and the thermal stratification in the nozzle produces non-axisymmetric loads. Two significant assumptions are necessary in order to analyze this nozzle using a 2D finite element model.

   a) The 3D structure can be approximated as a nozzle attached to a sphere whose radius is 3.2 times the radius of the hot leg. This assures that the pressure stress in the model will be equivalent to the maximum pressure stress in the actual structure at the critical location. The thermal stress from the model due to temperature gradients is approximately equal to those in the actual structure since thermal stress is not a strong function of the radius of the sphere.

   b) The circumferential temperature gradient is approximated by assuming the top and bottom of the nozzle is at a steady state condition for a thermal peak and valley, respectively. The transition between these two temperature fields is assumed to occur over the same 1" height of nozzle that contains the fluid interface zone between the hot and cold fluid. This is a conservative assumption since heat conduction in the circumferential direction of the nozzle will increase the height of the transition zone in the metal which would tend to reduce the thermal stresses.

2) The outside of surge line nozzle and hot leg are assumed to be fully insulated (no heat loss).

3) The surge line nozzle and hot leg are assumed to be at a steady state condition at the beginning of each up ramp (peak) or down ramp (valley). This is a conservative assumption since it maximizes the radial and axial gradients in the structure for each peak or valley.

4) The fluid temperature ramp rate (F/Hr) used in the analysis in determining the applicable base case is the maximum ramp rate at any time throughout the temperature change (PV) as defined in the design basis.

5) The transition between the nozzle and hot leg fluid temperatures is assumed to be a step change occurring at the intersection of the nozzle and hot leg pipe. This is a conservative assumption as a more gradual transition will actually occur which would reduce the thermal stresses in this region of the nozzle.

6) The stress indices from Table NB-3681(a)-1 for an "as-welded transition" are used in the evaluation of nozzle-to-surge line weld. This conservatively assumes the field weld was not ground flush on the inside surface of the nozzle.

7) The OBE seismic events are assumed to occur at steady state conditions and not at the point of maximum or minimum transient stress. Even if an event were to occur during a time of maximum transient stress, the effect on fatigue usage for only one occurrence of OBE would be minimal.

6.2.5. Thermal Analysis of Axisymmetric Loads

An axisymmetric heat transfer analysis using the finite element code ANSYS is performed to obtain the temperature distributions in the surge line nozzle and hot leg. The thermal transients evaluated are those specified in the design basis and discussed in Section 6.2.5.1. The resulting nodal temperatures from the thermal analysis will be used as input to the stress analysis.

The finite element model of a small segment of the surge line, surge nozzle, and hot leg is shown in Figure 6-9. These components are represented by isoparametric quadrilateral thermal elements, STIF 55. The required inputs for

this element are four nodal points and material properties: thermal conductivity, density, and specific heat.

6.2.5.1. Selection of Transients

The operating transients for the surge line (and nozzles) are identified in the design basis for the surge line and discussed in Section 4.5. A review of the transients revealed a significant number of temperature fluctuations during each transient. The temperature fluctuations involved approximately 40 different peaks or valleys per heatup and cooldown transient. The fluctuations include temperature changes (Delta-T) with magnitudes ranging from approximately 50 to 400 F. An example of one of these transients, HU1A1, is shown in Figure 6-10. As previously stated, an evaluation of each peak and valley is not practical, therefore only a few cases are considered. These cases are referred to as "base cases" and are selected to insure all peaks and valleys are enveloped. A summary of the base case parameters and resulting stresses is given in Table 6-4.

6.2.5.2. Thermal Boundary Conditions

The thermal boundary conditions consist of convective heat transfer at the inside surfaces of the model. Depending on the flow velocity in the nozzle and hot leg, either free or forced convection may be the predominant mode of heat transfer between the fluid and metal surfaces. For natural convection, the heat transfer is caused, primarily, by the difference in temperature between the metal surface and the reactor coolant fluid. The film coefficient versus Delta-T is input in tabular form to the ANSYS thermal runs. ANSYS uses the actual surface-to-fluid Delta-T at each time step (iteration) to determine the appropriate film coefficient. For forced convection, the film coefficient is constant for a given fluid velocity, temperature, and geometry. The film coefficient used in the analysis is the maximum of the coefficients for free or forced convection. A sample of the film coefficients for the two regions of the model is given below.

REGION	FILM COEFFICIENT (BTU/HR-FT^2-F)	
	FREE	FORCED
NOZZLE	140	185
HOT LEG	115	3000

The outside surfaces of the model are assumed to be fully insulated. In addition, for symmetry, the ends of the model are assumed to be adiabatic surfaces.

The transition between the nozzle and hot leg fluid temperatures is conservatively assumed to be a step change at the intersection of the nozzle and hot leg pipe.

6.2.5.3. Results of Thermal Analysis

The results of the thermal analysis are in the form of nodal temperatures. These nodal temperatures are read into the thermal stress analysis and provide the model with the axial and radial thermal gradients that produce the thermal stress. The times at which the maximum gradients occur are used for the thermal stress analysis since they are likely to produce the maximum stresses. To determine when the maximum gradients occur the ANSYS postprocessor, POST 26, is used. POST 26 provides a time history of the gradients at defined locations for the duration of the transient. For the surge nozzle evaluation fifteen pairs of nodes were used to examine the thermal response (Delta T) of the structure. The locations of these 15 node pairs are shown in Figure 6-11.

Figure 6-12 shows the temperature contours at an extreme Delta-T time point of a typical fluid temperature spike.

6.2.6. Stress Analysis of Axisymmetric Loads

An axisymmetric stress analysis using the finite element code ANSYS has been performed to obtain the stress distribution in the model for the base case axisymmetric loadings. The loadings for the analysis are the nodal temperatures from the thermal analysis (Section 6.2.5), a unit pressure load (1000 psi), and a unit axial force (10^5 lbs).

6.2.6.1. Description of Finite Element Model

The finite element model used for the thermal analysis was also used for the stress analysis. The only difference between the two models is the element type designation. The STIF 55 thermal element is replaced with an isoparametric quadrilateral stress element, STIF 42. The required inputs for this element are four nodal points and material properties: coefficient of thermal expansion, modulus of elasticity, and Poisson's ratio.

6.2.6.2. Structural Boundary Conditions

The structural boundary conditions applied are required to simulate those portions of the structure that are not modeled. The end of the model representing the hot leg was restrained from motion in the meridional direction (UY displacement = 0.0). This restraint simulates the restraint of the adjacent hot leg pipe material. The end of the surge line segment is assumed to be free. The location of this free boundary condition is sufficiently remote from the nozzle-to-surge line weld such that any stress induced by the assumed boundary condition will have attenuated to a negligible value at this critical section.

6.2.6.3. Selection of Transient Times

As stated in Section 6.2.5.3, the selection of transient times for use in the stress analysis is dependent upon the thermal gradients through the structure. The thermal gradients cause differential growth between adjacent material which results in thermal stresses. The times at which the maximum radial and axial gradients (Delta-T) occur are evaluated for stress.

6.2.6.4. Finite Element Stress Results

The results from the ANSYS stress runs are not in a format which can be directly compared to ASME code allowables. In order to get stresses compatible with the ASME code requirements it is necessary to use the ANSYS postprocessor POST 11. POST 11 performs stress linearization by converting the non-linear through-wall stress distributions into the stress components required for an ASME code evaluation: membrane stress, bending stress, and peak stress. The pertinent information about the linearization methods and detailed input is given in Section 6.31 of the ANSYS users manual. Eleven stress classification lines (SCL) were selected to evaluate stresses in the various regions of the model. The line locations are shown in Figure 6-13. The sum of the linearized stresses for a given load set is used to compare to the ASME code limit for the range of primary-plus-secondary stress intensities (3Sm limit). An example of the linearized and maximum thermal stresses for the various "base cases" evaluated is shown in Table 6-4. The tabulated stresses are those for the nozzle-to-surge line weld.

Also contained in Table 6-4 are the maximum stresses for the different "base cases". The maximum stresses represent the stresses at the surface of the

component and are given in the ANSYS element stress printout as the element surface stress. The sum of the maximum stresses for a given load set is used in the evaluation for fatigue usage.

6.2.7. Stress Analysis of Non-axisymmetric Loads

A non-axisymmetric stress analysis using the finite element code ANSYS has been performed to obtain the stress distribution in the model for the base case non-axisymmetric loadings. The loadings for the analysis are the circumferential nodal temperature gradients for two stratification cases and a nozzle bending moment as described in Section 6.2.3.

6.2.7.1. Description of Finite Element Model

The finite element stress model used for the axisymmetric loads was also used for the stress model for the non-axisymmetric loads. The only difference between the two models is the element type designation. The STIF 42 element is replaced with a harmonic element, STIF 25. The required inputs for this element are four nodal points and constant material properties: coefficient of thermal expansion, modulus of elasticity, and Poisson's ratio.

6.2.7.2. Structural Boundary Conditions

The structural boundary conditions are the same as was used for the axisymmetric loads in Section 6.2.6.2.

6.2.7.3. ANSYS Load Step Data

A harmonic element model requires the load to be input as a series of harmonic functions (Fourier series). The ANSYS preprocessor PREP6 is used to generate the Fourier series for the stratification temperature fields described in Section 6.2.3. Stresses were obtained for all the odd numbered modes up through mode number 33. These stress modes were then combined using the ANSYS postprocessor POST29. The unit (10^6 in-lb) nozzle bending moment was applied as described in Section 2.2.5, Case C of the ANSYS user's manual. This bending moment is represented by applying peak axial (nozzle) force values at the end of the nozzle. The load varies as a first harmonic wave (MODE - 1) with a cosine symmetry condition (ISYM = 1).

6.2.7.4. Finite Element Stress Results

The stresses output from POST29 were linearized at critical sections of the model. The results were then combined with linearized stresses from other loads and compared to the ASME code allowables as described in Section 6.2.8.

6.2.8. ASME Code Calculations

The linearized thermal, stratification, pressure, and external load stresses for each peak and valley were combined to obtain the total linearized stress. The linearized stresses for all peaks and valleys were tabulated and the difference between the maximum and minimum linearized stresses was used for comparison to the ASME code limit of 3Sm. When the 3Sm limit was exceeded, NB-3228.5 "Simplified Elastic-Plastic Analysis" was used to justify the stress conditions.

The maximum thermal, stratification, pressure, and external load stresses for each peak and valley were multiplied by the appropriate stress indices or stress concentration factor and combined to obtain the total maximum stress. The maximum stresses for all peaks and valleys were tabulated for evaluation of fatigue. A sample of the linearized and maximum stresses at the nozzle-to-surge line weld with the associated fatigue usage for a typical PV is given in Table 6-5. The fatigue evaluation took into account the number of cycles for each peak and valley, the maximum stress ranges, the linearized stress range associated with the maximum stress range, and the resulting Ke factor for the maximum stress range when the linearized stress range exceed the 3Sm allowable.

Fatigue usage due to thermal striping on the stainless steel regions of the nozzle is conservatively assumed to be equal to that calculated for the surge line.

The maximum linearized stress and fatigue usage factor for both the stainless steel and carbon steel portions of the surge nozzle are given in Section 6.2.9. All requirements of the ASME code are met.

6.2.9. Summary of Results and Conclusion

A summary of results for the hot leg surge nozzle evaluation is given in the following table. Although the 3Sm limit is exceeded for both the carbon steel and stainless steel, the requirements of the ASME code were satisfied by

performing a "Simplified Elastic-Plastic Analysis" as defined in NB-3228.5 of the code.

HOT LEG SURGE NOZZLE CALCULATED FATIGUE USAGE FACTORS						
LOCATION	Oconee Unit 1	Oconee Unit 2	Oconee Unit 3	TMI-1	CR-3	ANO-1
NOZZLE-TO-SURGE LINE WELD (STAINLESS STEEL)	.26	.26	.25	.19	.19	.20
NOZZLE-TO-HOT LEG CORNER (CARBON STEEL)	.59	.59	.59	.41	.42	.42
END OF NOZZLE TAPER (CARBON STEEL)	.42	.42	.42	.62	.62	.62

In conclusion, the hot leg surge nozzle and nozzle-to-surge line weld meet the requirements for Class 1 components of the ASME code, Section III, 1986 Edition with no Addenda for the revised design basis transients discussed in Section 4.5.

TABLE 6-1: BASE CASES

STRESS LINE 10, INSIDE SURFACE, SAFE END-TO-ELBOW WELD

Base Run, BR #	TRANSIENT INFORMATION Temperatures (F) Strt	End	Delta	Ramp Rate F/Hr	Press (psi)	STRESSES Linearized S12 (ksi)	S23 (ksi)	S31 (ksi)	Maximum (el. 376) S12 (ksi)	S23 (ksi)	S31 (ksi)
RU1a	80	482	402	900		11.1	-6.2	-4.9	14.7	-7.7	-7.0
RU1b	80	446	366	900		10.9	-6.0	-4.9	14.5	-7.4	-7.1
RU1c	80	373	293	900		10.2	-5.3	-4.9	13.7	-6.5	-7.2
RU1d	80	309	229	900		9.5	-4.6	-4.9	12.8	-5.7	-7.1
RU1e	80	253	173	900		8.7	-3.8	-4.9	11.9	-4.9	-7.0
RU1f	80	209	129	900		7.7	-3.0	-4.7	10.7	-4.0	-6.7
RU1g	80	172	92	900		6.5	-2.3	-4.2	9.2	-3.1	-6.1
RU2a	150	500	350	1500		15.8	-7.6	-8.1	21.4	-9.6	-11.6
RU2b	150	443	293	1500		15.1	-6.9	-8.2	20.4	-8.7	-11.7
RU2c	150	383	233	1500		13.8	-5.8	-8.0	18.9	-7.5	-11.4
RU2d	150	327	177	1500		12.2	-4.6	-7.6	16.9	-6.1	-10.8
RU2e	150	285	135	1500		10.7	-3.7	-7.0	15.0	-4.9	-10.1
RU2f	150	248	98	1500		8.7	-2.7	-6.0	12.4	-3.7	-8.7
RU2g	150	220	70	1500		6.7	-1.9	-4.9	9.8	-2.6	-7.2
RU3a	250	550	300	1000		11.1	-5.8	-5.3	14.8	-7.2	-7.6
RU3b	250	484	234	1000		10.5	-5.1	-5.4	14.1	-6.4	-7.7
RU3c	250	430	180	1000		9.7	-4.2	-5.4	13.2	-5.5	-7.7
RU3d	250	382	132	1000		8.5	-3.3	-5.2	11.7	-4.3	-7.4
RU3e	250	346	96	1000		7.2	-2.5	-4.7	10.1	-3.3	-6.8
RU3f	250	316	66	1000		5.6	-1.7	-3.9	8.0	-2.3	-5.7
RU3g	250	292	42	1000		3.8	-1.0	-2.8	5.6	-1.4	-4.2
RU4a	250	482	232	2000		16.4	-6.3	-10.1	22.6	-8.2	-14.4
RU4b	250	431	181	2000		14.6	-5.1	-9.5	20.3	-6.8	-13.5
RU4c	250	389	139	2000		12.4	-3.9	-8.5	17.5	-5.3	-12.2
RU4d	250	352	102	2000		9.8	-2.8	-7.0	14.1	-3.9	-10.2
RU4e	250	320	70	2000		7.0	-1.8	-5.2	10.3	-2.6	-7.7
RU5a	400	650	250	2000		16.8	-6.8	-10.0	22.9	-8.8	-14.1
RU5b	400	635	235	2000		16.5	-6.5	-10.0	22.5	-8.4	-14.1
RU5c	400	580	180	2000		14.6	-5.2	-9.4	20.3	-7.0	-13.3
RU5d	400	535	135	2000		12.6	-4.0	-8.6	17.6	-5.4	-12.2
RU5e	400	500	100	2000		10.2	-2.9	-7.3	14.6	-4.1	-10.5
RU6a	500	650	150	1000		8.7	-3.7	-5.0	11.9	-4.8	-7.1
RU6b	500	611	111	1000		7.8	-3.0	-4.8	10.7	-3.8	-6.9
RU6c	500	579	79	1000		6.5	-2.1	-4.3	9.1	-2.9	-6.2
RU6d	500	555	55	1000		5.0	-1.4	-3.6	7.1	-1.9	-5.2
RU7a	500	650	150	1500		11.2	-4.2	-7.0	15.4	-5.4	-10.0
RU7b	500	624	124	1500		10.2	-3.5	-6.7	14.2	-4.7	-9.5
RU7c	500	590	90	1500		8.4	-2.5	-5.8	11.8	-3.4	-8.4
S550	550	550	0	NONE		-0.3	0.2	0.1	-0.4	0.3	0.1

TABLE 6-1: BASE CASES

STRESS ZONE 10, INSIDE SURFACE, SAFE END-TO-ELBOW WELD

Base Run, BR #	TRANSIENT INFORMATION Temperatures (F) Strt	End	Delta	Ramp Rate F/Hr	Press (psi)	STRESSES Linearized S12 (ksi)	S23 (ksi)	S31 (ksi)	Maximum (el. 376) S12 (ksi)	S23 (ksi)	S31 (ksi)
S450	450	450	0	NONE		-0.3	0.2	0.1	-0.3	0.2	0.1
S300	300	300	0	NONE		-0.2	0.1	0.1	-0.2	0.1	0.1
SS70	70	70	0	NONE		0.0	0.0	0.0	0.0	0.0	0.0
RD1a	550	300	-250	-800		-9.7	5.2	4.5	-13.0	6.5	6.5
RD1b	550	332	-218	-800		-9.4	4.8	4.6	-12.6	6.1	6.5
RD1c	550	386	-164	-800		-8.6	4.1	4.5	-11.5	5.1	6.4
RD1d	550	432	-118	-800		-7.6	3.2	4.3	-10.3	4.2	6.1
RD1e	550	468	-82	-800		-6.4	2.4	3.9	-8.8	3.2	5.6
RD1f	550	493	-57	-800		-5.1	1.8	3.4	-7.2	2.4	4.8
RD1g	550	514	-36	-800		-3.6	1.1	2.5	-5.2	1.6	3.6
RD2a	482	160	-322	-4000		-28.1	9.8	18.3	-39.7	13.1	26.6
RD2b	482	218	-264	-4000		-25.0	8.1	16.9	-35.5	11.1	24.4
RD2c	482	276	-206	-4000		-21.1	6.4	14.7	-30.2	8.9	21.3
RD2d	482	321	-161	-4000		-17.3	4.9	12.4	-25.0	6.9	18.1
RD3a	450	100	-350	-3000		-25.2	9.8	15.4	-35.2	12.9	22.3
RD3b	450	135	-315	-3000		-24.0	9.1	15.0	-33.7	12.0	21.7
RD3c	450	198	-252	-3000		-21.4	7.5	13.9	-30.2	10.1	20.1
RD3d	450	254	-196	-3000		-18.4	6.0	12.5	-26.2	8.2	18.0
RD3e	450	296	-154	-3000		-15.6	4.7	10.9	-22.3	6.5	15.8
RD3f	450	338	-112	-3000		-11.9	3.3	8.6	-17.3	4.7	12.6
RD3g	450	373	-77	-3000		-8.2	2.1	6.1	-12.2	3.1	9.1
RD4a	450	100	-350	-1700		-17.7	8.3	9.4	-24.2	10.5	13.7
RD4b	450	145	-305	-1700		-17.0	7.6	9.4	-23.3	9.8	13.5
RD4c	450	215	-235	-1700		-15.3	6.3	9.0	-21.2	8.3	12.9
RD4d	450	270	-180	-1700		-13.6	5.2	8.5	-18.9	6.8	12.1
RD4e	450	315	-135	-1700		-11.6	4.0	7.6	-16.3	5.4	10.9
RD4f	450	350	-100	-1700		-9.5	3.0	6.5	-13.4	4.1	9.3
RD4g	450	380	-70	-1700		-7.1	2.1	5.0	-10.2	2.9	7.3
RD4h	450	405	-45	-1700		-4.6	1.2	3.3	-6.8	1.8	5.0
RD5a	300	100	-200	-700		-7.8	3.9	3.9	-10.6	4.9	5.7
RD5b	300	137	-163	-700		-7.4	3.4	3.9	-10.1	4.4	5.7
RD5c	300	183	-117	-700		-6.5	2.7	3.8	-9.0	3.6	5.4
RD5d	300	217	-83	-700		-5.5	2.1	3.4	-7.7	2.8	4.9
RD5e	300	243	-57	-700		-4.4	1.5	2.9	-6.2	2.1	4.1
PRS					2200	-9.1	-3.1	12.2	-10.3	-2.2	12.5

TABLE 6-2: LINEARIZED STRESSES, TRANSIENT 1A1

STRESS LINE 10, INSIDE SURFACE, SAFE END-TO-ELBOW WELD

PV #	Temperatures			Max Ramp Rate	Base Run	Thermal Stresses			Pressure Stresses				Piping Stresses			Linearized Stress (see Notes)		
	Strt (F)	End (F)	Delta (F)	(F/Hr)	Used	S12 (ksi)	S23 (ksi)	S31 (ksi)	Press (psi)	S12 (ksi)	S23 (ksi)	S31 (ksi)	pipe load pv #	Moment Mr(xyz) (in-lbs)	Stress Mc/I (ksi)	S12 (ksi)	S23 (ksi)	S31 (ksi)
PV1	70	70	0	0	SS70	0.0	0.0	0.0	0	0.0	0.0	0.0	1	24024	0.3	0.4	0.4	0.0
PV2	70	482	412	848	RU1a	11.1	-6.2	-4.9	578	-2.4	-0.8	3.2	2	2457310	29.8	46.8	31.1	-1.7
PV3	482	163	-319	-3954	RD2a	-28.1	9.8	18.3	578	-2.4	-0.8	3.2	3	522099	6.3	-22.4	17.1	21.5
PV4	163	482	319	758	RU3a	11.1	-5.8	-5.3	578	-2.4	-0.8	3.2	4	2508422	30.4	47.6	32.3	-2.1
PV5	482	97	-385	-3849	RD2a	-28.1	9.8	18.3	578	-2.4	-0.8	3.2	5	280908	3.4	-26.1	13.3	21.5
PV6	97	240	143	692	RU1f	7.7	-3.0	-4.7	578	-2.4	-0.8	3.2	6	2486005	30.1	43.9	34.7	-1.5
PV7	240	104	-136	-292	RD5c	-6.5	2.7	3.8	578	-2.4	-0.8	3.2	6	2486005	30.1	29.7	40.4	7.0
PV8	104	338	234	1305	RU2c	13.8	-5.8	-8.0	578	-2.4	-0.8	3.2	6	2486005	30.1	50.0	31.9	-4.8
PV9	338	101	-237	-2370	RD3c	-21.4	7.5	13.9	578	-2.4	-0.8	3.2	7	411227	5.0	-17.4	13.1	17.1
PV10	101	269	168	1218	RU2d	12.2	-4.6	-7.6	578	-2.4	-0.8	3.2	8	1829208	22.2	38.2	22.9	-4.4
PV11	269	135	-134	-651	RD5c	-6.5	2.7	3.8	578	-2.4	-0.8	3.2	9	483188	5.9	-1.4	9.4	7.0
PV12	135	178	43	1538	RU2g	[illegible]7	-1.9	-4.9	578	-2.4	-0.8	3.2	9	483188	5.9	11.8	4.8	-1.7
PV13	178	110	-68	-724	RD5d	[illegible]5	2.1	3.4	578	-2.4	-0.8	3.2	11	280977	3.4	-3.5	5.6	6.6
PV14	110	248	138	1390	RU2e	10.7	-3.7	-7.0	578	-2.4	-0.8	3.2	12	2195571	26.6	42.4	29.5	-3.8
PV15	248	114	-134	-376	RD5c	-6.5	2.7	3.8	578	-2.4	-0.8	3.2	13	429664	5.2	-2.2	8.5	7.0
PV16	114	266	152	1717	RU2d	12.2	-4.6	-7.6	578	-2.4	-0.8	3.2	14	1382962	16.8	31.3	16.0	-4.4
PV17	266	117	-149	-666	RD5b	-7.4	3.4	3.9	578	-2.4	-0.8	3.2	15	378492	4.6	-3.9	8.5	7.1
PV18	117	255	138	873	RU1f	7.7	-3.0	-4.7	578	-2.4	-0.8	3.2	16	1648571	20.0	30.9	21.7	-1.5
PV19	255	130	-125	-428	RD5c	-6.5	2.7	3.8	578	-2.4	-0.8	3.2	17	440821	5.3	-2.1	8.7	7.0
PV20	130	321	191	1192	RU2d	12.2	-4.6	-7.6	578	-2.4	-0.8	3.2	18	1695162	20.5	36.1	20.9	-4.4
PV21	321	140	-181	-823	RD5a	-7.8	3.9	3.9	578	-2.4	-0.8	3.2	19	395736	4.8	-4.1	9.2	7.1
PV22	140	478	338	1294	RU2a	15.8	-7.6	-8.1	578	-2.4	-0.8	3.2	23	139825	1.7	15.6	-6.2	-4.9
PV23	478	305	-173	-352	RD1c	-8.6	4.1	4.5	578	-2.4	-0.8	3.2	24	1536736	18.6	12.8	27.1	7.7
PV24	305	380	75	1767	RU4e	7.0	-1.8	-5.2	578	-2.4	-0.8	3.2	24	1536736	18.6	28.4	21.2	-2.0
PV25	380	253	-127	-395	RD5c	-6.5	2.7	3.8	578	-2.4	-0.8	3.2	24	1536736	18.6	14.9	25.7	7.0
PV26	253	300	47	1572	RU4e	7.0	-1.8	-5.2	578	-2.4	-0.8	3.2	24	1536736	18.6	28.4	21.2	-2.0
PV27	300	231	-69	-139	RD5e	-4.4	1.5	2.9	578	-2.4	-0.8	3.2	25	306030	3.7	-2.9	5.4	6.1
PV28	231	431	200	873	RU3c	9.7	-4.2	-5.4	578	-2.4	-0.8	3.2	[illegible]	1302842	15.8	27.5	15.2	-2.2
PV29	431	243	-188	-807	RD1c	-8.6	4.1	4.5	578	-2.4	-0.8	3.2	27	406195	4.9	-4.7	9.6	7.7
PV30	243	328	85	1466	RU4d	9.8	-2.8	-7.0	578	-2.4	-0.8	3.2	28	936974	11.3	21.9	10.9	-3.8
PV31	328	234	-94	-197	RD5d	-5.5	2.1	3.4	578	-2.4	-0.8	3.2	29	133506	1.6	-5.8	3.4	6.6
PV32	234	477	243	884	RU3b	10.5	-5.1	-5.4	578	-2.4	-0.8	3.2	31	428891	5.2	14.8	0.7	-2.2
PV33	477	234	-243	-350	RD1e	-9.7	5.2	4.5	578	-2.4	-0.8	3.2	30	1689142	20.5	14.1	30.6	7.7
PV34	234	418	184	1357	RU4b	14.6	-5.1	-9.5	578	-2.4	-0.8	3.2	32	1354047	16.4	33.2	15.1	-6.3
PV35	418	344	-74	-1400	RD4g	-7.1	2.1	5.0	578	-2.4	-0.8	3.2	33	929878	11.3	4.9	15.7	8.2
PV36	344	429	85	1241	RU3e	7.2	-2.5	-4.7	578	-2.4	-0.8	3.2	34	1248528	15.1	24.2	16.0	-1.5
PV37	429	276	-153	-997	RD1c	-8.6	4.1	4.5	659	-2.7	-0.9	3.7	35	458860	5.6	-4.2	10.3	8.2
PV38	276	411	135	1751	RU4c	12.4	-3.9	-8.5	708	-2.9	-1.0	3.9	36	1585180	19.2	34.1	19.7	-4.6
PV39	411	282	-129	-848	RD1d	-7.6	3.2	4.3	939	-3.9	-1.3	5.2	37	194453	2.4	-8.5	4.9	9.5
PV40	282	591	309	1058	RU3a	11.1	-5.8	-5.3	1543	-6.4	-2.2	8.6	38	2092208	25.3	37.2	24.5	3.3
PV41	591	524	-67	-2433	RD3g	-8.2	2.1	6.1	1551	-6.4	-2.2	8.6	39	1335898	16.2	[illegible]	20.6	14.7
PV42	524	584	60	659	RU6d	5.0	-1.4	-3.6	1587	-6.6	-2.2	8.8	40	1799577	21.[illegible]	[illegible]	24.3	5.2
PV43	584	469	-115	-494	RD1d	-7.6	3.2	4.3	1655	-6.8	-2.3	9.[illegible]	41	1446453	17.[illegible]	[illegible]	[illegible]	13.5
PV44	469	546	77	1406	RU7c	8.4	-2.5	-5.8	1674	-6.9	-2.4	9.[illegible]	42	[illegible]472581	[illegible]	[illegible]	[illegible]	3.5
PV45	546	376	-170	-946	RD1c	-8.6	4.1	4.5	1765	-7.3	-2.5	9.8	43	[illegible]281	[illegible]	[illegible]	[illegible]	4.3

TABLE 6-2: LINEARIZED STRESSES, TRANSIENT 1A1

STRESS LINE 10, INSIDE SURFACE, SAFE END-TO-ELBOW WELD

PV #	Temperatures			Max Ramp Rate	Thermal Stresses				Pressure Stresses				Piping Stresses			Linearized Stress (see Notes)		
	Strt (F)	End (F)	Delta (F)	(F/Hr)	Base Run Used	S12 (ksi)	S23 (ksi)	S31 (ksi)	Press (psi)	S12 (ksi)	S23 (ksi)	S31 (ksi)	pipe load pv #	Moment Mr(xyz) (in-lbs)	Stress Mc/I (ksi)	S12 (ksi)	S23 (ksi)	S31 (ksi)
PV46	376	468	92	2209	RU5e	10.2	-2.9	-7.3	1778	-7.4	-2.5	9.9	44	1567425	19.0	27.1	18.9	2.6
PV47	468	344	-124	-558	RD1d	-7.6	3.2	4.3	1968	-8.1	-2.8	10.9	45	356343	4.3	-10.2	6.0	15.2
PV48	344	481	137	1670	RU4c	12.4	-3.9	-8.5	2020	-8.4	-2.8	11.2	46	1805393	21.9	32.0	21.2	2.7
PV49	481	405	-76	-1412	RD4g	-7.1	2.1	5.0	2062	-8.5	-2.9	11.4	47	1068057	12.9	[illegible]	15.8	16.4
PV50	405	507	102	1239	RU7c	8.4	-2.5	-5.8	2118	-8.8	-3.0	11.7	48	1948405	23.6	29.8	24.7	5.9
PV51	507	395	-112	-1102	RD4f	-9.5	3.0	6.5	2208	-9.1	-3.1	12.2	49	237067	2.9	-15.0	3.6	18.7
PV52	395	646	251	819	RU3b	10.5	-5.1	-5.4	2208	-9.1	-3.1	12.2	50	1964924	23.8	31.8	22.3	6.8
PV53	646	450	-196	-652	RD1b	-9.4	4.8	4.6	2208	-9.1	-3.1	12.2	51	694340	8.4	-7.8	12.5	16.8
PV54	450	562	112	1857	RU5d	12.6	-4.0	-8.6	2208	-9.1	-3.1	12.2	52	1542314	18.7	27.4	16.8	3.6
PV55	562	448	-114	-489	RD1d	-7.6	3.2	4.3	2208	-9.1	-3.1	12.2	53	672901	8.2	-6.3	10.5	16.5
PV56	448	619	171	1493	RU7e	11.2	-4.2	-7.0	2208	-9.1	-3.1	12.2	56	1749913	21.2	29.2	19.8	5.2
PV57	619	471	-148	-678	RD1c	-8.6	4.1	4.5	2208	-9.1	-3.1	12.2	57	639273	7.7	-7.8	10.9	16.7
PV58	471	563	92	1582	RU7c	8.4	-2.5	-5.8	2208	-9.1	-3.1	12.2	58	1534824	18.6	23.1	18.2	6.4
PV59	563	508	-55	-291	RD1f	-5.1	1.8	3.4	2208	-9.1	-3.1	12.2	59	313303	3.8	-9.4	3.5	15.6
PV60	508	646	138	438	RU6a	8.7	-3.7	-5.0	2208	-9.1	-3.1	12.2	60	1265689	15.3	19.2	12.8	7.2
PV61	646	540	-106	-597	RD1d	-7.6	3.2	4.3	2208	-9.1	-3.1	12.2	61	686954	8.3	-6.[illegible]	10.7	16.5
PV62	540	602	62	1095	RU6d	5.0	-1.4	-3.6	2208	-9.1	-3.1	12.2	62	1137791	13.8	13.5	13.1	8.6
PV63	602	518	-84	-389	RD1e	-6.4	2.4	3.9	2208	-9.1	-3.1	12.2	63	571848	6.9	-6.7	8.2	16.1
PV64	518	650	132	1179	RU6e	8.7	-3.7	-5.0	2208	-9.1	-3.1	12.2	65	392579	4.8	5.7	-0.7	7.2
PV65	650	524	-126	-742	RD1d	-7.6	3.2	4.3	2208	-9.1	-3.1	12.2	67	525551	6.4	-8.6	8.2	16.5
PV66	524	575	51	1062	RU6d	5.0	-1.4	-3.6	2208	-9.1	-3.1	12.2	68	1104525	13.4	13.0	12.6	8.6
PV67	575	520	-55	-178	RD1f	-5.1	1.8	3.4	2208	-9.1	-3.1	12.2	69	471165	5.7	-6.9	6.0	15.6
PV68	520	640	120	1037	RU6b	7.8	-3.0	-4.8	2208	-9.1	-3.1	12.2	70	1108494	13.4	15.9	11.1	7.4
PV69	640	567	-73	-568	RD1e	-6.4	2.4	3.9	2208	-9.1	-3.1	12.2	71	582294	7.1	-6.5	8.3	16.1
PV70	567	608	41	794	RU6d	5.0	-1.4	-3.6	2208	-9.1	-3.1	12.2	71	582294	7.1	4.9	4.5	8.6
															MAXIMUM STRESS	50.0	40.4	21.5
															MINIMUM STRESS	-26.1	-6.2	-6.3
															MAXIMUM RANGE	76.1	46.7	27.8

Notes:
Linearized Stress (S12) = thermal stress + pressure stress + C2(piping stress), C2 = 1.28
Linearized Stress (S23) = thermal stress + pressure stress + C2(piping stress), C2 = 1.28
Linearized Stress (S31) = thermal stress + pressure stress, no piping stress
where: C2 = 1.28

TABLE 6-3: MAXIMUM STRESSES, TRANSIENT 1A1

STRESS LINE 10, INSIDE SURFACE, SAFE END-TO-ELBOW WELD

PV #	Strt Temp (F)	End Temp (F)	Delta Temp (F)	Max Ramp Rate (F/Hr)	Base Run Used	Thermal Stresses S12 (ksi)	S23 (ksi)	S31 (ksi)	Press (psi)	Pressure Stresses S12 (ksi)	S23 (ksi)	S31 (ksi)	pipe load pv #	Piping Stresses Moment Mr(xyz) (in-lbs)	Stress Mc/I (ksi)	Maximum Stress (see Notes) S12 (ksi)	S23 (ksi)	S31 (ksi)
PV1	70	70	0	0	SS70	0.0	0.0	0.0	0	0.0	0.0	0.0	1	24024	0.3	0.7	0.7	0.0
PV2	70	482	412	848	RU1e	14.7	-7.7	-7.0	578	-2.7	-0.6	3.3	2	2457310	29.8	87.8	55.8	-6.5
PV3	482	163	-319	-3954	RD2a	-39.7	13.1	26.6	578	-2.7	-0.6	3.3	3	522099	6.3	-48.0	33.8	43.4
PV4	163	482	319	758	RU3e	14.8	-7.2	-7.6	578	-2.7	-0.6	3.3	4	2508422	30.4	89.3	58.1	-7.4
PV5	482	97	-385	-3849	RD2a	-39.7	13.1	26.6	578	-2.7	-0.6	3.3	5	280908	3.4	-54.8	27.1	43.4
PV6	97	240	143	692	RU1f	10.7	-4.0	-6.7	578	-2.7	-0.6	3.3	6	2486005	30.1	82.2	62.6	-6.0
PV7	240	104	-136	-292	RD5c	-9.0	3.6	5.4	578	-2.7	-0.6	3.3	6	2486005	30.1	52.6	74.2	12.0
PV8	104	338	234	1305	RU2c	18.9	-7.5	-11.4	578	-2.7	-0.6	3.3	6	2486005	30.1	94.7	57.1	-13.1
PV9	338	101	-237	-2370	RD3c	-30.2	10.1	20.1	578	-2.7	-0.6	3.3	7	411227	5.0	-37.0	26.1	33.8
PV10	101	269	168	1218	RU2d	16.9	-6.1	-10.8	578	-2.7	-0.6	3.3	8	1829208	22.2	73.2	41.0	-12.2
PV11	269	135	-134	-651	RD5c	-9.0	3.6	5.4	578	-2.7	-0.6	3.3	9	483188	5.9	-3.3	18.3	12.0
PV12	135	178	43	1538	RU2g	9.8	-2.6	-7.2	578	-2.7	-0.6	3.3	9	483188	5.9	24.7	8.9	-6.7
PV13	178	110	-68	-724	RD5d	-7.7	2.8	4.9	578	-2.7	-0.6	3.3	11	280977	3.4	-7.0	11.4	11.2
PV14	110	248	138	1390	RU2e	15.0	-4.9	-10.1	578	-2.7	-0.6	3.3	12	2195571	26.6	80.5	53.1	-11.1
PV15	248	114	-134	-376	RD5c	-9.0	3.6	5.4	578	-2.7	-0.6	3.3	13	429664	5.2	-4.8	16.8	12.0
PV16	114	266	152	1717	RU2d	16.9	-6.1	-10.8	578	-2.7	-0.6	3.3	14	1382962	16.8	60.8	28.6	-12.2
PV17	266	117	-149	-666	RD5b	-10.1	4.4	5.7	578	-2.7	-0.6	3.3	15	378492	4.6	-8.0	16.6	12.4
PV18	117	255	138	873	RU1f	10.7	-4.0	-6.7	578	-2.7	-0.6	3.3	16	1648571	20.0	58.9	39.2	-6.0
PV19	255	130	-125	-428	RD5c	-9.0	3.6	5.4	578	-2.7	-0.6	3.3	17	440821	5.3	-4.5	17.1	12.0
PV20	130	321	191	1192	RU2d	16.9	-6.1	-10.8	578	-2.7	-0.6	3.3	18	1695162	20.5	69.5	37.3	-12.2
PV21	321	140	-181	-823	RD5e	-10.6	4.9	5.7	578	-2.7	-0.6	3.3	19	395736	4.8	-8.3	18.0	12.4
PV22	140	478	338	1294	RU2e	21.2	-9.6	-11.6	578	-2.7	-0.6	3.3	23	139825	1.7	32.9	-11.7	-13.3
PV23	478	305	-173	-352	RD1c	-11.5	5.1	6.4	578	-2.7	-0.6	3.3	24	1536736	18.6	22.1	50.2	13.5
PV24	305	380	75	1767	RU4e	10.3	-2.6	-7.7	578	-2.7	-0.6	3.3	24	1536736	18.6	54.8	38.3	-7.4
PV25	380	253	-127	-395	RD5c	-9.0	3.6	5.4	578	-2.7	-0.6	3.3	24	1536736	18.6	26.1	47.7	12.0
PV26	253	300	47	1572	RU4e	10.3	-2.6	-7.7	578	-2.7	-0.6	3.3	24	1536736	18.6	54.8	38.3	-7.4
PV27	300	231	-69	-139	RD5e	-6.2	2.1	4.1	578	-2.7	-0.6	3.3	25	306030	3.7	-4.0	11.0	10.1
PV28	231	431	200	873	RU3c	13.2	-5.5	-7.7	578	-2.7	-0.6	3.3	26	1302842	15.8	53.1	27.2	-7.5
PV29	431	243	-188	-807	RD1c	-11.5	5.1	6.4	578	-2.7	-0.6	3.3	27	406195	4.9	-9.4	18.6	13.5
PV30	243	328	85	1466	RU4d	14.1	-3.9	-10.2	578	-2.7	-0.6	3.3	28	936874	11.3	43.9	19.6	-11.2
PV31	328	234	-94	-197	RD5d	-7.7	2.8	4.9	578	-2.7	-0.6	3.3	29	133506	1.6	-11.1	7.3	11.2
PV32	234	477	243	884	RU3b	14.1	-6.4	-7.7	578	-2.7	-0.6	3.3	31	428891	5.2	30.2	1.3	-7.5
PV33	477	234	-243	-350	RD1e	-13.0	6.5	6.5	578	-2.7	-0.6	3.3	30	1689142	20.5	24.1	56.6	13.6
PV34	234	418	184	1357	RU4b	20.3	-6.8	-13.5	578	-2.7	-0.6	3.3	32	1354047	16.4	65.1	26.7	-16.2
PV35	418	344	-74	-1400	RD4g	-10.2	2.9	7.3	578	-2.7	-0.6	3.3	33	929878	11.3	7.5	29.6	14.7
PV36	344	429	85	1241	RU3e	10.1	-3.3	-6.8	578	-2.7	-0.6	3.3	34	1248528	15.1	46.7	29.1	-6.1
PV37	429	276	-153	-997	RD1c	-11.5	5.1	6.4	659	-3.1	-0.7	3.7	35	458860	5.6	-8.4	20.0	14.0
PV38	276	411	135	1751	RU4c	17.5	-5.3	-12.2	708	-3.3	-0.7	4.0	36	1585180	19.2	66.4	35.4	-13.3
PV39	411	282	-129	-848	RD1d	-10.3	4.2	6.1	939	-4.4	-0.9	5.3	37	194453	2.4	-15.5	10.7	15.5
PV40	282	591	309	1058	RU3a	14.8	-7.2	-7.6	1543	-7.2	-1.5	8.8	38	2092208	25.3	72.3	45.3	-0.8
PV41	591	524	-67	-2433	RD3g	-12.2	3.1	9.1	1551	-7.3	-1.6	8.8	39	1335898	16.2	10.6	40.0	23.9
PV42	524	584	60	659	RU6d	7.1	-1.9	-5.2	1587	-7.4	-1.6	9.0	40	1799577	21.8	51.9	45.4	3.1
PV43	584	469	-115	-494	RD1d	-10.3	4.2	6.1	1655	-7.7	-1.7	9.4	41	1146453	17.5	15.5	44.8	20.4
PV44	469	546	77	1406	RU7c	11.8	-3.4	-8.4	1674	-7.8	-1.7	9.5	42	1372581	22.7	60.5	45.1	-1.0
PV45	546	376	-170	-946	RD1c	-11.5	5.1	6.4	1765	-8.3	-1.8	10.0	43	685581	8.3	-8.3	25.0	21.6

TABLE 6-3: MAXIMUM STRESSES, TRANSIENT 1A1

STRESS LINE 10, INSIDE SURFACE, SAFE END-TO-ELBOW WELD

PV #	Strt Temp (F)	End Temp (F)	Delta Temp (F)	Max Ramp Rate (F/Hr)	Thermal Stresses Base Run Used	S12 (ksi)	S23 (ksi)	S31 (ksi)	Pressure Stresses Press (psi)	S12 (ksi)	S23 (ksi)	S31 (ksi)	Piping Stresses pipe load pv #	Moment Mr(xyz) (in-lbs)	Stress Mc/I (ksi)	Maximum Stress (see Notes) S12 (ksi)	S23 (ksi)	S31 (ksi)
PV46	376	468	92	2209	RU5e	14.6	-4.1	-10.5	1778	-8.3	-1.8	10.1	44	1567425	19.0	55.5	35.5	-3.5
PV47	468	344	-124	-558	RD1d	-10.3	4.2	6.1	1968	-9.2	-2.0	11.2	45	356343	4.3	-16.7	1.1	22.5
PV48	344	481	137	1670	RU4c	17.5	-5.3	-12.2	2020	-9.5	-2.0	11.5	46	1805393	21.9	65.2	39.9	-4.4
PV49	481	405	-76	-1412	RD4g	-10.2	2.9	7.3	2062	-9.7	-2.1	11.7	47	1068057	12.9	3.1	31.7	24.9
PV50	405	507	102	1230	RU7c	11.8	-3.4	-8.4	2118	-9.9	-2.1	12.0	48	1948405	23.6	60.2	46.7	2.0
PV51	507	395	-112	-1102	RD4f	-13.4	4.1	9.3	2208	-10.3	-2.2	12.5	49	237067	2.9	-25.8	10.2	28.9
PV52	395	646	251	819	RU3b	14.1	-6.4	-7.7	2208	-10.3	-2.2	12.5	50	1964924	23.8	63.9	42.2	3.6
PV53	646	450	-196	-652	RD1b	-12.6	6.1	6.5	2208	-10.3	-2.2	12.5	51	694340	8.4	-12.2	26.2	24.8
PV54	450	562	112	1857	RU5d	17.6	-5.4	-12.2	2208	-10.3	-2.2	12.5	52	1542314	18.7	57.1	32.2	-3.2
PV55	562	448	-114	-489	RD1d	-10.3	4.2	6.1	2208	-10.3	-2.2	12.5	53	672901	8.2	-9.2	22.6	24.2
PV56	448	619	171	1493	RU7a	15.4	-5.4	-10.0	2208	-10.3	-2.2	12.5	56	1749913	21.2	59.7	37.8	0.2
PV57	619	471	-148	-678	RD1c	-11.5	5.1	6.4	2208	-10.3	-2.2	12.5	57	639273	7.7	-12.1	23.2	24.6
PV58	471	563	92	1582	RU7c	11.8	-3.4	-8.4	2208	-10.3	-2.2	12.5	58	1534824	18.6	48.1	35.0	2.6
PV59	563	508	-55	-291	RD1f	-7.2	2.4	4.8	2208	-10.3	-2.2	12.5	59	313303	3.8	-14.4	9.8	22.2
PV60	508	646	138	438	RU6a	11.9	-4.8	-7.1	2208	-10.3	-2.2	12.5	60	1265689	15.3	40.9	25.3	4.5
PV61	646	540	-106	-597	RD1d	-10.3	4.2	6.1	2208	-10.3	-2.2	12.5	61	686954	8.3	-8.9	23.0	24.2
PV62	540	602	62	1095	RU6d	7.1	-1.9	-5.2	2208	-10.3	-2.2	12.5	62	1137791	13.8	30.0	26.2	7.3
PV63	602	518	-84	-389	RD1e	-8.8	3.2	5.6	2208	-10.3	-2.2	12.5	63	571848	6.9	-9.7	18.2	23.4
PV64	518	650	132	1179	RU6e	11.9	-4.8	-7.1	2208	-10.3	-2.2	12.5	65	392579	4.8	16.5	0.9	4.5
PV65	650	524	-126	-742	RD1d	-10.3	4.2	6.1	2208	-10.3	-2.2	12.5	67	525551	6.4	-13.4	18.5	24.2
PV66	524	575	51	1062	RU6d	7.1	-1.9	-5.2	2208	-10.3	-2.2	12.5	68	1104525	13.4	29.0	25.3	7.3
PV67	575	520	-55	-178	RD1f	-7.2	2.4	4.8	2208	-10.3	-2.2	12.5	69	471165	5.7	-10.0	14.2	22.2
PV68	520	640	120	1037	RU6b	10.7	-3.8	-6.9	2208	-10.3	-2.2	12.5	70	1108494	13.4	34.7	22.4	4.8
PV69	640	567	-73	-568	RD1e	-8.8	3.2	5.6	2208	-10.3	-2.2	12.5	71	582294	7.1	-9.4	18.5	23.4
PV70	567	608	41	794	RU6d	7.1	-1.9	-5.2	2208	-10.3	-2.2	12.5	71	582294	7.1	14.4	18.7	7.3
														MAXIMUM STRESS		94.7	74.2	43.4
														MINIMUM STRESS		-54.8	-11.7	-16.2
														MAXIMUM RANGE		149.5	85.9	59.6

Notes:
Maximum Stress (S12) = max thermal stress + (K3-1)(linear thermal stress) + K1(pressure stress) + C2(K2)(piping stress)
Maximum Stress (S23) = max thermal stress + (K3-1)(linear thermal stress) + K1(pressure stress) + C2(K2)(piping stress)
Maximum Stress (S31) = max thermal stress + (K3-1)(linear thermal stress) + K1(pressure stress), no piping stress
where: K1 = 1.2, K2 = 1.8, K3 = 1.7, C2 = 1.28

TABLE 6-4

THERMAL STRESS BASE CASES FOR THE NOZZLE-TO-SURGE LINE WELD

RAMP RATE (F/HR)	T START (F)	T END (F)	T HL (F)	INSIDE SURFACE STRESSES (PSI) LINEARIZED S12	LINEARIZED S23	LINEARIZED S31	SURFACE S2	SURFACE S3	OUTSIDE SURFACE STRESSES (PSI) LINEARIZED S12	LINEARIZED S23	LINEARIZED S31	SURFACE S2	SURFACE S3
10000	132	361	108	22723	-4214	-18510	-26737	-24593	-21377	4861	16516	19198	11686
3500	130	290	80	11618	-2360	-9259	-13332	-11909	-10631	3585	7346	10410	5341
3500	130	285	80	13465	-2738	-10728	-15353	-13703	-12663	4136	8532	12107	6239
3500	130	320	80	15829	-3271	-12558	-17882	-15882	-14892	4924	9968	14324	7344
1300	130	260	80	9811	-2333	-7478	-10770	-9102	-9231	4037	5194	9317	3920
1300	130	285	80	10847	-2666	-8182	-11856	-9910	-10206	4613	5593	10383	4246
1300	130	300	80	11428	-2864	-8565	-12443	-10326	-10753	4956	5797	10993	4420
-1000	265	145	80	-2413	-28	2441	3222	3790	2269	1931	-4200	-1220	-3029
-1000	265	125	80	-3145	223	2921	3984	4327	2957	1469	-6427	-1992	-3223
-2000	280	130	80	-5444	339	5105	6886	7433	5120	1773	-6893	-3615	-4943
-2000	280	100	80	-6890	728	6161	8438	8682	6480	1102	-7582	-5039	-5486
-3000	300	175	80	-4441	-58	4499	6063	7022	4176	2846	-7022	-2336	-4943
-3000	300	150	80	-6103	279	5824	7905	8660	5748	2322	-8062	-3862	-5725
-3000	300	115	80	-8207	739	7468	10223	10678	7719	1577	-9296	-5826	-6659
-10000	430	210	140	-13015	1203	11812	16541	17315	12242	3783	-16025	-8504	-11284
2500	250	345	250	11757	-3111	-8646	-12935	-10498	-11062	5636	5426	11381	4078
2500	250	410	250	16032	-4045	-11988	-17545	-14519	-15085	6983	8102	15348	6119
2500	250	480	250	19690	-5046	-14644	-21385	-17611	-18526	8499	10027	18921	7640
1500	200	300	200	10379	-2695	-7684	-11329	-9246	-9766	4874	4892	10061	3712
1500	200	530	200	18763	-5579	-13185	-19880	-15332	-17655	9603	8052	18799	6379
1500	200	600	200	20189	-6246	-13943	-21280	-16088	-18997	10740	8257	20442	6624
-700	360	280	250	2745	-1674	-1072	-2289	-292	-2584	4876	-2292	4028	-1503
-700	360	250	250	1669	-1308	-361	-1162	521	-1572	4261	-2689	2912	-1836
-1500	410	315	255	1943	-1755	-187	-1153	1116	-1830	5603	-3774	3703	-2530
-1500	410	255	255	-1048	-971	2019	2072	3766	984	4382	-5365	816	-3769
-3000	495	310	250	-3290	-835	4125	4990	6943	3093	5297	-8390	-565	-5900
-3000	495	250	250	-6492	-90	6581	8460	9906	6105	4147	-10252	-3586	-7327
-10000	495	250	250	-13620	1216	12404	17265	18187	12811	4429	-17240	-8796	-12194
2500	300	400	300	14295	-3840	-10455	-15592	-12551	-13450	6978	6471	13927	4902
2500	300	500	300	20053	-5263	-14789	-21666	-17641	-18867	9114	9754	19463	7475
2500	300	600	300	23796	-6538	-17258	-25467	-20391	-22390	11018	11372	23323	8833
1500	350	450	350	14559	-4226	-10333	-15512	-11977	-13699	8080	5619	14647	4389
1500	350	500	350	16723	-4862	-11862	-17775	-13752	-15735	9054	6682	16804	5243
1500	350	600	350	19647	-5951	-13696	-20738	-15763	-18486	10765	7721	19904	6151
-1000	440	350	350	2753	-1961	-792	-2112	326	2592	5980	-3388	4434	-2271
-2000	560	400	400	-290	-1480	1770	1503	3901	270	6429	-6699	2137	-4705
-3000	480	350	350	-1098	-1355	2454	2584	4875	1031	5932	-6963	1437	-4817
-10000	550	370	330	-6855	-212	7067	9653	11461	6446	6280	-12726	-2788	-8878
1500	500	600	500	19132	-5814	-13318	-20254	-15281	-18002	10961	7061	19458	5594
1500	500	650	500	20646	-6410	-14236	-21791	-16291	-19427	11777	7650	21064	6112
1500	500	680	500	21310	-6743	-14567	-22448	-16635	-20051	12187	7863	21795	6318
-700	615	560	550	7080	-3206	-3874	-6647	-3090	-6664	9097	-2433	8980	-1516
-1500	625	530	530	2857	-2235	-622	-1869	1101	-2691	8212	-5521	5247	-3822
-2200	650	530	530	-82	-1614	1696	1521	4174	74	7864	-7938	2757	-5609
0	70	70	70	0	0	0	0	0	0	0	0	0	0
0	615	615	550	11750	-4299	-7452	-11843	-7593	-11058	10299	759	13210	889

TABLE

STRESSES AND FATIGUE USAGE FOR A TYPICAL PV AT THE NOZZLE-TO-SURGE LINE WELD

SECTION NO. 9 AT THETA = 39. DEGREES FOR S12 ON THE INSIDE SURFACE

PV#	PV#	TMAX (F)	TMIN (F)	3*SM (PSI)	SY (PSI)	E (PSI)	ALPHA (IN/IN/F)	SN (PSI)	SP (PSI)	KE	SA (PSI)	NACTUAL	NALLOW	U	USUM
22	46	550.	200.	56250.	19350.	.2555E+08	.9500E-05	64711.	118415.	1.501	98460.	13.	.19012E+04	.0068	.0068

PL + PB + Q - THERMAL BENDING = 39992. PSI

ALLOWABLE THERMAL STRESS RANGE AS PERMITTED BY RATCHETING RULES = 103212. PSI

TRANS. NAME	PV#	LOAD	COMPUTER RUN NAME		INSIDE SURFACE STRESSES (PSI)						OUTSIDE SURFACE STRESSES (PSI)					
					LINEARIZED			SURFACE			LINEARIZED			SURFACE		
					S12	S23	S31	S1*	S2*	S3*	S12	S23	S31	S1*	S2*	S3*
HU1A1	22	FX		GOMY	[illegible]	[illegible]	-59.	0.	-742.	-57.	803.	-713.	-90.	0.	-960.	-116.
HU1A1	22	PRESS		GOMV	-3778.	-4830.	8609.	-1527.	[illegible]	7119.	-4642.	-2029.	6671.	0.	5627.	6881.
HU1A1	22	MZ		GOJU	7688.	-6985.	-703.	0.	-7766.	-645.	11248.	[illegible]	-1555.	0.	-12977.	-1769.
HU1A1	22	STRAT	GFAE	GOMV	14357.	-13736.	-621.	0.	-13546.	1443.	15360.	-12364.	-2997.	0.	-17583.	-1509.
HU1A1	22	TRANS	GBUG	GILA	23796.	-6538.	-17258.	0.	-25667.	-20391.	-22390.	11018.	11372.	0.	23323.	8853.
HU1A1	22	TOTAL			42802.	-32769.	-10032.	77539.	66535.	-11004.	380.	-13782.	13402	2264.	-14547.	12329.

TRANS. NAME	PV#	LOAD	COMPUTER RUN NAME		INSIDE SURFACE STRESSES (PSI)						OUTSIDE SURFACE STRESSES (PSI)					
					LINEARIZED			SURFACE			LINEARIZED			SURFACE		
					S12	S23	S31	S1*	S2*	S3*	S12	S23	S31	S1*	S2*	S3*
CD1B1	46	FX		GOMY	33.	-35.	-3.	0.	-38.	-3.	41.	-56.	-5.	0.	-49.	-6.
CD1B1	46	PRESS		GOMV	-1047.	-1338.	2385.	-423.	593.	1972.	-1286.	-562.	1848.	0.	1559.	1906.
CD1B1	46	MZ		GOJU	1004.	-912.	-92.	0.	-1014.	-84.	1469.	-1366.	-203.	0.	-1695.	-230.
CD1B1	46	STRAT	GOEY	GOMV	-7706.	2471.	5234.	0.	6446.	4737.	7386.	-2184.	-5202.	0.	-7718.	-4650.
CD1B1	46	TRANS	EOBJ	EOEJ	-14198.	1312.	12886.	0.	18045.	18889.	13355.	4127.	-17482.	0.	-9277.	-12310.
CD1B1	46	TOTAL			-21908.	1499.	20410.	-60876.	-14942.	25934.	20965.	78.	-21043.	18742.	-3453.	-15289.

* NOTE, FOR TOTAL LOAD, THESE REPRESENT STRESS DIFFERENCES S12, S23, AND S31.

FIGURE 6-1

GEOMETRY OF PRESSURIZER SURGE NOZZLE

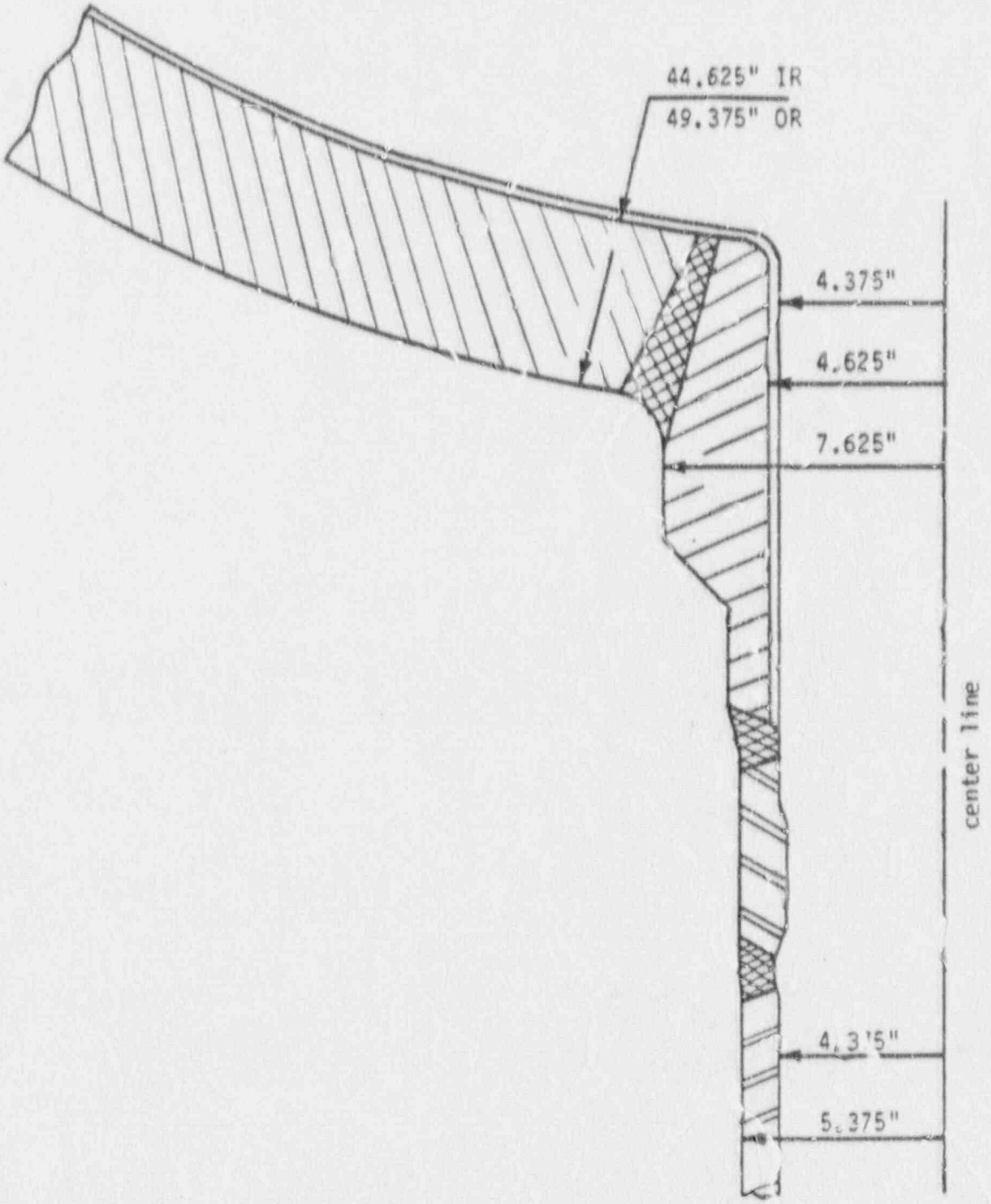

FIGURE 6-2

FINITE ELEMENT MODEL OF PRESSURIZER SURGE NOZZLE

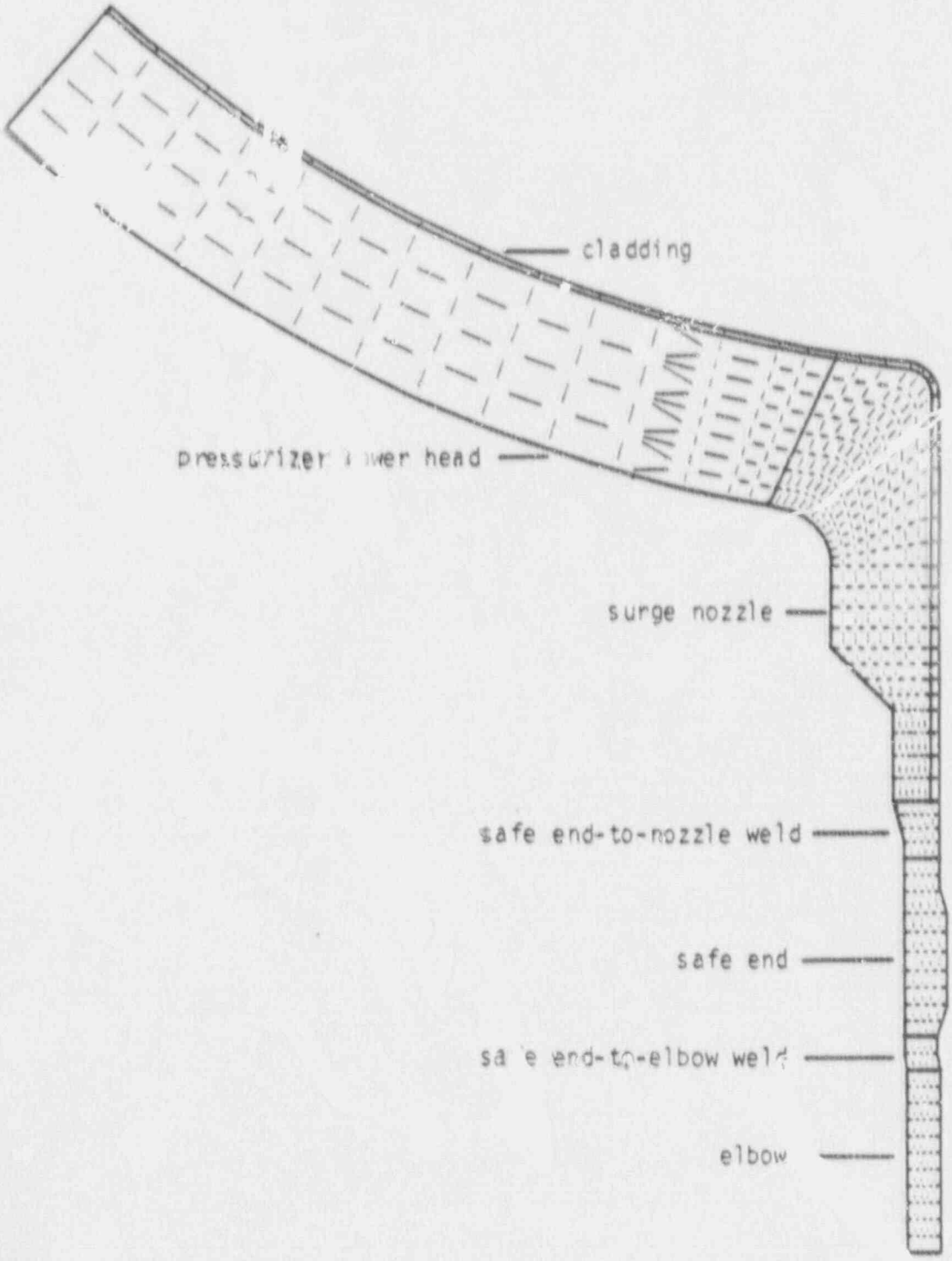

FIGURE 6-3

EXAMPLE OF TYPICAL TRANSIENT

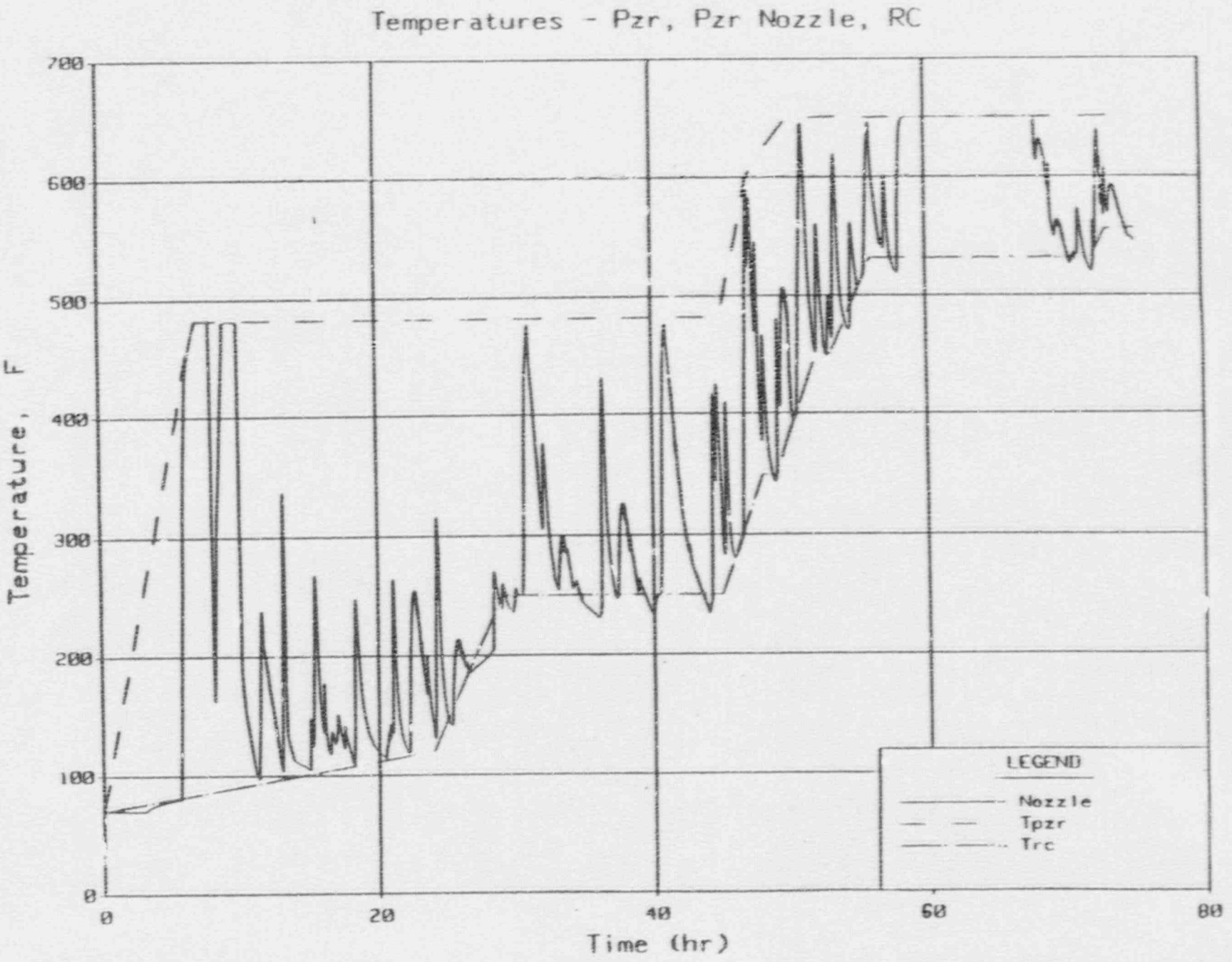

FIGURE 6-4

SUMMARY OF THERMAL BOUNDARY CONDITIONS
(pressurizer surge nozzle)

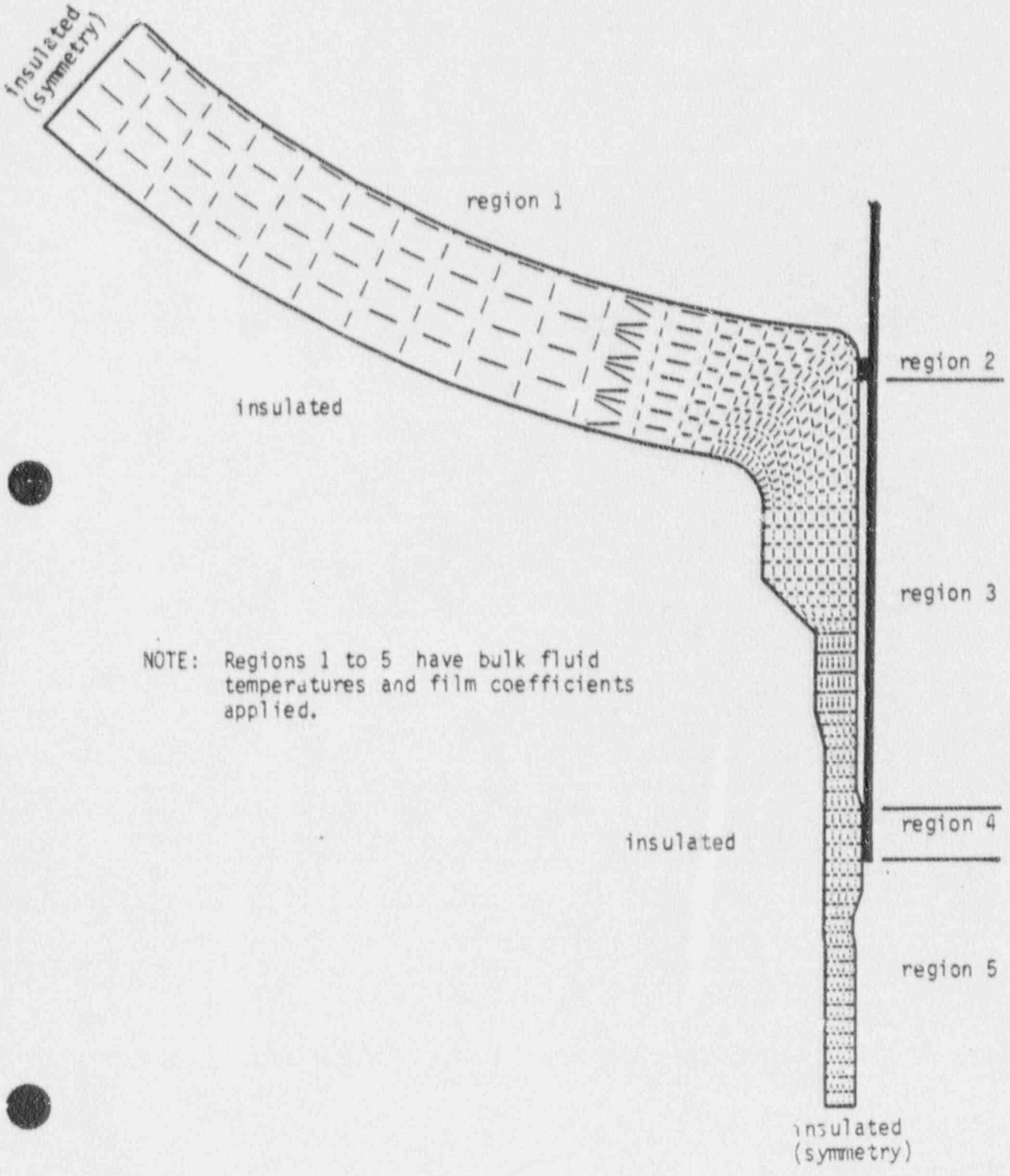

FIGURE 6-5

LOCATION OF DELTA-T VALUES
(pressurizer surge nozzle)

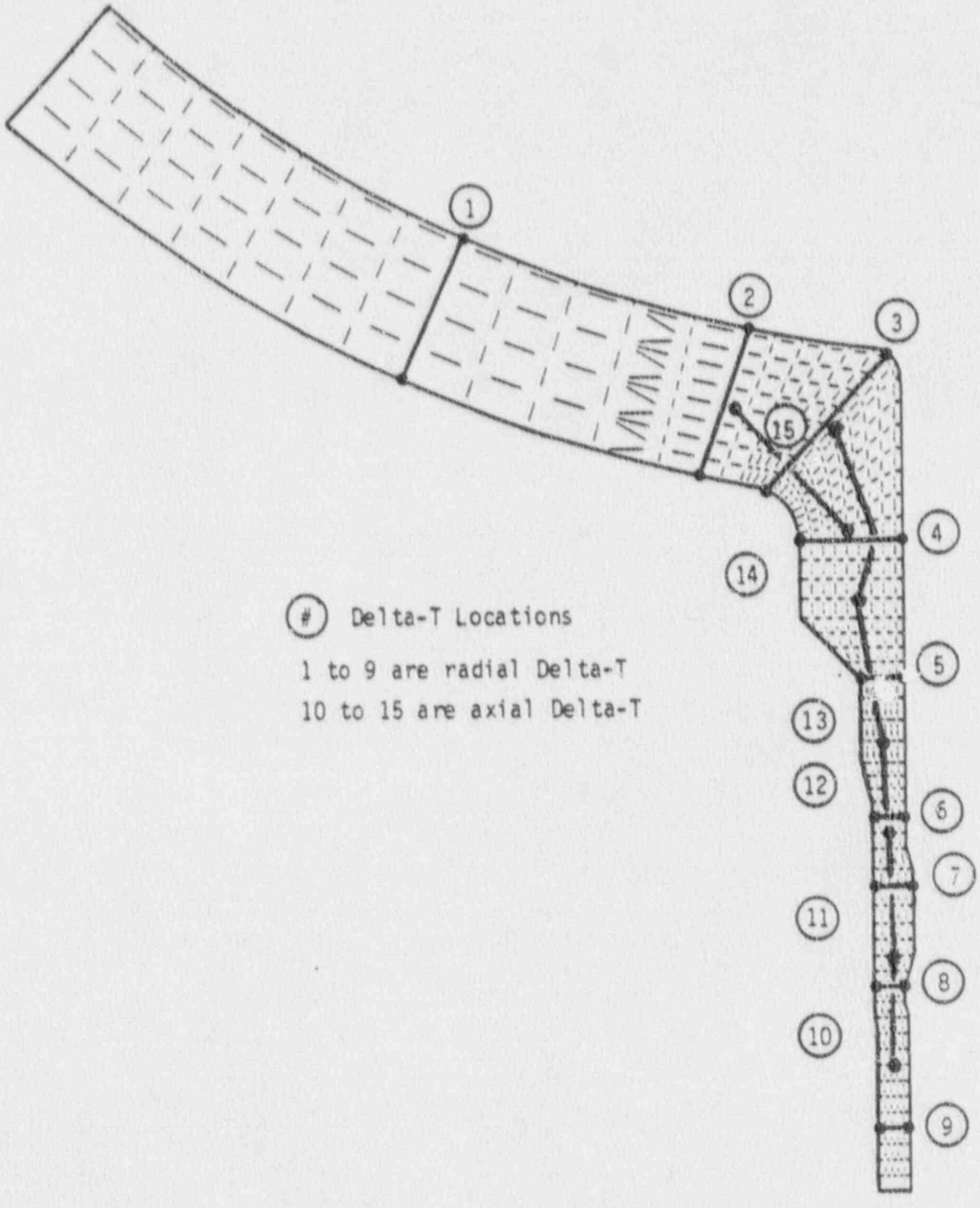

FIGURE 6-6

STRUCTURAL BOUNDARY CONDITIONS
(pressurizer surge nozzle)

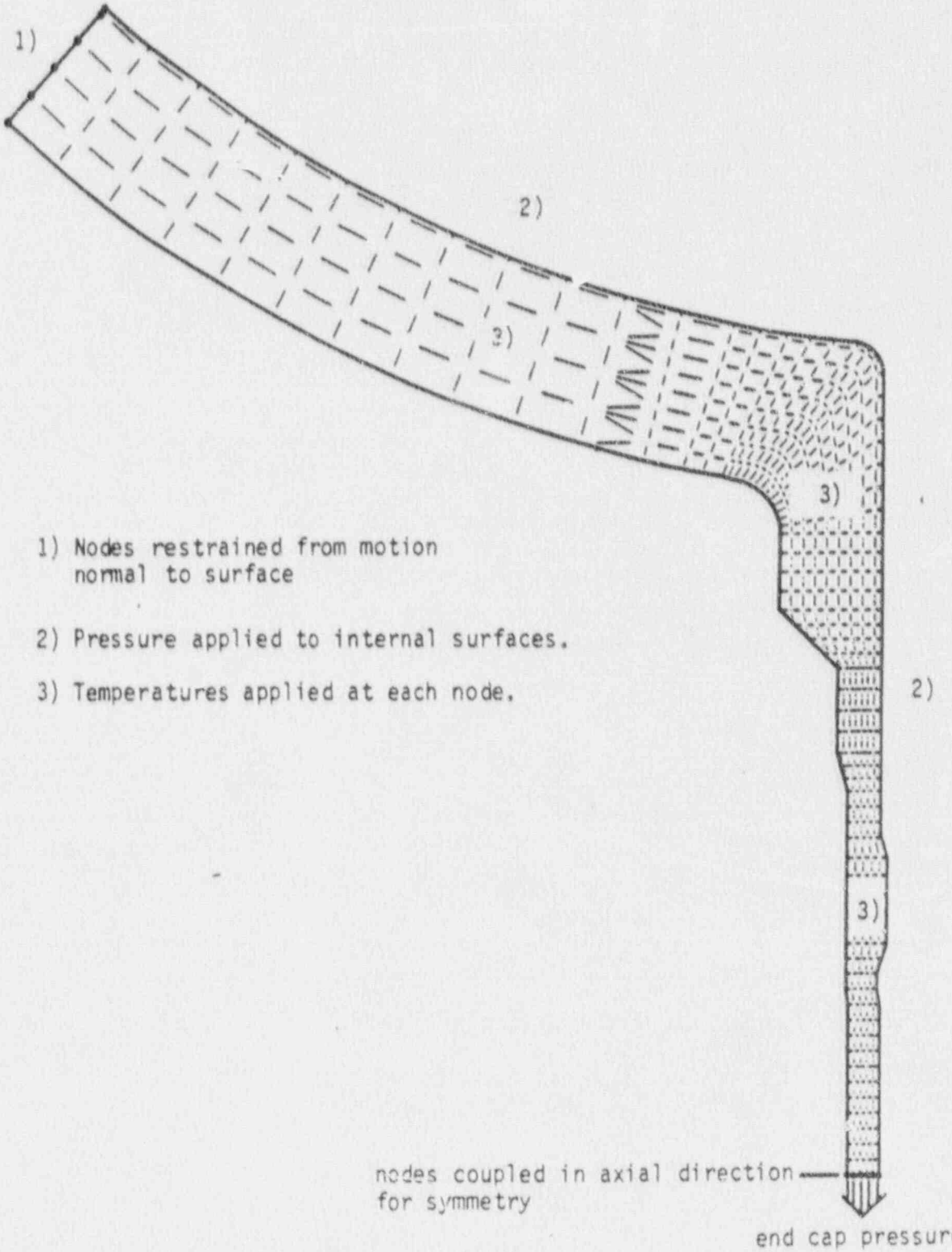

1) Nodes restrained from motion normal to surface

2) Pressure applied to internal surfaces.

3) Temperatures applied at each node.

FIGURE 6-7

LOCATION OF STRESS CLASSIFICATION LINES
(pressurizer surge nozzle)

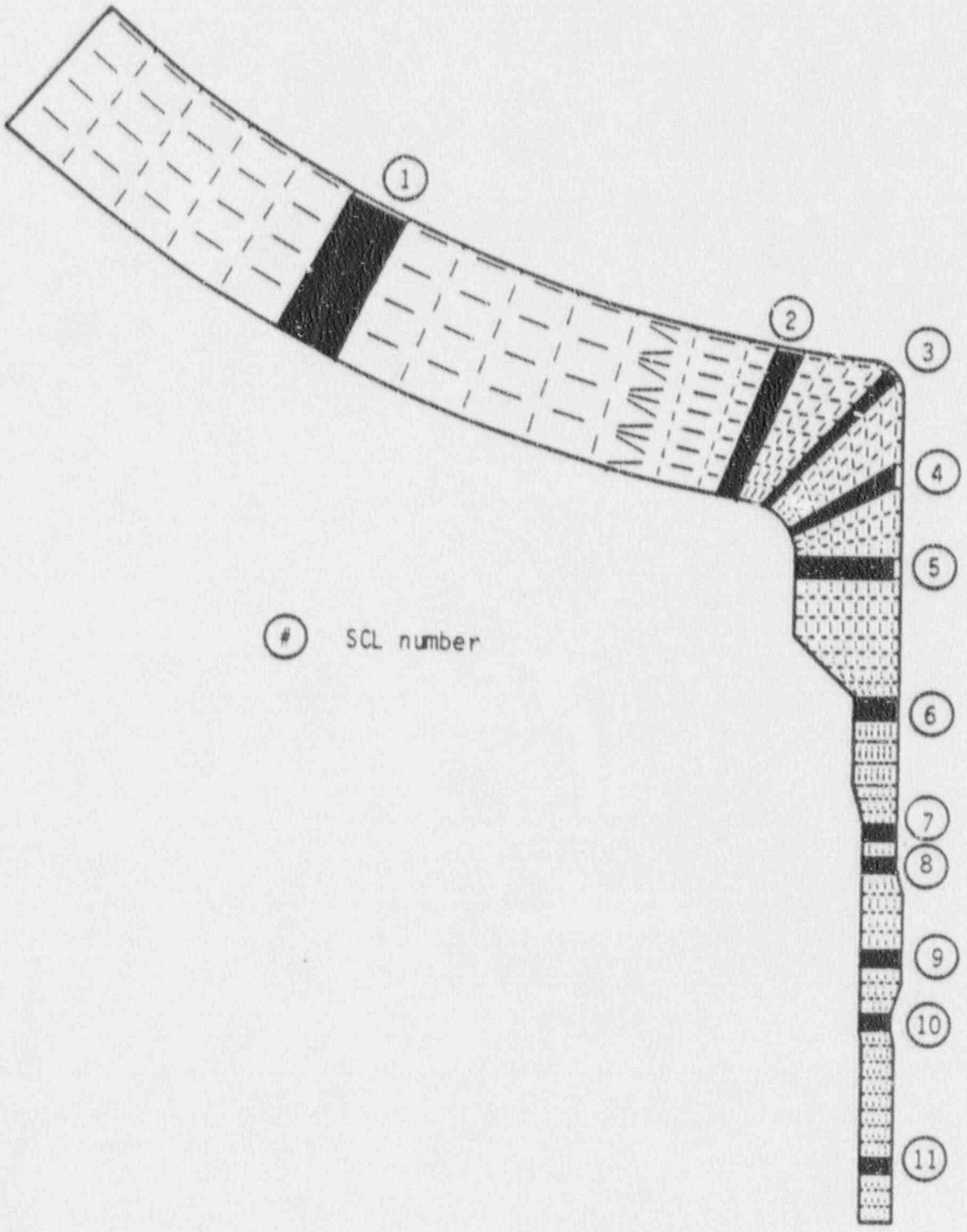

FIGURE 6-8

GEOMETRY OF HOT LEG SURGE NOZZLE

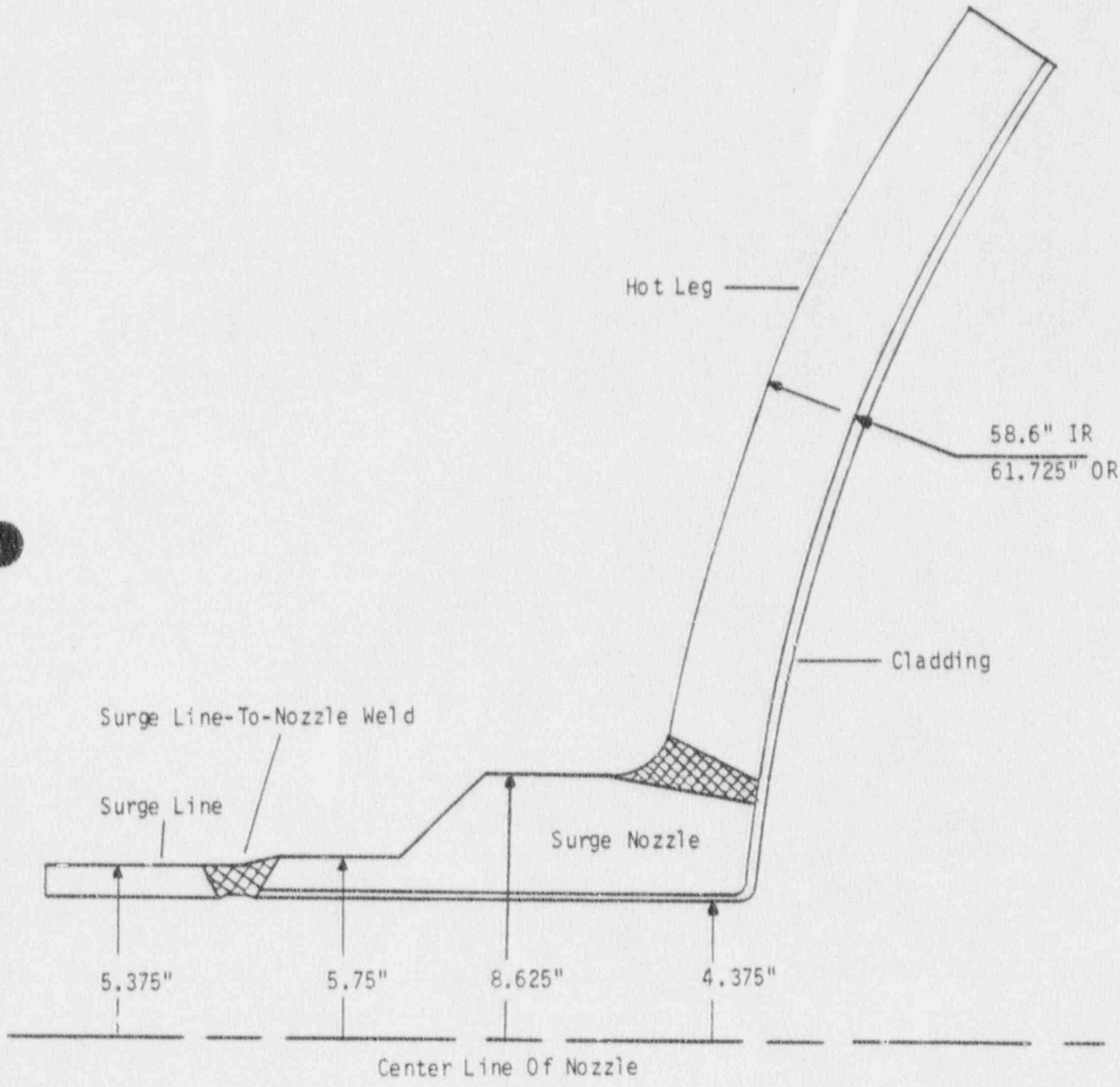

FIGURE 6-9

FINITE ELEMENT MODEL OF HOT LEG SURGE NOZZLE

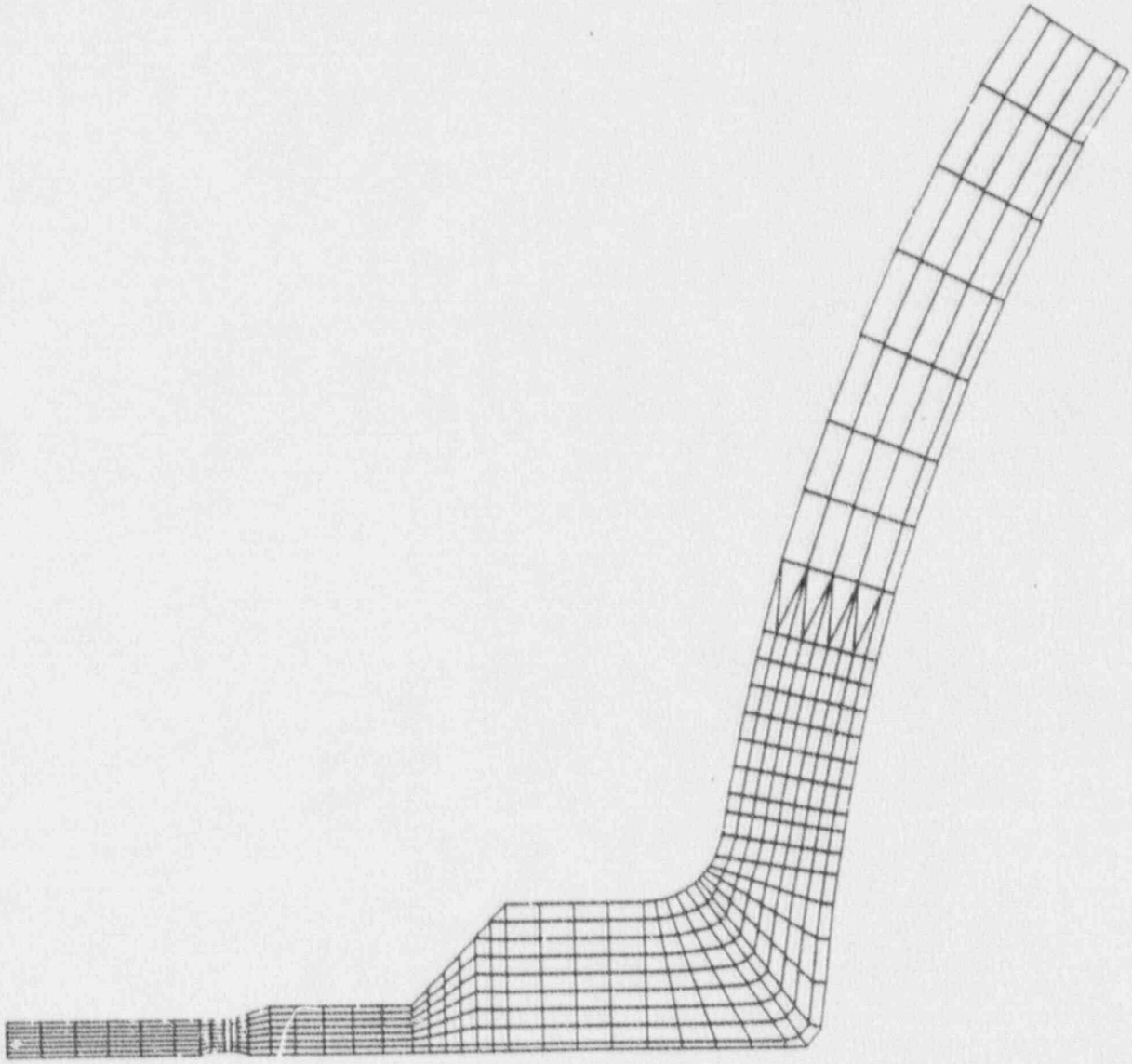

FIGURE 6-10

EXAMPLE OF A TYPICAL TRANSIENT FOR THE HOT LEG SURGE NOZZLE

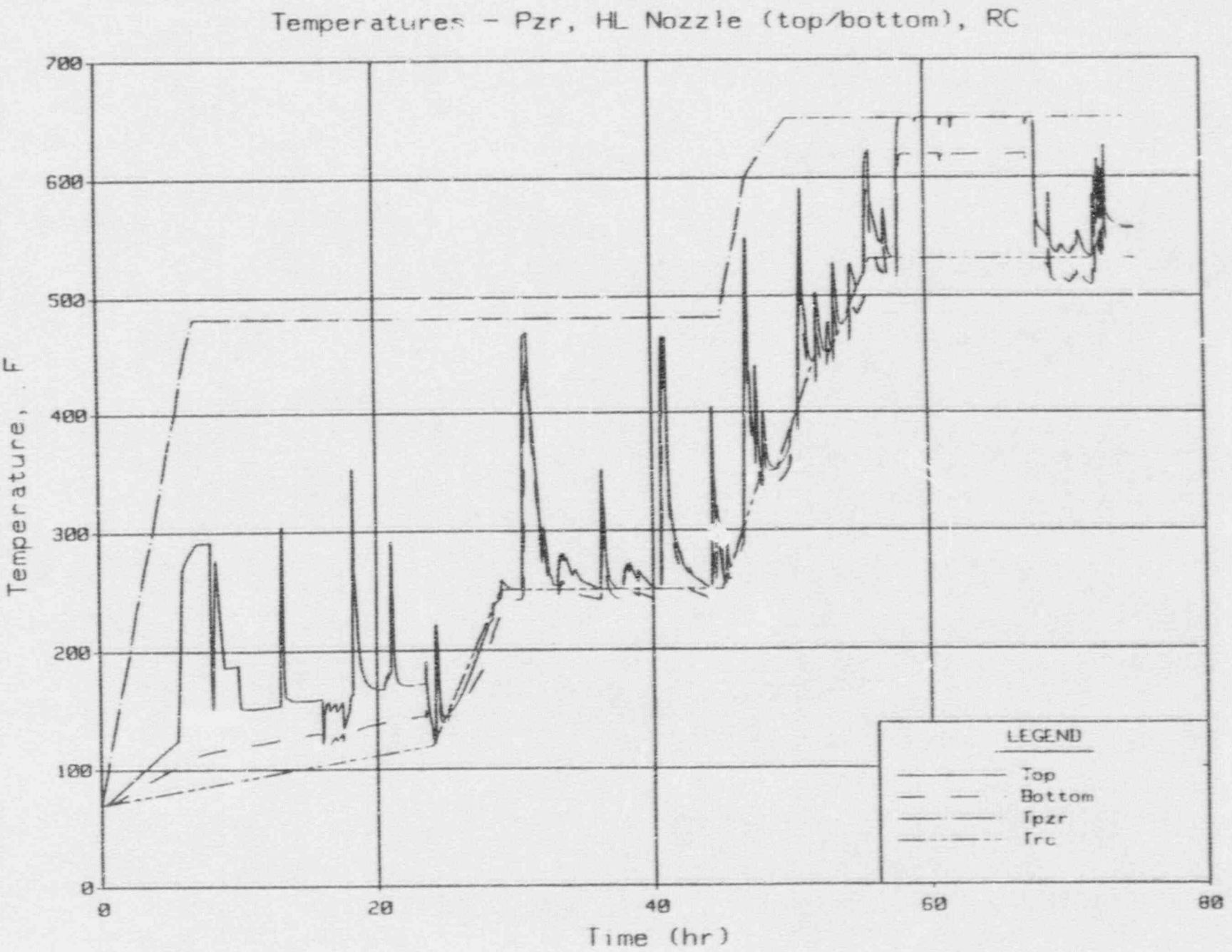

FIGURE 6-11

LOCATION OF DELTA-T VALUES
(hot leg surge nozzle)

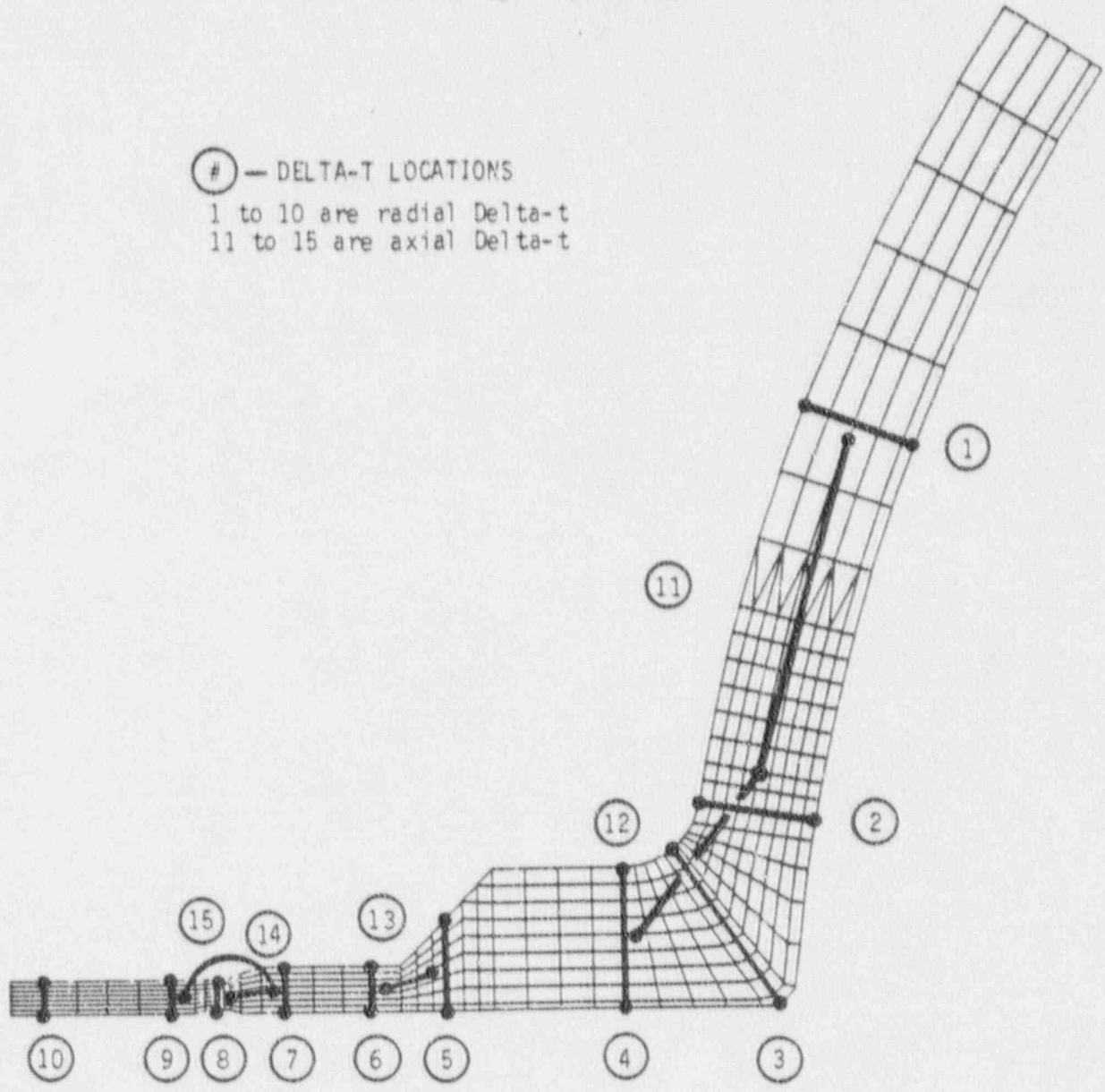

FIGURE 6-12

HOT LEG SURGE NOZZLE TEMPERATURE CONTOURS (F) FOR A TYPICAL PV

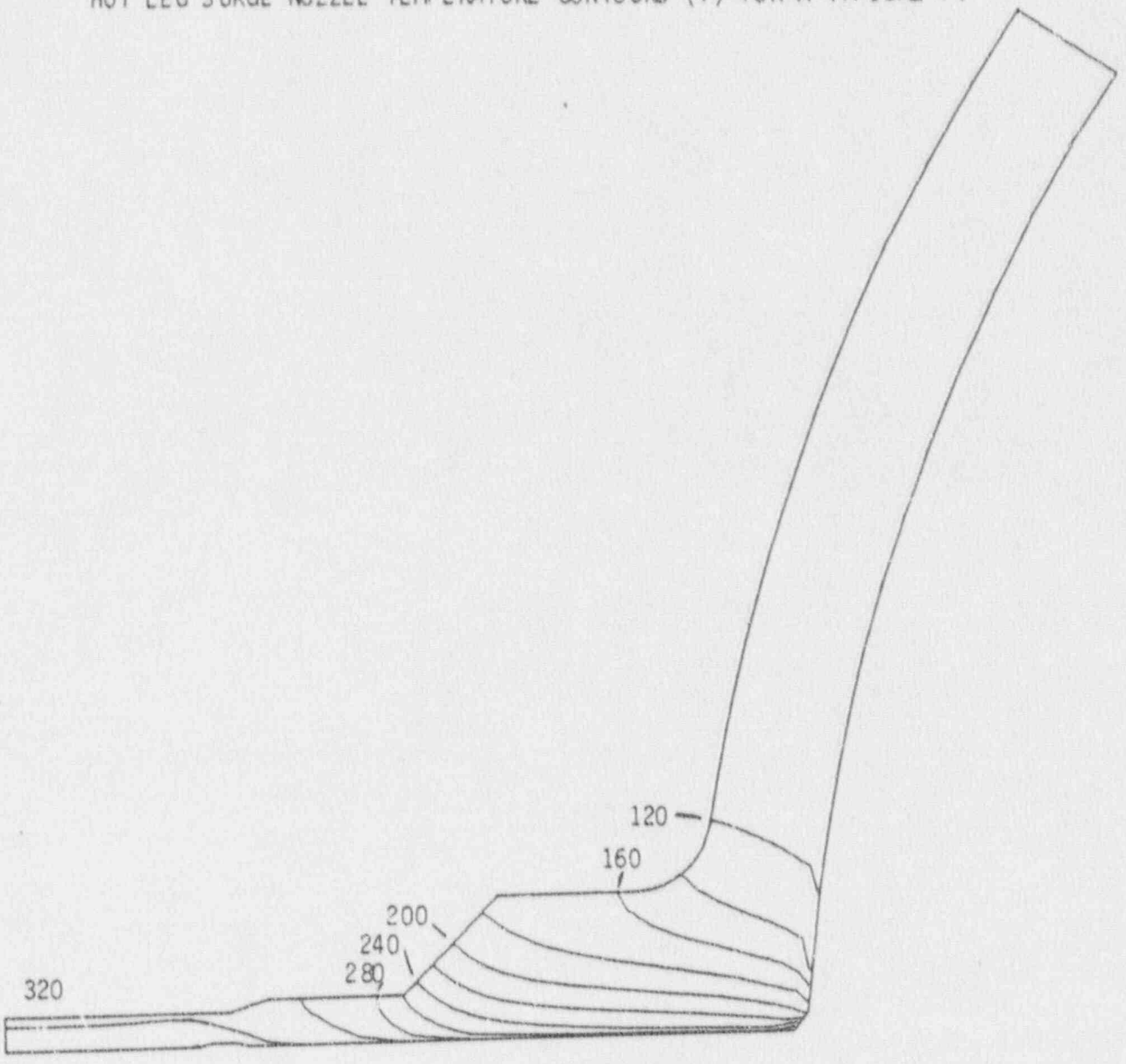

FIGURE 6-13

LOCATION OF STRESS CLASSIFICATION LINES
(hot leg surge nozzle)

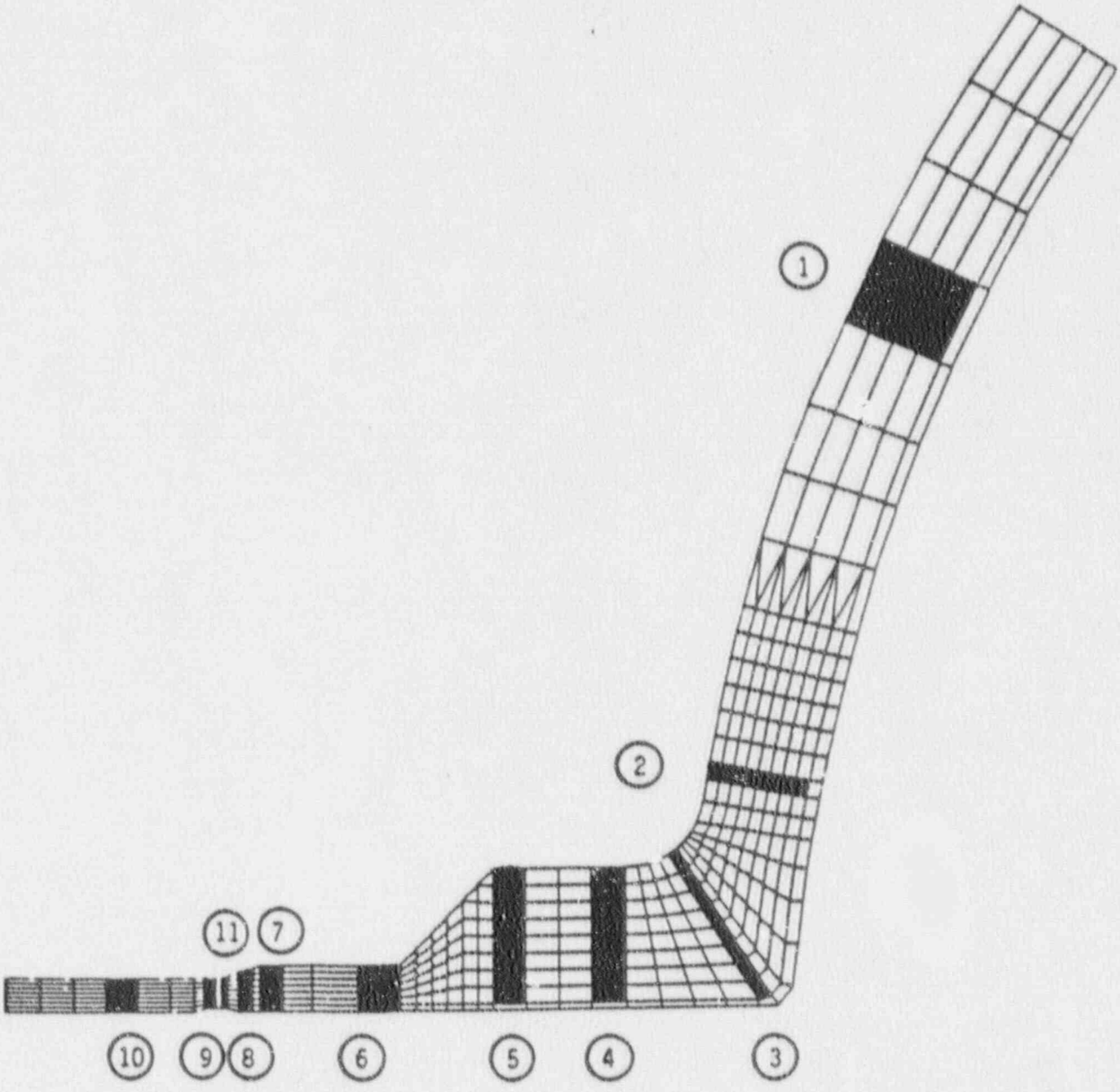

7. SUMMARY OF RESULTS

The B&W Owners Group has developed a program to comprehensively address the requirements of NRC Bulletin 88-11, "Pressurizer Surge Line Thermal Stratification". The Owners have collected the necessary information required to evaluate the surge line. In addition to operational records and plant design information, plant thermal stratification data and thermal striping test data have been obtained.

It has been determined that the lowered loop plant configuration and plant operations are sufficiently similar for a generic development of the design basis transients. Stratification data for the lowered loop plants has been obtained by monitoring the thermal conditions of the Oconee Unit 1 surge line during normal operations. This data made it obvious that the original design basis did not adequately represent surge line thermal conditions. The details of the Owners plan have been subsequently developed to correlate the Oconee Unit 1 stratification data and other information for use in generating a set of transients accurately representing the surge line conditions for the operating conditions in the plants.

Davis-Besse Unit 1 (DB-1), a raised loop plant, requires its own instrumentation and a separate plant specific set of design basis transients because of inherent differences in its design. These differences are discussed in Section 3 and the DB-1 analysis will be addressed in a supplement to this report.

Revised surge line design basis transients accounting for plant evolutions affecting the surge line for the 40 year design life of each B&W plant have been developed. The number of occurrences for each transient varies among the plants due to differences in operational history. The plant heatup and cooldown transients have been the most significant contributor to the fatigue usage factor for surge line components.

A structural loading analysis of the surge line has been performed to take into account the global effects due to thermal stratification. The resulting internal forces and moments have been applied for the fatigue stress analysis of the surge line and the associated nozzles.

The fatigue stress analysis takes into consideration the stress ranges for the global effects due to thermal stratification, the localized effects due to thermal stratification, the pressure ranges, the Operating Basis Earthquake, the thermal striping and the fluid flow conditions. All resulting stress intensities have been shown to be within their allowable limits. As a result of the fatigue analyses, the cumulative usage factor is less than 1.0 at all locations of the surge line and its nozzles.

In summary, the following is a tabulation of the highest usage factor of all six lowered loop plants for the most important surge line components.

Surge Line Component	Usage Factor (40 year Life)
Surge Line Elbow	0.82
Straight Pipe Section	0.48
Drain Nozzle Branch Connection	0.37
Pressurizer Nozzle	0.41
Hot Leg Nozzle	0.62

In view of the conservatism accumulated in the synthesis of the design transients and in the analysis of resultant stresses, these fatigue usage values provide assurance that the 40 year licensed life of the lowered loop B&W plants will be met with considerable margin to accommodate normal variations in operations.

8. BASES FOR THE B&WOG ANALYSIS - FOR PLANT SPECIFIC APPLICATION

The generation of the revised Design Basis transients and the thermal stratification fatigue stress analysis of the surge line have been based on conditions stated in this section.

The thermal stratification fatigue stress analysis has been based on:

- no interference of the surge line with any other structure,
- surge line movement within the travel range of each snubber,
- surge line movement within the travel range of each hanger, and
- branch moments at the surge line drain nozzle connection within their respective maximum allowables (for Deadweight, Operating Basis Earthquake and thermal stratification).

The generation of the revised Design Basis transients (for future events) has been based on the incorporation of operational guidelines which:

- limit the pressurizer to RCS temperature difference during plant heatups and cooldowns (imposed with pressure/temperature limits), and
- prevent surveillance tests which cause rapid additions of water to the RCS from being performed with a pressurizer to RCS temperature difference greater than 220F.

The heatup and cooldown Design Basis transients which were defined for future operation should remain conservative if the pressure is limited in accordance with Figure 8-1. The curve shown in Figure 8-1 is a composite of variable subcooling limits that change with RCS temperature. The operating procedures of each of the lowered loop plants are to maintain pressure and temperature during heatup and cooldown operations to the right of the selected maximum allowed subcooling limits.

To meet the pressure limit specified for heatup in the temperature range 70F to 150F, preheating the RCS has been recommended. This may be accomplished by throttling back on the decay heat system cooling water (i.e. component cooling water) and/or bypassing reactor coolant flow around the decay heat removal heat exchanger. The availability of decay heat and the requirements of the heatup schedule will dictate the capability of maintaining the recommended P/T profile prior to achieving the conditions necessary for starting an RC pump. The fatigue evaluation has been performed on the basis that 85% of the heatups for the remainder of the plant life can meet the recommended limit shown by path CDEN in Figure 8-1. For those heatups involving pressurization at an RC temperature of 70F to 120F, a less restrictive limit is included in order to permit RC pump operation at lower RCS temperatures (path ABEN in Figure 8-1) when core decay heat is not adequate for raising RC temperature. The fatigue evaluation has been performed on the basis that 15% of the heatups for the remainder of the plant life will follow this heatup path. In summary, future heatups have been divided into path CDEN (85%) and path ABEN (15%).

Figure 8-1. Surge Line Operational Limit

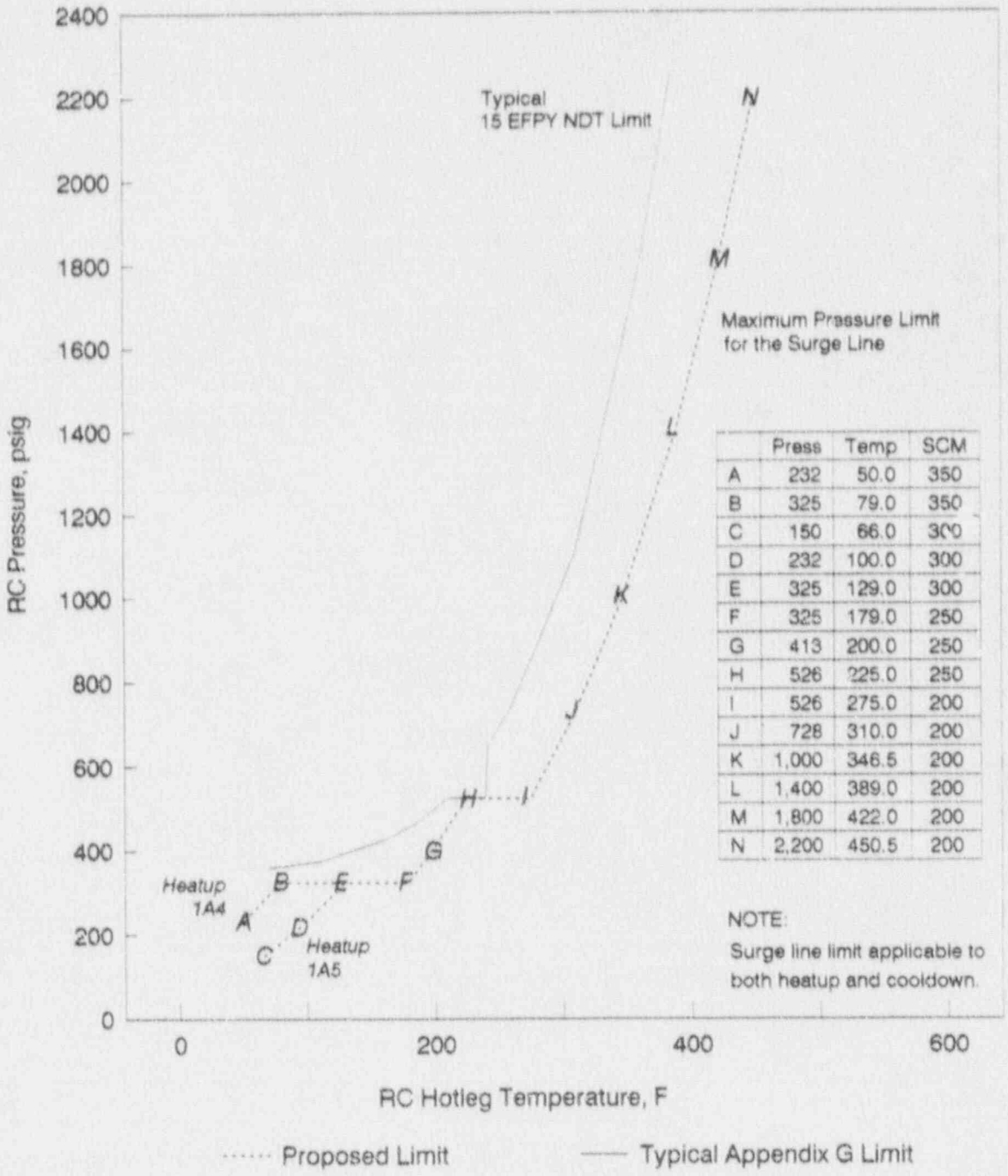

	Press	Temp	SCM
A	232	50.0	350
B	325	79.0	350
C	150	66.0	300
D	232	100.0	300
E	325	129.0	300
F	325	179.0	250
G	413	200.0	250
H	526	225.0	250
I	526	275.0	200
J	728	310.0	200
K	1,000	346.5	200
L	1,400	389.0	200
M	1,800	422.0	200
N	2,200	450.5	200

9. REFERENCES

1) NRC Bulletin 88-11, "Pressurizer Surge Line Thermal Stratification", dated Dec. 20, 1988.

2) BAW-2085, "Submittal in Response to NRC Bulletin 88-11, Pressurizer Surge Line Thermal Stratification", dated May 1989.

3) NRC Letter dated May 18,1990, J.T. Larkins to M.A. Haghi, "Evaluation of Babcock & Wilcox Owners Group Bounding Analysis Regarding NRC Bulletin 88-11".

4) H.O. Fuchs et al, "Shortcuts In Cumulative Damage Analysis" in Fatigue Under Complex Loading, R.M. Wetzel (ed.), SocAutoEng, 1977.

5) H.Watanabe, "Boiling Water Reactor Feedwater Nozzle/Sparger Final Report,"NEDO-21821-A (February 80).

6) W.S. Woodward, "Fatigue of LMFBR Piping due to Flow Stratification", ASME Pressure Vessel and Piping Conference, Portland, Paper 83-PVP-59, CONF-830607-27 (June 83).

7) T.Fujimoto, K. Swada, K. Uragami, A. Tsuge, and K. Hanzawa, "Experimental Study of Striping at the Interface of Thermal Stratification", Thermal Hydraulics in Nuclear Technology, K.H. Sun et al (ed), ASME (81).

8) T.M. Kuzay and K.E. Kasza, "Thermal Oscillations Downstream of an Elbow in Stratified Pipe Flow", FBR Thermal Hydraulics, Trans ANS, 46, 794-796 (June 84).

9) T.M. Kuzay and K.E. Kasza, "Thermal Striping Downstream of a Horizontal Elbow Under Thermally Stratified Flow Conditions", Joint Mtg. ANS and AIF, Washington, CONF-841105-10 (Nov.84).

10) T.M. Kuzay and K.E. Kasza, "Resolution of Thermal Striping Issue Downstream of a Horizontal Pipe Elbow in Stratified Pipe Flow," ANS Annual Meeting, Boston, CONF-850610-4 (June 85).

11) L. Wolf and U. Schygulla, "Experimental Results of HDR-TEMR Thermal Stratification Test in Horizontal Feedwater Lines," Trans 9th SMIRT, D, pp.361-367 (87).

12) L. Wolf, U. Schygulla, M. Geiss and E. Hansjosten, "Thermal Stratification Test in Horizontal Feedwater Pipelines," Proc 15th WRSRIM, NUREG/CP-0091, 5, pp. 437-464 (Feb 88).

13) L. Wolf, U. Schygulla, M. Geiss and E. Hansjosten, and A. Talja, "Temperature and Wall Strain Fluctuations During the TEMR Thermal Stratification Tests AT HDR," 10th SMIRT, Anaheim, CA (Aug 89).

14) L. Wolf, M. Geiss, E. Hansjosten, and A. Talja, "Evaluation of the Thermal Stratification Tests at the HDR Facility," NURETH-4 Conference, 2, Karlsruhe, FRG (Oct 89).

15) A. Talja and E. Hansjosten, "Results of Thermal Stratification Tests In a Horizontal Pipe Line At the HDR Facility," TRANS 10th SMIRT, E (89).

16) U. Schygulla and L. Wolf, "Design Report - Thermal Stratification Experiments In a Horizontal Piping Section," HDR-Test group TEMR T33, Battelle-FRG (November, 1986).

17) "ANSYS" Computer Code, Versions 4.1c and 4.3. Engineering Analysis System, User's Manual Volumes I and II, Swanson Analysis Systems, Inc.

18) "ASME Boiler and Pressure Vessel Code", Section III, 1986 Edition with no Addenda.

19) "ABAQUS" Computer Code, Version 4.8.5, 1989, User's Manual, Hibbitt, Karlsson and Sorensen, Inc.

20) J.B. Truitt and P.P. Raju, "Three Dimensional Versus Axisymmetric Finite-Element Analysis of a Cyclindrical Vessel Inlet Nozzle Subject to Internal Pressure - A Comparative Study", ASME Pressure Vessel and Piping Division, Paper No. 78-PVP-6.

10. DOCUMENT SIGNATURES

This document has been prepared by:

M T Matthews 12/15/90
M.T. Matthews

R. Gurdal 12/18/90
R.J. Gurdal

D E Costa 12/18/90
D.E. Costa

G. L. Weatherly 12/18/90
G.L. Weatherly

The report has been reviewed for technical content and accuracy by:

James R. Gloudemans 12/18/90
J.R. Gloudemans, Analysis Services

J. F. Shepard 12/18/90
J.F. Shepard
Material & Structural Analysis

Verification of independent review.

C W Tally 12/19/90
C.W. Tally, Manager
Performance Analysis

K. E. Moore
K.E. Moore, Manager
Materials & Structural Analysis

This document has been approved for release.

W R Gray 12/19/90
W.R. Gray, Program Manager

APPENDIX A

A. Surge Line Data Acquisition at Oconee Unit 1

CONTENTS

Oconee Unit 1 was instrumented as part of the B&WOG program as discussed in Section 4.1. This appendix supplements Section 4.1 with additional detail on the data acquisition.

1. Thermocouple Fabrication and Instrumentation Qualification

The thermocouple assemblies and associated extension wire assemblies required for instrumenting Oconee Unit 1, including spares, were fabricated by the Babcock & Wilcox Alliance Research Center (ARC). Seventy thermocouple assemblies were fabricated from ANSI Type K, 20 gage solid Chromel-Alumel commercial grade assembly wire having parallel conductors individually insulated with ceramic fiber braid, an overall jacket of ceramic fiber braid and Inconel protective overbraid. The hot junction, or bead of each thermocouple was formed by heliarc welding (fusing) the two conductors together, then swaging the bead to a flat disk to ensure intimate contact with the surge line pipe. Standard 2-pole connector plugs with integral cable clamp were attached to the ends of the thermocouple wires opposite the hot junction. Ninety-five thermocouple extension cable assemblies were fabricated from ANSI Type K, 20-gage solid Chromel-Alumel commercial grade extension wire having twisted connectors individually insulated with Teflon, Mylar-backed aluminum foil shielding with drain wire, and an overall extruded Teflon insulation jacket.

Qualifying the commercial grade thermocouples fabricated for the safety-related pressurizer surge line temperature measurement application was accomplished by the standard practice of "type" testing. In this approach, six additional thermocouple assemblies prepared from the same materials and following the same procedures that applied to fabricating the thermocouples installed at Oconee were placed in ovens along with certified Platinum Resistance Thermometers (RTDs) and heated. Comparison between the temperature registered by these qualification test thermocouples and the reference temperature monitored by the RTDs provided a means of qualifying the surge line thermocouples. Also, as part of the qualification test, the string potentiometers and the linear variable differential transformers (LVDTs) were connected to the assigned channels of the data acquisition system instrumentation cabinet, as configured for the surge line field test, and operated. Transducers were arbitrarily chosen (four LVDTs and four PTs) and exposed to simulated ambient temperatures expected to exist at Oconee Unit 1 during heatup. At these various test conditions, reference

displacements were imposed to assess the functional performance of the transducer types.

Comparison of thermocouple data and the RTD reference indications demonstrated that thermocouple readings were consistently within 1.5F of the reference temperature. This agreement was well within the established acceptance criteria at all test conditions for qualifying surge line thermocouples. From the testing and evaluations of the two types of displacement transducers, it was evident that both the LVDTs and string potentiometers are well suited for the surge line test application. The qualification results demonstrated acceptable displacement transducer operating and performance characteristics when subjected to the range of expected surge line and pressurizer room ambient temperatures. Finally, the qualification testing process demonstrated the adequacy of the Helios-based data acquisition system for the ambient temperatures expected during plant operations.

2. Data Acquisition System Description and Operation

The schematic in Figure A-1 depicts the general interface of components which make up the data acquisition system. The system included a Fluke Helios mainframe controlled by a host Compaq computer utilizing LabTech Notebook software which was configured to receive the desired data. The computer and Helios front end, which were located in the Oconee 1 control room, interfaced with a remote Helios extender chassis housed in an instrumentation cabinet located in the reactor containment building near the pressurizer surge line. This instrument cabinet also contained the power supply, signal conditioning and other interfacing equipment required for the surge line thermocouples and displacement transducers.

With the system installation complete, the integrity of each instrument and acquisition component was checked. Proper electrical loop resistances for the thermocouples, lead wires, and extension cables were verified. A polarity test and a complete checkout were then performed for all instrument channels. Data collection was started one hour before the pressurizer heaters were turned on and continued until the plant had reached full power and remained there for several days. There were only short time periods in which data collection was interrupted in order to download the data from the host computer.

In addition to overseeing Data Acquisition System operation, members of the surge line data acquisition team logged important plant events as the control room operators and plant computer system kept the acquisition team informed of the heatup procedural steps being taken. After the heatup was complete, the control room logbooks and procedural checklist were also obtained to assist in associating plant operations to surge line transients.

3. General Description of Data

The temperature and displacement of the surge line were monitored, as well as the reactor coolant system (RCS) conditions. A list of recorded parameters is contained in Table A-1. To monitor the thermal conditions of the surge line, thermocouples were spot welded to the outer diameter of the pipe at nine different axial locations (see Figure A-2). The movement of the surge line was monitored with displacement transducers at 23 locations (see Figure A-3). Fifty-four thermocouples were installed, with either three, seven, or ten being placed at the nine axial locations. Each vertical location (locations 2, 4, and 13) contained three thermocouples placed symmetrically around the pipe. The horizontal locations (locations 1, 5, 7, 9, 11, and 12) contained seven thermocouples spaced from top to bottom down one side of the surge line. Location 9 contained an additional three thermocouples evenly spaced along the other side of the surge line for a total of ten thermocouples at this axial location. The thermocouples were identified by axial location and relative position as follows: "12-T5" means the thermocouple at axial position 12, fifth from the top of the line.

Plant data has been recorded for four heatups, three cooldowns and during periods of power operation. The data was stored for the first heatup and cooldown (2/89) with a sample time of 20 seconds which was nearly the fastest update time possible for the Data Acquisition System. The subsequent heatups and cooldowns were primarily monitored with an update time of 60 seconds which was deemed acceptable based on the 20 second data. The large quantity of data (more than 180 Megabytes of disk space) was stored in ASCII format and transferred to the BWNS HP9000 Series 800 computer where the data was processed into functional information (plots, calculations, etc.).

Table A-1. Oconee Stratification Test Signal List

SIGNAL NAME	SIGNAL DESCRIPTION
1-T1-E	Surge Line Location 1, Thermocouple 1-E
1-T2-E	Surge Line Location 1, Thermocouple 2-E
1-T3-E	Surge Line Location 1, Thermocouple 3-E
1-T4-E	Surge Line Location 1, Thermocouple 4-E
1-T5-E	Surge Line Location 1, Thermocouple 5-E
1-T6-E	Surge Line Location 1, Thermocouple 6-E
1-T7-E	Surge Line Location 1, Thermocouple 7-E
10-L3-Y	3" LVDT, S/N 648
10-SP-X	5" Celesco String Pot, S/N 2516
10-SP-Y	5" Celesco String Pot, S/N 2513
11-L2-Y	2" LVDT, S/N 1996
11-SP-X	5" Celesco String Pot, S/N 2520
11-T1-S	Surge Line Location 11, Thermocouple 1-S
11-T2-S	Surge Line Location 11, Thermocouple 2-S
11-T3-S	Surge Line Location 11, Thermocouple 3-S
11-T4-S	Surge Line Location 11, Thermocouple 4-S
11-T5-S	Surge Line Location 11, Thermocouple 5-S
11-T6-S	Surge Line Location 11, Thermocouple 6-S
11-T7-S	Surge Line Location 11, Thermocouple 7-S
12-L2-Y	2" LVDT, S/N 1995
12-T1-S	Surge Line Location 12, Thermocouple 1-S
12-T2-S	Surge Line Location 12, Thermocouple 2-S
12-T3-S	Surge Line Location 12, Thermocouple 3-S
12-T4-S	Surge Line Location 12, Thermocouple 4-S
12-T5-S	Surge Line Location 12, Thermocouple 5-S
12-T6-S	Surge Line Location 12, Thermocouple 6-S
12-T7-S	Surge Line Location 12, Thermocouple 7-S
13-T1-W	Surge Line Location 13, Thermocouple 1-W
13-T2-NE	Surge Line Location 13, Thermocouple 2-NE
13-T3-SE	Surge Line Location 13, Thermocouple 3-SE
2-SP-X	5" Celesco String Pot, S/N 2518
2-SP-Z	5" Celesco String Pot, S/N 2529
2-T1-N	Surge Line Location 2, Thermocouple 1-N
2-T2-SE	Surge Line Location 2, Thermocouple 2-SE
2-T3-SW	Surge Line Location 2, Thermocouple 3-SW
2HPI152B	Loc 2 HPI Nozzle Temperature 152, Bottom
2HPI152T	Loc 2 HPI Nozzle Temperature 152, Top
2HPI153B	Loc 2 HPI Nozzle Temperature 153, Bottom
2HPI153T	Loc 2 HPI Nozzle Temperature 153, Top
3-SP-X	5" Celesco String Pot, S/N 2521
3-SP-Z	5" Celesco String Pot, S/N 2522

Table A-1. (cont.)

SIGNAL NAME	SIGNAL DESCRIPTION
3HPI152B	Loc 3 HPI Nozzle Temperature 152, Bottom
3HPI152T	Loc 3 HPI Nozzle Temperature 152, Top
3HPI153B	Loc 3 HPI Nozzle Temperature 153, Bottom
3HPI153T	Loc 3 HPI Nozzle Temperature 153, Top
4-SP-X	5" Celesco String Pot, S/N 2527
4-SP-Z	5" Celesco String Pot, S/N 2525
4-T1-N	Surge Line Location 4, Thermocouple 1-N
4-T2-SE	Surge Line Location 4, Thermocouple 2-SE
4-T3-SW	Surge Line Location 4, Thermocouple 3-SW
4HPI152	Loc 4 HPI Nozzle Temperature 152
4HPI153T	Loc 4 HPI Nozzle Temperature 153, Top
5-L2-Y	2" LVDT, S/N 1977
5-SP-Z	5" Celesco String Pot, S/N 2514
5-T1-E	Surge Line Location 5, Thermocouple 1-E
5-T2-E	Surge Line Location 5, Thermocouple 2-E
5-T3-E	Surge Line Location 5, Thermocouple 3-E
5-T4-E	Surge Line Location 5, Thermocouple 4-E
5-T5-E	Surge Line Location 5, Thermocouple 5-E
5-T6-E	Surge Line Location 5, Thermocouple 6-E
5-T7-E	Surge Line Location 5, Thermocouple 7-E
6-L3-Y	3" LVDT, S/N 645
6-SP-Y	5" Celesco String Pot, S/N 2530
6-SP-Z	5" Celesco String Pot, S/N 2512
7-L2-Y	2" LVDT, S/N 1974
7-SP-Z	5" Celesco String Pot, S/N 2515
7-T1-E	Surge Line Location 7, Thermocouple 1-E
7-T2-E	Surge Line Location 7, Thermocouple 2-E
7-T3-E	Surge Line Location 7, Thermocouple 3-E
7-T4-E	Surge Line Location 7, Thermocouple 4-E
7-T5-E	Surge Line Location 7, Thermocouple 5-E
7-T6-E	Surge Line Location 7, Thermocouple 6-E
7-T7-E	Surge Line Location 7, Thermocouple 7-E
8-L2-Y	2" LVDT, S/N 1988
8-SP-Z	5" Celesco String Pot, S/N 2531
9-L2-Y	2" LVDT, S/N 1978
9-SP-Z	5" Celesco String Pot, S/N 2519
9-T1-E	Surge Line Location 9, Thermocouple 1-E
9-T2-E	Surge Line Location 9, Thermocouple 2-E
9-T3-E	Surge Line Location 9, Thermocouple 3-E
9-T4-E	Surge Line Location 9, Thermocouple 4-E
9-T5-E	Surge Line Location 9, Thermocouple 5-E
9-T6-E	Surge Line Location 9, Thermocouple 6-E
9-T7-E	Surge Line Location 9, Thermocouple 7-E
9-T9-W	Surge Line Location 9, Thermocouple 9-W

Table A-1. (cont.)

SIGNAL NAME	SIGNAL DESCRIPTION
HPI152-1	HPI Nozzle Temperature 152-1
HPI152-2	HPI Nozzle Temperature 152-2
HPI152-3	HPI Nozzle Temperature 152-3
HPI153-1	HPI Nozzle Temperature 153-1
HPI153-2	HPI Nozzle Temperature 153-2
HPI153-3	HPI Nozzle Temperature 153-3
HPI188T	HPI Nozzle Temperature 188, Top
Lpzr	Pressurizer Level
LsgAop	Steam Generator A Operate Level
LsgAsu	Steam Generator A Startup Level
LsgBop	Steam Generator B Operate Level
LsgBsu	Steam Generator B Startup Level
MT Trip	Main Turbine Trip
Pms	Main Steam Pressure
Prcsnr	Narrow Range RC Pressure
Prcswr	Wide Range Reactor Coolant Pressure
PsgA	Steam Generator Pressure A
PsgB	Steam Generator Pressure B
Rate Ch2	Channel 2 Rate of Change > 2% FP
Ref-L2	2" LVDT, S/N 1976
Ref-SP	5" Celesco String Pot, S/N 2528
RxPower	Reactor Power
TcldAwr	Wide Range RC Loop A Cold Leg Temperature
TcldBwr	Wide Range RC Loop B Cold Leg Temperature
Tcold avg	Average Tcold
Tdas	Data Acquisition System Temperature
Tfw	Feedwater Temperature
Thot avg	Average Thot
ThotA	RC Loop A Hot Leg Temperature
ThotB	RC Loop B Hot Leg Temperature
Tmi	Mirror Insulation Temperature
Tpt	String Pot Temperature
TsgA	Steam Generator A Temperature
TsgB	Steam Generator B Temperature
WfwA	Feedwater Loop A Flow
WfwB	Feedwater Loop B Flow
Wrcs	Reactor Coolant Total Flow

Figure A-1. Oconee Data Acquisition Hardware Configuration

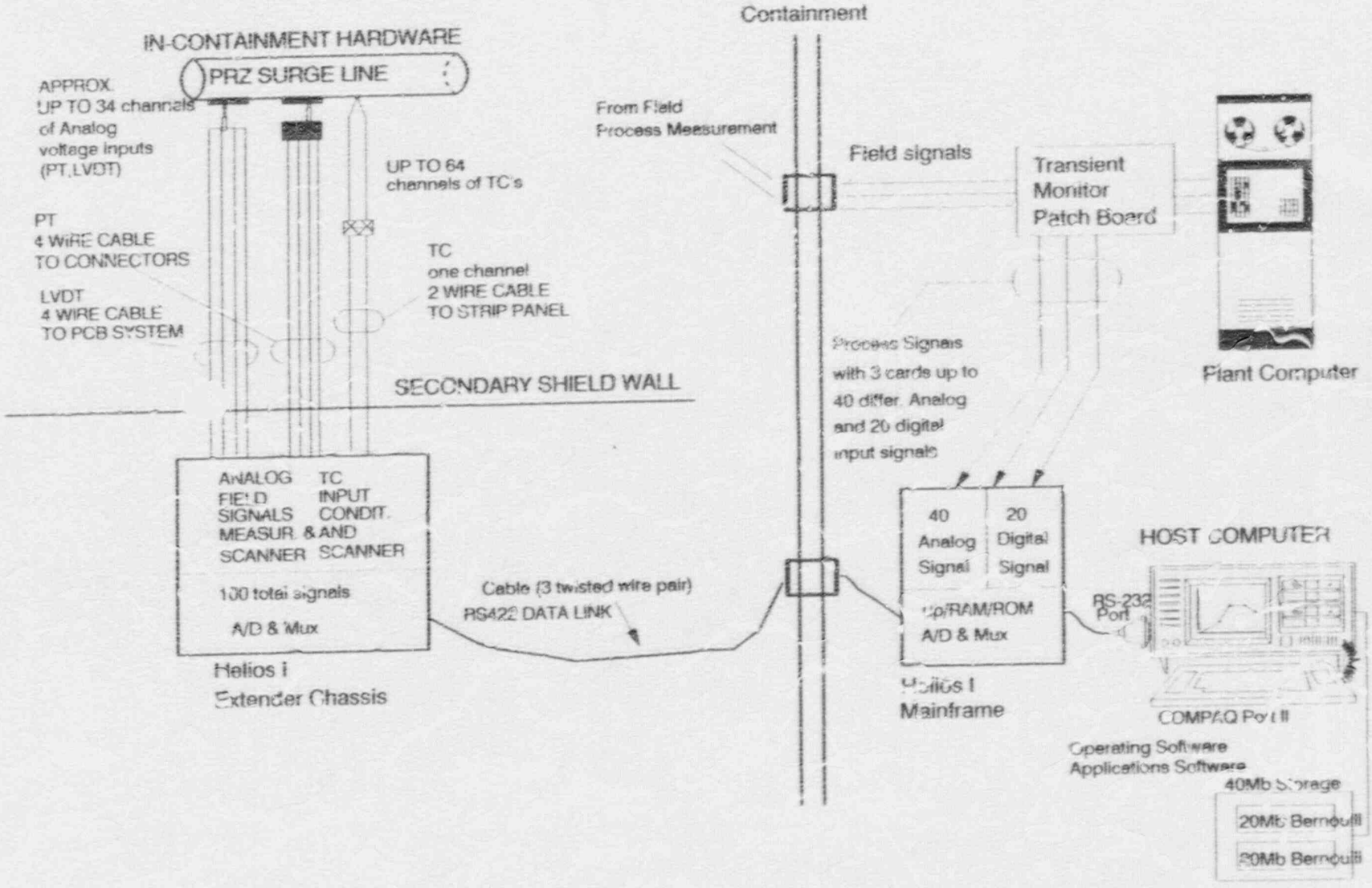

Figure A-2. Thermocouple Locations at Oconee Unit 1

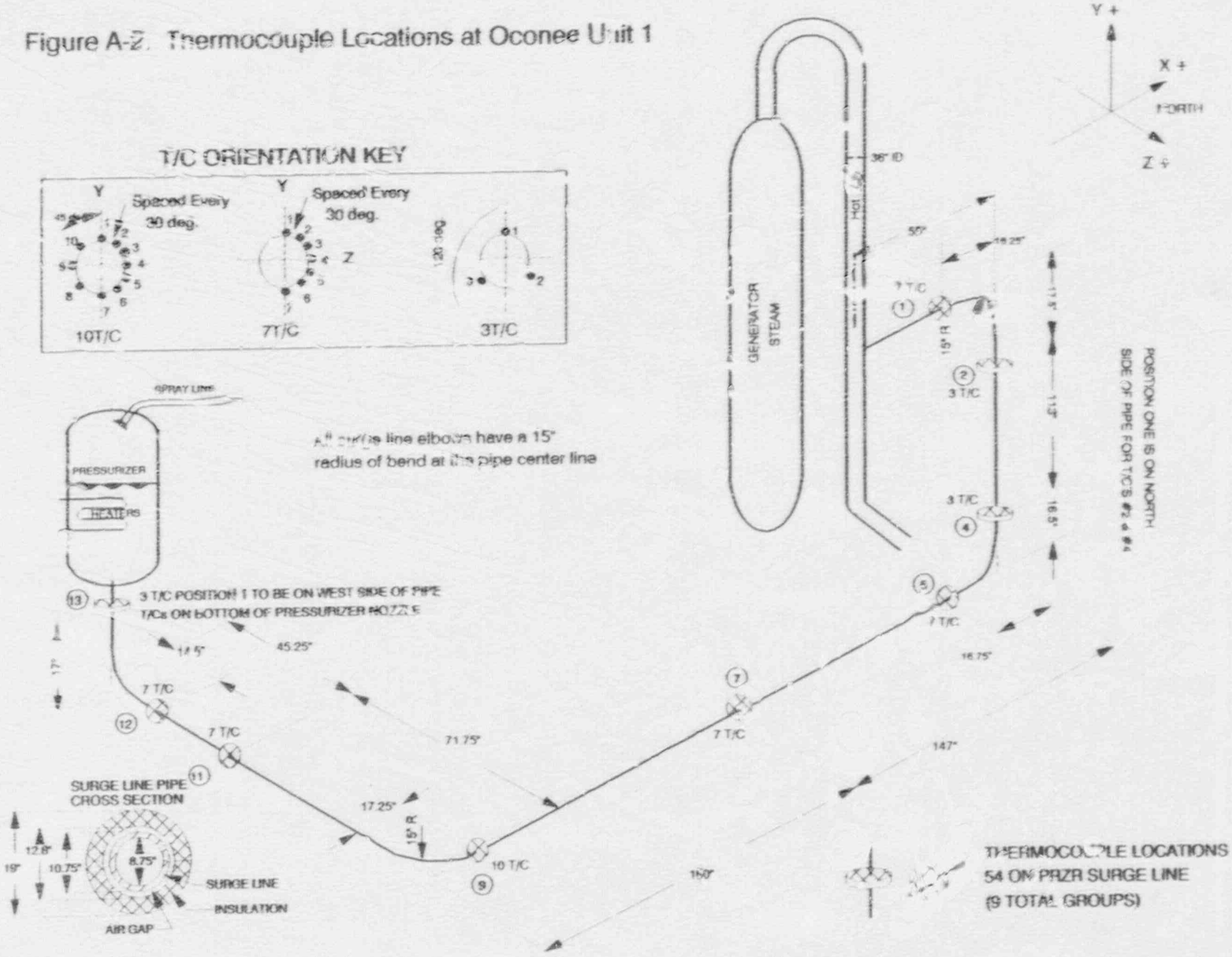

Figure A-3. Displacement Transducer Locations at Oconee Unit 1

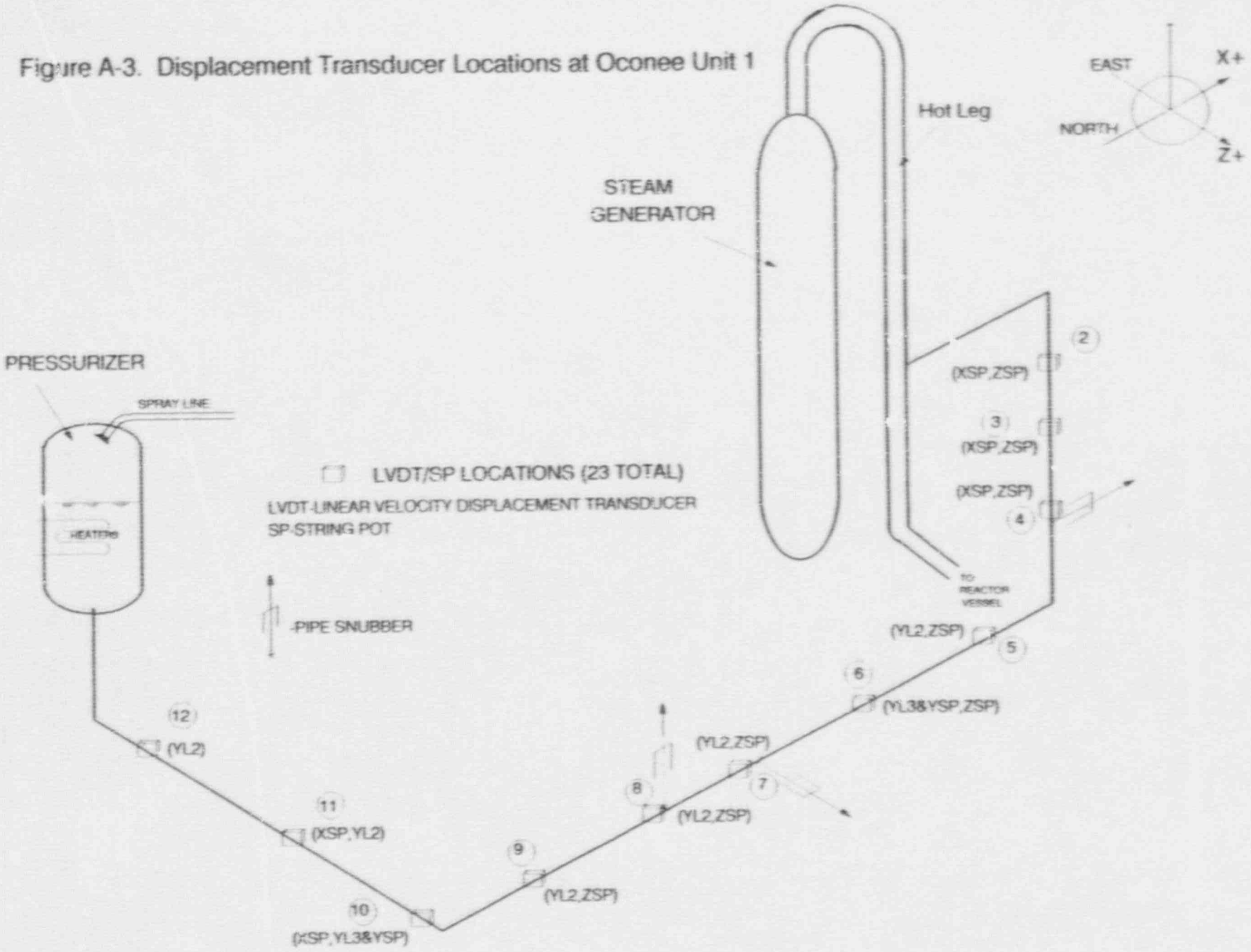

APPENDIX B

B. Utilization of Oconee Data for B&W Owners Group Program

CONTENTS

Numerous observations pertaining to plant operations and the resulting effect on surge line thermal stratification have been made based on the Oconee data. The effect of the HPI check valve tests on stratification discussed in the first subsection provides an example surge line transient. This subsection provides a more detailed view of stratification and the operations that cause it to occur. The second subsection consolidates the conclusions drawn from the data.

1. HPI Check Valve Test - An Example Surge Line Transient

The most significant stratification cycles during the February 7, 1989 heatup were due to High Pressure Injection (HPI) check valve functional testing (2/10/89, 0100 to 0600). A stratification cycle of 280F resulted from changes in pressurizer level at a time when the temperature difference between the pressurizer and the reactor coolant system (RCS) was approximately 300F. Figure B-1 shows the relationship of key parameters during this test period and Figure B-2 is a diagram of the tested flow paths.

At Oconee, the HPI Borated Water Storage Tank (BWST) check valves (HP-101, HP-102 - see Figure B-2) were tested for free movement to open by pumping from the BWST into the RCS (Oconee Functional Test PT/1/A/251/09 Enclosure 13.2). This test is required if it has not been performed in the last 90 days or if maintenance has been performed on either of the check valves. By monitoring the BWST level and the Letdown Storage Tank (LDST) level while opening the shutoff valves (HP-24, HP-25) in the flow path between the BWST and an RC cold leg, it could be determined if the suction check valves (HP-101, HP-102) were allowing flow. After opening HP-24, the operating HPI pump should take suction from the BWST. At Oconee, the makeup control valve has been throttled open to establish greater than 30 gpm, or 150 gpm if following a refueling outage. After a refueling outage, 150 gpm of makeup flow is established to verify the check valves operate with a full stroke (approximately 150 gpm is the maximum flow obtainable with the valves in the full open position). If the BWST level decreases or the Letdown Storage Tank (LDST) level increases, HP-101 was determined to be operating correctly. The test was repeated by opening HP-25 and testing for flow through HP-102 in the same manner.

The Oconee HPI-BWST suction check valve testing had a large impact on surge line stratification, due to 1) large RCS inventory changes, and 2) the large

temperature difference between the pressurizer and the RCS at the time of the testing. Because letdown flow is driven by the RC pressure, a maximum of 75 gpm was available at the time of the HPI check valve test. The pressurizer level was controlled at approximately 100 inches during this part of the heatup. Thus, an outsurge was initiated after each insurge to restore pressurizer level. During these outsurges, the pressurizer temperature was between 340F and 410F, while the RC temperature was only 100F (RC pumps had not been started). As a result of the outsurges, stratification nearly as large as the pressurizer-RC temperature difference develops. Figure B-1 is a plot of key parameters for this time period with the detailed operational events annotated.

The 1A HPI pump was started at 0140 and turned off 10 minutes later. Inventory was added to the RC system as soon as the pump was turned on. Because the pressurizer level was well above 100 inches at this time, the makeup control valve was closed trying to control level to 100 inches. The makeup control valve has not been known to allow leakage, even with the large delta P across it in this early part of the heatup. Duke personnel suspect that the inventory addition had been due to seal injection throttle valve (HP-31) leakage. At this time, the RC pressure (65 psig) was not sufficient to establish the proper seal back pressure. The seal return throttle valve (HP-277) was adjusted for the proper back pressure after an RC pressure of 295 psig was reached. This does not occur for another two hours. The pressurizer level fell when the HPI pump was turned off due to no inventory addition with a constant letdown of approximately 50 gpm.

The outsurges that occur between 0250 and 0520 were a result of the HPI-BWST check valve testing. The insurges that begin at 0355 and 0415 were due to inventory addition during the HPI BWST suction valve test. Although not directly verified, it appears the same test was the reason for the other insurges occurring between 0250 and 0320. The evidence for this has been based on the similar time span for each insurge (5 to 10 minutes), the rate of pressurizer level increase, and the fact that these tests have often been redone for additional verification.

A portion of the RCS inventory changes up until 0530 were possibly due to leakage by the seal injection throttle valve (HP-31). This was due to the proper back pressure not being established until 0530. Adjustment of HP-277 to establish the

proper seal back pressure occurred at 0531. The pressurizer level was relatively steady after that time.

The top to bottom temperature difference at the horizontal surge line locations at the time of the peak stratification (0449) was as follows:

Oconee Unit 1 Surge Line Location	Approximate Top to Bottom Temperature Difference
5	275
7	190
9	200
11	280
12	250

The top thermocouples indicate approximately 400F for these locations. The bottom thermocouples at the two middle locations in the surge line (location 7 and location 9) were affected by the large outsurges but the bottom thermocouples at the other locations were not. This accounts for the lower peak stratification at surge line locations 7 and 9.

The relationship between pressurizer level change and stratification can be seen in Figure B-1. All decreases in pressurizer level cause the stratification to increase. However, stratification was more dependant on the rate of pressurizer level change than it was the total level change. This was evident at 0310 and 0330 on 2/10 as shown in Figure B-1.

2. Operational Conclusions and Recommendations

The surge line data taken at Oconee Unit 1 have confirmed that the design basis transients have not been adequate for the surge line structural analysis. The B&W Owners Group program has been established for the development of new surge line design basis transients in which the Oconee Unit 1 data collected played a key role in addressing surge line thermal stratification.

The Oconee data has indicated which plant operations are important in determining that the plants could be generically evaluated and for specifying the events to

be included in the design basis transients. The following conclusions in regard to operations have been drawn from the data:

1) The RCS conditions in which the pressurizer to RC hot leg temperature difference was large have been determined to be of the most concern. Power operations have been determined to generally be of less concern than heatup and cooldown events,

2) For outsurges, the surge line top temperatures increase with a smaller effect on the surge line botton. In addition, surge line bottom temperatures lag those of the top. Thus, quick changes in surge line top temperatures cause increased stratification before the bottom of the surge line responds. Insurges decrease stratification during most RCS conditions,

3) The first RC pump start results in a sharp outsurge due to reactor coolant mixing and subsequent contraction. Additional RC pump starts generally cause an insurge and pump stops cause an outsurge due to changes in loop pressure,

4) The operation of full pressurizer spray flushes the entire surge line and reduces stratification to a negligible magnitude. However, a stratification cycle resulted because the surge line returned to its previous thermal condition after the spray flow was stopped, and

5) Operations which involve inventory additions might result in large stratification cycles. During the Oconee HPI check valve test, inventory was added to the system at a greater rate than it could be discharged by letdown. After the inventory addition was stopped, restoration of pressurizer level resulted in an outsurge. The largest top to bottom temperature observed during the 2/89 heatup resulted from the HPI check valve test.

The October 2, 1989 heatup data (key parameters shown in Figure B-3) have been used to correlate thermal stratification to surge line boundary conditions. This computerized set of correlations developed by BWNS relates the transient surge line conditions to the imposed boundary conditions (hot leg temperature, saturation temperature, and pressurizer level) as discussed in Section 4.2.

Plant operation recommendations have been made based collectively upon the Oconee surge line data and other available plant data. The first recommendation has been to implement a surge line pressure-temperature limit in order to limit the temperature difference between the pressurizer and the RC hot leg. The second recommendation stemmed from the HPI check valve test discussed earlier in this section. It has been recommended that surveillance tests that require large makeup or letdown from the RC system be performed only when the RCS subcooled margin is less than 200F in order to limit the pressurizer to RC hot leg temperature difference.

Figure B-1. Oconee Unit 1 data taken 2/10/89

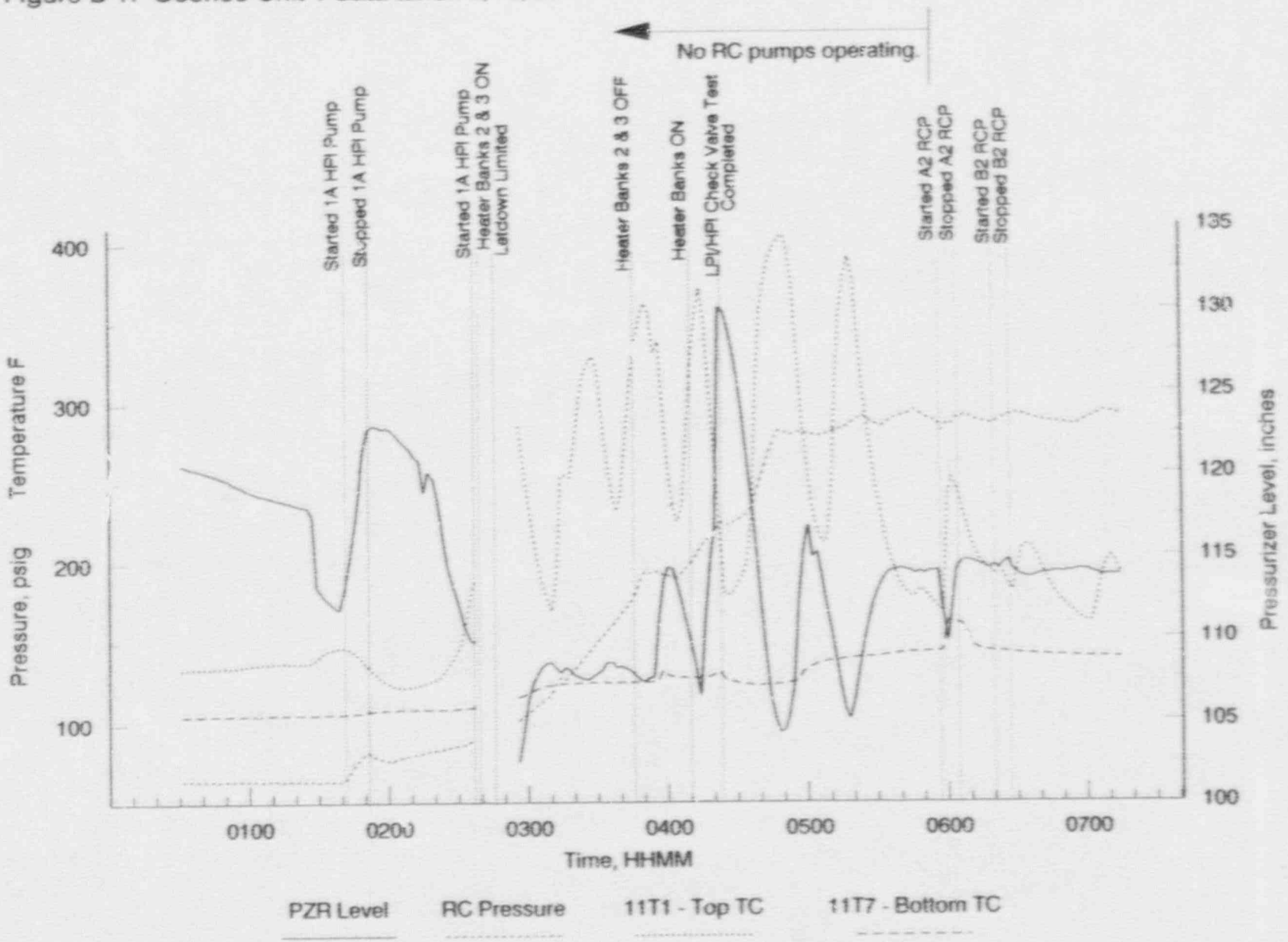

Figure B-2 HPI FLOWPATH - BWST TO RCS

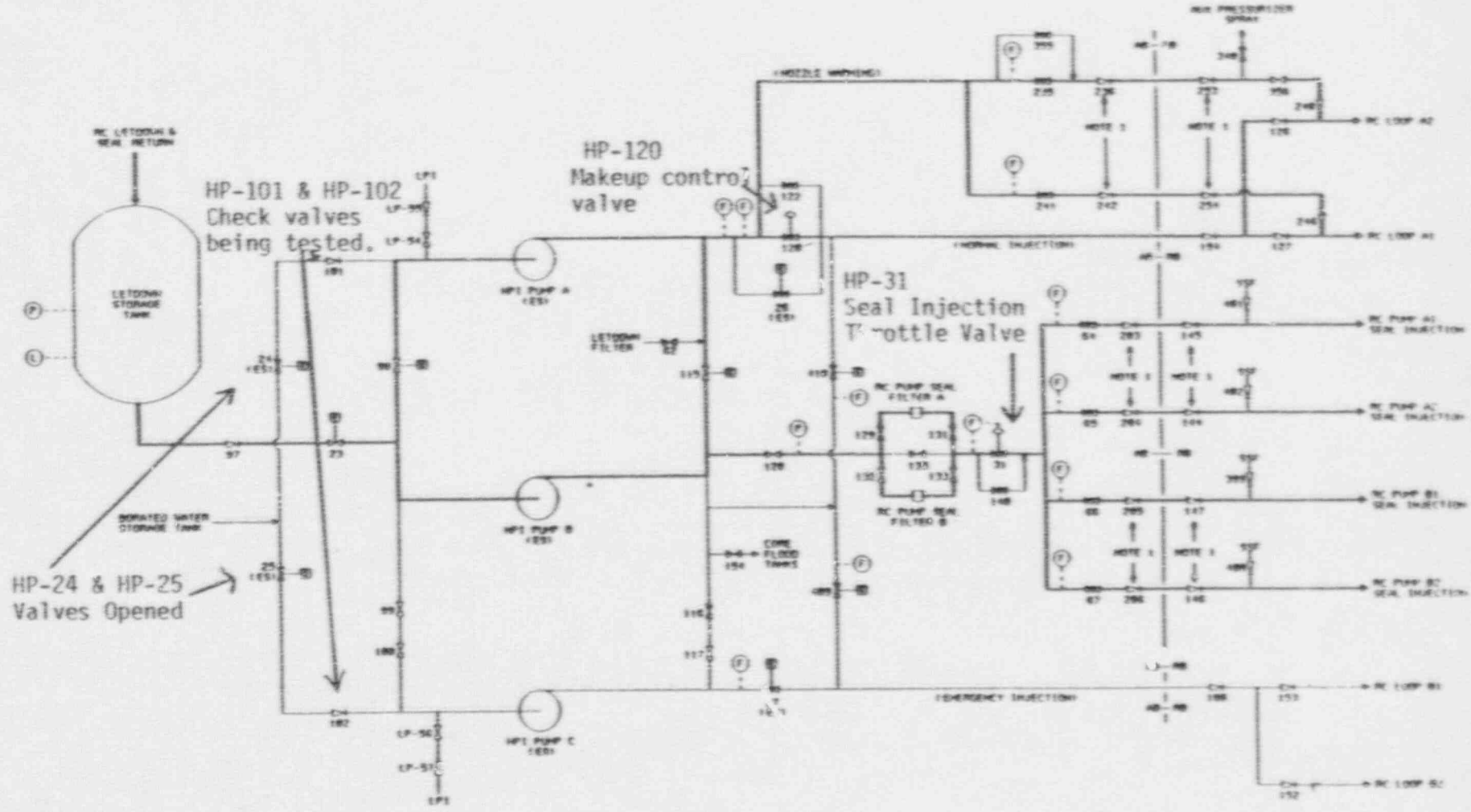

Figure B-2. Oconee 1 Surge Line Data: Heatup, 22 Oct 89

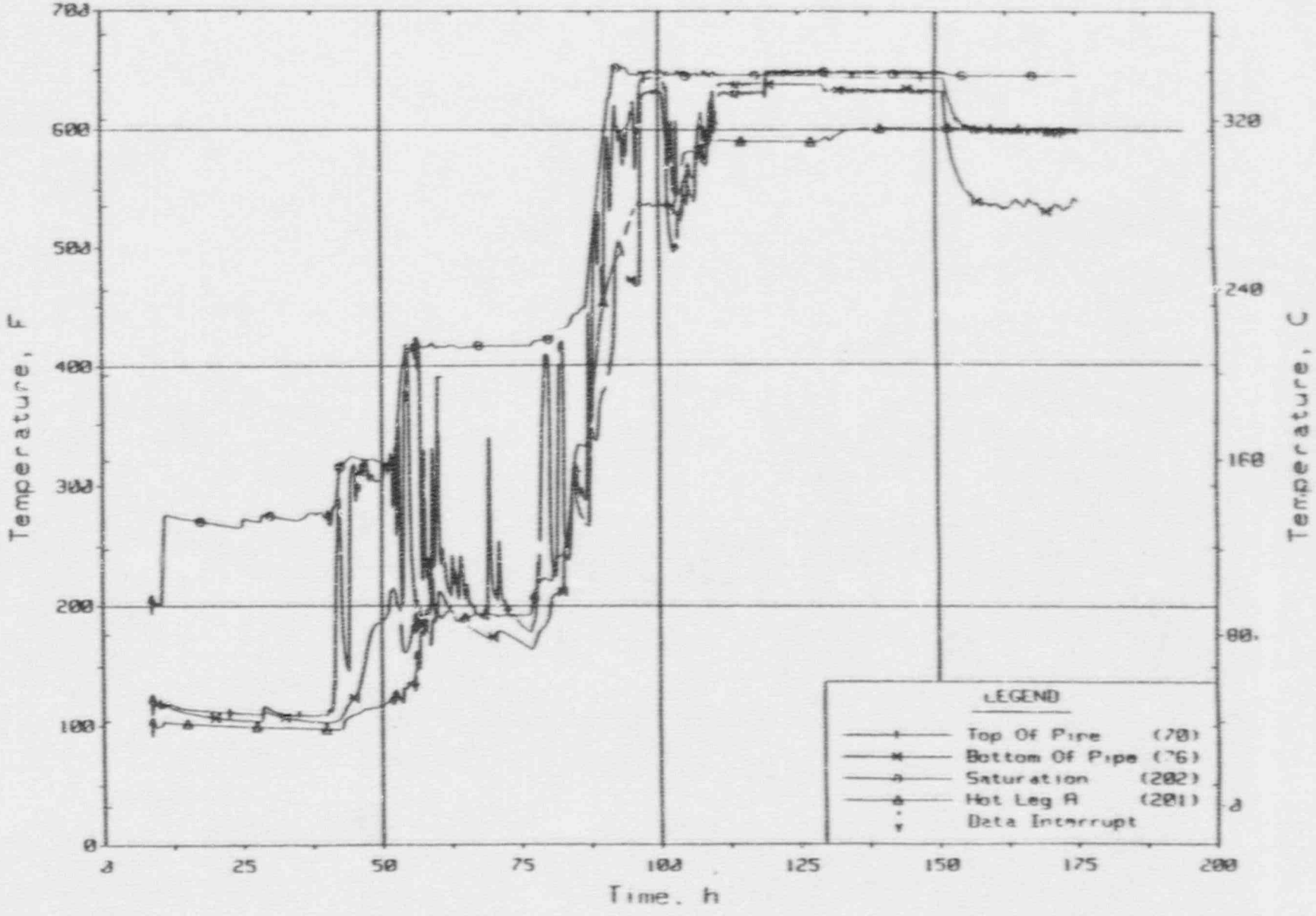

APPENDIX C.

C. Supplementary Striping Information

CONTENTS

1. Thermal Striping Literature

Thermal striping is the localized metal stress caused by repetitive fluctuations of the temperature at a fluid-metal interface. The fluid temperature fluctuations are due to the interactions between forced flow and buoyancy. The buoyant forces tend to stratify the fluid, obtaining vertical segregation (in a horizontal flow component) by temperature and density. The fluid shear forces associated with forced convection and fluid viscosity, on the other hand, tend to mix the fluid. The combination of these effects can generate undulations of the fluid-fluid interface, resulting in thermal striping. The existence and characteristics of these fluctuations depend primarily on the simultaneous occurrence of buoyant forces and fluid shear forces which are of comparable magnitude. The fluctuations are also responsive to the flow geometry; for example, they may be greatly amplified by the helical, secondary fluid motion induced by axial flow in a pipe bend. Finally, the fluctuations of the pipe surface temperature are directly responsive to the interactions between convective and conductive heat transfer at the fluid-pipe interface.

The thermal-hydraulic characteristics of thermal striping have been examined in the following four major areas of research:

1. BWR feedwater nozzle tests,
2. LMFBR tests (Westinghouse),
3. Argonne National Laboratory (ANL) tests, and
4. Project HDR (FRG) tests.

These programs are summarized below, and are described in more detail in the subsequent paragraphs.

The BWR feedwater nozzle studies (reference 1) were extensive, but the geometry of interest was quite unlike that of the pressurizer surge line. The BWR studies did demonstrate the ability to combine low-temperature data with high-temperature data and with plant striping data, by suitably adjusting the low-temperature results. The application of the BWR feedwater nozzle results illustrated the use of probability density functions. Thermal fluctuations were analyzed to determine the frequency of occurrence of cycles having discrete ranges of

amplitudes. These incremental-amplitude analyses were carried through the nozzle stress analysis by introducing plant time-at-conditions data. These BWR feedwater nozzle studies are described in detail in Section 1.

Woodward (reference 2) examined the fluid temperature fluctuations in transparent horizontal pipes. The amplitudes of the near-wall fluid temperature fluctuations reached 60% of the imposed fluid temperature difference, with most of the cycles exhibiting amplitudes of 10 to 35%. The frequency of fluctuations ranged from 0.1 to 0.5 Hz. A film heat transfer coefficient was needed to determine the wall thermal fluctuations from those of the near-wall fluid. Woodward referred to the studies of Fujimoto et al. Fujimoto et al (reference 3) also studied striping in a transparent horizontal pipe. A fluid density difference was imposed by adding calcium chloride to the warmer fluid stream. Thin squares of copper were used to measure wall striping. The striping amplitude was less than 10% of the imposed temperature difference (the temperature difference between the interacting hot and cold fluid streams). The film heat transfer coefficient was 1.25 to 7 times the Dittus-Boelter coefficient. The studies of Woodward, and of Fujimoto et al, are described in detail in Section 2.

Kasza et al at ANL (reference 4-14) have extensively tested thermal stratification and striping in transparent horizontal piping with bends in both the vertical and horizontal planes. Based on a limited amount of published power-spectral-density information, the higher-amplitude fluctuations occurred at lower frequencies, 0.1 to 0.6 Hz, with amplitudes of 30 to 40% of the imposed temperature difference. The amplitude of fluctuations drops off sharply with increasing frequency. These ANL studies are outlined in Section 4.

Wolf et al (reference 15-27), in the TEMR test series of Project HDR, measured striping in metal, horizontal pipes at plant-typical temperatures. Typical striping frequencies were 0.1 to 10 Hz. The amplitudes of the wall temperature fluctuations were generally from 10 to 40% of the imposed fluid temperature difference, with peak amplitudes from 25 to 50%. Examining a single test of the nine "PWR" tests, the maximum striping amplitude was approximately 30% and the frequency of occurrence of the larger fluctuations was approximately 0.2 Hz. Wolf et al noted the interactions between convective and conductive effects, and hence the difficulty of extrapolating to a plant the results of tests performed using a transparent model. They also noted the insensitivity of temperatures

measured at the outside of a metal pipe to inside interactions. The TEMR tests are described later in Section 4.

Finally, the characteristics of thermal striping were addressed in a 1980 report by the NRC which summarized pipe cracking in PWRs. (reference 28) The range of frequencies was 0.1 to 10 Hz. The reduction of amplitude due to film heat transfer was described, resulting "... in a peak metal temperature variation at the surface of roughly one-fourth to one-half the water temperature variation."

1.1. BWR Feedwater Nozzles Tests

The BWR feedwater nozzle configuration was examined in relation to observed feedwater line cracks. The thermal striping of this configuration has been obtained from two test facilities, Two-Temperature and Moss Landing, as well as from plant measurements (reference 1). The Two-Temperature Test Facility was limited to atmospheric pressure; hot and cold fluid temperatures of 160 and 70F were used. The Moss Landing Test Facility, on the other hand, achieved plant-typical temperatures. The results of the two test facilities were combined with plant data by adjusting the Two-Temperature results to account for the changes of fluid density, viscosity, and thermal conductivity between the test and reactor conditions.

The composite data was processed to obtain the number of cycles having discrete ranges of stress amplitudes. These amplitude ranges, or windows, were prescribed to be relatively small at the higher amplitudes, [illegible]p to 20% wide at the smallest amplitudes. The results of this analysi[illegible]e presented in tabular form. (reference 1) This data has been restated in terms of windows of equal amplitudes, 10%, and plotted in Figure C-1. The frequency of occurrence decreases rapidly and regularly up to a stress amplitude of 50% of the maximum stress, and then more slowly at the higher amplitudes. Although most of the fluctuations had low amplitudes, approximately 1% of the metal temperature fluctuations obtained stress amplitudes approaching the maximum stress.

It is estimated that the observed amplitudes of the near-wall fluid temperature fluctuations were reduced by one-half to obtain the amplitudes of the wall temperature fluctuations and hence the wall stress amplitudes. The maximum stress of Figure C-1 thus corresponds to a wall temperature fluctuation of approximately 50% of the imposed temperature difference, the temperature

difference between the two fluid streams of unequal temperatures and densities. Most of the fluctuations had stress amplitudes less than 50% of the maximum stress, which corresponds to wall temperature fluctuations less than 25% of the imposed fluid temperature difference.

1.2. LMFBR Tests

Woodward (reference 2) investigated stratification and striping in a 1/5-scale model of an LMFBR at the Waltz Mills Test Facility. The model was plexiglass, therefore the hot and cold water temperatures were limited to 130F and 70F. Two lengths of horizontal piping, of 4" and 6.5" inside diameter, were examined. The tests were conducted in the turbulent transition range, with Reynolds Numbers (based on half-pipe flow areas) of 2×10^3 to 8×10^3. Dye and thermocouples were used, the thermocouples were typically inserted 1/32" into the fluid.

The thickness of the interface region, over which the fluid temperature changed from hot to cold, ranged from 0.6" to 2". The striping frequency was 0.1 to 0.5 Hz and the fluctuations were approximately sinusoidal. The amplitudes of the temperature fluctuations (of the near-wall fluid) approached 60% of the imposed temperature difference, and were most pronounced at low Richardson Numbers. Probability-of-occurrence information was presented for only three ranges of amplitudes (or windows). This information has been converted to the fractional occurrence for constant window widths of 10% amplitude, and plotted in Figure C-2. Most of the fluctuations had mid-range amplitudes, 10 to 35%. The probability of occurrence dropped rapidly at the higher amplitudes, approaching zero at 60% amplitude.

A heat transfer coefficient was needed to obtain wall temperature information from the near-wall fluid temperature measurements. The heat transfer coefficients determined by Fujimoto et al were referenced by Woodward. Fujimoto et al (reference 3) tested striping in a 14.2" horizontal pipe made of acrylite. Calcium chloride was added to the warmer fluid stream to obtain plant-typical density differences. (The fluid temperatures were used simply to track the streams of differing densities.) Wall striping was measured on thin squares of copper. The amplitude of the fluid temperature fluctuations was observed to decrease near the wall. The fluctuations at the interface between the fluids of differing densities evidenced frequencies of 0.3 to 3.0 Hz. The amplitude of the

wall fluctuations was less than 10% of the imposed temperature difference. The convective heat transfer coefficient was calculated to be from 1.25 to 7 times that of the Dittus-Boelter correlation (for forced convection in tubes). The information obtained by Woodward and by Fujimoto et al was referenced in the evaluation of thermal stratification of the pressurizer surge lines of the South Texas Project power plants.

1.3. ANL Tests

Kasza et al have conducted extensive experimental studies of stratification and striping at ANL (references 4-14). These studies have generally used water flowing turbulently in transparent pipes of 6-in inside diameter. Combinations of horizontal and vertical piping lengths have been tested, including bends in the horizontal plane. Vertical lengths of piping were observed to interrupt stratification. Stratification in horizontal lengths began at a Richardson Number of approximately 0.05; flow stagnation and reversal occurred near a Richardson Number of 0.7. Kasza et al applied the buoyancy index of Jackson and Fewster, namely

$$\gamma = Ri\ Re^{-0.625} / Pr$$

Kasza et al observed a correlation between buoyant effects and this buoyancy index. The threshold of buoyant effects was found to correspond to a γ on the order of 10^{-4}; a γ on the order of 10^{-2} or larger obtained strong buoyant effects.

The more-recent investigations of Kasza et al (references 7-14) obtained some details of the thermal fluctuations. Whereas the bulk fluid temperature fluctuations were about 75% of the imposed temperature difference, the amplitude of the wall fluctuations was 30 ↔ 40% of the imposed temperature difference. On the basis of the limited published power-spectral-density information, most of the signal energy was concentrated below 1 Hz, peaking between 0.1 and 0.6 Hz, and decaying approximately exponentially with increasing frequency. These maximum fluctuations were observed approximately one diameter downstream of a horizontal elbow. Kasza et al have obtained many additional, as yet unpublished, striping power spectral density distributions. These distributions confirm the trends of the published distribution.

1.4. HDR Tests

Wolf et al have conducted extensive examinations of thermal mixing in the HDR project at Karlsruhe, FRG (references 15-27). The TEMB test series examined pressurized thermal shock using a large-scale pressure vessel and various high-pressure injection configurations; the experimental results were compared to the predictions of many codes and correlations (references 15-22). Fluid temperature fluctuations were observed and recorded, but received little emphasis.

The TEMR test series concentrated on thermal stratification in horizontal feedwater lines (references 23-27). The test section was a 20-foot length of 15.6-in inside diameter metal pipe, extensively instrumented with 11-ms thermocouples. Cold water entered one end of the horizontal run through a bend from vertical upflow, the opposite end of the horizontal run was attached to a reservoir of hot fluid. The TEMR tests consisted of 3 subseries, 2 of which were labelled "BWR" and "PWR." In the BWR tests, a plate with slit orifices was installed at the junction of the horizontal run with the reservoir, to simulate the holes of a typical BWR feed sparger. The horizontal-to-reservoir junction was unobstructed in the PWR tests. The third subseries of TEMR tests considered the buildup and decay of hot water pockets. The horizontal-to-reservoir junction was blocked except for a horizontal slit at the bottom of the pipe cross-section.

The PWR tests of the TEMR series are most relevant to the surge line configuration. The ranges of conditions of the 9 PWR tests are listed in Table C-1. The average fluid temperature ranged from approximately 200 to 300F, and the imposed fluid temperature differences ranged from approximately 200 to 400F; the volumetric flow rates spanned 10 to 200 gpm. The Reynolds Numbers based on the flow area (rather than on a reduced flow area to account for stratification) were in the turbulent range. Kasza and Kuzay have employed a buoyancy index which is dependent on the Reynolds, Richardson, and Prandtl Numbers. In an order-of-magnitude sense, the threshold of buoyant effects occurs at an index of 10^{-4}, and strong buoyant effects occur for an index of 10^{-2} and larger. Applying this index to the PWR test conditions, all the PWR tests of Wolf et al were in the strong buoyant range.

The interface between the fluid of unequal densities was characterized as being wavy, with typical frequencies between 0.1 and 10 Hz (reference 11). Within the

mixing layer, the fluid temperature fluctuations were not damped near the wall (reference 10). The fluid mixing did reduce the local maximum temperature difference from the imposed temperature difference, however. The amplitude of the wall temperature variations, expressed as a fraction of the amplitude of the fluid temperature fluctuations, was stated in two contexts (reference 11). For all the BWR and PWR tests, the fractional amplitude was 10 to 40%, but the peak fractional amplitude was 25 to 50%.

Measurements from one of the PWR tests, Test 33.19, were presented (reference 11). The conditions of Test 33.19 are listed in Table C-1. Test 33.19 was characterized by a relatively high flow rate and ratio of inertial to viscous forces (Re) and by a mid-range temperature difference. The resulting ratio of buoyant to inertial forces (Ri) was low compared to that of the other PWR tests, as was the index of buoyant effects (χ). The temperatures measured in the fluid, on the inside pipe metal surface, and on the outside pipe surface were presented. (references 10,11) Examining these figures, the fluid temperature fluctuated with an amplitude which was almost equal to the imposed temperature difference. the difference between the temperatures of the hot and cold fluid streams. The temperature of the inside pipe wall fluctuated with an intermediate amplitude, but the temperature of the outside surface of the pipe evidenced no fluctuations.

The inside pipe surface temperature exhibited irregular fluctuations. The maximum amplitude of these fluctuations was approximately 30% of the imposed temperature difference; the larger-amplitude fluctuations occurred at intervals of approximately 5 seconds. This interval corresponds to a frequency of occurrence (of relatively large fluctuations) of 0.2 Hz. This frequency of occurrence must be distinguished from the characteristics of the individual fluctuations. Because the larger-amplitude variations generally occurred within groups of fluctuations of much smaller amplitude, the frequency of all fluctuations was approximately 1 Hz. That is, the larger-amplitude fluctuations, which occurred at intervals of approximately 5 seconds, each persisted for only approximately 1 second. These characterizations were obtained by examining the figures presented for PWR Test 33.19.

The HDR experimentalist drew the following conclusions from the TEMR results: (reference 10,11)

- The extrapolation of model data to a plant, using a transparent model, is made difficult by the complex interactions between convective and conductive phenomena,
- There is no simple, unique correspondence between the thermal response of the exterior of the pipe and that of the interior, and
- The region of fluctuating temperatures was extremely narrow (reference 26).

1.5. Comparison of Thermal Striping Conditions

Figure C-3 provides an overview of thermal striping. Both dimensional and dimensionless axes are presented. The dimensional axes, flow rate versus temperature difference, apply specifically to the surge line geometry and conditions. The dimensionless axes, Reynolds number (Re) versus Grashof number (Gr), both correspond to the surge line quantities and provide a more general basis with which to assess the thermal-hydraulic interactions. The Reynolds number indicates the ratio of inertial to viscous forces whereas the Grashof number provides a measure of the ratio of buoyant to viscous forces. The information presented in Figure C-3 is to be regarded in an order-of-magnitude sense. For example, flow rates were converted to velocities using the whole-pipe flow area, rather than reducing the area to accommodate stratification; and the surge line fluid properties were evaluated at 300F and slightly subcooled - they are relatively insensitive to pressure, but quite sensitive to temperature.

Regions of relatively weak and of relatively strong buoyant effects, compared to inertial effects, were estimated by evaluating the Richardson Number (Ri), and the buoyancy index (δ) which has previously been described. The conditions of interest to surge line stratification and striping lie in the "strong buoyant effects" range shown in Figure C-3. The range of interest is further refined by considering the surge line temperature difference (DT): there is no fatigue concern for DTs less than 90F, and the maximum DT is approximately 300F. The conditions of interest are thus approximately $10^{11} < Gr < 10^{12}$ and $Re < 10^{5}$. (There is probably a lower-Re bound, below which the buoyant effects predominate to the extent that interface instabilities and thus striping are suppressed; this

limit has not been quantified, except that Kasza et al have observed such a limit for the case of fluctuations downstream of a bend in the horizontal plane.)

The dimensionless axes of Figure C-3 provide a convenient basis on which to compare the several investigations of striping. These are the singly cross-hatched regions in the figure. The conditions of Woodward, and of Kasza et al, lie far below the range of Grashof numbers of interest. Both these striping investigations were conducted at atmospheric pressure, thus the reduced thermal expansion coefficient and DT, as well as the increased viscosity, resulted in relatively small Grashof Numbers. The conditions of Wolf et al, on the other hand, are just on the high-Gr side of the conditions of interest, due only to their larger pipe diameter compared to that of the surge line.

Several data sets are not shown on the figure. The data of Fujimoto et al was obtained at atmospheric conditions, but with the inter-fluid density difference enhanced toward that encountered at surge line conditions. The viscosity remained in the low-temperature range, however, and the data evaluation of Fujimoto et al depended on a correspondence between mixing and diffusion within a thermal gradient and a concentration gradient. The EDF data is also not shown. This data, although unpublished, was apparently obtained at atmospheric pressure and correspondingly low Grashof numbers. Finally, the conditions of the BWR feedwater nozzle research are not shown because of the pronounced geometric dissimilarities between the nozzle and the surge line.

Notwithstanding their dissimilar Grashof number ranges, the published striping characteristics of the three investigations plotted in Figure C-3 are quite similar. But, it is uncertain whether the low-Gr data of Woodward and of Kasza et al apply at the conditions of interest for the surge line. Certainly the visualizations available with the low-Gr tests provide valuable insight regarding striping mechanisms, characteristics, and limiting regions, but these insights may apply only at the tested conditions, even if the Richardson number is preserved in the translation of conditions to those of interest. Hence, the work of Wolf et al thus seems singularly pertinent to surge line applications.

2. Description of HDR Experiments

The subject tests were conducted at Battelle-Karlsruhe under the direction of Dr. Lothar Wolf et al, in October 1986 (reference 29). They were conducted in a

larger series of tests in horizontal piping with various configurations of the flow area at the pipe-to-vessel interface.

2.1. Configuration

Stratification and striping were measured in an 18-foot, straight run of horizontal piping. The pipe inside diameter was 15.6 in (397mm), its thickness was 0.634 in (16.1mm). The steel pipe (15NiCuMoNb5, WB36) was insulated with glass wool. One end of the pipe was connected to a pressure vessel through a nozzle, and the opposite end to a gradual bend downward to a 21-foot vertical run (Figure C-4). The nozzle was unobstructed throughout the series of tests analyzed herein. The pressure vessel and horizontal pipe were initially hot and isothermal, cold water was introduced at the bottom of the vertical run during testing.

2.2. Conditions

The ranges of imposed conditions were as follows:

Average Temperature (F): 187 to 323

Temperature Difference (F): 190 to 420

Flow Rate (gpm): 15 to 229

In terms of nondimensional variables, these ranges of conditions were:

Gr: 5 x 10**11 to 3.5 X 10**12

Re: 9.4 x 10**3 to 2.5 x 10**5

Ri: 2.7×10^{1} to 1.1×10^{4}

γ : 1.2×10^{-2} to 2.4×10^{1}

where γ is the buoyancy index:

$$\gamma = Ri\ Re^{-0.625}\ Pr^{-0.5}$$

These dimensionless variables are global rather than local; the imposed temperature difference rather than a local gradient was used, and velocity was calculated using the whole pipe flow area.

2.3. Tests

There were 7 tests conducted with an unobstructed pipe-to-vessel interface, Tests 14 through 19 and Test 25. Test 25 consisted of 3 distinct phases, making a total of 9 sets of test conditions for analysis (Table C-2). The 3 phases of Test 25 have been separated, and reidentified as Tests 51 through 53, for ease of analysis and identification (Table C-3). The imposed injection flow rate, fluid temperature difference, and average fluid temperature were varied among these 9 sets of test conditions. The warmer fluid was kept subcooled throughout each test.

Starting with a hot and isothermal system, cold water injection was begun with a prescribed flow rate and temperature. Data recording was initiated as the cold-to-hot fluid interface ascended the vertical run toward the horizontal piping run. Time zero was set as this interface approached the bend to the horizontal run, such that the effects of the imposed flow rate and temperature difference began to be observed just after time zero. Testing was generally continued until the fluid and metal temperatures approximately stabilized. During this time, system pressure and the injection flow rate and temperature, were to be held constant. The hot fluid was replenished by inherent (rather than imposed) backflow from the heated pressure vessel. The tests were terminated by interrupting the injection flow and stopping the data recording.

2.4. Thermocouples

The horizontal pipe was instrumented with multiple strain gauges and thermocouples. Displacement, pressure, and flow rate measurements were also performed. This investigation deals almost exclusively with the temperature measurements, and usually with those at the instrument cross section located approximately two-thirds of the way from the bend to the pressure vessel. This cross section was equipped with thermocouple triplets at 30° increments from 0 to 180°, at 15° increments from 105 to 120°, and at 2-1/2° increments from 90 to 105° (Figure C-5). Each triplet consisted of a near-wall fluid thermocouple, and thermocouples on the inside surface of the pipe and on the outside surface. The near-wall fluid thermocouples were located 0.4 in (10mm) from the wall, compared to the pipe inside diameter of 15.6 in (397mm). The surface thermocouples were held to the wall using thin foils which covered the thermocouples almost to their

tips and which were welded to the wall. The diameter of the Chromel-Alumel thermocouple junction was 0.02 in (.05mm).

2.5. Data Acquisition Rate

The data analyzed herein was recorded at a frequency of 10 Hz. Examination of the temperature traces revealed that this frequency was completely adequate to document the temperature-versus-time fluctuations; multiple points were recorded for most of the fluctuations. The point density was sufficient to reconstruct the actual fluctuations with confidence. The predominant striping frequency obtained herein, approximately 1 Hz, supports the adequacy of the 10-Hz measurements (but would itself have been biased had the predominant frequency approached the frequency of data recording).

3. References

1. H. Watanabe, "Boiling Water Reactor Feedwater Nozzle/Sparger Final Report," NEDO-21821-A (February 80).

2. W.S. Woodward, "Fatigue of LMFBR Piping Due to Flow Stratification," ASME Pressure Vessel and Piping Conference, Portland, Paper 83-PVP-59, CONF-830607-27 (June 83).

3. T. Fujimoto, K. Swada, K. Uragami, A. Tsuge, and K. Hanzawa, "Experimental Study of Striping at the Interface of Thermal Stratification," Thermal Hydraulics in Nuclear Technology, K.H. Sun et al (ed), ASME (81).

4. K.E. Kasza, J.P. Bobis, "Thermal-Transient Induced Pipe Stratification," ANS, 35, 675-676 (80).

5. K.E. Kasza, J.P. Bobis, W.P. Lawrence, and T.M. Kuzay, "Heat Exchanger Thermal-Buoyancy Effects: Design and Performance Comments (Phase I)," ANL-CT-81-31 (April 82).

6. J.J. Oras and K.E. Kasza, "Thermal Transient Induced Buoyant Flow Channeling in a Vertical Steam Generator Tube Bundle," ANL-83-109 (Oct 83).

7. K.E. Kasza, T.M. Kuzay, and J.J. Oras, "Overview of Thermal-Buoyancy-Induced Phenomena in Reactor Plant Components," Proc 3rd Intl Conf - Oxford, pp. 187-194, (April 84).

8. K.E. Kasza, J.P. Bobis, W.P. Lawrence to J.C. Liljegren, "Thermal Transient Induced Pipe Flow Stratification Phenomena and Correlations (Phase II)," ANL-CT-81-19 (Feb 81).

9. K.E. Kasza and T.M. Kuzay "Thermal Transient Induced Pipe and Elbow Flow Stratification Phenomena and Correlations (Phase III)," ANL-82-85 (Oct 82).

10. T.M. Kuzay and K.E. Kasza, "Thermal Oscillations Downstream of an Elbow in Stratified Pipe Flow," FBR Thermal Hydraulics, Trans ANS, 46, 794-796 (June 84).

11. T.M. Kuzay and K.E. Kasza, "Experiments and Analysis of a Horizontal Pipe Elbow in Stratified Pipe Flow," Liquid Metal Thermal Hydraulics, pp 459-460.

12. T.M. Kuzay and K.E. Kasza, "Thermal Striping Downstream of a Horizontal Elbow Under Thermally Stratified Flow Conditions," Joint Mtg. ANS and AIF, Washington, CONF-841105-10 (Nov. 84).

13. K.E. Kasza, J.J. Oras and R. Kolman, "Measurement of Velocity Profiles in a Stratified Pipe Flow Recirculating Shear Zone using Laser Flow Visualization" Liquid Metal Reactor Thermal Hydraulics, pp. 458-460.

14. T.M. Kuzay and K.E. Kasza, "Resolution of Thermal Striping Issue Downstream of a Horizontal Pipe Elbow in Stratified Pipe Flow," ANS Annual Meeting, Boston, CONF-850610-4 (June 85).

15. L. Wolf, K. Fischer, W. Hafner, W. Baumann, U. Schygulla, and K-H Scholl, "Overview of HDR Large Scale PTS Thermal Mixing Experiments and Analyses with 3-D Codes and Engineering Models," Trans 8th SMIRT, 5, pp. 359-365 (85).

16. L.Wolf, U. Schygulla, W. Hafner, K. Fischer, and W. Baumann, "Results of Thermal Mixing Tests at HDR-Facility and Comparisons with Best-Estimate and Simple Codes," Trans 8th SMIRT, E, 8E.1-9 (85).

17. L. Wolf, U. Schygulla, F. Gorner, and G.E. Neubrech, "Thermal Mixing Processes and RPV Wall Loads for HPI-Emergency Core Cooling Experiments in the HDR-Pressure Vessel," NED, 96, pp. 337-362 (Oct. 86).

18. L. Wolf, U. Schygulla, W. Hafner, K. Fischer, W. Baumann, and T.G. Theofanous, "Application of Engineering and Multi-Dimensional, Finite Difference Codes to HDR Thermal Mixing Experiments TEMB," Proc 14th WRSRIM, NUREG/CP-0082 5, pp. 396-416 (Feb. 87).

19. L. Wolf, W. Hafner, U. Schygulla, W. Baumann, and W. Schnellhammer, "Experimental and Analytical Results for HDR-TEMB Thermal Mixing Tests for Different HPI-Nozzle Geometrics," Trans 9th SMIRT, G, pp. 319-324 (87).

20. U. Schygulla, E. Hansjosten, H.J. Bader, and K. Jansen, "Assessment of Heat Transfer and Fluid Dynamics in Cold Leg and Downcomer of HDR-TEMB Experiments," Trans 9th SMIRT, G, pp. 313-317 (87).

21. W. Hafner, K. Fischer, and L. Wolf, "Computations of the HDR Thermal Mixing Experiments and Analysis of Mixing Phenomena," Trans 9th SMIRT, G, pp. 301-312 (87).

22. L. Wolf, W. Hafner, K. Fischer, U. Schygulla, and W. Baumann, "Application of Engineering and Multi-Dimensional Finite Difference Codes to HDR Thermal Mixing Experiments TEMB," NED, 108, pp. 137-165 (June 88).

23. L. Wolf and U. Schygulla, "Experimental Results of HDR-TEMR Thermal Stratification Test in Horizontal Feedwater Lines," Trans 9th SMIRT, D, pp. 361-366 (87).

24. L. Wolf, U. Schygulla, M. Geiss and E. Hansjosten, "Thermal Stratification Tests in Horizontal Feedwater Pipelines," Proc 15th WRSRIM, NUREG/CP-0091, 5, pp. 437-464 (Feb 88).

25. L. Wolf, M. Geiss, W. Hafner, E. Hansjosten, and A. Talja, "Temperature and Wall Strain Fluctuations During the TEMR Thermal Stratification Tests At HDR," 10th SMIRT, Anaheim, CA (Aug 89).

26. L. Wolf, M. Geiss, E. Hansjosten, and A. Talja, "Evaluation Of the Thermal Stratification Tests at the HDR Facility," NURETH-4 Conference, 2, Karlsruhe, FRG (Oct 89).

27. A. Talja and E. Hansjosten, "Results Of Thermal Stratification Tests In a Horizontal Pipe Line At the HDR Facility." TRANS 10th SMIRT, E (89).

28. "Investigation and Evaluation of Cracking Incidents in Piping in Pressurized Water Reactors," NUREG-0691 (Sept 80).

29. U. Schygulla and L. Wolf, "Design Report - Thermal Stratification Experiments in a Horizontal Piping Section," HDR-Test group TEMR T33, Battelle-FRG (November, 1986).

Table C-1. HDR Test Series TEMR-PWR: Ranges of Conditions and Conditions of Test 33.19 (Ref. 24)

- The extreme conditions are listed for any of the 9 tests, rather than for the tests having extreme combinations of conditions.
- The flow rates and dimensionless numbers use the flow area of the whole pipe; properties are evaluated at the average fluid temperature.
- γ is the buoyancy index used by Kasza and Kuzay, where $\gamma > 10^{-2}$ obtains strong buoyancy effects.

Condition	Minimum	Maximum	Test 33.19
Fluid temperatures, F			
Hot	314	486	417
Cold	79	130	130
(Hot-Cold)	201	391	287
Average	198	290	274
Flow Rates			
Volumetric, gpm	10	200	200
Velocity, ft/s	0.016	0.34	0.34
$Re = vd/\nu$	10^4	2×10^5	1.8×10^5
$Ri = g\beta\Delta T\, d/v^2$ $(= 1/Fr^2)$	5×10^1	3×10^4	5.5×10^1
$\gamma = Ri\, Re^{-0.625}/\, Pr^{.5}$	0.025	84	0.026

Table C-2. Test Conditions(Entries Rounded)

TEST	14	15	16	17	18	19	51	52	53
Thot, F	313	315	313	413	417	417	486	485	484
Initial Tcold, F	61	74	77	63	77	85	65	66	117
Maximum Tcold, F	62	98	123	65	111	148	66	116	162
Temp Diff. Thot-Max. Tcld, F	252	217	190	349	306	269	420	369	322
Avg.Temp. (Thot+Max .Tcld)/2	137	206	218	239	264	283	276	300	323
Flow Rate, lbm/hx10^{-4}	0.77	5.4	10.1	0.72	5.4	10.2	0.88	6.0	10
Pressure, psia	98	96	94	328	339	329	634	634	631
Gr x 10^{-12}	0.50	0.59	0.61	1.5	1.8	1.9	2.8	3.2	3.5
Re x 10^{-4}	0.95	7.4	15	1.2	10	21	1.7	13	25
Ri x 10^{-2}	56	1.1	0.27	100	1.8	0.45	91	1.8	0.55
Buoyancy Index	13	0.071	0.012	24	0.11	0.019	18	0.11	0.023

Table C-3. Phases of Test 33.25

Times in seconds

The imposed boundary conditions were varied among the three phases of Test 33.25, as shown in table C-2.

Times Extracted from Test 33.25

Phase	Test Number	Start	Zero	End
1	51	-122.5	0	920
2	52	900	925	1195
3	53	1180	1200	1604.9

Figure C-1. Frequency of Occurrence Versus Amplitude

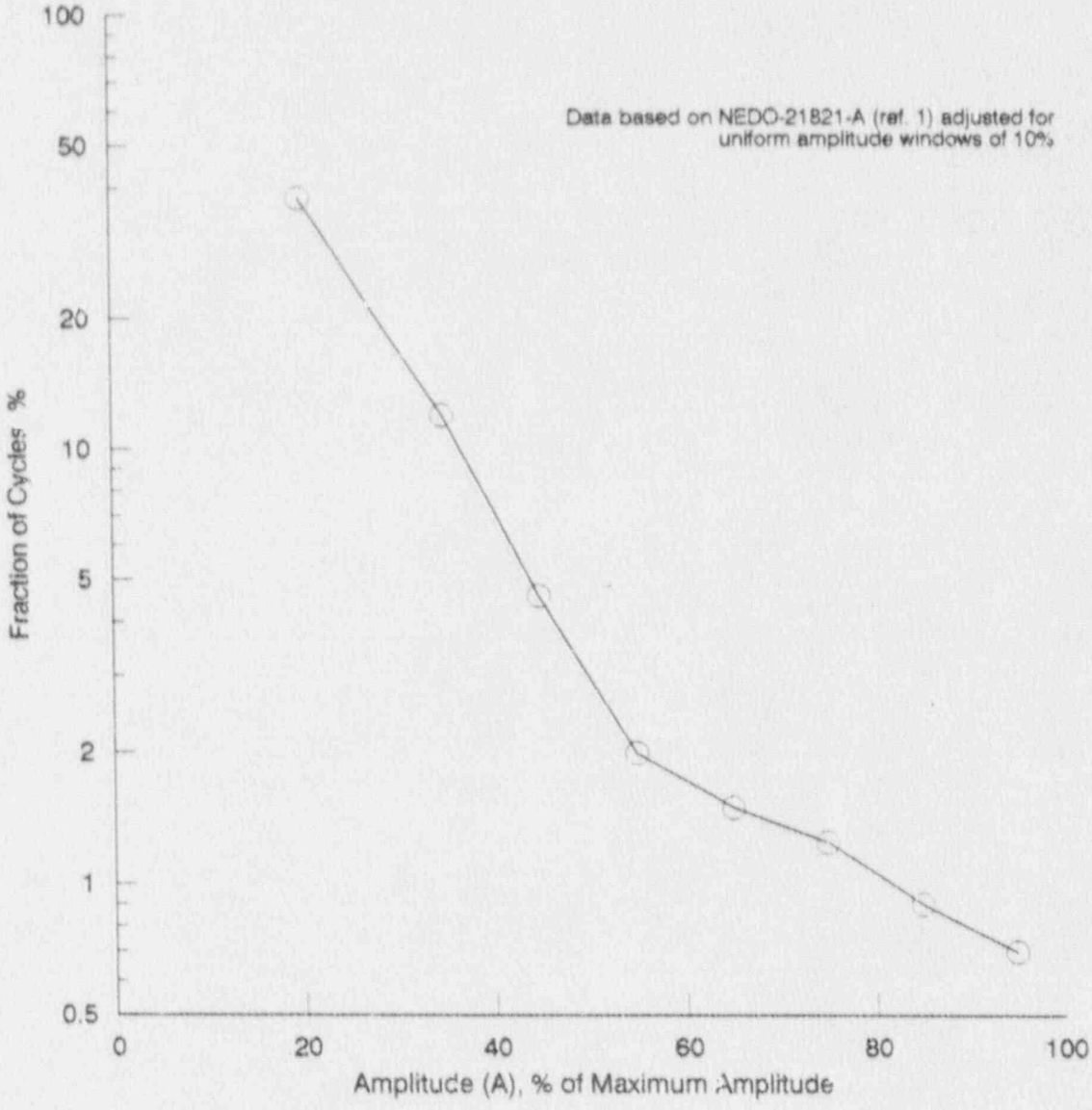

Figure C-2. Frequency of Occurrence Versus Amplitude of Near-Wall Fluid Temperature Fluctuations

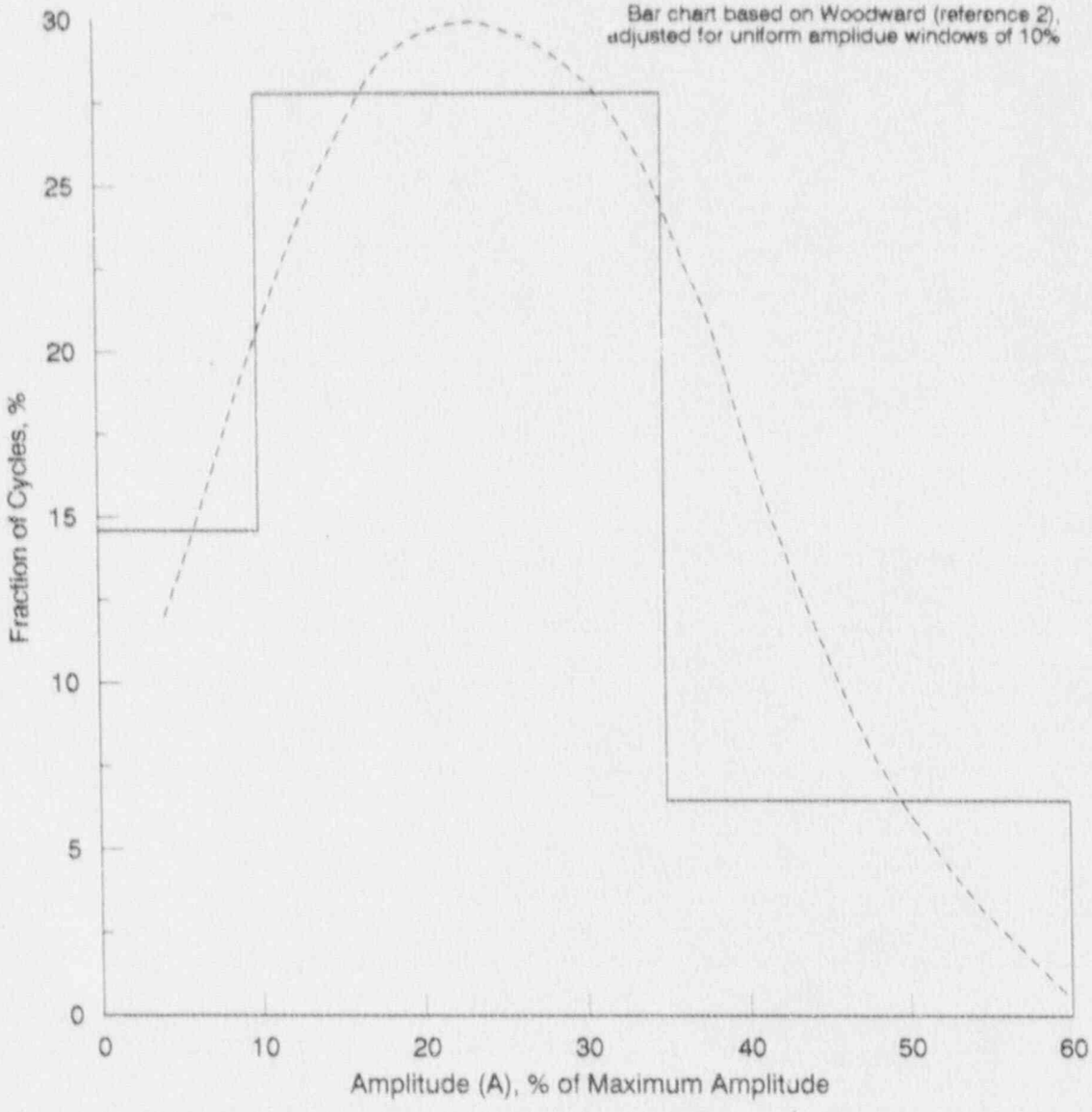

Figure C-3. Striping Conditions

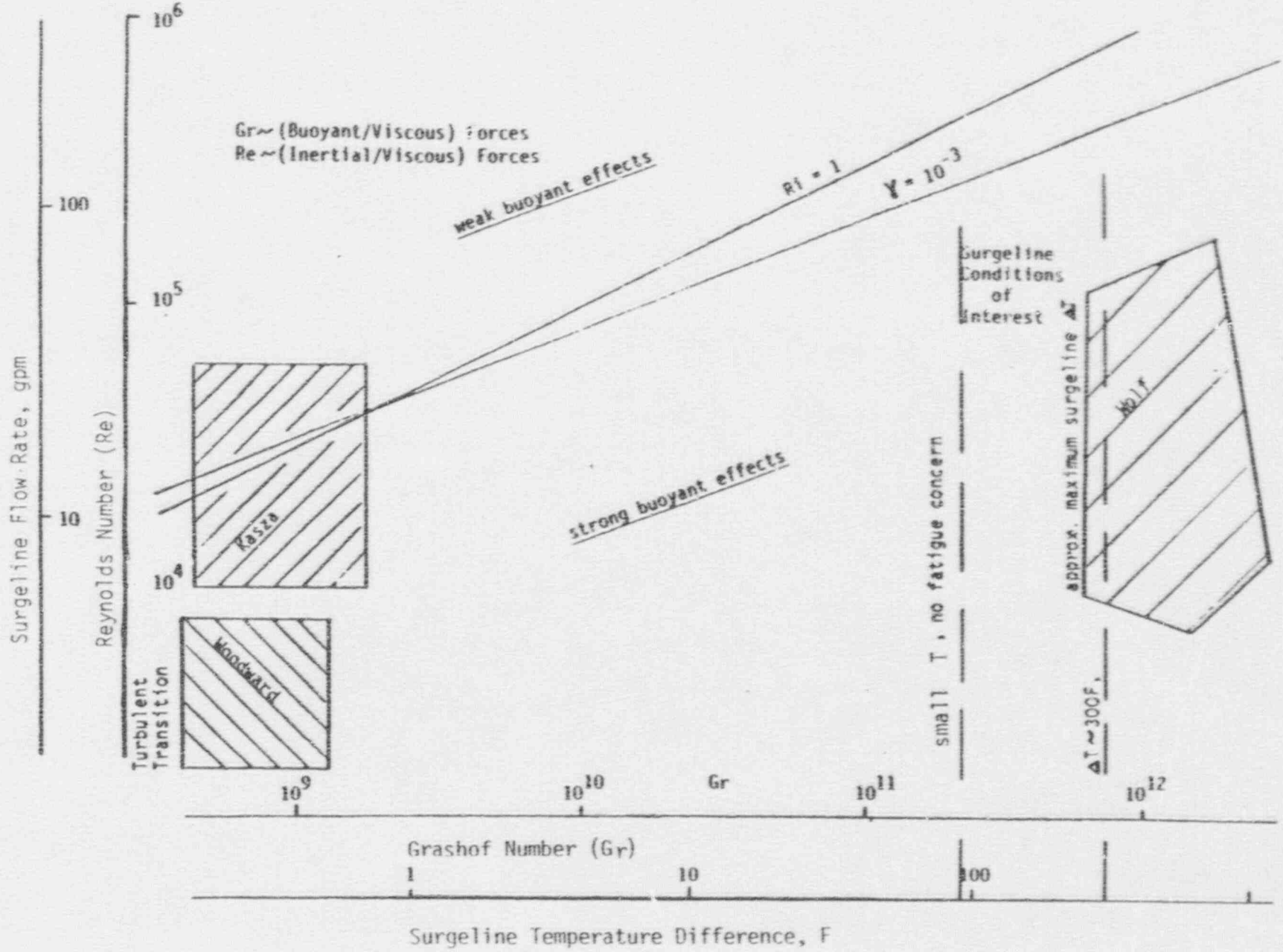

Figure C-4. Test Loop

Extracted from Figure 4.2-1 of reference 1.
Dimensions in mm.

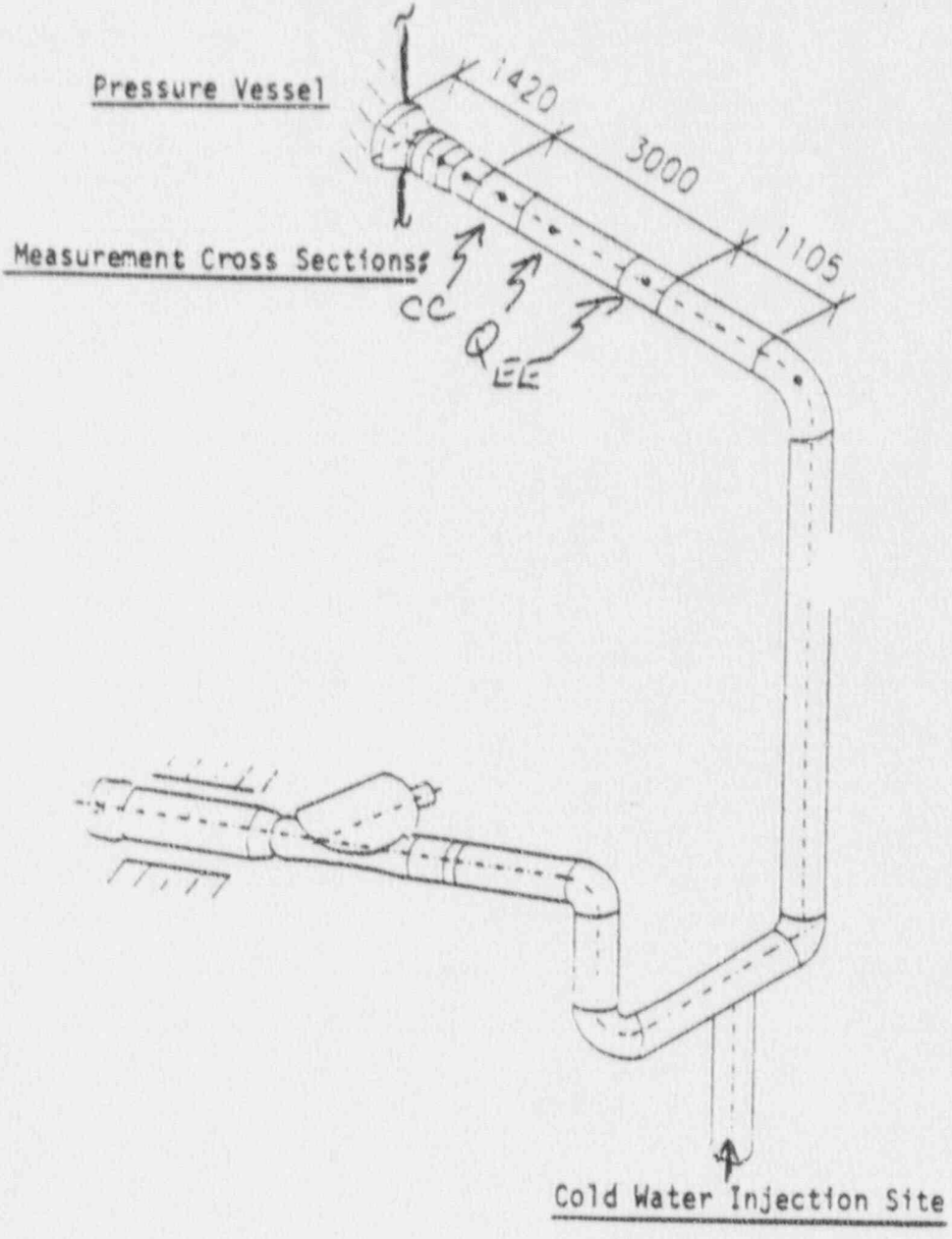

Figure C-4. Test Loop

Extracted from Figure 4.2-1 of reference 1.
Dimensions in mm.

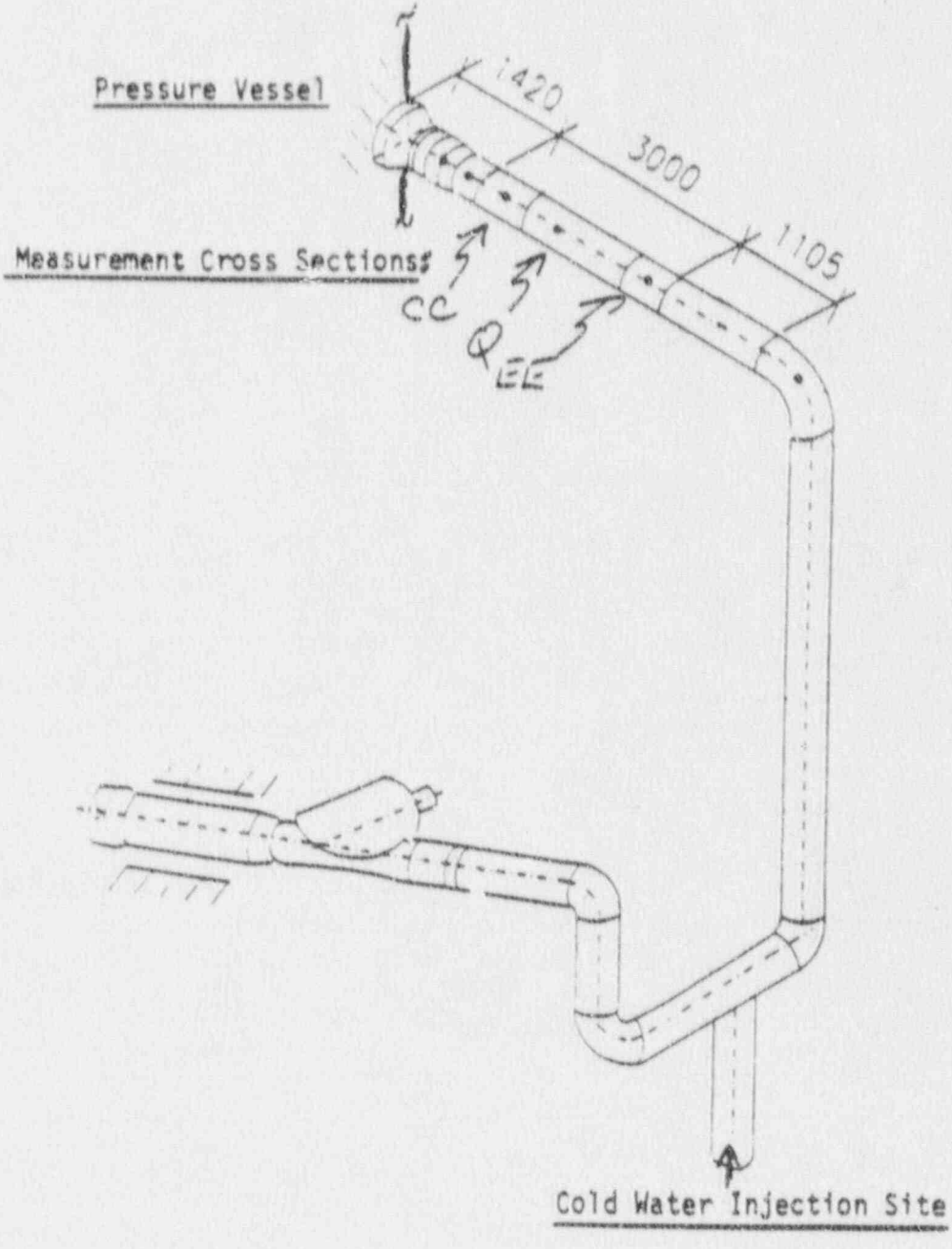

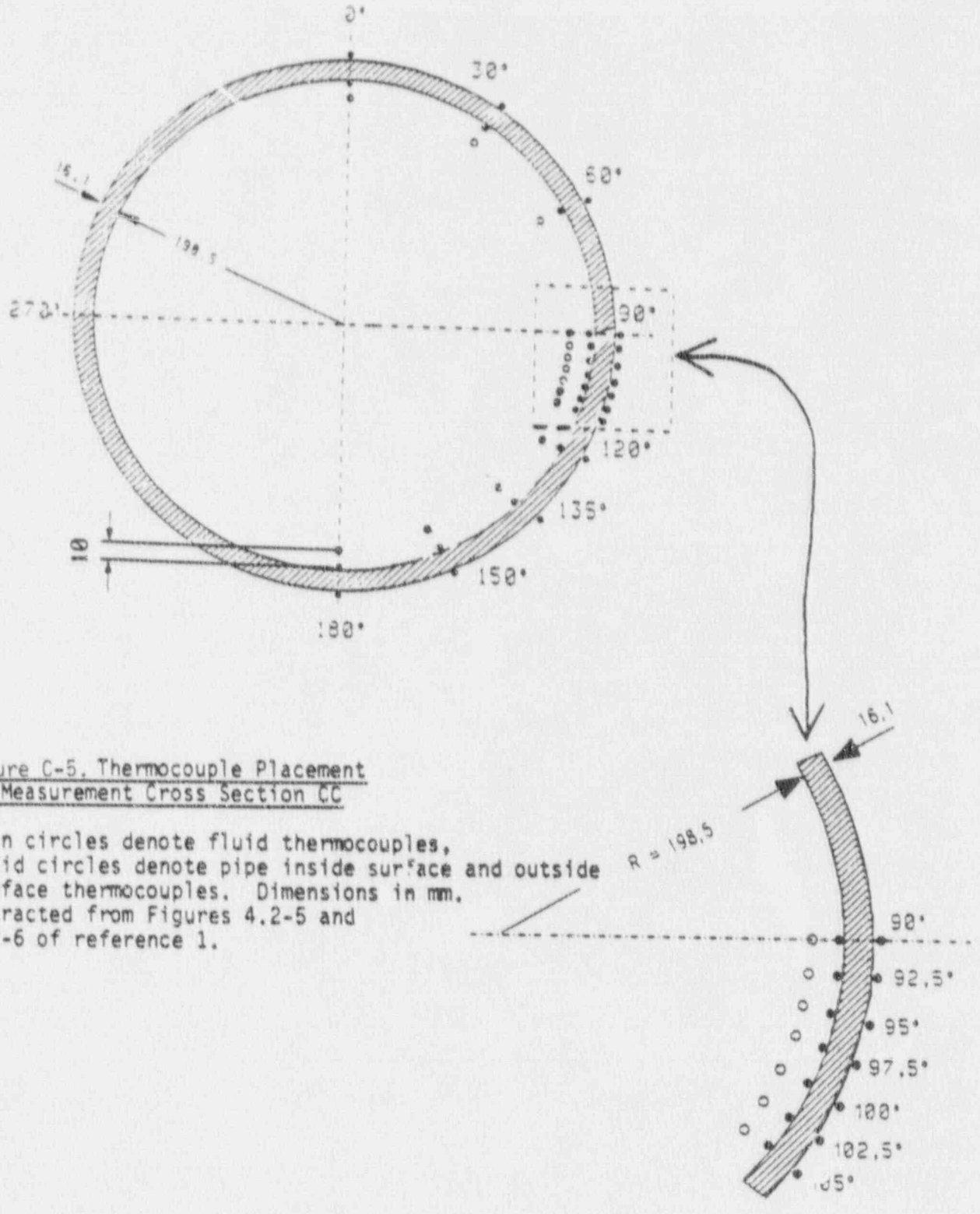

Figure C-5. Thermocouple Placement
At Measurement Cross Section CC

Open circles denote fluid thermocouples,
Solid circles denote pipe inside surface and outside surface thermocouples. Dimensions in mm.
Extracted from Figures 4.2-5 and
4.2-6 of reference 1.